University of Stavanger

Faculty of Science and Technology

MASTER'S THESIS

Study program/ Specialization: A Master's Thesis in Structural Engineering Faculty of Science and Technology Department of Mechanical and Structural Engineering and Materials Science	Spring semester, 2015 Open / ~~Restricted access~~
Writer: Arnstein Stangeland Waldeland	Arnstein Waldeland (Writer's signature)

Faculty supervisor: Ove Tobias Gudmestad (University of Stavanger)

External supervisor: Meric Pakkan (Subsea 7)

Thesis title:
Structural design and application of concrete protection covers in shallow waters

Norwegian title:
Dimensjonering og bruk av beskyttelsesdeksler av betong på grunne havdyp

Credits (ECTS): 30

Keywords: concrete, protection cover, subsea, structural design, trawl loads, dropped object, full scale impact test, finite element analysis, Eurocode 2, Norsok U-001, Ansys Workbench, STAAD.Pro	Pages: 22 + 206 + enclosure: 104 Stavanger, 12/6-2015 Date/year

Structural design and application of concrete protection covers in shallow waters

by

Arnstein Stangeland Waldeland

A Master's Thesis in Structural Engineering

University of Stavanger

Faculty of Science and Technology

Department of Mechanical and Structural Engineering and Materials Science

In cooperation with Subsea 7

June 15th 2015

Abstract

The objective of this Master's thesis was to investigate whether or not using protection covers made of reinforced concrete is a viable option for protection of subsea installations on the seabed. The main focus of the thesis is on the structural design of the cover. The original problem, raised by Subsea 7, was that in shallow waters of about 100m depth, the protection covers made of GRP experience problems with on-bottom stability due to the hydrodynamic forces from currents and waves. Unless tons of ballast steel is added to increase the mass of the cover, and rock-dumping on the sides of the cover is performed, the covers are prone to be unstable or possibly moved by the currents and waves. The hypothesis behind the thesis is that the slightly higher density of concrete and the thicker walls of the concrete covers, as well as some slight changes to the typical shape of the cover, will make them heavy enough to be stable on the seabed on its own without added ballast weight and rock-dumping.

The type of cover assessed in the thesis is a simple tunnel or arch cover, which is typically used to cover pipelines or spools. The inner diameter of the cover was set to 2 m, so that it can protect pipelines or spools up to size 16" with the necessary clearances to walls and roof.

A 3D model of the reinforced concrete cover was created, and a finite element analysis performed using the software *Ansys® Workbench, Release 14.5*. The trawl design loads of 300 kN from *NORSOK standard U-001* was applied to the cover. A dynamic dropped object simulation on the reinforced concrete cover model was also performed. The analyses showed that the concrete protection covers had sufficient strength to withstand the force from the trawl board and to withstand the energy from the dropped objects without damaging the product underneath.

A 2D beam model of the cover was created in *STAAD.Pro V8i* in order to get the design forces and moments in the cover. The concrete protection cover was designed according to the concrete standard *Eurocode 2*. This design resulted in the necessary amount of reinforcement to withstand the design forces and moments, and proved that the cross-

section of concrete and reinforcement of the protection cover was able to withstand the design loads from trawl gear impacts.

A full scale dropped object test of impact energies 5 kJ, 20 kJ, 30 kJ and 50 kJ, according to *NORSOK standard U-001* was performed on doubly reinforced concrete protection covers of 215 mm thickness and inner radius of 1000 mm. The test was performed on concrete covers provided by Multiblokk AS. The objects used in the test had masses of 140 kg, 550 kg, 850 kg and 1400 kg and was dropped onto the cover from approximately 3,7 m height. An initial test was performed on gravel on Multiblokk AS' premises, and the four main tests were performed with the cover submerged in the basin at the laboratories at the University of Stavanger. The covers in the main tests cracked slightly, but none were penetrated or collapsed. The dropped object tests proved that the strength of the protection covers was more than enough to withstand the dropped object energies, and that the initial design of the cover is suitable to build upon further.

Based on the results from the structural assessment of the cover, the tests and analyses, the concept of using concrete protection covers was found to be a feasible concept that should be investigated further and in more detail. Its heavy weight, high strength and the possibility of liberation from rock-dump requirements gives the concrete protection cover a competitive edge that is well worth exploring further.

Acknowledgement

There are many who have helped me make this Master's thesis possible, and they all have my sincerest thanks! I would especially like to thank my supervisors Ove Tobias Gudmestad (Professor at the University of Stavanger) and Meric Pakkan (Principle Engineer at Subsea 7) for all their ideas, help, support and comments along the road.

From Subsea 7, I would also like to thank Pål Myge (Discipline Manager) and Endre Ulversøy (Engineer Level I) for all of their help and input into making the 3D-model work as it should. For the same reason, I would also like to thank the support staff at EDR Medeso who was very helpful in regards to Ansys software.

I would also very much like to thank the guys from Multiblokk AS for their proactive efforts into making the full scale dropped object impact test possible. Especially Rune Egeland (General Manager), who has very much helped to arrange everything from their side and has put up with the seemingly endless stream of e-mails and phone calls to and from me, but also Egil Lillebø, Jan Herbert Sandsmark, Egil Pedersen, Kalle Tagamets, Arvid Lillebø and the rest of the guys at Multiblokk AS for making the preparation to and the execution of the dropped object test a smooth sail.

In addition, I would like to thank John Charles Grønli (Chief Engineer) of the University of Stavanger for allowing the potentially destructive dropped object test to be performed in the basin in the laboratories in the University of Stavanger, and for helping out with preparation and making the execution of the test possible.

And last, but not least, I would like to extend my thanks to my friends and family for support over the years. Thanks to my grandfather Rolv for helping out with the dropped object test. Thanks to my brothers Øyvind and Kristian for stepping up whenever needed. A special thanks to my dear Martine for everything, and a last special thanks to my father Rolv for love and support through it all.

This one is for you, Mum.

/Arnstein Stangeland Waldeland

Disclaimer

The work in this thesis has been done to my best abilities, and with as much care as I could possibly muster. I have double and triple checked everything myself, but alas, errors can always happen. Neither I nor Subsea 7 can be held responsible should you choose to use these results in your work.

Table of Contents

List of Figures

List of Tables

1 Introduction

Since the dawn of the Norwegian petroleum adventure, starting with the discovery of the Ekofisk oil field in the North Sea in 1969, important and expensive production equipment have been installed on the seabed in large parts of the Norwegian continental shelf. The equipment is connected together in a complex system all over the seabed, and represents considerable investments for the companies and owners of the petroleum fields. Naturally, it is in the companies' interest to protect these installations from damage to ensure a functional and reliable production system, but also from an environmental perspective is it important to protect the equipment properly. The DROPS Resource Centre states that 'where such pipelines and other facilities bear hydrocarbons, any damage or breach of containment could have potentially catastrophic consequences' (DROPS online, 2010). Leaks, spills, blowouts and other accidents represent dangers to the environment, and could have severe consequences on marine life and ecosystems. It is important to minimize the chances of such an event.

1.1 Protection methods

To repair an already damaged system can be a lot more costly than to plan for and implement proper protection of the system from the beginning of the project. There are many ways of protecting subsea equipment. Det Norske Veritas AS lists a number of different protection methods used to protect subsea pipelines in the Recommended Practice document *Risk Assessment of Pipeline Protection* (Det Norske Veritas AS, 2010):

- 'Concrete coating may be used to shield pipelines from potential impact damage' as it will absorb some of the impact energy (Det Norske Veritas AS, 2010).
- 'Polymer coating may be used to protect from potential damage. Polymer normally consist of a combination of several layers of different thickness and material properties' (Det Norske Veritas AS, 2010).
- Gravel dump (rock-dump) is the most common protection methods for pipelines. Using natural backfill is also a used method, but 'energy absorption in natural back-filled sand is considerably lower than for gravel' and 'can be assumed to be 2 – 10 % of the gravel resistance' (Det Norske Veritas AS, 2010).

- ‘Concrete blankets are well suited for low energy impacts’ (Det Norske Veritas AS, 2010) such as trawl board impacts, with typical impact capacity of approximately 3 kJ per individual concrete cone (several cones can be activated at the same time).
- Trenching is also a widely used method of protecting pipelines, often in combination with rock-dumping or natural backfilling. By using large ploughs on the seabed it is possible to create trenches that the pipes are placed in. ‘Trenching without backfilling will have a positive but limited effect against dropped objects, ships sinking, etc., as these will reduce the possibility to hit the pipeline/umbilical depending on the width of the trench and the size of the impacting object’ (Det Norske Veritas AS, 2010).
- One of the most used methods of protection is the use of tunnel covers, especially in the areas near significant installations where it is not practical to bury the pipeline with rock or sand, because it might be important to have easy access to the structure at a later point. In addition, Det Norske Veritas state that ‘tunnel structures are normally introduced in order not to restrain pipeline movements. Tunnel structures can be made up with a variety of geometry and material. Thus almost any required capacity level can be obtained’ (Det Norske Veritas AS, 2010).

1.2 Protection covers

This thesis will deal with the method of using tunnel structures as a protection cover for the equipment. These protection covers come in many different shapes, sizes and materials, but they are usually designed as a fully enclosed shell or a simple tunnel structure, and are placed over and around the exposed sides of the equipment. The cover's main objective is to protect the equipment against damage from external sources such as accidental drop loads and loads from fishing gear. According to the International Organization for Standardization, 'Accidental loads can include dropped objects, snag loads (fishing gear, anchors), abnormal environmental loads (earthquake) etc.' (International Organization for Standardization, 2010). This means that, for protection covers in general, the most important damages to consider (unless there are project specifics to include) are accidental impact loads from dropped objects such as anchors and dropped objects overboard from lifting operations, and loads from fishing gear. Especially trawl gear represent a substantial hazard for the covers, both as impact and snag loads. The on-bottom stability due to hydrodynamic forces on the cover is also important to consider so that the cover is not unstable or potentially moved by the hydrodynamic forces, as well as lift and installation loads on the cover, such as snap loads from wave force interactions during installation.

The design lifetime requirements for the protection covers are usually between 20 to 50 years (Subsea 7, 2015). The material used in the cover needs to withstand the corrosive subsea environment and still be structurally sound after the specified time. In the later years in Norway, the most used materials for protection covers have been steel and glass-reinforced plastic (GRP), also known as fibreglass. Covers made of polyurethane or concrete reinforced with steel are also known alternatives. The last two are more rarely used in the Norwegian sector in the later years, but in e.g. the UK sector, concrete protection covers, especially concrete blankets, are more widely used.

GRP protection covers have been more or less the industry standard in Norway for a long time due to the fact that it is a fairly cheap way to get robust covers that are easily fabricated, transported, installed, maintained and recovered. The covers are also very flexible in regards to design; they can be made into almost any shape needed, even curved shapes, see Figure 1.2-1 (Subsea 7, 2015). The fact that the GRP covers usually have relatively low mass is normally positive in regards to transportation and lifting. In recent years and projects, Subsea 7 has found, however, that its light weight can be a problem that require extra measures to overcome, especially in regards to the on-bottom stability of the cover.

Figure 1.2-1 Example of GRP protection cover

1.3 On-bottom stability problems

The problem with the GRP cover's weight is in regards to its on-bottom stability. This means its ability to be stable on its own on the seabed due to its mass, and to not have it capsize or move due to the hydrodynamic forces along the sea bottom. This problem is especially evident in shallow waters of approximately 100 m depth, where the hydrodynamic forces from waves and currents are larger than for deeper waters. Because of this weight issue with GRP covers, several tons of steel bars and plates are usually added to the covers as ballast, which will help against capsizing of the cover. The added weight increases the load on the ground, and might exceed the bearing capacity of the seabed. For this reason, extra horizontal so called mud mats are added to the cover to lower the stresses on the seabed and to gain soil bearing capacity (Subsea 7, 2015). Examples of steel ballast and mud mats can be seen on Figure 1.2-1. In addition, the sides of the covers are often being dumped rock upon after installation, which quite effectively minimizes the problem from the hydrodynamic forces after installation. Before installation, however, the covers are often placed in so called wet-storage areas near the installation site for some time while awaiting the installation. There have been cases throughout the earlier subsea history where the cover was placed in wet storage awaiting installation at a later time, only to discover upon return to the area that the protection cover had disappeared and was nowhere to be found. The cover had been moved away by the forces from currents and waves. It is therefore important that the cover weighs enough on its own so that it is stable on the seabed even during rough seas.

1.3.1 Linear wave theory

Marine technology and all of its branches of different technologies is an entire field of study on its own, and the process of determining the forces acting upon the cover e.g. through for instance computational fluid flow (CFD) analysis could have been an entire thesis on its own. Thus, this will not be attempted in this thesis, as the main focus is the structural design of the cover. A small summary of some key aspects and formulas of the theory behind the waves and currents will however be presented here.

The hydrodynamic forces that work on the cover are a combination of current forces and wave forces. Ocean currents are continuous movement of water that are affected by several local conditions like tidal effects, temperature differences in the water, the salinity of the water, the Coriolis effect as well as wind and storm effects (Gudmestad, 2015) , (National Oceanic and Atmospheric Administration, 2015). Surface waves are a result from the wind blowing over an area of water, and are created by the friction forces between the water surface and the wind.

Linear wave theory, also called Airy wave theory, is the 'core theory of ocean surface waves used in ocean and coastal engineering and naval architecture' (Gudmestad, 2015). It is an approximation of the real wave behaviour based upon linearized boundary conditions. Higher order wave theories are not based on the same boundary conditions, and are thus able to describe the wave behaviour more accurately. 'In real life, there is hardly anything like a sinusoidal wave, we normally have a combination of many different waves with different heights and different periods. These are called irregular waves and are analysed by Fourier analysis as a sum of regular waves. The closest we get to a sinusoidal-looking wave is the swell. Wind from one direction over a long time will also generate very large waves, close-to-regular waves.' (Gudmestad, 2015)

In linear wave theory the velocity potential function of the regular wave - which can be used to describe the water particle movements, given that the fluid is incompressible and non-rotational, is given as:

$$\varphi(x,y,z) = \frac{\xi_0 * g}{\omega} * \frac{cosh * k(z+d)}{\cosh(kd)} * \cos(\omega t - kx)$$

Where $\omega = 2\pi$ = frequency, $k = 2\pi/L$, T = wave period, L = wave length, ξ_0 = wave amplitude, g = acceleration of gravity, t = time, d = water depth, x = direction of propagation and z = vertical coordinate, positive upward, and origin at still water level (Gudmestad, 2015), (Krogstad & Arntsen, 2000).

When deriving the potential function for movement, we get the water particle velocities. The horizontal particle velocity u can be described as

$$u = \frac{\xi_0 * k * g}{\omega} * \frac{cosh * k(z + d)}{\cosh(kd)} * sin(\omega t - kx)$$

and the vertical particle velocity w can be described as

$$w = \frac{\xi_0 * k * g}{\omega} * \frac{sinh * k(z + d)}{\cosh(kd)} * cos(\omega t - kx)$$

By deriving these functions again, we get the particle accelerations. The horizontal particle acceleration $\dot{u}$ is

$$\dot{u} = \xi_0 * k * g * \frac{cosh * k(z + d)}{\cosh(kd)} * cos(\omega t - kx)$$

and the vertical particle acceleration $\dot{w}$ is

$$\dot{w} = -\xi_0 * k * g * \frac{sinh * k(z + d)}{\cosh(kd)} * sin(\omega t - kx)$$

These functions can be used to describe the wave forces acting on submerged structures. In order to find the wave forces, two different load cases need to be considered: submerged cylinder exposed to a constant current (constant velocity of the water) and submerged cylinder in a constant accelerating current (F = m*a), see *Marine Technology and Operations* (Gudmestad, 2015) for the complete derived formulas.

Based on velocity, diameter of cylinder and its roughness, the cylinder exposed to constant current will typically experience two forces along the flow: drag forces f_D in current direction and lift forces f_L perpendicular to the current direction. The forces are caused by the 'friction between the fluid and the cylinder, which causes eddy currents', the 'difference in pressure between upstream and downstream sides' of the cylinder (from the Bernoulli equation of fluid flow, which is the principle behind lift force from wind around airplane wings), and that the 'water will have to flow back into a stagnation point behind the cylinder' (Gudmestad, 2015).

Assuming that the cylinder is slender and fulfils the requirement D/L < 0,2 (small cylinder diameter compared to wavelength), experiments have shown that the drag forces f_D can be approximated as

$$f_D = \frac{1}{2} * \rho * C_D * D * u * |u|$$

where ρ is the density of the water, C_D is the drag coefficient, D is the diameter of the cylinder and u is the horizontal water particle velocity. The C_D drag coefficient is a function of parameters such as the roughness k of the cylinder surface and the Reynolds number R_e.

Experiments have shown that the lift forces f_L can be approximated as

$$f_L = \frac{1}{2} * \rho * C_L * D * u * |u|$$

where C_L is the lift coefficient.

When the cylinder is submerged in a constant accelerating current, 'the fluid near the cylinder will be dragged along the flow. We will therefore get an additional mass (added mass) which is accelerated' (Gudmestad, 2015). The total mass (or inertial) force on the cylinder is

$$f_M = m * \dot{u} = \frac{\pi}{4} * \rho * D^2 * C_M * \dot{u}$$

The cylinder will experience a combination of velocities and accelerations from the water particles in the case of waves, and thus all three forces will play a role on the behaviour of the cylinder. The horizontal forces are described by the Morison's equation as

$$f_{(z,t)} = f_M + f_D$$

In *Marine Technology and Operations* (Gudmestad, 2015), a simplified approach for stability assessment during pipeline operations is given. The same principles can be applied to the protection cover on the seabed, see Figure 1.3.1-2.

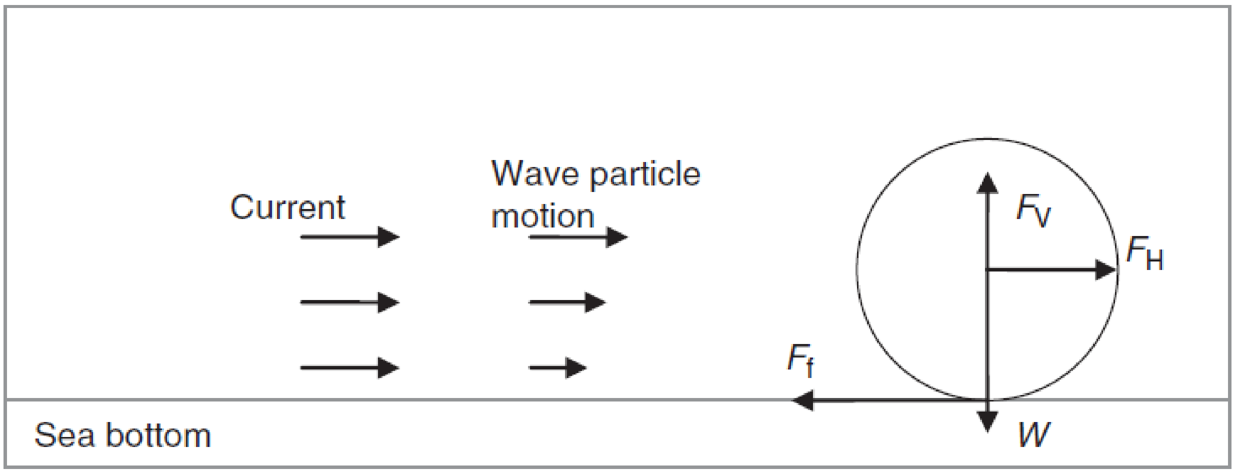

Figure 1.3.1-2 Assessment of on-bottom stability for pipeline operations. Source: (Gudmestad, 2015)

The horizontal stability of the pipeline or cover is secured when

$$F_f > F_H = \gamma_{st}(f_D + f_M)$$

where F_f is the friction force, γ_{st} is a safety factor. The friction force is a function between the weight of the cover (including buoyancy) and the vertical lift force. The friction force increases with increased weight of the cover, and also limits the effect of the lifting force.

$$F_f = f(W - F_V)$$

The functions above show that water particle movements, velocities and accelerations are dependent on the depth, z, and it can be shown that the effects of the waves stretch deep into the sea, diminishing with depth. The same is the case for the wave forces, which are directly related to the water particle velocities and accelerations. 'The deeper down into the water we go, the smaller the wave action is. However, underwater currents can still be very large, and currents in general have huge impact on the sea' (Gudmestad, 2015), see Figure 1.3.1-3. This proves the necessity of on-bottom stability assessments of the protection covers, as the hydrodynamic forces in shallow waters can be quite large. This assessment will however not be taken further in this thesis.

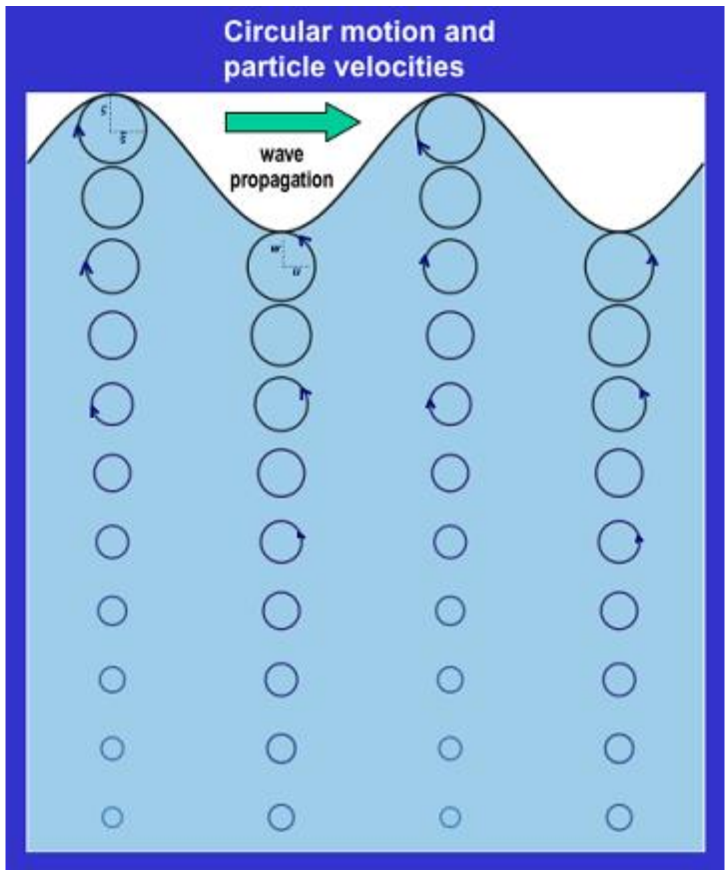

Figure 1.3.1-3 Description of the circular motion and particle velocities in waves and its relation to the water depth. Source: http://fcit.usf.edu/florida/teacher/science/mod2/images/waves/Slide4.png, downloaded 27/1-15

1.3.2 GRP and steel protection covers

The combination of forces from currents and the wave forces is what has been troubling Subsea 7 in regards to the on-bottom stability. In shallow waters (i.e. approximately 100 m water depth), the hydrodynamic forces due to currents and wave action may lead to sliding and overturning of the cover; it is not stable on its own. The solution to this problem has been, as mentioned above, to rock-dump the mud mats of the cover after installation and to add ballast weight in the form of steel bars or plates.

This combination of GRP covers and steel ballast have been the go-to choice for a long time. However, in certain cases the amount of ballast steel needed can be many times the mass of the GRP cover itself. In addition, there are cases where rock-dumping is not possible, and the process of designing a completely stable cover can be a lot of work. In such scenarios it could be beneficial to explore other options where the cover itself will have enough self-weight to be stable on the seabed by itself.

It is possible to use steel for this purpose as well. Steel has a high structural stiffness, has practically no size limits and its density makes it heavy enough to be stable on its own on the seabed. Due to its weight, it is also possible to install during heavier sea states and wind. There are, however, some negative aspects to using steel. The corrosion in the subsea environment is aggressive, and requires several preventive actions such as protective paint and sacrificial anodes, which can snag the trawling gear. Further, steel is expensive due to the fabrication process and the possible need for steels with high alloy content such as Super Duplex Stainless Steel. The heavy weight of the structure also means that the soil bearing capacity could become a problem, and this needs to be addressed (Subsea 7, 2015).

1.4 Objective of the thesis - Concrete protection cover

The objective of this thesis is to investigate whether or not the third material alternative, using reinforced concrete, is a viable option to solve the problems regarding the on-bottom stability. The density of GRP is given as 2124 kg/m^3, and reinforced concrete is given as 2400 kg/m^3 (Subsea 7, 2015). For reference, the density of steel is in the same document given as 7850 kg/m^3. The difference in density between GRP and concrete is quite small at only 12 %, but the difference in shapes of the covers from the two materials can be significantly different. GRP covers are usually around 20-30 mm thick, but concrete covers will most likely need to be in the thickness area of minimum 200-250 mm. This will in the end make a huge difference in the total weight of the cover, and could possibly be enough to be able to place the concrete cover as it is on the seabed, without rock-dumping, and without having to worry about the hydrodynamic forces and the on-bottom stability.

In this thesis an attempt will be made to design a reinforced concrete protection cover that fulfils the various requirements to material and geometry, trawl gear impact and dropped object impact given by the relevant governing standards such as *Eurocode 2* (Norsk Standard, 2004), *NORSOK standard U-001* (Norwegian Technology Centre (NTS), 2002), *NORSOK standard M-001* (Norwegian Technology Centre (NTS), 2004) and *DNV-RP-F107* (Det Norske Veritas AS, 2010). In addition, the *Subsea Protection Structure Design Guideline* by Subsea 7 will be used (Subsea 7, 2015).

The main focus of the thesis will be on the structural design of the cover, and will include a finite element analysis of a model of the cover performed in *Ansys® Workbench, Release 14.5* according to the requirements in *NORSOK standard U-001*. The finite element analysis will include both a static trawl impact analysis as well as a dynamic dropped object analysis. In addition, a simple beam model of the cover will be made in *STAAD.Pro V8i* in order to output the design forces and moments from the trawl board impact. Based on these results, a design of the reinforced concrete cross-section of the cover will be performed according to the requirements of *Eurocode 2*. And last, but not least, a full scale dropped object test will be performed on the protection cover to verify its ability to withstand the impact energies given in *NORSOK standard U-001*.

The type of protection cover that will be considered in this thesis is a spool or pipeline cover, which is a tunnel-shaped cover. There are several possible shapes to choose from: square, dome shaped, arched etc.; this thesis will consider arched covers, more specifically a protection cover shaped like a half circle. The reason for this is to get comparable results between the different analyses and the dropped object test.

2 Technology Qualification

Det Norske Veritas As outlines in the recommended practice document *DNV-RP-A203 Technology Qualification* (Det Norske Veritas AS, 2013) a process that provides 'evidence that a technology will function within specified operational limits with an acceptable level of confidence' (Det Norske Veritas AS, 2013).

By following the technology qualification process, see Figure 2-1, through the separate steps of Concept evaluation, Pre-engineering and then an iteration process of Detailed engineering one can ensure that the technology will be taken successfully from development to goal. This thesis will operate in one stage, the concept evaluation stage, due to time limitations. It will not be possible to follow every step of the process down to the last detail in the thesis. The focus of the thesis is a structural assessment of the cover, and the most important parts in regards to this will be included in the qualification process.

The Technology Qualification Process is outlined in Figure 2-1 below. It must be repeated through the stages of concept evaluation, pre-engineering and detailed engineering until the technology qualification is complete.

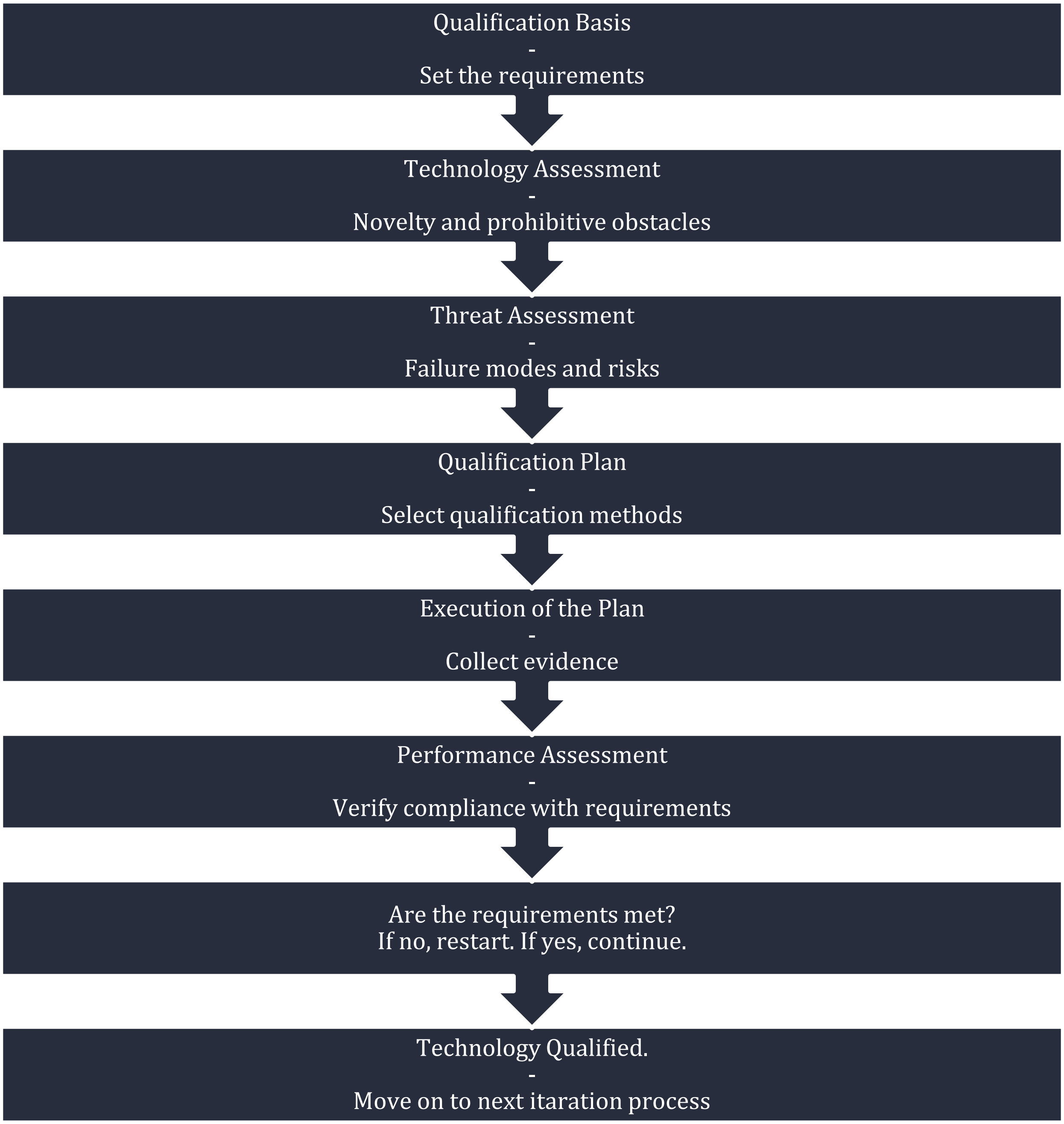

Figure 2-1 The steps in the Technology Qualification Process from (Det Norske Veritas AS, 2013).

2.1 Qualification Basis

The goal of this stage is to define 'criteria against which all qualification activities and decisions will be assessed' and 'shall describe the technology; define how the technology will be used; the environment in which it is intended used; specify its required functions, acceptance criteria and performance expectations' (Det Norske Veritas AS, 2013).

The protection cover is to be placed on the seabed around and covering pipelines or spools in order to protect it. Several covers will be connected on the sea bottom to a chain of covers. Its required functions are to protect the pipeline from fishing gear impacts and snag loads etc. It shall also protect it from falling objects such as anchors or other loads dropped over board. The cover is allowed to be damaged and to deform, but shall be of continuous protection to the pipeline even after the impact, until it can be replaced. This means that the protection cover is not allowed to be penetrated, have too much concrete debris knocked off from the roof of the cover, or to deform so much that the necessary clearance to roof and walls are compromised. It shall also be stable on the sea bottom, preferably on its own due to its weight.

2.2 Qualification Assessment

The purpose of this stage is to 'determine which elements require technology qualification, and identify their key challenges and uncertainties' (Det Norske Veritas AS, 2013). In this case, the concrete protection cover as a whole can be considered the element that requires technology qualification. The cover shall be made of concrete and reinforcement steel according to the relevant standards with the necessary material quality and fabrication methods. The design of the protection cover will be performed later in the thesis, and will include documents such as detailed drawings, material specifications etc. In addition, some details about some of the various life cycle phases, such as design, fabrication and testing, transportation and storage, installation, activation, operation, retrieval and abandonment, will be included.

The main challenges and uncertainties concerning the protection cover must also be addressed. For this thesis, where the structural design is the main focus, this could for instance mean the strength of the materials and the cover, which are addressed by safety factors for the materials. Uncertainties in regards to the loads needs to be addressed as well, and safety factors for the loads will be used as well, in accordance with the LRFD design approach. Since the cover is to be submerged, challenges such as keeping the materials free of corrosion by choosing suitable material qualities and protective methods must be addressed. In addition, the various hazards to the protection cover must be assessed, such as dropped or dragged anchors; trawl gear impact, dropped objects into the sea, ROV impact, and sunken ship etc. see chapter 3.1 Hazards and risk for more details about the hazards and risks.

2.3 Threat Assessment

The failure modes and the underlying failure mechanisms must be identified, the consequences of failure, the probabilities of failure and the associated risks must be assessed. The hazards from the previous step will be assed in regards to the risk it poses to the cover. The focus of the thesis is mainly on trawl gear impact and objects dropped into the sea. See chapter 3.1 Hazards and risk for more info about the risk assessment.

2.4 Qualification Plan

A qualification plan 'shall be developed to provide the evidence needed to manage the critical failure modes identified' (Det Norske Veritas AS, 2013) in the previous step. Qualification methods must be chosen and described in sufficient detail so that it is possible to carry out the qualification methods and acquire the necessary evidence and documentation of verification of the various criteria.

In regards to the trawl gear load, a finite element analysis will be performed on a 3D model of the protection cover using *Ansys® Workbench, Release 14.5.* The verification criteria are that the cover does not deform more than the specified allowed deformation, see chapter 4.5.2.2 Verification criteria, and that the stresses in the concrete and reinforcement does not exceed the maximum allowed stresses.

In addition, a 2D beam model of the cover will be made in *STAAD.Pro V8i* and a static analysis will be performed to find the design forces and moments acting in the cover. These will be used to design the concrete and reinforcement according to the requirements in *Eurocode 2*. The verification criteria are that the design forces and moments in the cover do not exceed the force and moment capacities of the cover. Suggestions to the necessary amount of reinforcement in the cover will be made.

The dropped objects requirements will be tested in full scale by dropping objects onto the protection cover and inflicting specific impact energies. The protection covers used will be half concrete drain pipes with similar shape, material strength, reinforcement, thickness and diameter as the designed protection cover will have. The verification criteria are that the covers shall not be penetrated by the objects, debris that can damage the equipment underneath shall not be knocked from the roof of the cover, and the cover is not allowed to deform so that the required clearances are compromised.

A dynamic finite element analysis of the dropped objects tests will be performed in *Ansys® Workbench, Release 14.5.* The simulations will be compared to the results from the dropped object test.

A simple assessment of the weight and stability of the cover will be performed, in order to find the necessary weight of the cover in order to be stable on its own on the seabed when impacted by the trawl gear loads.

The on-bottom stability due to wave forces and currents will not be investigated in this thesis more than what has been explained in chapter 1.3.1 Linear wave theory and chapter 3.4 On-bottom stability requirements.

2.5 Execution of the Plan

The execution of the qualification plan means to perform the analyses and tests described in the plan. It is important that all results are collected, traceable and documented. See the chapter 4 Theory, modelling, experiments and calculations for the explanation of the entire execution process for this thesis. The results from the various analyses and tests can be seen in chapter 5 Results, as well as in the appendices A to G.

2.6 Performance Assessment

The objective of this step is to measure the success by comparing the available qualification evidence against the criteria and the qualification basis. 'In the final iteration, this implies confirmation that the technology meets all its requirements, and both risk and uncertainty have been reduces to acceptable levels' (Det Norske Veritas AS, 2013). This process is performed in chapter 6 Discussion.

Based on this assessment, a conclusion whether or not the requirements have been met will be made, see chapter 7 Conclusion.

If the protection cover meets the requirements outlined earlier, the first step of the technology qualification process can be deemed successful and passed. The next step would then be to refine the details of the protection cover based on the findings, and then to do another iteration of the technology qualification process until a finalized design for the protection cover qualifies all the necessary requirements.

3 Design data

The input design data that the protection cover will need to withstand is mainly based on the *NORSOK standard U-001* (Norwegian Technology Centre (NTS), 2002), which gives additional load in regards to the protection structures of the subsea production systems described in *ISO standard 13628-1:2005+A1:2010* (International Organization for Standardization, 2010).

3.1 Hazards and risk

The possible hazards than can cause damage to subsea structures needs to be assessed based on the available information about activities in the area. Det Norske Veritas AS lists possible hazards that can cause damage to pipelines in the recommended practice document *DNV-RP-F107 Risk Assessment of Pipeline Protection* (Det Norske Veritas AS, 2010), see Table 3.1-1.

Table 3.1-1 Possible external hazards to pipelines (Det Norske Veritas AS, 2010)

Possible external hazards		
Operation/activity	**Hazard**	**Possible consequence to pipeline**
Installation of pipeline	Dropped and dragged anchor/anchor chain from pipe lay vessel Vessel collision during laying leading to dropped object, etc.	Impact damage
	Loss of tension, drop of pipe end, etc.	Damage to pipe/umbilical being laid or other pipes/umbilicals already installed
	Damage during trenching, gravel dumping, installation of protection cover, etc.	Impact damage
	Damage during crossing construction.	Impact damage
Installation of risers, modules, etc. (i.e. heavy lifts)	Dropped objects	Impact damage
	Dragged anchor chain	Pull-over and abrasion damage
Anchor handling (Rig and lay vessel operations)	Dropped anchor, breakage of anchor chain, etc.	Impact damage
	Dropped anchor	Hooking (and impact damage)
	Dropped anchor chain	Pull-over and abrasion damage
Lifting activities (Rig or Platform operations)	Drop of objects into the sea	Impact damage
Subsea operations (simultaneous operations)	ROV impact	Impact damage
	Manoeuvring failure during equipment installation/removal	Impact damage
Trawling activities	Trawl board impact, pull-over or hooking	
Tanker, supply vessel and commercial ship traffic	Collision (either powered or drifting)	Impact damage
	Emergency anchoring	Impact and/or hooking damage
	Sunken ship (e.g. after collision with platform or other ships)	Impact damage

The risks connected to the hazards and consequences should be assessed in regards to the frequency of the end-events. This can be done for instance by using the As Low As Reasonably Practicable (ALARP) principle. Figure 3.1-1 ALARP principle Figure 3.1-1 below identifies an area where the risk is acceptable (Det Norske Veritas AS, 2010).

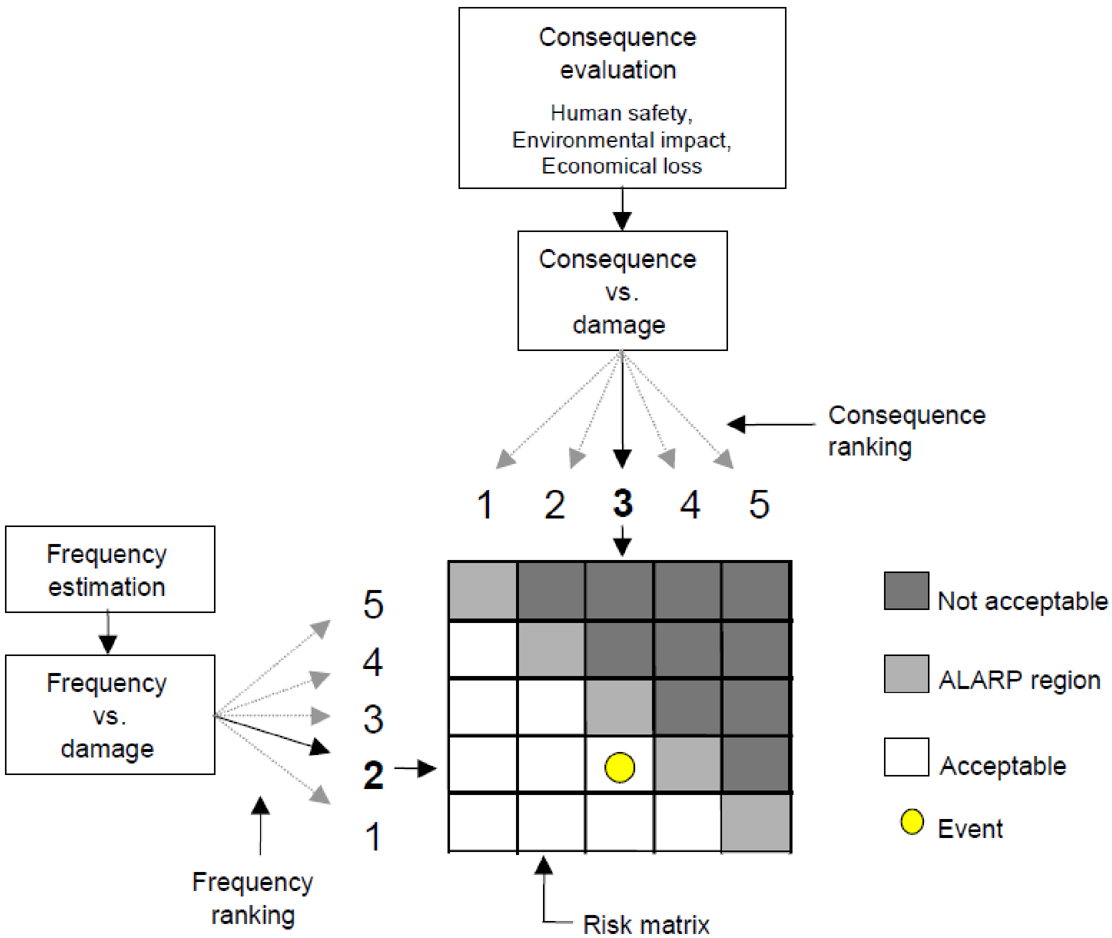

Figure 3.1-1 ALARP principle (Det Norske Veritas AS, 2010)

In the case the estimated risk is above the relevant acceptance criterion, the risk can be reduced by either reducing the frequency of the event, reducing the consequence of the event or a combination of the above. Some examples of frequency reducing measures are to limit lifting, or lift of certain objects, to certain zones, introduce safety distances or safe areas, or to introduce weather restrictions for operations. Some consequence reducing measures are to stop production in pipeline during activity, or to increase the protection around the pipeline (Det Norske Veritas AS, 2010).

Introducing safety distances and limiting lifting to certain zones can go a long way in reducing the risk in regards to trawling and dropped objects. Nevertheless, it is good practice to also reduce the consequences to the pipelines in the event that the hazards happen. This can be done by methods mentioned in chapter 1.1 Protection methods.

The most likely hazards with potentially large consequences from Table 3.1-1 are various dropped objects and trawl gear impacts.

3.2 Trawl Design Data

The Subsea 7 Engineering Standard *Subsea Protection Structure Design Guideline* states that 'subsea installations attract fish, and hence fishing activity' (Subsea 7, 2015). To understand why trawling is such an important factor to consider in the load scenario for the protection cover, a short explanation of trawling will follow. It is based on the info by Fiskeridirektoratet (Fiskeridirektoratet, 2010), the Atkins Boreas study about trawl loads (Atkins Boreas, Shell UK Ltd, 2009) and the *Subsea Protection Structure Design Guideline* (Subsea 7, 2015).

3.2.1 About trawling

To fish by trawling means to drag a large and submersed net behind a trawler boat at various depths to catch the fish, shrimp and other marine life. This is an effective way of commercial fishing that is widely used outside most of the coasts in the world, and especially in the North Atlantic Sea and the North Sea (Puig, et al., 2012). There are two main types of trawling, demersal and pelagic trawling. When the trawl net is dragged along the seabed, it is called demersal trawling. This is the fishing method that is most likely to interact with subsea pipeline systems, in contrast to pelagic trawling, which takes place higher up in the water column and is therefore not relevant to impacts or snags on subsea structures on the seabed (Atkins Boreas, Shell UK Ltd, 2009). Pelagic trawling will thus be disregarded in this thesis.

There are two main categories of trawl gear for demersal fishing; otter trawling and beam trawling. For beam trawling the net is held open by heavy beams that drag along the seabed. This type of trawling is mainly carried out in the southern part of the North Sea (UK sector), specifically south of the latitude 58° North (Fiskeridirektoratet, 2010), and will be disregarded in this thesis.

Otter trawling, utilizes a pair of otter boards, also called trawl doors, marked by A and B in Figure 3.2.1-2, that are heavy enough to remain on the seabed while being pulled by the boat. They are fastened on each side of the trawl net (D in Figure 3.2.1-2). The otter boards are designed to provide a hydrodynamic spreading of the net and force it open. The otter boards are heavy equipment that is considered important in the impact energy evaluations (Subsea 7, 2015). The otter boards are connected to the towing trawler with steel wire ropes known as trawl warps, and to the net with wires or ropes called bridles or sweeps. The typical spreading between the trawl doors are 80m-120m, the net opening is 30m-50m and typical trawl speed is 2-4 knots, or 1-2 m/s (Atkins Boreas, Shell UK Ltd, 2009).

Impacts on subsea structures may occur from the otter boards hitting the structure as it passes by. The otter boards may even get stuck on the structure unless care is taken to make the structure overtrawlable, i.e. that the walls on the structure are not steeper than 58° so that the otter board will pass over it (Norwegian Technology Centre (NTS), 2002). The ropes around the mouth of the trawl net may wrap around the structure, get stuck and make the vessel come to a halt. This creates snag loads between the moving boat and equipment and the subsea structure as the trawler is forced to a halt or the structure is moved. For this reason, it is important to make the structure snag free, i.e. that there are no protuberances on the structure on which the trawl can get caught.

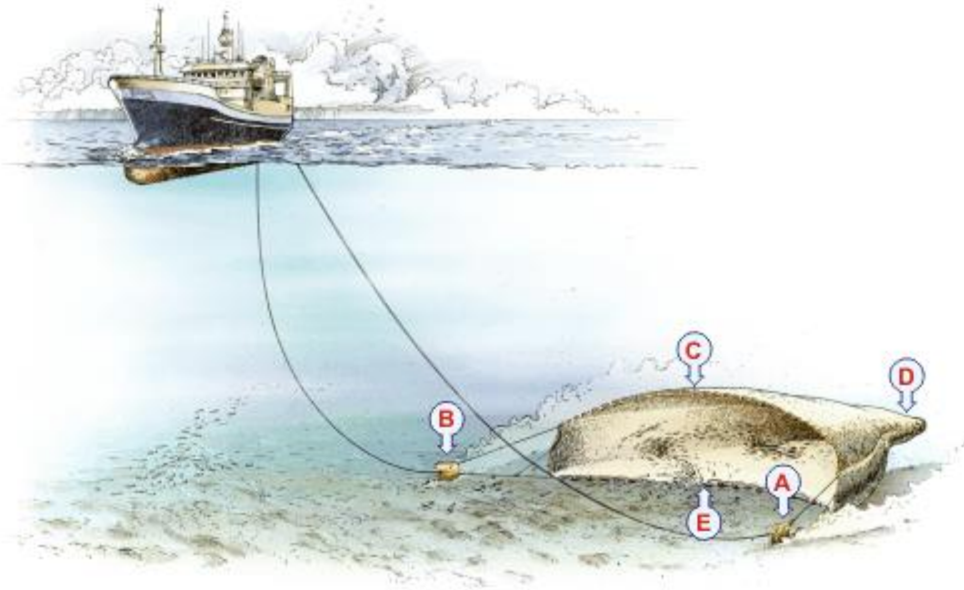

Figure 3.2.1-2 Illustration of Single otter trawl set-up
Source: http://www.simrad.com/www/01/NOKBG0240.nsf/AllWeb/ BC3D9D7D34DDF33AC12573C60049D1F8?OpenDocument, downloaded 27/3-15

Figure 3.2.1-3 Typical otter trawl doors
Source: http://www.codend.ca/en/images/ty2j6n0nzc_24111e59 _e184_3bfc_7323_7ad3524c3772.jpg, downloaded 27/3-15

There are other types of demersal trawling as well, for instance twin rig demersal trawl, which means that one boat tows two trawl nets side by side. The nets share one clump weight in the middle and each have one otter door on the outer warps, see Figure 3.2.1-4. The clump weight is often designed to be able to roll over hindrances to prevent snagging, but it can create powerful impact energies on the subsea structure as it passes over.

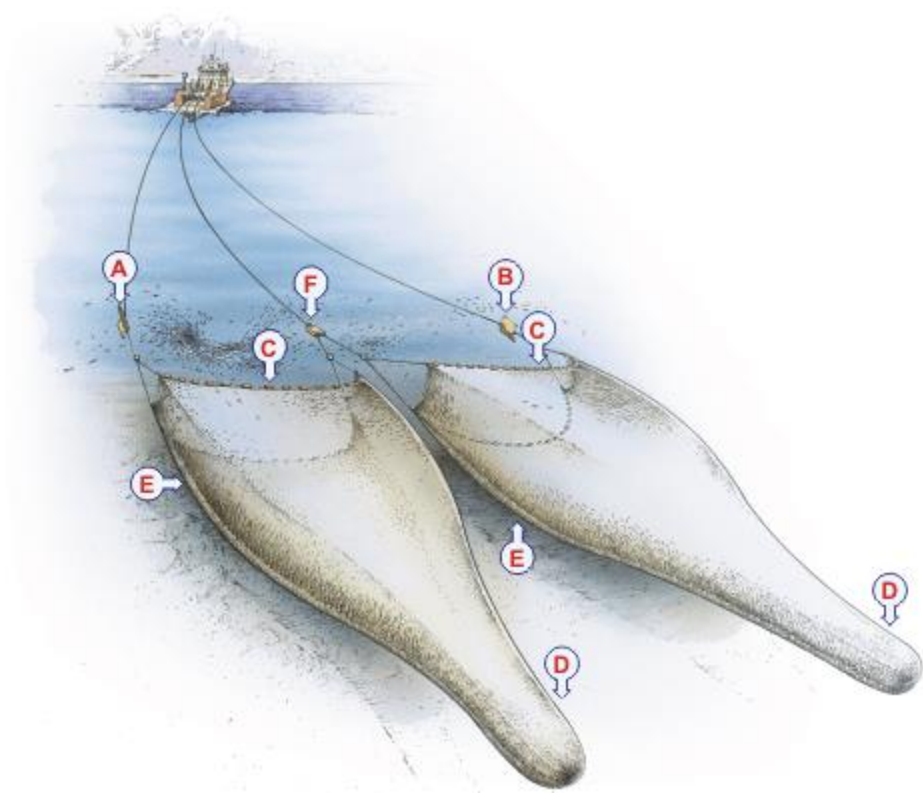

Figure 3.2.1-4 Illustration of Twin Rig Demersal Trawl
Source: http://www.simrad.com/www/01/NOKBG0240.nsf/AllWeb/ BAB035356DD4CA94C12573C500490F53?OpenDocument, downloaded 27/3-15

A third variant of the demersal trawl is Pair Trawling, in which two boats, each connected to a side of a single trawl net, holds the net open by their relative positions. Due to this, otter boards may not be used, but heavy chain bridles keep the sweeps and foot-rope on the seabed. The chain bridles can get caught under or around a seabed structure, and create powerful snag loads (Subsea 7, 2015).

Common to all the above methods are the use of trawl warps, or wires between otter boards or clump weight and the trawler. According to the Atkins Boreas report, ‘diverting the warps around the obstructions will largely deflect the gear; equally, snagging the wire will cause the gear to snag as well, perhaps irretrievably' (Atkins Boreas, Shell UK Ltd, 2009). This means that special care should be taken not to snag the warps, on the grounds that it might be inaccessibly stuck on the subsea structures.

3.2.2 Critical trawl gear

In *Interference between Trawl Gear and Pipelines,* Det Norske Veritas AS states that 'it should be observed; when considering the most critical trawling equipment, velocities, impact frequencies and area of application; that these parameters are subject to change. As an example, the largest trawl board in the North Sea and the Norwegian Sea has increased from about 1500 kg in the late 1970's and 1980's to 5000 kg in 2005 and 7300 in 2014. The largest trawl doors have been observed being used by industrial and prawn trawlers. The largest clump weights are observed for trawlers which aim to catch prawns. In the Barents Sea clump weights up to 9000 kg are currently being used by prawn trawlers' (Det Norske Veritas AS, 2014).

Table 3.2.2-1 lists appropriate data for the largest trawl boards, beam trawls and clump weights in the North Sea and the Norwegian Sea in 2014. However, this data varies from time to time, and the following specific data needs to be established for each new project (Det Norske Veritas AS, 2014):

- The types and maximum size of trawl gear that normally is used in the area
- Expectations for the future (mass, velocity, new types and shapes)
- The expected trawling frequency in the area

The trawl gear impact frequency can change a lot during the lifetime of a pipeline or structure, and the following aspects should be addressed to get a good estimate of the impact frequency from the trawl gear (Det Norske Veritas AS, 2014):

- Density of fishing vessels in the area
- Prevailing trawling direction relative to the pipeline
- Distribution of different trawl equipment and sizes

With this information, an estimate of the trawl gear impact frequency can be made:

$$f_{imp} = n_g * I * V * \alpha_e * \cos\phi$$

'Where n_g is the number of trawl boards, beam shoes or clump weight for each vessel, I is the expected density (i.e. annual mean number of trawlers per unit seabed area), V is the trawling velocity, α_e is the proportion of the pipeline length exposed to trawl loads, and φ is the angle of prevailing trawling direction relative to the pipeline perpendicular.' (Det Norske Veritas AS, 2014).

Table 3.2.2-1 Largest trawl gears in use in the North Sea and the Norwegian Sea in 2014 (Det Norske Veritas AS, 2014)

Data for largest trawl gears in use in the North Sea and the Norwegian Sea in 2014						
	Trawl boards			Clump weights		Beam
	Consumption		Industrial	Consumption		
	Prawn	Fish		Prawn	Fish	
Mass [kg]	6500	5000	7300	8000	6500	5000
Dimension Lxh [m]	4.6 x 4.0	4.0 x 3.5	5.2 x 4.4	1)	1)	12.0, 2)
Trawl velocity [m/s]	1.7	2.0	2.0	1.7	2.6	3.6

1) Typical dimension of the clump weights of 8 tonnes are L = 3.0 m wide (i.e. length of roller) by 0.8 meter diameter cross section. For smaller size roller type clump weights (i.e. 6 500 kg), the width L is shorter, whereas the roller diameter is unchanged. Typically length of the roller is between 2.0 to 3.0 m.

2) Beam trawl length (i.e. distance between outside of each shoe)

3.2.3 Trawl Design Loads in *NORSOK standard U-001*

In *NORSOK standard U-001 Rev. 3* (Norwegian Technology Centre (NTS), 2002) it is stated that the following fishing gear design loads shall apply as an addition to *ISO 13628* (International Organization for Standardization, 2010), see Table 3.2.3-1. The loads are design loads, and do thus include safety load factors for the Ultimate Limit State (ULS) load case.

Table 3.2.3-1 Fishing gear loads from NORSOK standard U-001 (Norwegian Technology Centre (NTS), 2002)

Design load type	Design load figure		
Trawlnet friction	2 x 200 kN	0° to 20° horizontal	ULS
Trawlboard overpull	300 kN	0° to 20° horizontal	ULS
Trawlboard impact	13 kJ		ULS
Trawlboard snag	600 kN	0° to 20° horizontal	PLS (If not overtrawlable/snagfree)
Trawl ground rope snag	1000 kN	0° to 20° horizontal	PLS (If not overtrawlable/snagfree)
Trawlboard snag on sealine	600 kN		PLS (If not overtrawlable/snagfree)

According to chapter 5.3.2 in *NORSOK standard U-001*, model tests may be used to document smaller trawl loads. In addition, 'when an overtrawlable/snag free concept or geometry can be documented through model test or a geometric evaluation combined with data from relevant model tests, the following design loads can be disregarded: trawlboard snag, trawl ground rope snag and trawlboard snag on sealine' (Norwegian Technology Centre (NTS), 2002). An overtrawlable structure will be assumed for this thesis, and the three load types at the bottom of Table 3.2.3-1 will thus be disregarded. The trawlnet friction force will be disregarded as well, as this is used for geotechnical assessment of the ground beneath the cover. See chapter 3.3.1 Dropped Objects in NORSOK standard *U-001* for more information about the trawlboard impact load.

3.2.4 Trawl Design Loads from NORNE Test

Such a test as described above was performed by Stolt Offshore Systems AS (previous name of Acergy, which was merged with Subsea 7 in 2011) and Marintek in March 2005 (Fokk, 2005). Model tests were performed in the Ocean Basin Laboratory at Marintek in scale 1:10 to investigate the overtrawlability of the Norne Satellites protection covers. Two different cover shapes were tested, and various fishing equipment at different angles for different water depths were tested.

The test showed that design loads lower than the values specified by *NORSOK standard U-001* can be documented, as well as an overtrawlable shape. It will however not be possible to include the details or the results of this test in this thesis, due to the fact that the results are classified and that the documented forces are still in use by Subsea 7 today. It would undermine one of their commercial advantages to publish it in this thesis. For this reason, the load cases and values specified by *NORSOK standard U-001* will be used in this thesis.

3.2.5 Design requirements for overtrawlability in *NORSOK standard U-001*

The *NORSOK standard U-001* (Norwegian Technology Centre (NTS), 2002) defines the following design requirements for overtrawlable structures:

a) 'the protective structure shall deflect all fishing equipment;
b) structural corners shall have maximum true angle of 58° from the horizontal to assist trawl and trawl wire deflection;
c) corners, ramps and equivalent structures shall penetrate the seabed to avoid snagging from trawl warp lines and ground rope. Effects from installation tolerances and expected scouring shall be accommodated;
d) the overall geometry of the structure and the size of openings, shall be such that trawl doors are prevented from entering into the structure;
e) if vertical side bracings are included, these shall be spaced to prevent intrusion and rotation of trawl equipment, without restricting subsea structure access for the intervention systems;
f) all protuberances shall be designed to prevent snagging of nets;
g) all external edges/members which are not part of a closed protection structure shall have a minimum radius of 250 mm;
h) minimum trawl speed shall be 3,0 m/s' (Norwegian Technology Centre (NTS), 2002).

3.3 Dropped Objects

It is important to test the cover's ability to resist and absorb impact energies from potential dropped objects or other impacts, so that the protection of the pipeline or structure does not breach upon impact. Typical sources of loads in this category are items dropped overboard from vessels, anchor impacts on the structure, impact from trawl otter doors or even sunken ships etc., see Table 3.1-1.

Impact energy testing is usually performed on GRP or other brittle materials, where failure mode is difficult to predict or analyse (Subsea 7, 2015). Steel is for instance not considered brittle, but has a fairly predictable deformation pattern and can be verified through simplified limit state analyses. Concrete, on the other hand, can be considered a brittle material. It behaves differently under loading to ductile materials like steel. It differs quite a bit from ideally brittle materials in many ways, such as its considerable hardness and resistance to compression, and weakness of tensile strain. Due to this, T.L. Anderson defines concrete as a quasi-brittle material (Anderson, 2004). It is therefore deemed necessary to perform impact tests on the concrete protection cover in order to validate its resistance to the impacts and ability to absorb the impact energies.

3.3.1 Dropped Objects in *NORSOK standard U-001*

The *NORSOK standard U-001* (Norwegian Technology Centre (NTS), 2002) states that the dropped object impact energy requirements in Table 3.3.1-1 below shall be tested. The requirements are split into Multi well structures and other structures, where multi well structures are protective structures in connection to or around a well structure. Other structures mean less critical protective structures. The dropped objects are to have a circular impact area of given diameters; this is to simulate the impact of a drill pipe dropped over board.

The standard also states that impact loads from dropped objects shall be treated in the Progressive Collapse Limit State (PLS) condition. This means that plastic deformation of the cover is allowed, so long as the protected structure beneath is unharmed, and still has the required clearance to walls and roof of the protection cover.

Table 3.3.1-1 Impact energies for dropped objects (Norwegian Technology Centre (NTS), 2002)

Group	Impact energy, kJ	Impact area	Object diameter, mm
Multi well structures	50	Point load	700
	5	Point load	100
Other structures	20	Point load	500
	5	Point load	100

No requirements for velocity of impact or mass of the impact object are mentioned in the *NORSOK standard U-001*. It is assumed that this means that impact energy and impact diameter that are most important factors, and that impact velocity and mass can be more or less chosen by the tester. It is a good idea to make the impact test representative of an impact that actually could happen in a real life situation. Since the dropped object test is supposed to simulate the impact of a drill pipe dropped over board, where the terminal velocity of the falling pipe is 6 m/s according to the *Subsea Dropped Objects* (DROPS online, 2010), a decision was made to make sure that the velocity of the covers are at least 6 m/s, and preferably slightly above.

In addition to the impact energies above, a new impact requirement of 30 kJ, which most likely will be published in a new revision of the *NORSOK standard U-001* later in 2015, will be included in the tests. This is in fact a trawl impact situation; as opposed to the dropped object PLS load cases. The current value of this impact is 13 kJ, see Table 3.2.3-1. The validity of use of impact velocity of 6 m/s or more in this situation can be discussed, as the normal trawl velocity is in the area of 3 and 4 m/s, but, as argued above, the impact energy and impact diameter seems to be the most important aspect of the test, and the increased impact velocity of the trawl impact is considered to be conservative in terms of damage on the concrete structure.

3.4 On-bottom stability requirements

The following load combinations for on-bottom stability design of submarine pipelines are listed in *DNV-RP-F109 On-Bottom Stability of Submarine Pipelines* (Det Norske Veritas AS, 2011):

For a temporary phase (prior to rock-dumping for GRP covers) with duration less than 12 months but in excess off three days, a 10-year return period for the actual seasonal environmental condition applies. An approximation to this condition is to use the most severe condition among the following two combinations:

1) The seasonal 10-year return condition for waves combined with the seasonal 1-year return condition for seasonal current.
2) The seasonal 1-year return condition for waves combined with the seasonal 10-year return condition for current.

For permanent operational conditions (e.g. post rock-dumping) and temporary phases with duration in excess of 12 months, a 100-year return period applies, i.e. the characteristic load condition is the load with 10^{-2} annual exceedance probability.

1) The 100-year return condition for waves combined with the 10-year return condition for current.
2) The 10-year return condition for waves combined with the 100-year return condition for current.

'One must make sure that the season covered by the environmental data is sufficient to cover uncertainties in the beginning and ending of the temporary condition, e.g. delays. For a temporary phase less than three days an extreme load condition may be specified based on reliable weather forecasts' (Det Norske Veritas AS, 2011).

According to the Subsea 7 Engineering standard, 'the wave acceleration close to the seabed should always be checked when doing on-bottom stability analyses in shallow water to determine whether inertia effects should be included.

The applicability of linear wave theory should be checked. A Computational Fluid Dynamics (CFD) analysis should be considered either for obtaining drag, added mass and lift coefficients for a simplified (spreadsheet) analysis or for simulating the oscillating flow around the structure due to waves and current' (Subsea 7, 2015). This, however, falls outside the scope of this thesis.

As a simple example of in what area the effective submerged weight of the protection cover should be, the results from a 2D CFD analysis for a protection cover of fairly similar shape and depth, but slightly smaller size, is that for 10-year wave return period the cover needs to have an effective mass of 6 tons submerged, and for 100-year wave return period, the cover will need to have a mass of 9 tons submerged (Subsea 7, 2014).

3.5 Material requirements

The *NORSOK standard U-001* states that 'Material selection and corrosion protection shall be in accordance with NORSOK M-001' (Norwegian Technology Centre (NTS), 2002).

The *NORSOK standard M-001* states the following about using concrete as structural material: 'For offshore load bearing concrete structures, concrete materials' properties shall comply with NS 3420, Exposure Class Ma – Highly Aggressive Environment, and NS 3473 or equivalent standards. Maximum water to binder ratio shall be 0,45' (Norwegian Technology Centre (NTS), 2004).

NS3473 has been retracted and replaced by the *Eurocode 2* (Norsk Standard, 2004) for concrete structures. According to Table 4.1 in *Eurocode 2*, also called EC2 further, the exposure class related to environmental conditions will for structures that are permanently submerged in seawater be Class 4, XS2, where the risk of corrosion stems from chloride induction from the sea water (Norsk Standard, 2004).

The EC2 Table NA.4.4N states that for the exposure class XS2, the minimum durability class of the concrete shall be M40. The minimum concrete cover of the reinforcement, $C_{min,dur}$, shall be 40 mm for 50 years of design working life and 50 mm for 100 years of design working life based on environmental conditions. Protection covers have, as mentioned earlier, a design working life between 20 and 50 years, which makes the use of 40 mm cover acceptable for $C_{min,dur}$ (Norsk Standard, 2004). The minimum concrete cover of the reinforcement c_{min} will be calculated later.

According to EC2 Table NA.E.1N, the anticipated lowest strength class of the concrete is B40 based on the minimum durability class M40, which should give a characteristic strength of 40 MPa (cylinder tested, f_{ck}) and 50 MPa for cube tested, $f_{ck,cube}$ (Norsk Standard, 2004).

The yield strength of the reinforcement steel shall be in the area $f_{.yk}$ = 400 to 600 MPa (Norsk Standard, 2004). The amount of reinforcement necessary will be calculated later.

The Offshore Standard *DNV-OS-H102 Marine Operations, Design and Fabrication* (Det Norske Veritas AS, 2012) does not give specific material factors for concrete or reinforcement, but states that 'material factors for materials not mentioned in B400 through B600 e.g. concrete, concrete reinforcement [...] shall be in accordance with a recognized code or standard' (Det Norske Veritas AS, 2012).

Thus, the governing standard in regards to material factors for concrete and reinforcement is the *Eurocode 2* (Norsk Standard, 2004), and in EC2 Table NA.2.1.1N the material factors for ultimate limit states can be found, see Table 3.5-1:

Table 3.5-1 Material factors for limit states (Norsk Standard, 2004)

Design situations	$\gamma_{.c}$ for concrete	$\gamma_{.s}$ for reinforcing steel	$\gamma_{.s}$ for prestressing steel
Persistent & Transient	1,5	1,15	1,15
Fatigue	1,5	1,15	1,15
Accidental	1,2	1,0	1,0

3.6 Load factors in the Ultimate Limit State

Det Norske Veritas AS gives in *DNV-OS-H102 Marine Operations, Design and Fabrication* the load factors for the ultimate limit state (Det Norske Veritas AS, 2012).

Two load conditions a) and b) shall be considered, see Table 3.6-1.

Table 3.6-1 Load factors for ULS (Det Norske Veritas AS, 2012)

Load factors for ULS					
Load Condition	Load categories				
	G	Q	D	E	A
a)	1.3	1.3	1.0	0.7	NA
b)	1.0	1.0	1.0	1.3	NA
Load categories G, Q, D, E and A are described in Sec.3 B of DNV-OS-H102 (Det Norske Veritas AS, 2012)					

G is permanent loads, Q is variable functional loads, D is deformation loads, E is environmental loads and A is accidental loads.

Load factors is however not needed for the loads in this thesis because the trawl board overpull load already is a design load, and has the load factor built in. In the analyses where the weight of the cover is included, the effect of using a load factor on it would not be conservative. The dropped object load case is regarded in the accidental progressive collapse limit state, where load factors are not applied.

4 Theory, modelling, experiments and calculations

4.1 Finite Element Analysis using Ansys® Workbench, Release 14.5

Structural finite element analyses of the cover was performed using the multi-purpose finite element software *Ansys® Workbench, Release 14.5*. The newest version of the software was at the time of writing *Ansys® Workbench, Release 16*, but this version was not available for use in the thesis. This led to some troubles with the chosen method of reinforcing the concrete which will be addressed in the following chapters.

Using *Ansys® Workbench, Release 14.5*, several pre-set analysis systems are available. For this analysis, the Static Structural system was used for simulating the effect of the trawl load requirements; and the Explicit Dynamics system was used for simulation of the dropped object impact testing of the cover.

4.1.1 Modelling of concrete and reinforcement

Concrete is a composite ceramic material mainly made up of aggregate (sand and stone), cement and water, as well as other chemicals and additives to gain specific material properties. The cement reacts with the water and forms a matrix which binds the aggregate and forms a hard and versatile cohesive mass and construction material. The ingredients must be added in the correct proportions to optimize the workability and strength. Concrete is a brittle material and has much higher compressive strength than tensile strength, which is why it is important to add steel reinforcement bars in the concrete to absorb and bear the tension (Callister & Rethwisch, 2010).

Concrete is a mix of different materials, and because the properties of the ingredients and the proportions can vary, the material properties of concrete are varied by nature. The material properties can vary due to differences in the water-to-binder ratio, by which cement type has been used, by the grading curve, shapes and sizes of the aggregate, by how well the concrete is vibrated, by how well the cement matrix binds to the aggregate, and by the porosity in the concrete as well as other factors. The properties vary during the curing process as well by factors such as air humidity, temperature and time. Factors such as creep, shrinkage and cracking need to be taken into consideration as well.

Because of these embedded variances in the concrete material, and the differences in what material properties that are wanted in certain situations, finding a material model that describes them all perfectly is not possible. Therefore, in order to achieve efficient progress during the work with the thesis, a decision to use the material model for concrete (and steel) embedded in *Ansys® Workbench, Release 14.5* was made.

There are several possible ways of modelling reinforcement bars inside a concrete beam available in *Ansys® Workbench, Release 14.5*. One of the traditional ways to model concrete has been to model the concrete beam using 3D elements of type Solid65 and reinforcement using element type Link180 or similar. The Solid65 element is an element used specifically for modelling of concrete and has eight nodes and three degrees of freedom in each node. It has the special ability to model cracking under tension and crushing under compression. Although this element is available for use, it has reached a legacy status and has been replaced by the element Solid185 which utilizes newer technology. In the documentation of *Ansys® Workbench, Release 14.5*, the use of Solid185 elements instead of Solid65 is recommended.

The Solid185 is also an eight node element with three degrees of freedom in each node, see Figure 4.1.1-1. It does not support cracking or crushing, but was nevertheless chosen for the thesis due to the recommendation as well as its support of the reinforcing element type Reinf264. This thesis is not a study on crack patterns of the concrete, and hence this advantage of the Solid65 elements was not necessary. The default keyoptions (element properties) of the Solid185 are the options recommended by the documentation of *Ansys® Workbench, Release 14.5* as the closest equivalent to the Solid65 element (ANSYS, Inc.),.

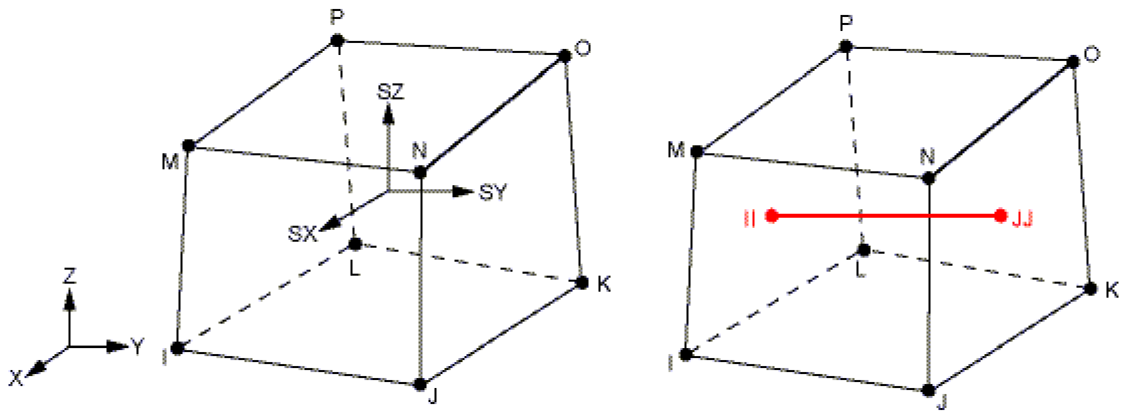

Figure 4.1.1-1 The Solid185 element (left) and Reinf264 element (right). Source: (ANSYS, Inc.)

Using the Solid185-approach, there are several ways to model reinforced concrete. The perhaps simplest way to imagine is to model the concrete body, cut away holes in the concrete body and fill these holes with steel reinforcement bodies sized equal to the holes. *Ansys® Workbench, Release 14.5* generates the contact between reinforcement and concrete automatically. This results in a multi-body part that should work well without the need of commands or clever solutions. For simple, straight beams and reinforcement bars, this procedure should give fairly accurate results without much hassle. The problem with this method is evident when the model is slightly more complicated due to curves and the many small reinforcement bars compared to the relatively thick concrete material. The method was attempted, and the result was a large, bad mesh with a very high number of badly shaped elements of various sizes that would simply use up all available computational resources and then result in an abortion of the analysis procedure. Due to this, other alternative methods to model reinforcement had to be considered. Two methods in particular stood out as the most reasonable approaches: using Reinf264-elements in the Static Structural system and using line bodies in the Explicit Dynamics system.

Reinf264 is a reinforcing element that is applied in the *Ansys® Workbench, Release 14.5* environment by classic Mechanical APDL commands. The element can simulate reinforcing fibres with arbitrary orientation in a base element – in this case the Solid185 element, see Figure 4.1.1-1. The reinforcing fibres are modelled separately in each element as a spar, and are thus limited to axial stiffness (ANSYS, Inc.). As a consequence, it is only able to output nodal displacements and axial stress and strains, see Figure 4.1.1-2.

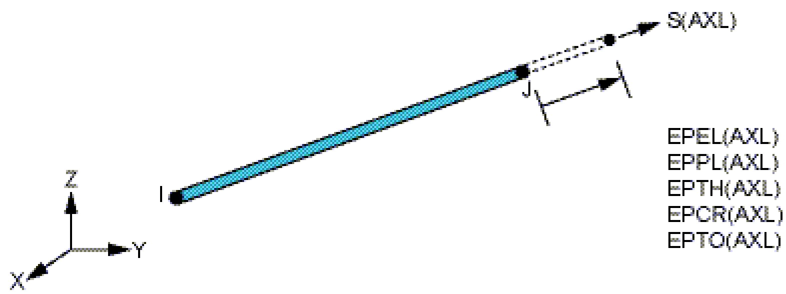

Figure 4.1.1-2 The Reinf264 element's stress and strain output. Source: (ANSYS, Inc.)

The line body-approach used in the Explicit Dynamics systems utilizes an embedded body interaction function in the software that applies discrete reinforcement to solid line bodies. All elements of line bodies that are contained within a solid body in the model will be converted to discrete reinforcement bars. The nodes of the reinforcing beam will be constrained to follow the displacement of the body element they reside within (ANSYS, Inc.).

4.1.2 Procedure and design decisions from the modelling of the protection cover

The modelling of the cover and the various analyses was performed using software available in the *Ansys® Workbench, Release 14.5* package, such as *DesignModeler* and *Mechanical,* except for viewing results for the Reinf264 elements, for which the classic *Mechanical APDL* was used.

The following is a chronological explanation of the procedure used to model the reinforced concrete covers, as well as discussions and explanations of the choices made in the process.

4.1.2.1 Engineering Data

The material data requirements presented in chapter 3.5 are required for the actual production of the protection cover. In the finite element analyses however, due to the extensive material data required to create a properly functioning material model in *Ansys® Workbench, Release 14.5*, and the amount of material testing needed to acquire this data, a decision to use the material data model included in the software was made. The material requirements listed in chapter 3.5 Material requirements have slightly higher requirements in regards to material strength than the material data included in *Ansys® Workbench, Release 14.5*, and for that reason, the finite element models are considered slightly conservative in regards to material strength. The difference is especially evident for concrete in the Explicit Dynamics system where the included material data has a compressive strength of 35 MPa, while the material requirement states a minimum of 40 MPa in compressive strength. For the Static Structural system, the included compressive ultimate strength of the concrete material is 41 MPa. The Young's Modulus is given as 30 GPa and the Poisson's rate is given as 0,18. The Bulk Modulus is given as 15,6 GPa and the material has a density of about 2300 kg/m^3.

The steel material data included in *Ansys® Workbench, Release 14.5* has a Compressive Yield Strength of 250 MPa and a Tensile Ultimate Strength of 460 MPa. The Young's Modulus is 200 GPa, the Poisson's Ratio is 0,3 and the Bulk Modulus is 166 GPa. The material has a density of 7850 kg/m^3.

In addition, in order to get realistic plastic behaviour of the steel material, the Bilinear Isotropic Hardening material data was added. Yield Strength was set to 355 MPa and the Tangent Modulus to 741 MPa according to Table A.3-4 in *NORSOK Standard N-004* (Norwegian Technology Centre, 2013).

$$E = Elastic\ modulus = 210000\ MPa$$

$$H = Plastic\ stiffness\ factor = 0{,}0034\ (for\ steel\ grade\ S355)$$

$$Tangent\ Modulus = H * E = 714\ MPa$$

This has been done in order to get a realistic picture of how the stresses and strains redistribute to neighbouring regions when the material reaches its yield limit and starts to strain plastically. The Bilinear Isotropic Hardening data has been added to the material data in both the Static Structural and the Explicit Dynamics systems.

The complete material data which was used in the thesis can be seen in the figures below.

Properties of Outline Row 3: Concrete

	A	B	C
1	Property	Value	Unit
2	Density	2300	kg m^-3
3	Isotropic Secant Coefficient of Thermal Expansion		
4	Coefficient of Thermal Expansion	1,4E-05	C^-1
5	Reference Temperature	22	C
6	Isotropic Elasticity		
7	Derive from	Young's Modulus and Poisson's R...	
8	Young's Modulus	3E+10	Pa
9	Poisson's Ratio	0,18	
10	Bulk Modulus	1,5625E+10	Pa
11	Shear Modulus	1,2712E+10	Pa
12	Tensile Yield Strength	0	Pa
13	Compressive Yield Strength	0	Pa
14	Tensile Ultimate Strength	5E+06	Pa
15	Compressive Ultimate Strength	4,1E+07	Pa

Figure 4.1.2-3 The engineering data for concrete in the Static Structural system.
Source: ***Ansys® Workbench, Release 14.5***

4		Fatigue Data at zero mean stress comes from 1998 ASME BPV Code, Section 8, Div 2, Table 5-110.1

Properties of Outline Row 4: Structural Steel

	A	B	C
1	Property	Value	Unit
2	Density	7850	kg m^-3
3	Isotropic Elasticity		
4	Derive from	Young's Modulus and Poisson's R...	
5	Young's Modulus	2E+11	Pa
6	Poisson's Ratio	0,3	
7	Bulk Modulus	1,6667E+11	Pa
8	Shear Modulus	7,6923E+10	Pa
9	Bilinear Isotropic Hardening		
10	Yield Strength	3,55E+08	Pa
11	Tangent Modulus	7,14E+08	Pa
12	Specific Heat	434	J kg^-1 C^-1

Figure 4.1.2-4 The engineering data for steel in the Explicit Dynamics system.
Source: ***Ansys® Workbench, Release 14.5***

3	Riedel et al."Penetration of Reinforced Concrete" ISIEMS'99 pp315. Riedel W. "Beton unter dynamischen Lasten" Ed. Frauhhofer EMI, IRB-Verlag, 2004, ISBN 3-8167-6340-5 Riedel, et al. "Numerical Assessment for Impact Strength" IJIE 36 (2009) pp283.

Properties of Outline Row 3: CONC-35MPA

	A	B	C	D	E
1	Property	Value	Unit		
2	Density	2314	kg m^-3		
3	Specific Heat	654	J kg^-1 C^-1		
4	RHT Concrete Strength				
5	Use cap on Elastic Surface	Yes			
6	Compressive Strength fc	3,5E+07	Pa		
7	Tensile Strength ft/fc	0,1			
8	Shear Strength fs/fc	0,18			
9	Intact Failure Surface Constant A	1,6			
10	Intact Failure Surface Exponent n	0,61			
11	Tension/Compression Meridian Ratio Q2.0	0,6805			
12	Brittle to Ductile Transition BQ	0,0105			
13	Hardening Slope	2			
14	Elastic Strength/ft	0,7			
15	Elastic Strength/fc	0,53			
16	Fracture Strength Constant B	1,6			
17	Fracture Strength Exponent m	0,61			
18	Compressive Strain Rate Exponent α	0,032			
19	Tensile Strain Rate Exponent δ	0,036			
20	Maximum Fracture Strength Ratio SFMAX	1E+20			
21	Damage Constant D1	0,04			
22	Damage Constant D2	1			
23	Minimum Strain to Failure	0,01			
24	Residual Shear Modulus Fraction	0,13			
25	~~Bulk Modulus~~	3,527E+10	Pa		
26	Shear Modulus	1,67E+10	Pa		
27	Polynomial EOS				
28	Parameter A1	3,527E+10	Pa		
29	Parameter A2	3,958E+10	Pa		
30	Parameter A3	9,04E+09	Pa		
31	Parameter B0	1,22			
32	Parameter B1	1,22			
33	Parameter T1	3,527E+10	Pa		
34	Parameter T2	0	Pa		
35	P-alpha EOS				
36	Solid Density	2750	kg m^-3		
37	Porous Soundspeed	2920	m s^-1		
38	Initial Compaction Pressure Pe	2,33E+07	Pa		
39	Solid Compaction Pressure Ps	6E+09	Pa		
40	Compaction Exponent n	3			

Figure 4.1.2-5 The engineering data for concrete in the Explicit Dynamics system. Source: ***Ansys® Workbench, Release 14.5***

4			Fatigue Data at zero mean stress comes from 1998 ASME BPV Code, Section 8, Div 2, Table 5-110.1

Properties of Outline Row 4: Structural Steel

	A	B	C
1	Property	Value	Unit
2	Density	7850	kg m^-3
3	Isotropic Secant Coefficient of Thermal Expansion		
4	Coefficient of Thermal Expansion	1,2E-05	C^-1
5	Reference Temperature	22	C
6	Isotropic Elasticity		
7	Derive from	Young's Modulus and Poisson's R...	
8	Young's Modulus	2E+11	Pa
9	Poisson's Ratio	0,3	
10	Bulk Modulus	1,6667E+11	Pa
11	Shear Modulus	7,6923E+10	Pa
12	Bilinear Isotropic Hardening		
13	Yield Strength	3,55E+08	Pa
14	Tangent Modulus	7,41E+08	Pa
15	Alternating Stress Mean Stress	Tabular	
16	Interpolation	Log-Log	
17	Scale	1	
18	Offset	0	Pa
19	Strain-Life Parameters		
20	Display Curve Type	Strain-Life	
21	Strength Coefficient	9,2E+08	Pa
22	Strength Exponent	-0,106	
23	Ductility Coefficient	0,213	
24	Ductility Exponent	-0,47	
25	Cyclic Strength Coefficient	1E+09	Pa
26	Cyclic Strain Hardening Exponent	0,2	
27	Tensile Yield Strength	2,5E+08	Pa
28	Compressive Yield Strength	2,5E+08	Pa
29	Tensile Ultimate Strength	4,6E+08	Pa
30	Compressive Ultimate Strength	0	Pa

Figure 4.1.2-6 The engineering data for steel in the Static Structural system.
Source: ***Ansys® Workbench, Release 14.5***

4.1.2.2 Geometry

Due to the differences in reinforcing methods in the Static Structural and the Explicit Dynamics systems, the geometry in the two systems needed to be made slightly different to one another. Both models were created in the *DesignModeler* software in the *Ansys® Workbench, Release 14.5* software package, but following different procedures. These will both be explained in the following sub-chapters.

4.1.2.2.1 Static Structural

In the Static Structural system the reinforcing elements were generated by commands in the base elements. In this case the base elements are the elements of the concrete cover mesh. In the *Ansys® Workbench, Release 16* this can be done easily by simply picking the elements from the mesh that shall be reinforced; this cannot be done in the *Ansys® Workbench, Release 14.5*, and a workaround was needed to make this procedure work.

It is known from details provided by Multiblokk AS, see chapter 4.5.3.1 Concrete Protection Cover, that the inner radius of the concrete cover used for testing is 1000 mm and that the outer radius is 1215 mm. The thickness of the concrete cover is therefore 215 mm. A total of 24 reinforcement bars was inserted in the pipe in a double pattern of 2x12 bars. The inner bar has a radius of 1031 mm and the outer bar has a radius of 1184 mm. The reinforcement bars will have a centre distance between each circle of approximately 100 mm.

In order to enable the Reinf264 elements along the arc of the cover in their specific locations, the base body of the cover had to be split into several parts that could be picked separately to generate a named selection in the next section. In order to simplify this process without compromising accuracy too much, a decision to split the thickness of the cover into three separate parts was made. As default the reinforcing Reinf264 elements will be generated in the midpoints of the element faces. Splitting the thickness into three separate bodies made it possible to generate reinforcing elements with an inner radius of 1035,8 mm and an outer radius of 1179,2 mm, see Figure 4.1.2-7 .

$$\frac{215\ mm}{3} = 71{,}7\ mm\ per\ element$$

$$inner\ radius = \frac{71{,}7\ mm}{2} = 35{,}8\ mm$$

$$outer\ radius = (71{,}7\ mm \times 2) + 35{,}8\ mm = 179{,}2\ mm$$

The length of the pipe supplied by Multiblokk AS was 1500 mm. In order to place the 12 bars evenly along the X-axis of the cover, a decision to split the base body into 14 separate bodies was made. Since the Reinf264 elements by default are generated in the midpoints of the elements, this approach results in an even placement of the double reinforcement rings with a centre distance of 100 mm, as the 12 inner bodies were given a length of 100 mm. The two outer bodies were each 150 mm long, resulting in a total of 1500 mm.

In order to achieve this in the *DesignModeler* software, three sketches were drawn, see Figure 4.1.2-7, and extruded to a total length of 1500 mm, resulting in three solid layers along the thickness of the cover. Next, thirteen new planes were created along the X-direction of the cover which allowed for the slice function to slice the cover in these locations along the YZ-plane. This resulted in a 3x14 grid of bodies which could easily be combined into a single part, while still allowing bodies to be picked separately in the next section, see Figure 4.1.2-8.

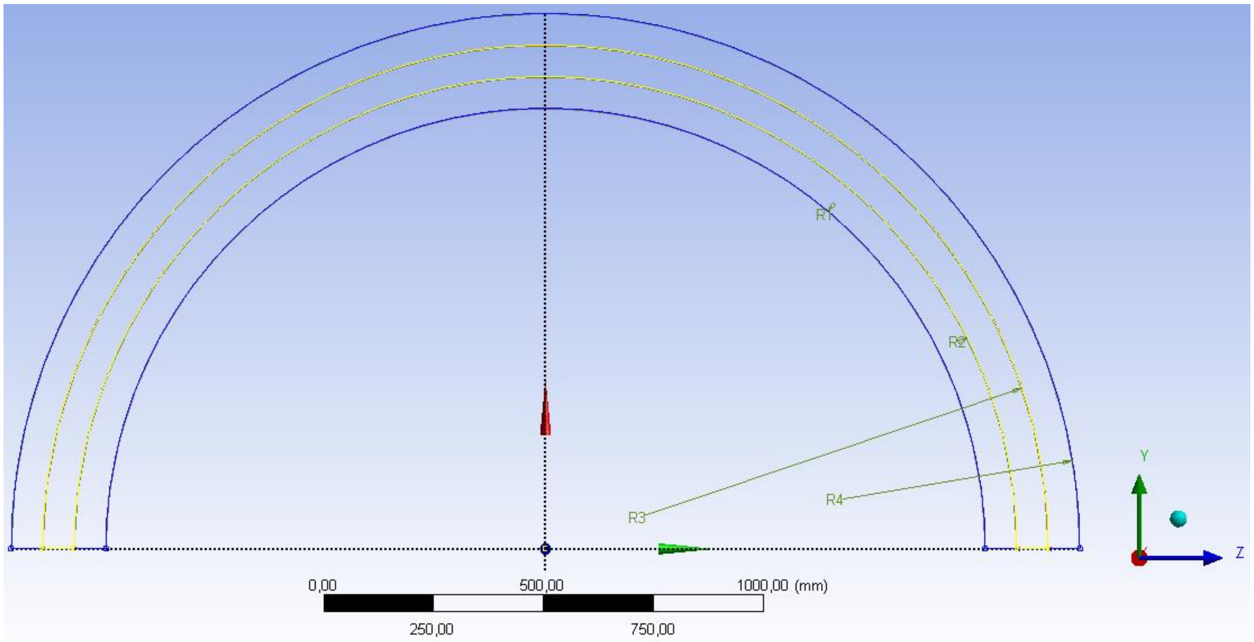

Figure 4.1.2-7 YZ-plane of the sketch from *DesignModeler*. Source: *Ansys® Workbench, Release 14.5*

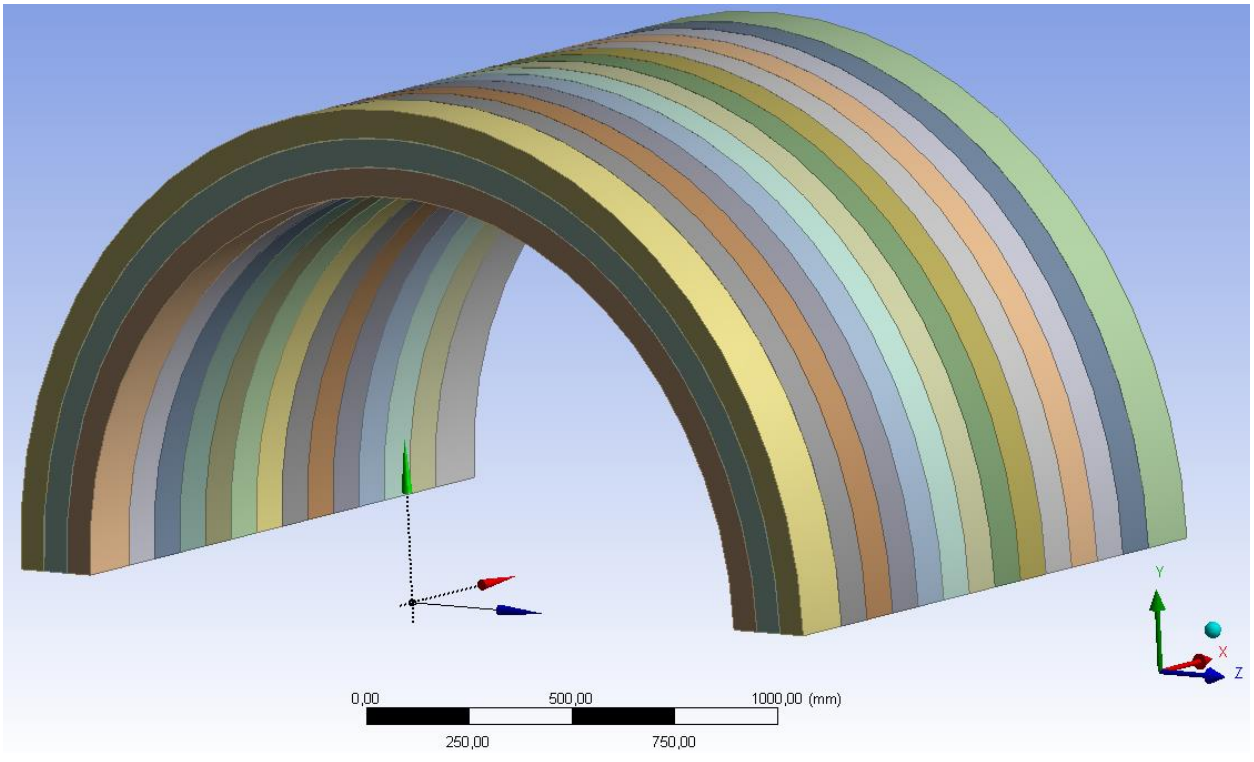

Figure 4.1.2-8 3D-model of the 3x14 part body used in the analysis.
Source: *Ansys® Workbench, Release 14.5*

4.1.2.2.2 Explicit Dynamics

In the Explicit Dynamics system, the process of modelling the concrete cover and the reinforcement bars was much simpler. As explained earlier, the Explicit Dynamics system has a built in function to convert line bodies to reinforcement bars. Therefore, the cover itself could easily be created using only one sketch over the full thickness of 215 mm which was extruded to a length of 1500 mm. Next, a new coordinate system was created at X coordinates 200 mm, which is the location of the first pair of reinforcement bars. These could be created simply by drawing a sketch of two half circles with the inner and outer reinforcement radiuses. The sketches could then be turned into Line Bodies by using the Lines From Sketches-function in the software. Further, a pattern was created to copy the pair of reinforcement bars 11 times with a distance of 100 mm, resulting in a total of 2x12 bars, with the same locations of the reinforcement bars as the Static Structural system (except for reinforcement radiuses, which differ by approximately 5 mm). Next, the line bodies needed a cross-section area to function, and therefore, a circular cross section with radius 6 mm representing the diameter Ø12 mm reinforcement bars was created and assigned to all the line bodies.

Next, the impact objects needed to be created. Four separate bodies and three different diameters needed to be created to account for the testing of the dropped objects requirements. They should impact the cover with energies of 50 kJ, 30 kJ, 20 kJ and 5 kJ. The bodies were given masses of 1400 kg, 850 kg, 550 kg and 140 kg, with impact diameters of 700 mm, 500 mm, 500 mm and 100 mm accordingly. The needed height of the bodies for the simulations is 463 mm, 551 mm, 357 mm and 2271 mm accordingly using the density of steel of 7850 kg/m^3, see full calculations in Appendix D Impact Calculations. A new coordinate system was created at (X,Y,Z) coordinates (750 mm, 1215 mm, 0 mm), directly in the centre of and on top of the cover. Sketches of the three diameters were drawn and extruded into the four objects with the needed object heights. In total, 29 bodies were created; 1 cover, 24 reinforcement bars and 4 dropped objects.

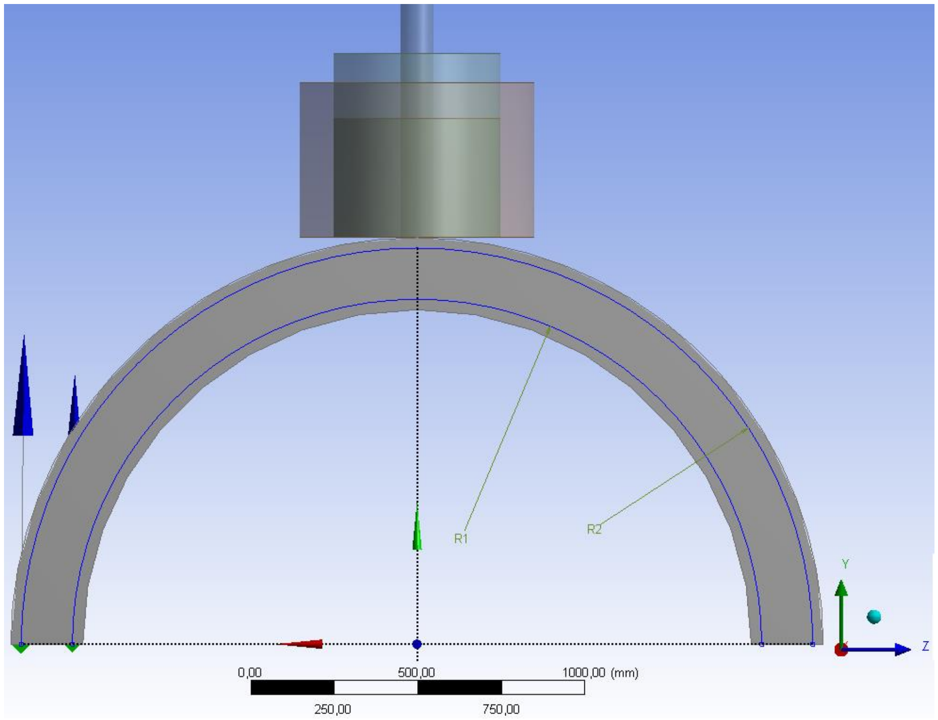

Figure 4.1.2-9 The YZ-view of the objects created for the Explicit Dynamics system
Source: ***Ansys® Workbench, Release 14.5***

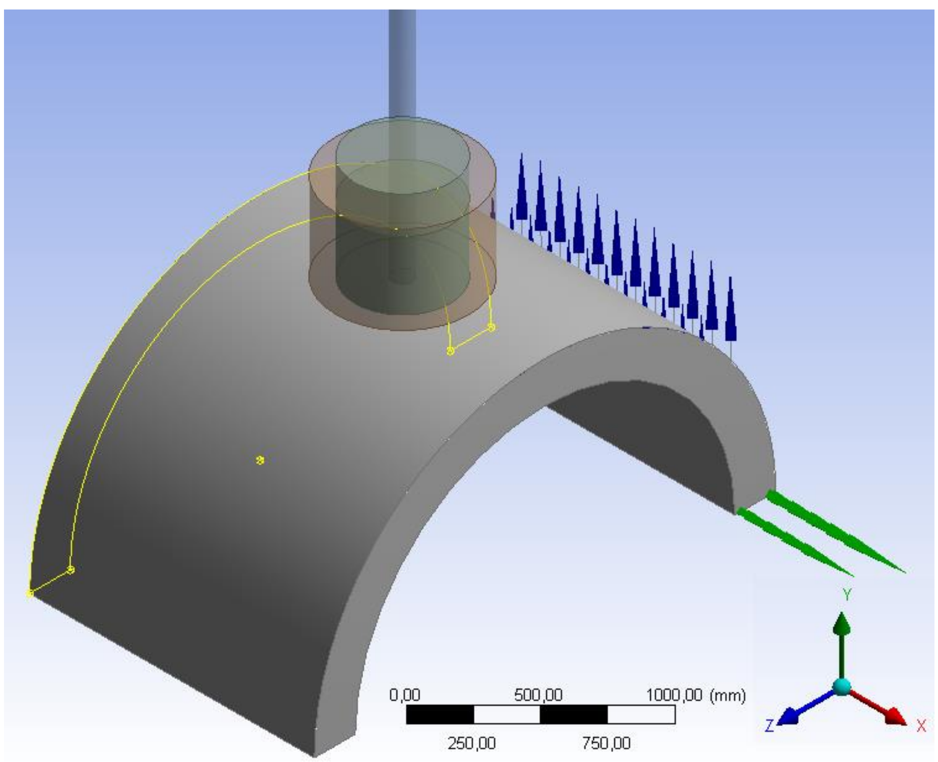

Figure 4.1.2-10 3D-view of the objects created for the Explicit Dynamics system
Source: ***Ansys® Workbench, Release 14.5***

4.1.2.3 Model

By opening the model generated by the *DesignModeler* software in the *Mechanical* software, which is also a part of the *Ansys® Workbench, Release 14.5* software package, the details about loads, boundary conditions and other details and inputs to the model can be applied.

The Subsea 7 Engineering standard *Subsea Protection Structure Design Guideline* states that 'for the software analysis of GRP covers, the boundary conditions to be applied on the cover are the following: at one end of the mud mad the cover shall be constrained in all degrees of freedom, and on the other end it shall be constrained in the vertical direction. Rock dump loads can be applied as a hydrostatic pressure by using the submerged weight of the rock dump on the model' (Subsea 7, 2015).

On the GRP covers, the mud mat is a horizontal plate on the bottom that increases the surface area of the cover when placed upon the seabed. This makes geotechnical assessment of the seabed easier, since the surface area of the cover is increased. In addition, the mud mats are used to hold the cover in place after rock-dumping is performed on the sides of the cover. One of the premises for this thesis is however to investigate the possibility of use of concrete protection covers where rock-dumping on GRP covers is not possible.

When a protection cover is placed on the seabed it is not bolted or otherwise completely fastened to the ground, as the quote above might be misunderstood as. This means that the part about constrained in all degrees of freedom is a simplified truth. The cover shall not be fixed to the ground, as it will be able to rotate - however limited due to the rock-dump. In order to still constrain movements, but not limit rotation, a pinned support is chosen for the outer bottom line of the cover. The other side of the cover also needs to be able to rotate, and the inner line in the bottom corner of the cover will be given a roll support, limiting movement in vertical direction, but still allowing rotation. In practice, this is done by applying a displacement constriction on the outer corner line limiting all movement, and a displacement constriction of movement in the X- and Y-direction on the inner corner line on the opposite side of the cover. This is done slightly different for the dropped object analyses, as will be explained later.

Due to the aforementioned premise of the thesis, the extra hydrostatic pressure caused by rock-dumping will not be considered for the concrete protection cover. This might, however, create some stability issues in the analyses, because the rock-dump pressure restricts any movement of the cover due to e.g. trawl loads or from wave forces and currents.

The *Subsea Protection Structure Design Guideline* also states that 'loads from trawl board (the otter board) overpull, is applied on a small area, while trawl net friction can be applied as a line load over several meters' (Subsea 7, 2015). The loads from trawl board overpull will be applied in a 300 mm x 300 mm area on the side of the cover that is roll supported, and it will be tested on a set of various locations to determine the worst load case. The trawl net friction load will be ignored in this thesis, as it requires extensive geotechnical calculations that fall outside of the scope of the thesis.

4.1.2.3.1 Static Structural

From here on and forward, the analysis settings differ quite a lot between the two systems. This first part will cover only the Static Structural analysis settings and the Explicit Dynamics settings will follow after.

4.1.2.3.1.1 Geometry

The grid of 3x14 bodies from the Static Structural system is combined into one single part, thus eliminating the need to specifically define the connections between the bodies; the *Mechanical* software of the *Ansys® Workbench, Release 14.5* software package assume automatically that the parts stick together.

4.1.2.3.1.2 Mesh

The mesh of the cover is given an element size of 100,0 mm, which creates one element in the X-direction per separate body part of the cover, except for the three outer bodies on both ends, which are split into two separate elements in the X-direction. This makes the placement of the reinforcement elements simple. The Relevance setting is kept at 0, and the Relevance Center is set to Coarse. These are the main settings to control the mesh and element sizes, see Figure 4.1.2-11 for the resulting mesh.

Activation of the option to drop element midside nodes makes sure that the elements stay Solid185 with eight nodes per element, as opposed to the higher order element Solid186 with 20 nodes. As can be seen in Figure 4.1.2-12 below, the quality of the mesh elements are very high, with a minimum of 0,92 and a maximum of 0,97, with an average of 0,94. This number is a composite quality metric that ranges between 0 and 1. It is based on the ratio of the volume to the edge length for the elements. The value 1 indicates a perfect cube, while the value 0 indicates that the element has zero or negative volume (ANSYS, Inc.).

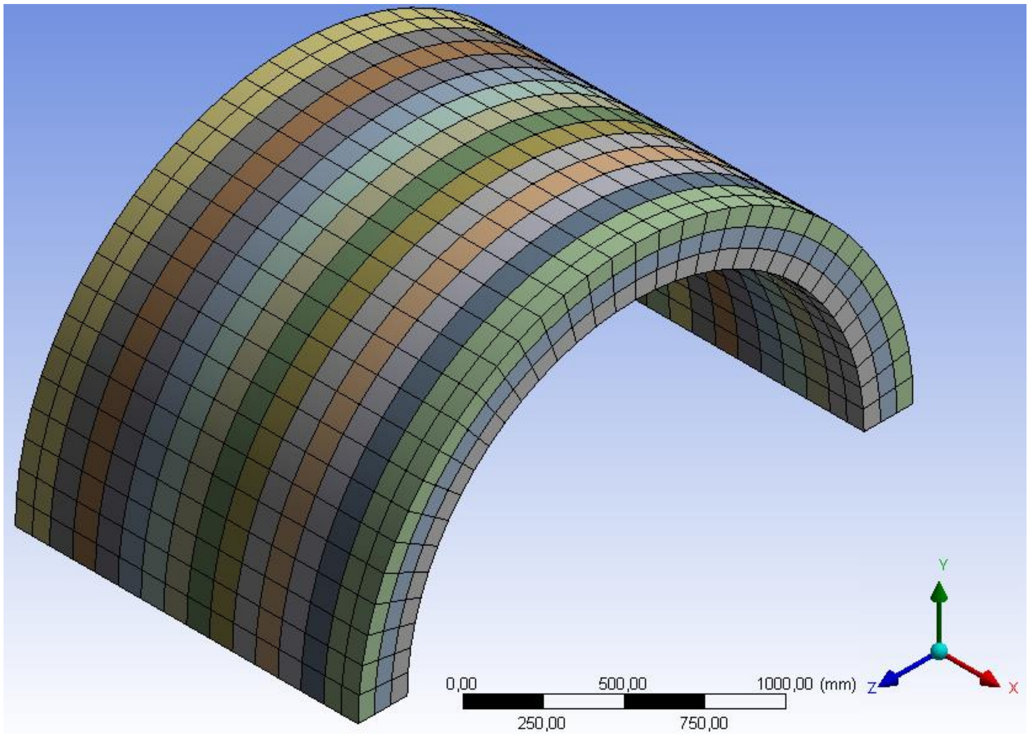

Figure 4.1.2-11 The element mesh of the cover in the Static Structural system.
Source: ***Ansys® Workbench, Release 14.5***

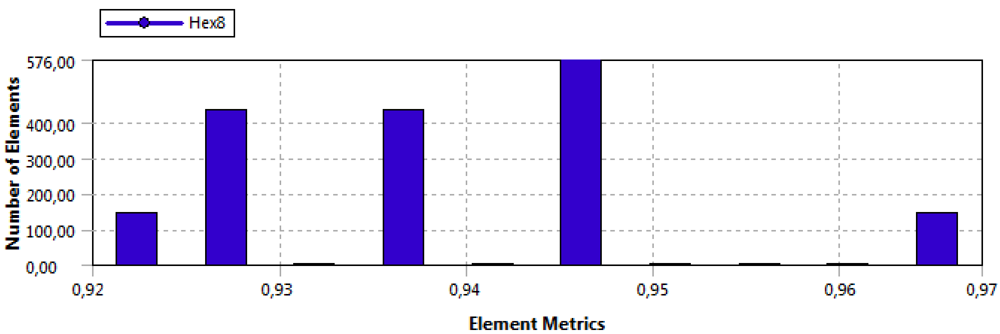

Figure 4.1.2-12 The element metrics of the mesh in Figure 4.1.2-11.
Source: ***Ansys® Workbench, Release 14.5***

4.1.2.3.1.3 Named Selections

The next step was to create the various named selections of bodies or nodes needed in the analysis. In order to test a range of attack points of the trawl board overpull load, a set of twelve nodal selections were made. These locations were split into three separate locations on the X-axis, Outer, Left and Mid. In each of these locations four different heights in the Y-direction was made, resulting in twelve force attack points.

A grid of 3x3 nodes were selected in each location, which means that the horizontal 300 kN design load will be applied evenly in an approximately 300 mm by 300 mm area. Applying the loads directly into the nodes is a slightly conservative approach, as opposed to creating an impact plate or area on which the load is applied, because the nodes affected will be slightly more strained than if the whole element was affected. This approach was chosen due to the carefully chosen mesh grid of elements were to be reinforced by Reinf264 elements. The other two methods would have messed up the mesh in that area, and made the chosen reinforcing method difficult.

The following three figures show all the force locations:

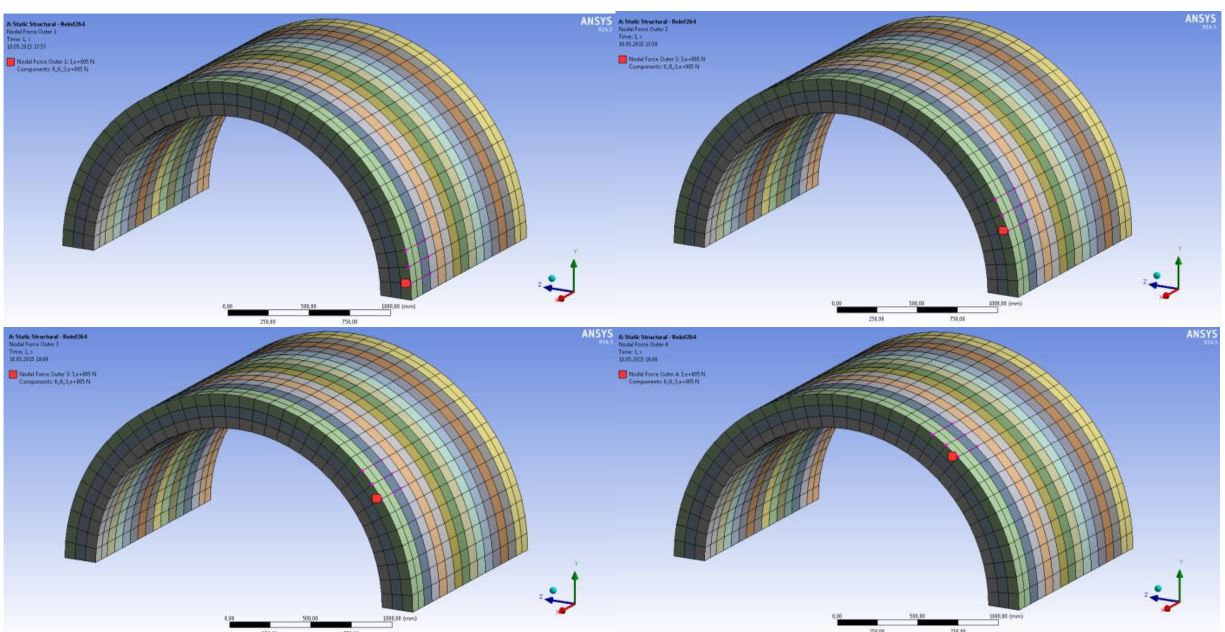

Figure 4.1.2-13 The four impact locations on the outer part of the cover.
Source: ***Ansys® Workbench, Release 14.***

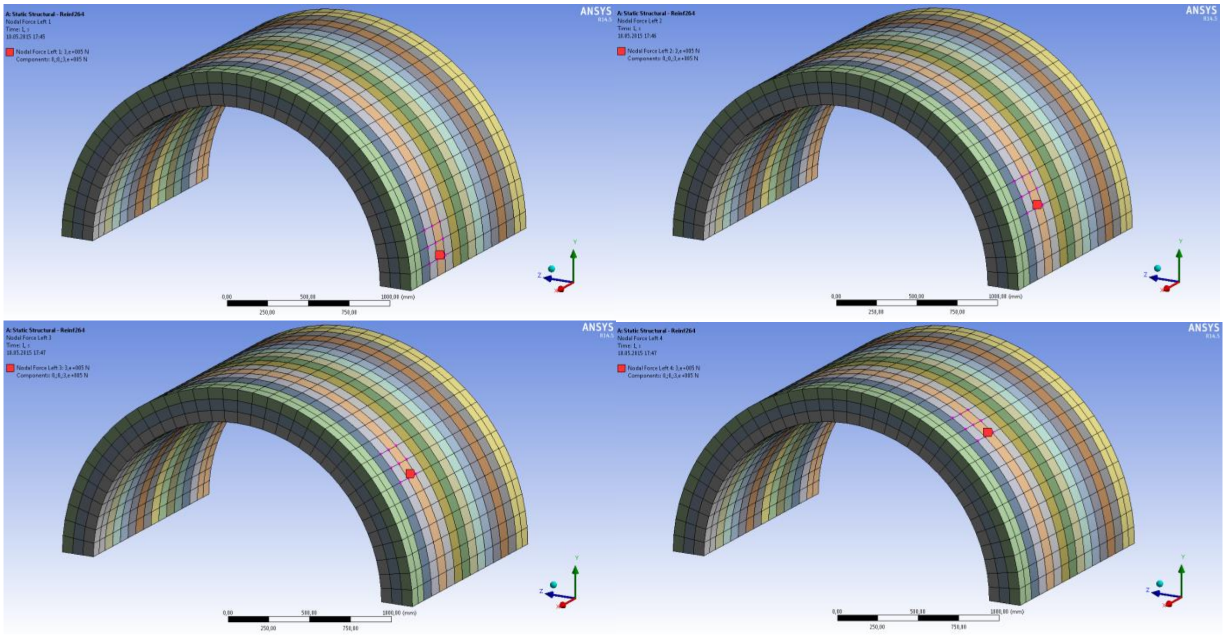

Figure 4.1.2-14 The four impact locations on the left part of the cover.
Source: *Ansys® Workbench, Release 14.5*

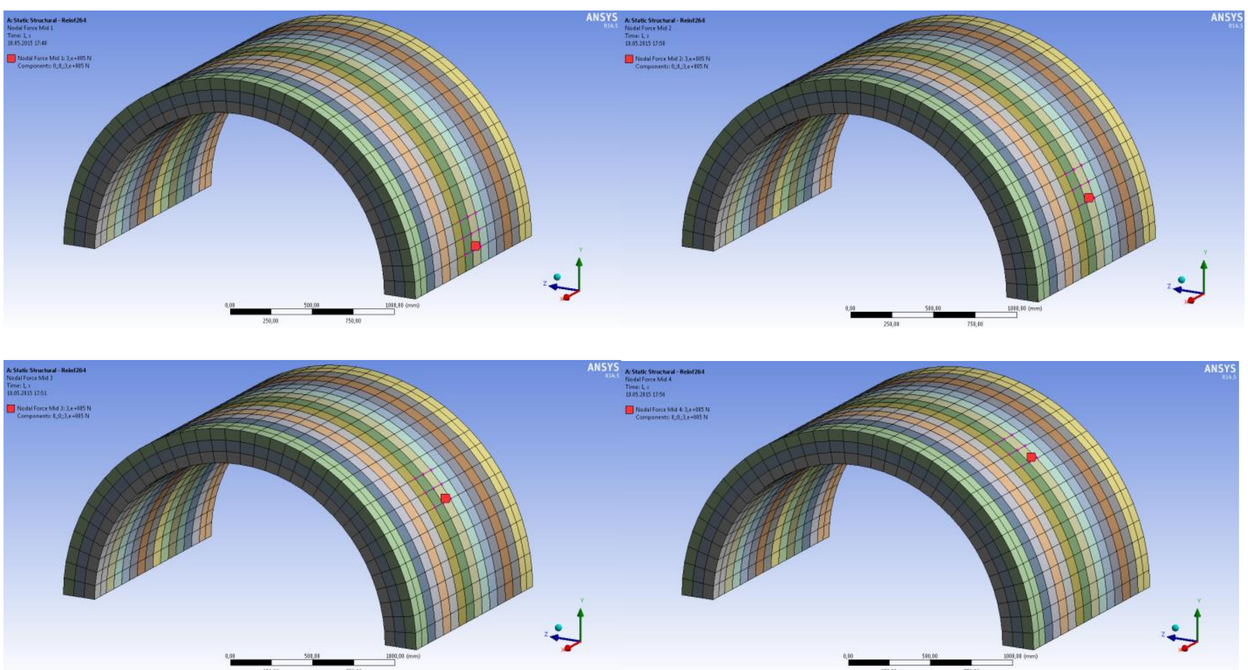

Figure 4.1.2-15 The four impact locations on the mid part of the cover.
Source: *Ansys® Workbench, Release 14.5*

The next selections that needed to be made were to choose which bodies and elements of the cover that the Reinf264 elements were to be generated in. Three separate selections were needed to get the best possible result in *Ansys® Workbench, Release 14.5*. A selection of 22 bodies was made in which Reinf264 elements were to be generated in the midpoints of the elements of the selected bodies, see Figure 4.1.2-16. Next, a selection of two separate bodies was necessary due to a different orientation of those elements, which generated reinforcement elements with wrong direction, see Figure 4.1.2-17. Lastly, a selection of lines on the lower edges of the cover needed to be made in order to correct the generation of Reinf264 elements of the wrong direction due to different orientation of the lower elements, see Figure 4.1.2-18.

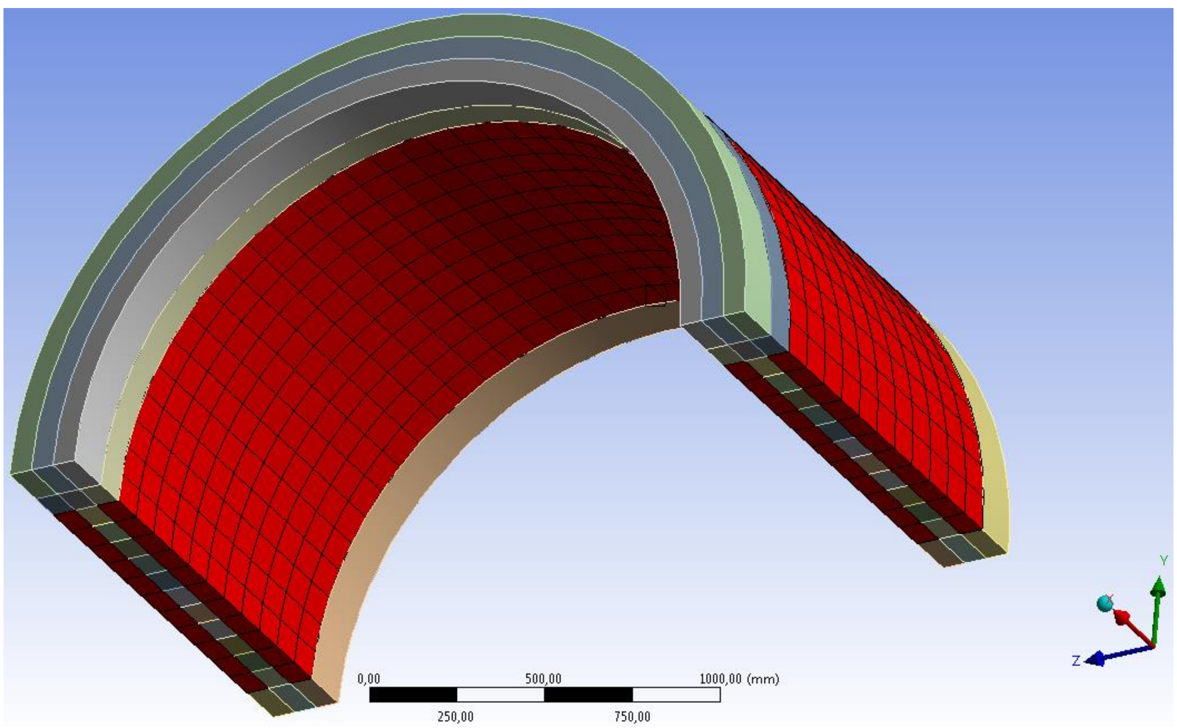

Figure 4.1.2-16 The body selections in which to generate reinforcing elements.
Source: *Ansys® Workbench, Release 14.5*

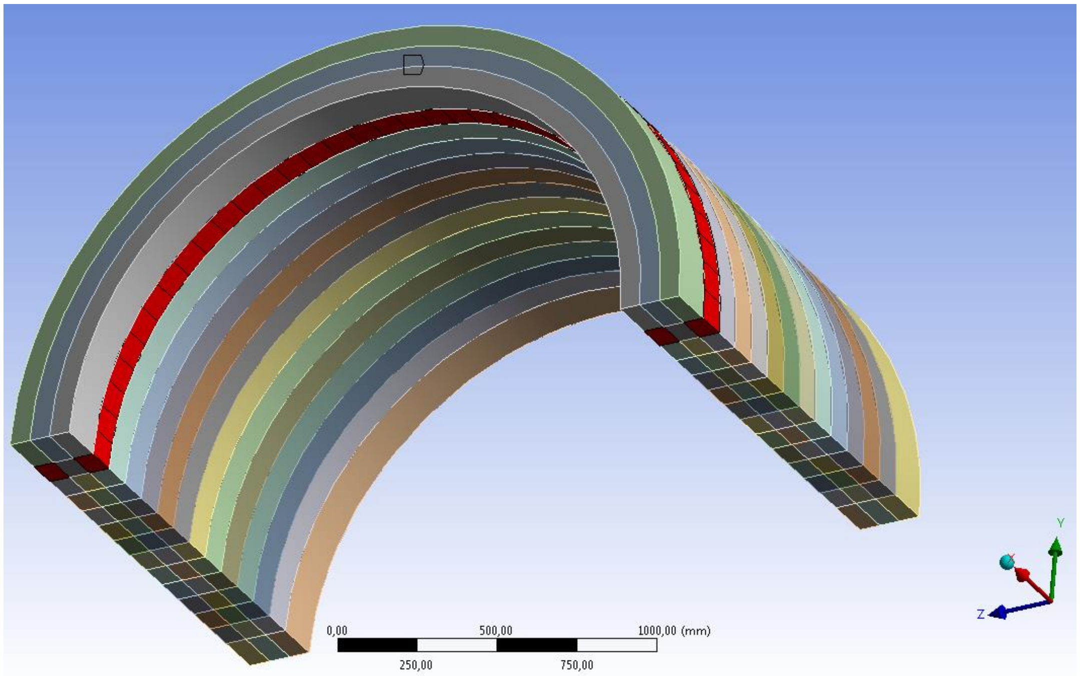

Figure 4.1.2-17 Two body selections in which to generate reinforcing elements.
Source: *Ansys® Workbench, Release 14.5*

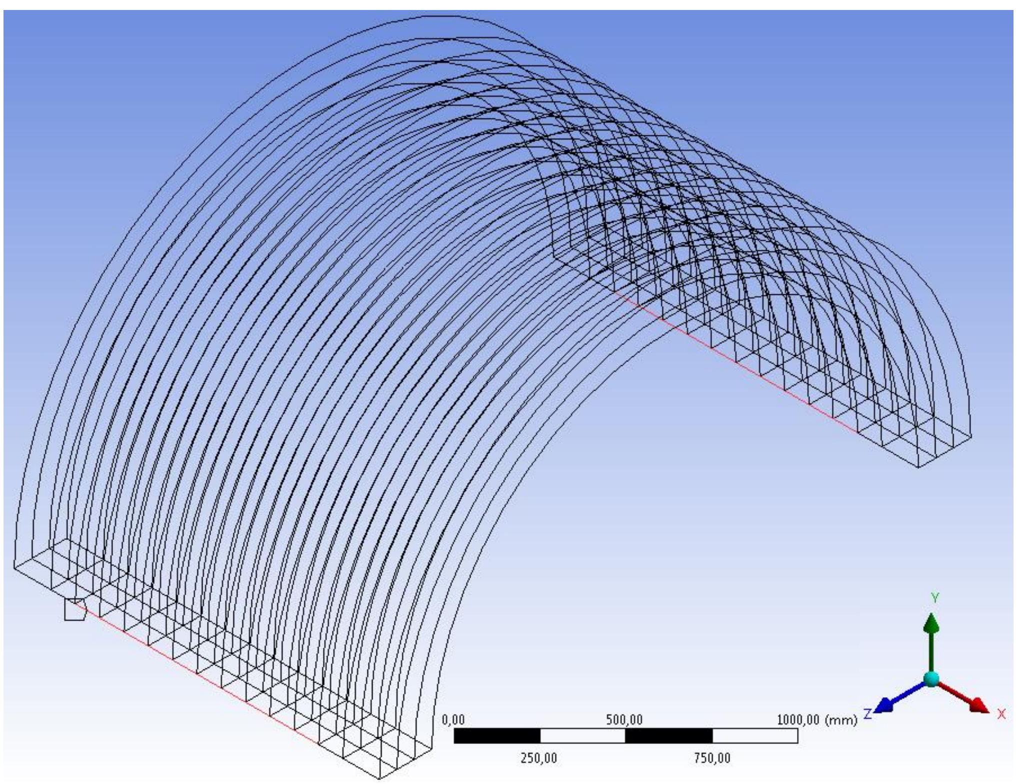

Figure 4.1.2-18 Line selections, where reinforcing elements were generated in the nearby elements.
Source: *Ansys® Workbench, Release 14.5*

This procedure is not perfect, however, as can be seen in the resulting locations and orientations of the Reinf264 elements. The bottom element of the left, outer corner and the right, inner corners have been assigned two reinforcement bars with different orientations, see Figure 4.1.2-19. In addition, two reinforcing elements are missing in the two front corners, see Figure 4.1.2-20. Many attempts to amend this problem were made, but none yielded a result better than the present one, and all of them made a mess of the reinforcing elements somewhere else in the model. A decision was made to keep the model as it is, despite its obvious flaws. These flaws are however rather minor, and thus deemed non-critical to the overall result from the model.

By using the pick element function in *Ansys® Workbench, Release 16*, the result would have been much more elegant, and the problem with picking certain elements and rotating the reinforcement element would have been avoided.

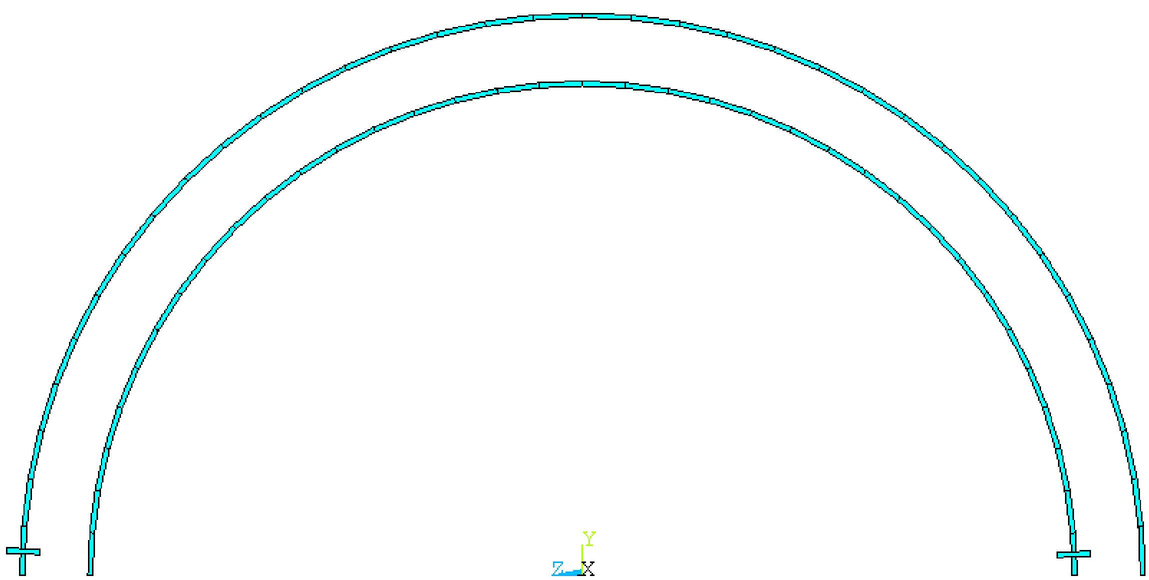

Figure 4.1.2-19 Front view (YZ-plane) of the reinforcing elements. Note the double cross-reinforcing of the nether elements. Source: *Ansys® Workbench, Release 14.5*

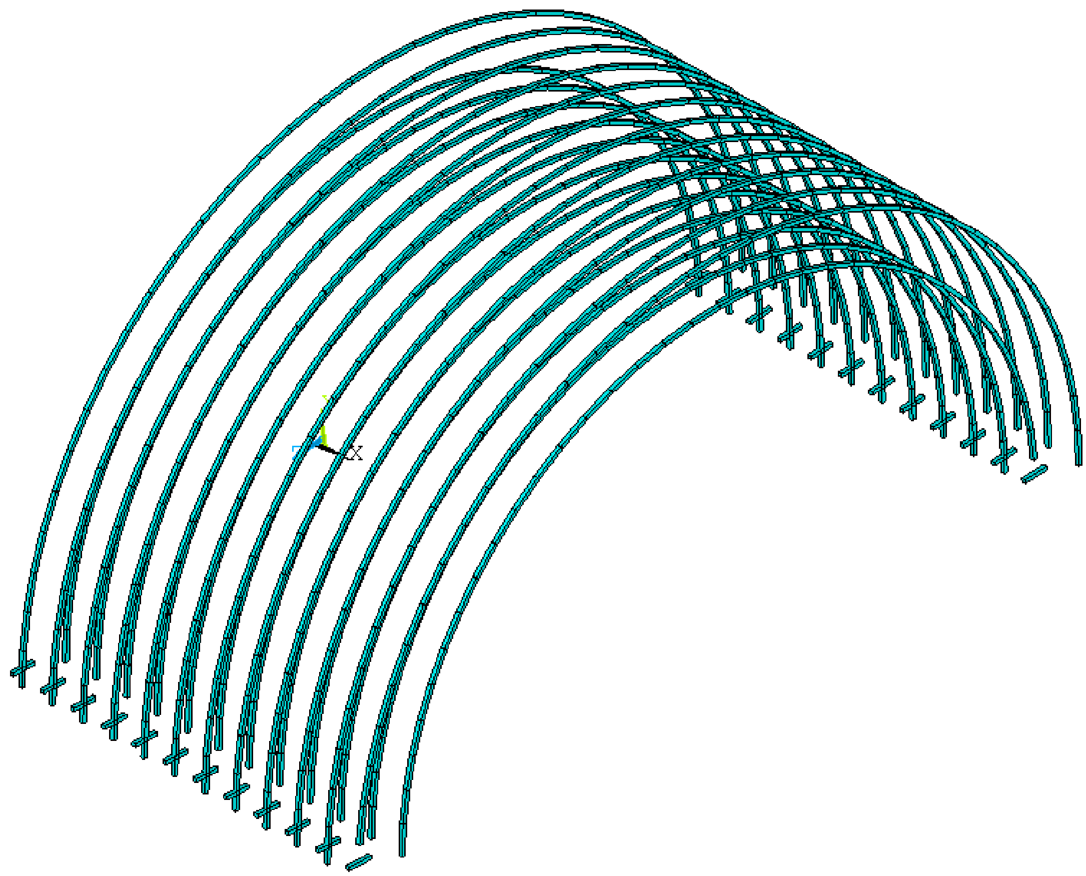

Figure 4.1.2-20 3D view of the reinforcing elements. Note the two missing elements in front, as well as the double cross-reinforcing of the nether elements. Source: *Ansys® Workbench, Release 14.5*

4.1.2.3.1.4 Static Structural (settings)

Under the Analysis Settings page of the Static Structural system, the only setting that was changed was to change Save MAPDL db to Yes in order to be able to open the solution in the Mechanical APDL software to view the Reinf264-elements.

Supports and boundary conditions were added according to the discussion in chapter 4.1.2.3 above4.1.2.3.1.2 above. As mentioned, this is done by applying a displacement constriction on the outer corner line limiting all movement, but not rotations; and a displacement constriction of movement, but not rotations, in the X- and Y-direction on the inner corner line on the opposite side, see Figure 4.1.2-21.

The limitation of movement in the X-direction on both supports was necessary to keep the model stable. This will however make any movements in the X-direction due to rotation small and negligible, and they will thus not be recorded in this thesis. In a real situation, several covers will be stacked next to one another like a snake, and will thus naturally limit movement in X-direction.

In order to include the effects of the weight of the cover, the inertial boundary condition of Standard Earth Gravity was added. It was given a Y-component of -9806,6 mm/s^2 by standard.

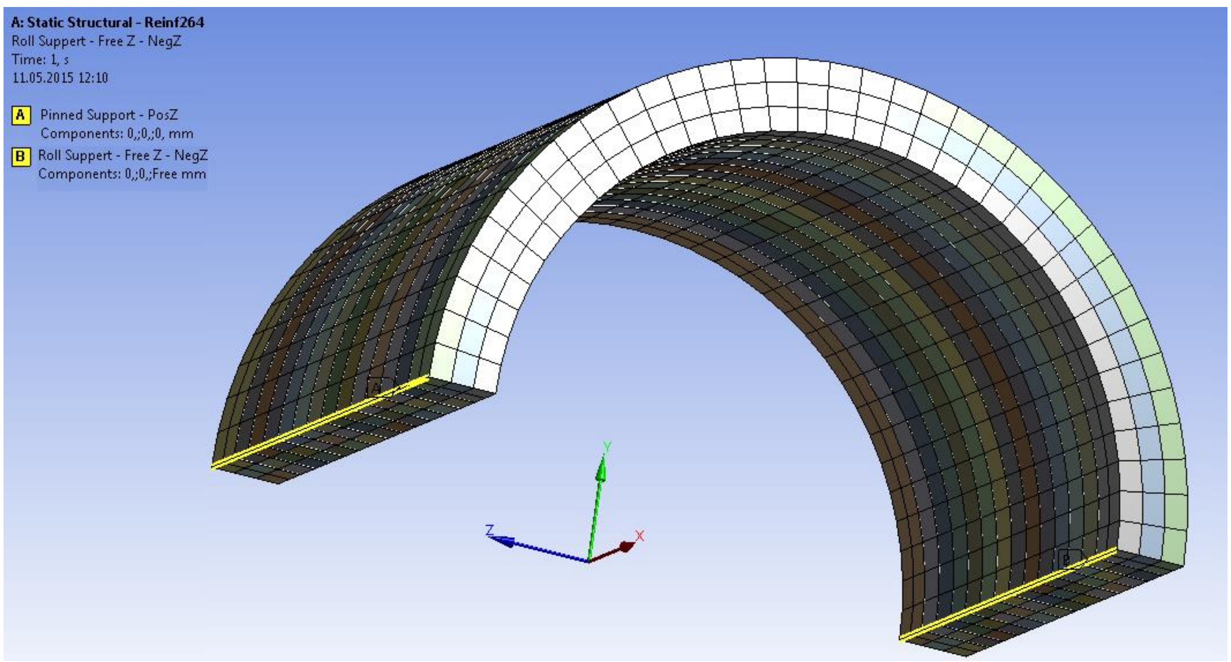

Figure 4.1.2-21 Support conditions for the Static Structural system.
Source: *Ansys® Workbench, Release 14.5*

Nodal Forces are applied to all the named nodal selections one at a time, as shown in Figure 4.1.2-22, resulting in twelve different impact areas that will be analysed. The horizontal design loads of 300 kN are applied in the positive Z-direction, on the opposite side of the pinned support, and effectively shared equally between the 9 nodes in the selection. In a real situation, the force may have components in both X and Y direction as well, but this effect will not be regarded in this thesis.

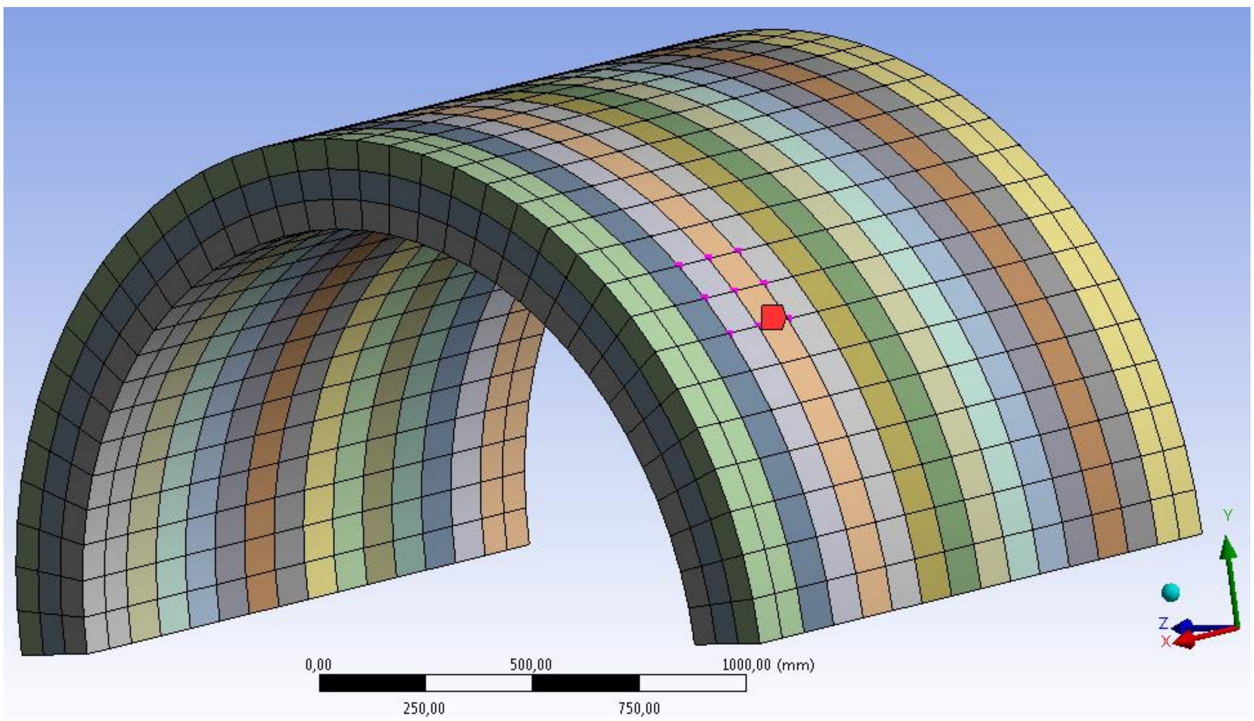

Figure 4.1.2-22 Application of nodal forces, represented by load case Left 3
Source: ***Ansys® Workbench, Release 14.5***

A set of APDL Commands needs to be inserted to activate the Reinf264 elements. The command snippet with explanations annotated by ! can be seen below:

```
! Commands inserted into this file will be executed just prior to the ANSYS SOLVE command.
! These commands may supersede command settings set by Workbench.

! Active UNIT system in Workbench when this object was created: Metric (mm, t, N, s, mV,
mA)
! NOTE:  Any data that requires units (such as mass) is assumed to be in the consistent
! solver unit system.
!                See Solving Units in the help system for more information.

! Notes about SECTYPE-command:
! Discrete or smeared reinforcing fibers

! Notes about SECDATA-command (for discrete fibers):
! Define material model, cross-section area and location of the reinforcing fiber

! Notes about SECCONTROL-command (for discrete fibers):
! Tension and compression (VAL1= 0), tension-only (VAL1= 1) or compression-only (VAL1= -1)

! Notes about EREINF-command:
! Generates reinforing elements directly from selected base elements

FINISH

! PREP7 starts the preprocessor

/PREP7

! Selects the maximum material and section numbers and adds +1,
! so that the Reinf264-elements are always the highest number.
! Clever solution for making sure that there are no collsions of assigned ID's.

*GET, Max_MATtype, MAT, 0, NUM, MAX
my_MATtype = Max_MATtype + 1

*GET, Max_SECtype, SECP, 0, NUM, MAX
my_SECtype = Max_SECtype + 1
my_SECtype2 = my_SECtype + 1
my_SECtype3 = my_SECtype + 1

! Material data for the Reinf264-elements:
! ex = Elastic module. prxy = Major Poisson's ratio

mp,   ex, my_MATtype, 210000
mp, prxy, my_MATtype, 0.3


!xxxxxxxxxxxxxxxxxxxxxxxxxxxxxxxxxxxxxxxxxxxxxxxxxxxxx
! Generation of Reinf264 elements:

! Sectype: Associate section type information with a section ID number.
! SECTYPE, SECID, Type, Subtype, Name, REFINEKEY
! Defines that the reinforcement bars shall be discrete reinforcement bars,
! as opposed to a smeared type of reinforcement.

sectype, my_SECtype, reinf, disc

! Secdata: Describes the geometry of a section.
! SECDATA, MAT ID, CROSS-SECTION AREA, PATTERN, V1
! Pattern EDGo: The orientation of the discrete reinforcing fiber is similar to one of
! the specified element edges. The fiber orientation can be further adjusted via offsets
! with respect to the specified element edge.
```

```
! The orientation of the reinforcing bar can be changed by changing number from 1 to 3.

secdata, my_MATtype, 113.1, edgo, 2

! Seccontrol: Supplements or overrides default section properties.
! 0 = Provide both Tension and Compression in the value field (VAL1) of SECDATA

seccontrol, 0

! Esel selects a subset of elements. Here of names from Solid185 to Solid186.

ESEL, S, ENAM,, 185, 186

! Cmsel selects a subset of components and assemblies.
! Here it selects the Named Selection called "Selection" consisting of 22 bodies.

CMSEL, S, Selection

! Secnum sets the element section attribute pointer.

secnum, my_SECtype

! Ereinf generates reinforcing elements from selected existing (base) elements.

EREINF

!xxxxxxxxxxxxxxxxxxxxxxxxxxxxxxxxxxxxxxxxxxxxxxxxxxxxxx

! Same as above, except change of selection and reinforcing element orientation.
! Now the selection points to the two bodies of different element orientation.

sectype, my_SECtype2, reinf, disc
secdata, my_MATtype, 113.1, edgo, 1
seccontrol, 0

ESEL, S, ENAM,, 185, 186
CMSEL, S, Selection2

secnum, my_SECtype2
EREINF

!xxxxxxxxxxxxxxxxxxxxxxxxxxxxxxxxxxxxxxxxxxxxxxxxxxxxxx

! Same as above, except change of selection and reinforcing element orientation.
! Now the selection points to the lines on the lower edges of the cover.

sectype, my_SECtype3, reinf, disc
secdata, my_MATtype, 113.1, edgo, 1
seccontrol, 0

ESEL, S, ENAM,, 185, 186
CMSEL, S, Selection3

! ESLN selects the elements that are attached to the nodes of the selected lines.

ESLN

secnum, my_SECtype3
EREINF

! alls selects everything

alls

! /solu starts the solution processor

/solu
```

Lastly, the following outputs will be generated in *Ansys® Workbench, Release 14.5*:

- Equivalent (von-Mises) Stress
  - Plots the stress distributions in the cover
- Total Deformation
  - Plots the total deformation of the cover in any direction
- Directional Deformation X
  - Plots the X-component of the deformation of the cover

    The deformation in the X-direction is negligible due to constriction in both supports.
- Directional Deformation Y
  - Plots the Y-component of the deformation of the cover
- Directional Deformation Z
  - Plots the Z-component of the deformation of the cover

The *Mechanical* software in *Ansys® Workbench, Release 14.5* is not able to output the stresses in the Reinf264-elements. Therefore, the solution needs to be transferred into the *Mechanical APDL* software, from where the reinforcement elements are viewable. This is done by adding a Mechanical APDL system in the Project Schematic and linking it to the Solution from the Static Structural system, as seen in Figure 4.1.2-23.

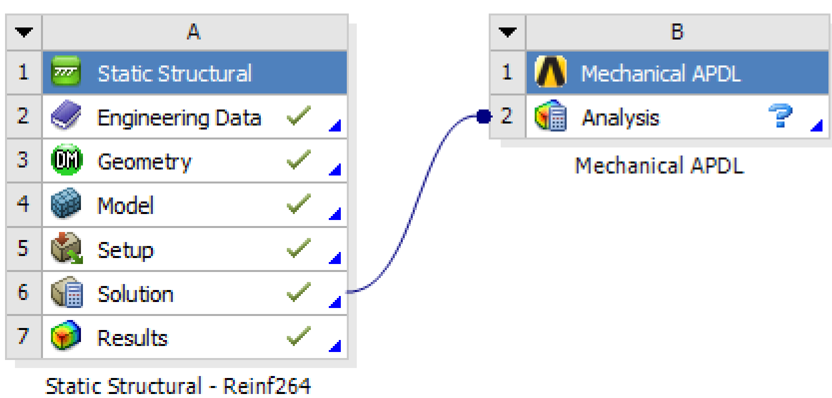

Figure 4.1.2-23 Project Schematic overview of the project, where the solution is linked to the *Mechanical APDL* software. Source: *Ansys® Workbench, Release 14.5*

By clicking Edit in Mechanical APDL and following by clicking RESUM_DB, the model and results will load into *Mechanical APDL*. From there, clicking Preprocessor < Sections < Reinforcing < Display Options < Reinf Only will plot the reinforcing elements alone.

Next, by clicking PlotCtrls < Style < Size and Shape and tick Display of Element < On, the reinforcing elements will show better and be able to display the colour coded stress output.

Further, by clicking PlotCtrls < Style < Colors < Reverse Video the background colour will change from black to white, making it easier to examine the results.

By clicking General Postproc < Read Results < First Set the software will load the results from *Ansys® Workbench, Release 14.5.*

Lastly, by clicking General Postproc < Plot Results < Contour Plot < Nodal or Element Solution, and then choosing to output the axial X-component of stress, the colour coded stress plot of the results from the analysis will appear.

4.1.2.3.2 Explicit Dynamics
In the Explicit Dynamics system, the process of modelling reinforcement bars is much simpler than in the Static Structural system. As explained earlier, a simple model of the concrete is created, and line bodies with a given cross-section area are placed in the locations of the reinforcement bars. The dropped objects have been modelled directly on top of the midpoint of the cover.

4.1.2.3.2.1 Geometry
The geometry consists of 1 body which is the cover, 24 reinforcing line bodies and 4 dropped object bodies. Only one dropped object body can be active at a time. The dropped object bodies are given rigid stiffness behaviour. This means that the bodies will not deform, and the software will not waste processing time on calculating their deformation.

4.1.2.3.2.2 Connections
The *Mechanical* software in *Ansys® Workbench, Release 14.5* automatically assumes connection between the cover and the dropped objects due to the connection at the top of the cover. These contact regions needs to be suppressed, as there is no pre-contact or connection between the two bodies.

Next, a new connection type needs to be added, specifically a Body Interaction, in addition to the already present Body Interaction. The first one will remain at Type: Frictionless, while the new Body Interaction shall be set to Type: Reinforcement. This will automatically convert all line bodies contained within any solid body in the model to discrete reinforcement bars.

4.1.2.3.2.3 Mesh
The size option in the mesh settings is left at default, and Relevance is left at 0 and Relevance Center at Medium. Element Midside Nodes are dropped in this mesh as well, so that the elements are Solid185 instead of the higher order Solid186 element. This results in a mesh that is similar to the one from the Static Structural system.

The quality of the mesh elements are very high in this model as well, with a typical minimum of 0,67 and maximum of 0,99, with an average of 0,92. Most of the elements of lower quality are located in the dropped object, and are thus of little importance, especially since the objects were rendered rigid, and little computation time was spent on analysing its deformation. The mesh needed to be regenerated between every change of dropped object body, but the element metrics were quite similar between the four load cases, and the figures below are representable of the other three meshes as well.

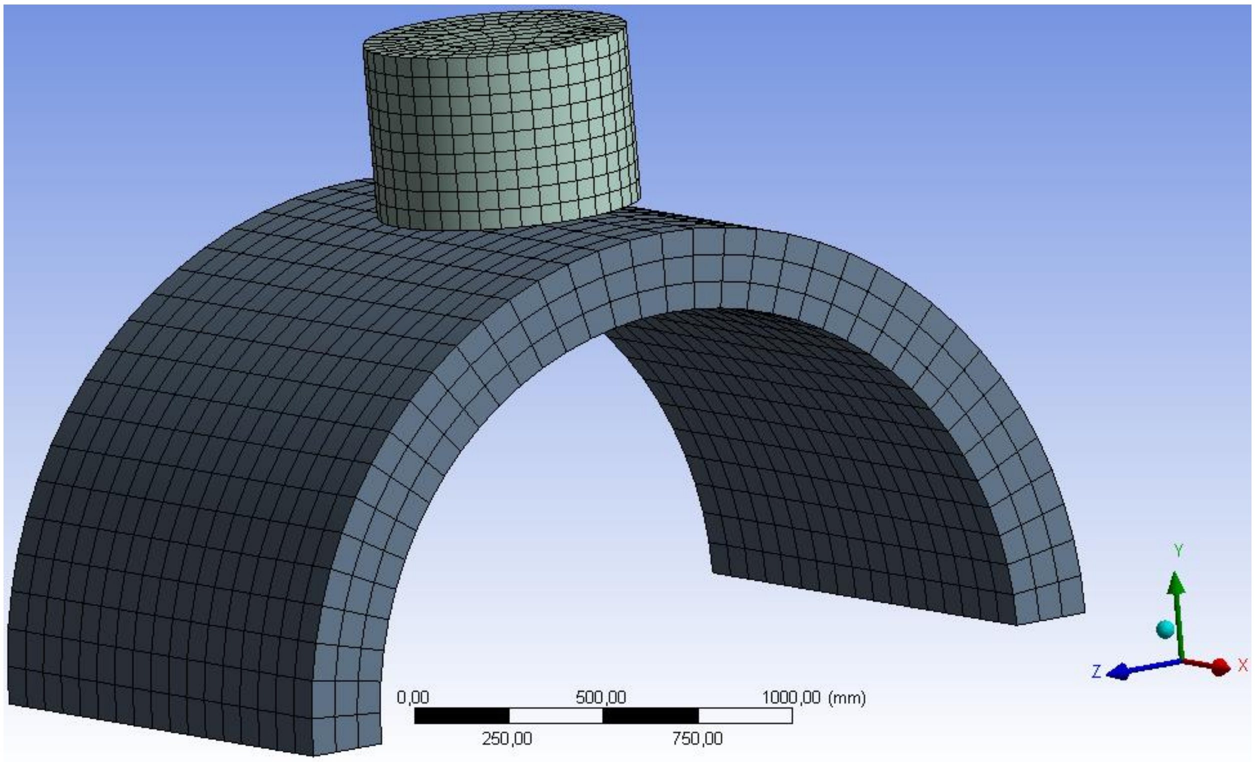

Figure 4.1.2-24 Mesh of the cover and the 50 kJ object. Source: *Ansys® Workbench, Release 14.5*

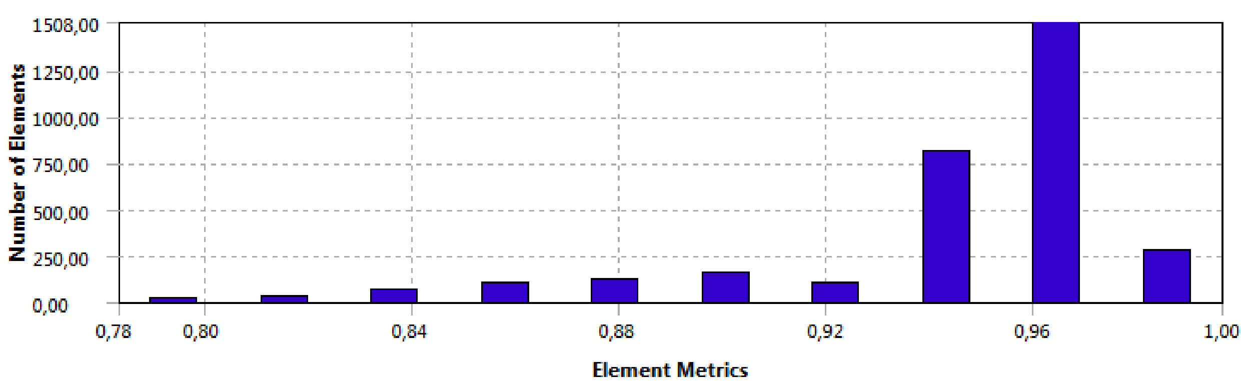

Figure 4.1.2-25 Typical element mesh metrics for the Explicit Dynamics analyses. Source: *Ansys® Workbench, Release 14.5*

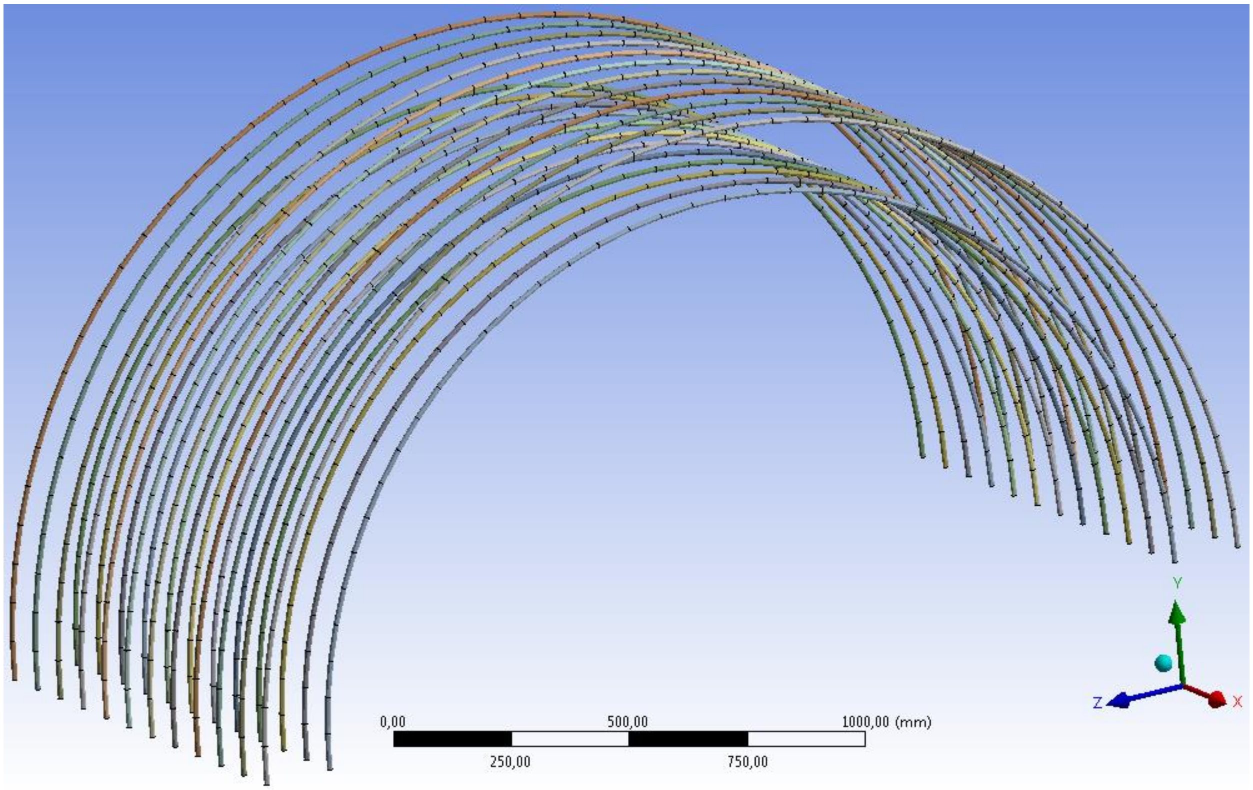

Figure 4.1.2-26 Mesh of the reinforcement bars. Source: *Ansys® Workbench, Release 14.5*

4.1.2.3.2.4 Explicit Dynamics (settings)

The solver of the Explicit Dynamics systems differs quite significantly from the one of the Static Structural system, and needs different input.

Under Initial Conditions, the Pre-Stress is left at None, while a new condition, Velocity, is added. The geometry selected for this initial condition is the active dropped object. It was given a Y-component velocity of roughly -8450 mm/s (depending on the weight of the object); see Table 4.1.2-1, which is slightly over the terminal velocity of a drill pipe falling through water (DROPS online, 2010).

$$Kinetic\ energy = E_K = \frac{1}{2}mv^2$$

$$Necessary\ velocity = v = \sqrt{\frac{2 * E_I}{m}}$$

Table 4.1.2-1 Masses and velocities necessary to gain certain impact energies.

Impact energy	Mass	Velocity
5 kJ	140 kg	8,452 m/s
20 kJ	550 kg	8,528 m/s
30 kJ	850 kg	8,402 m/s
50 kJ	1400 kg	8,452 m/s

Next, the Analysis Settings needed to be changed to fit this type of impact. In *Ansys® Workbench, Release 14.5*, an impact of velocity less than 100 m/s is characterized as low velocity. The recommended settings for such a low velocity and low deformation simulations are automatically set by choosing the pre-set type of analysis. A couple of the most important settings will be mentioned here.

The needed End Time, or total simulation time can be adjusted to the point where all of the kinetic energy has been absorbed to internal energy in the cover. From testing, it was determined that a simulation time of 0,06 seconds was just enough time to convert the energy without compromising accuracy or wasting computational time. In reality, the movements of the impact might last a couple of seconds before everything is at rest, but it is not necessary to simulate several seconds to get the maximum stresses and deformations, as these happen fairly momentarily after the impact. Every second after this is more or less a waste of time and computational resources. The model has been designed so that the impact will happen instantaneously after the start of the simulation.

One of the most important settings that needed to be specified, was how the software should dampen the solution, and specifically how it should deal with damping of hourglass instabilities. Hourglassing is a state of strain of the mesh elements which results from the excitation of zero-energy degrees of freedom, and usually manifests as hourglass-like shaped elements, see Figure 4.1.2-27. This typically happens in hexahedral elements when the simulation is run with the time saving setting of using reduced one-point integration in the middle of the element. This does not properly describe the deformation of the elements, and instabilities in the model are introduced (ANSYS, Inc.). Therefore, using the hourglass dampening formulas by Flanagan Belytschko is recommended when large rotations of hexahedral elements are expected. The result from this setting can be seen in the results under the Energy Summary from each run. As a rule of thumb, the documentation of *Ansys® Workbench, Release 14.5* recommends that the added hourglass energy do not surpass 10 % of the kinetic energy (ANSYS, Inc.).

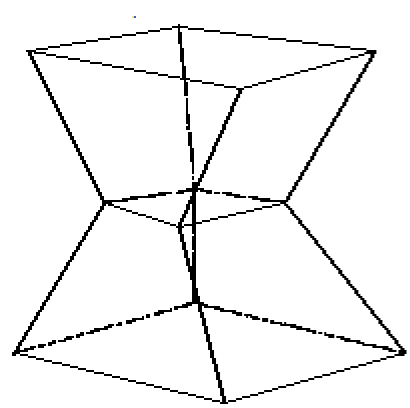

Figure 4.1.2-27 Hourglass shaped elements. Source: (ANSYS, Inc.)

In order to ensure that the object behaves normally after impact, the inertial boundary condition of Standard Earth Gravity was added to the model. It was given a Y-component of -9806,6 mm/s^2.

The supports are slightly different to that of the Static Structural system. Since the cover does not experience any load in the Z-direction, only in the Y-direction, it was decided to keep both sides free to move in the Z-direction. This ensures that the cover deforms symmetrically, but is dependent on the material strength of the cover to be strong enough to withstand the impact without the model becoming unstable. This is one of the typical reasons for the need of stabilizing hourglass energy in the system. Next, both sides are constrained in the Y-direction, meaning that they cannot be pushed down, nor be pushed up because of the impact. The right support is also constrained in the X-direction, see Figure 4.1.2-28.

Another option, which would have been more realistic, would have been to model a floor on which the cover is placed on top of. Next, the friction coefficient from contact between concrete and the seabed conditions could have been added to dampen movement in Z-direction. With the supports as described above, oscillatory movement of the cover occurred when the end time of the analysis was set sufficiently high. Such movement is not necessarily realistic, as it would be dampened by the above mentioned friction between cover and seabed.

In addition, the model is not able to realistically show how the cover will be pushed into the ground during impact. The seabed upon which it will be placed will probably have a slight dampening effect on the deformations of the cover, as well as allowing for the cover being pushed down into the ground, which is not possible in this model.

The dampening effects from the water around and inside the cover have not been included. The model is however deemed sufficiently realistic for the purposes of this thesis, as physical drop tests on the covers will be performed to test the strength of the covers. The results of the analyses will be used in comparison to the results in order to examine the similarities and differences between the model and the real world situation.

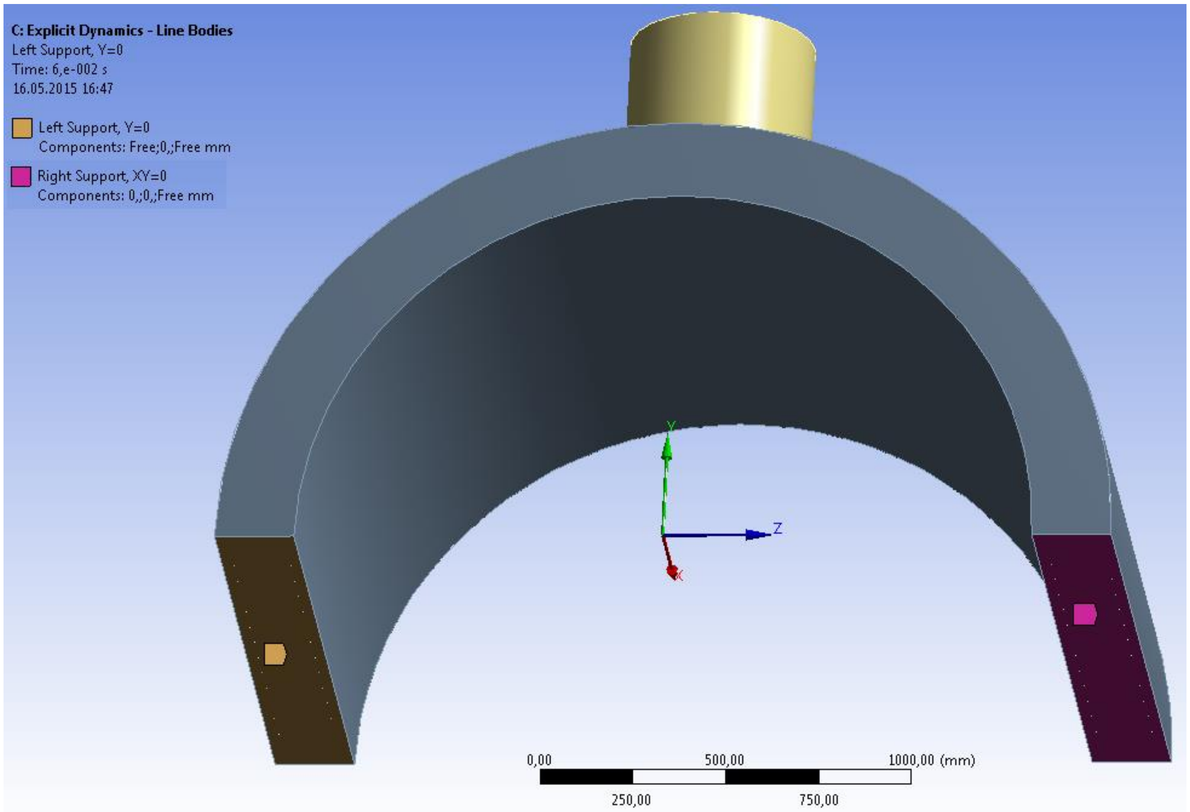

Figure 4.1.2-28 Support conditions for the Explicit Dynamics system.
Source: ***Ansys® Workbench, Release 14.5***

Lastly, the following outputs will be generated in *Ansys® Workbench, Release 14.5*:

- Energy Summary
  - Shows the absorption of kinetic energy into the cover as internal energy, and the hourglass energy added to keep the model stable.
- Total Cover Deformation
  - Plots the total deformation of the cover in all directions
- Directional Cover Deformation X
  - Plots the X-component of the deformation of the cover
- Directional Cover Deformation Y
  - Plots the Y-component of the deformation of the cover
- Directional Cover Deformation Z
  - Plots the Z-component of the deformation of the cover

- Equivalent (von-Mises) Stress
    - Plots the stress distributions in the cover
- Reinforcement Stress (User Defined Result: BEAM_MISES_STR)
    - Plots the stress distribution in the reinforcing line bodies
- Damage (User Defined Result: DAMAGEALL)
    - This is a plot of the Cumulative Damage Model implemented in *Ansys® Workbench, Release 14.5*. It can be 'used to describe the macroscopic inelastic behaviour of material such as ceramics and concrete where the strength of the material can be significantly degraded by crushing' (ANSYS, Inc.). The damage model describes the progressive crushing of a material by reduces the material's strength. The model computes a damage factor which is related to the amount of strain that the material is subjected to. The value 0 means that the material is intact, while 1 means fully fractured. The damage factor is used to reduce the elastic module and the yield strength of the material as the calculation proceeds. Fully damaged material has some residual strength in compression, but none in tension (ANSYS, Inc.).

4.2 Stability Calculations

A stability issue was discovered in the model in the Static Structural system; specifically because of the tipping moment from the trawl board overpull force on the cover. The 300 kN design load represents approximately a massive 30 tons of impact on the cover with a weight of 2560 kg. As can be seen from the stress results from *Ansys® Workbench, Release 14.5*, this results in unrealistic forced stresses in the cover above the roll support. This can also be seen in the reaction forces in the roll support, where there is a large downwards force that holds the cover down from tipping due to the trawl force.

In reality, the cover will be longer than 1,5 m, and will thus have a higher mass to counteract the tipping moment from the trawl force. This would eliminate both the forced stresses, and give a realistic upwards reaction force. Due to the command method used to generate reinforcement bars, and the elaborate system of mesh elements and selections that was created to make it work, simply extending the length of the cover was not an option, as this would have messed up the reinforcement end the elements, and much would have to be redone. In *Ansys® Workbench, Release 16*, however, this process would not have been resulted in that much extra work.

Therefore, a system of static equilibrium was set up in order to get a picture of how long the cover would need to be to counteract the tipping moment from the trawl force, see Figure 4.2-29. In addition, the effects of the trawl board deflectors were included, see Figure 4.2-30.

The boundary conditions were kept equal to those of the 3D model, with a pinned support to the left, and a roll support on the right.

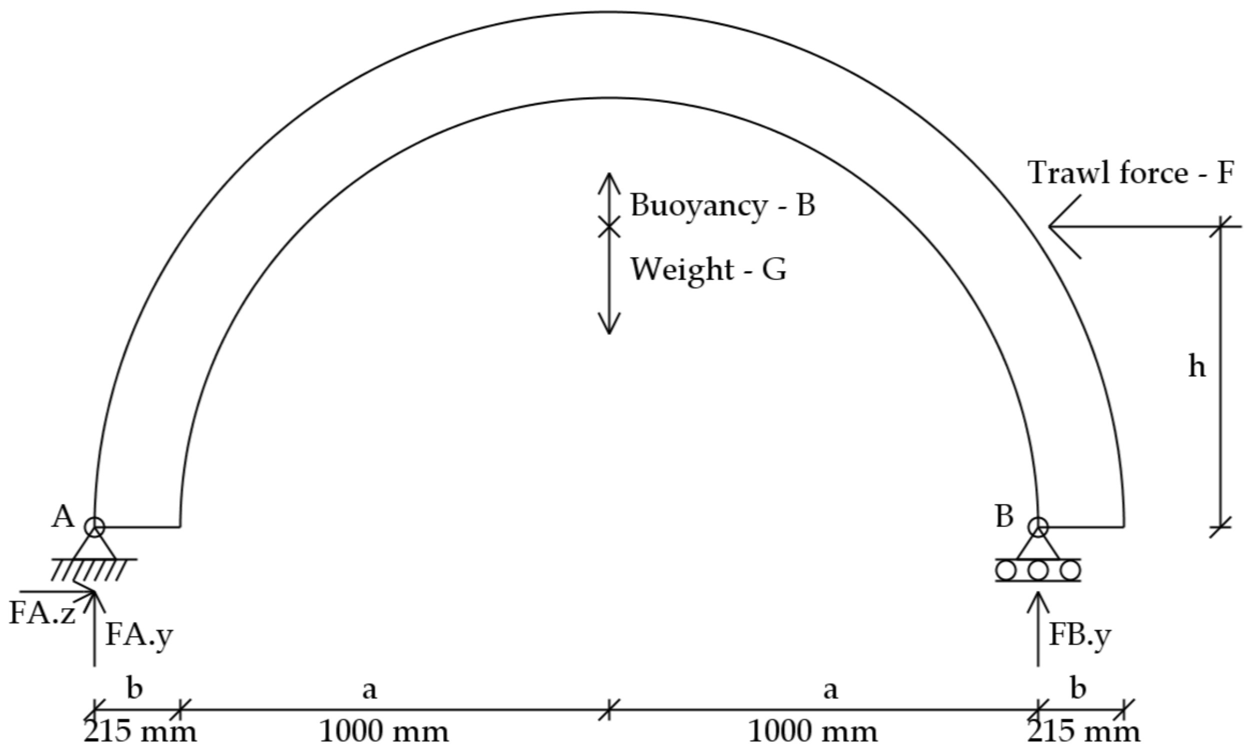

Figure 4.2-29 The system of static equilibrium set up to investigate the stability issue.

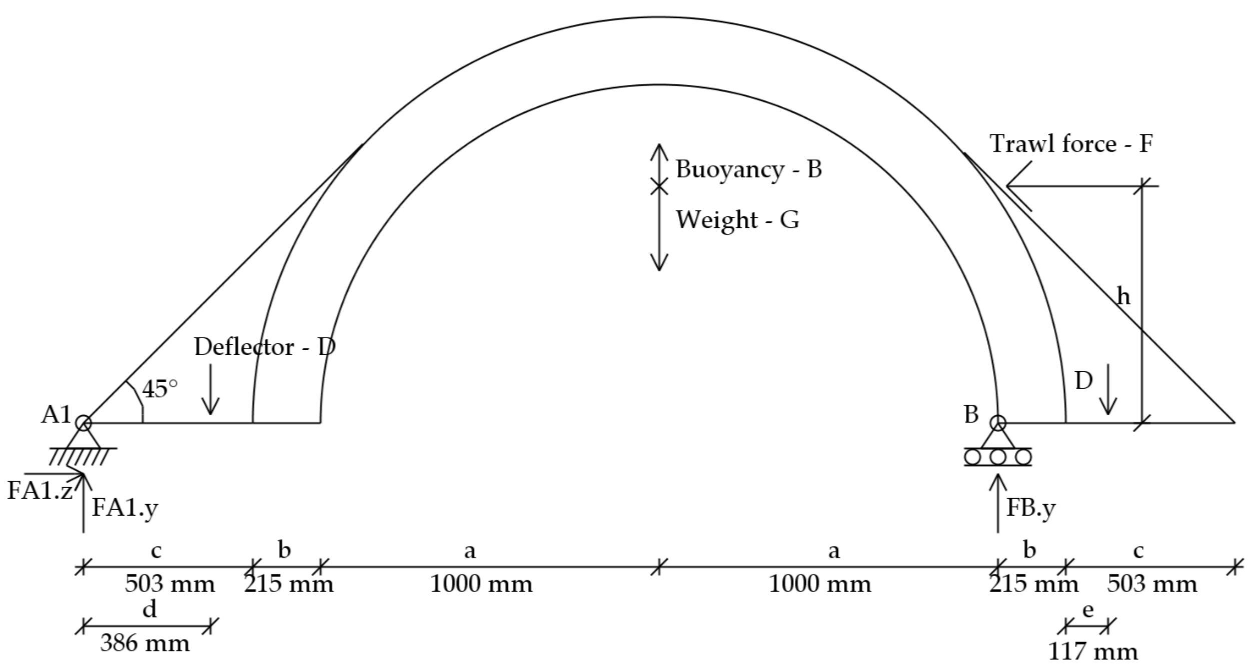

Figure 4.2-30 The system of static equilibrium including the trawl deflectors set up to investigate the stability issue.

4.3 2D model in *STAAD.Pro V8i*

A simple 2D beam model of the cover was made in *STAAD.Pro V8i* to output the shear forces, moment, axial forces and diagrams of the cover when subjected to the design trawl force of 300 kN. This was necessary due to the fact that *Ansys® Workbench, Release 14.5* does not output these values separately, but converts them to a stress total.

The simple beam model was made with pinned support on the left and roll support on the right. The radius of the center line of the cover is the mid line between inner radius (1000 mm) and outer radius (1225 mm); 1107,5 mm to be exact. This is the radius chosen for this model, and the nodal coordinates was calculated using the following formulas, where x_0 and y_0 is 0 mm, r=1107,5 mm and the α increases with 5 degrees every step from 0° to 180°, see Figure 4.3-31.

$$x = x_0 + r * \cos(\alpha) \quad and \quad y = y_0 + r * \sin(\alpha)$$

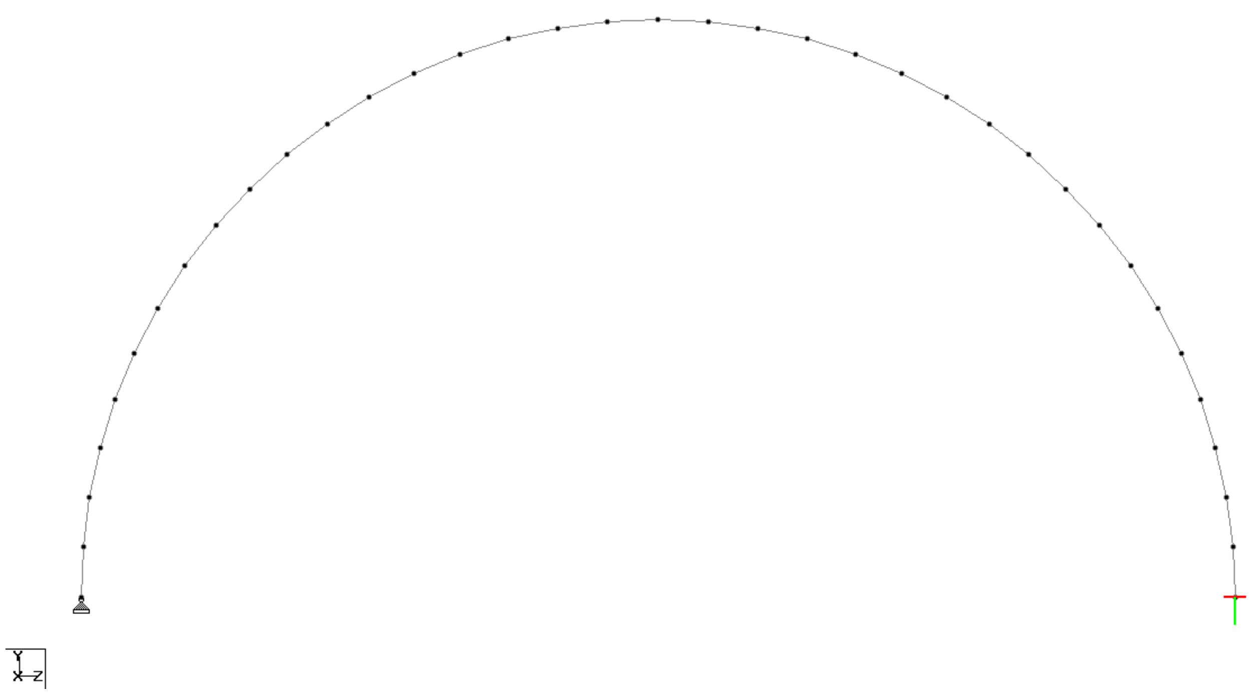

Figure 4.3-31 The beam model used in the analysis. Source: *STAAD.Pro V8i*

In order to get the model to work, the beams have been assigned a prismatic type of section, with a width and height of 215 mm. This does not matter however, as *STAAD.Pro V8i* will not run a code check against e.g. the concrete standard *Eurocode 2*.

The mass of the cover from the *Ansys® Workbench, Release 14.5* model has been added as a uniform load on each beam. The mass is 2560 kg, which converts to a total force of 25,105 kN. The circumference of the half circle with a radius of 1107,5 mm is 3,479 m. By distributing the total force evenly on the beams, a uniform load of 7,215 kN/m was added to each beam in the model.

$$\frac{25{,}105\ kN}{3{,}479\ m} = 7{,}216\ \frac{kN}{m}$$

Next, the design trawl design load of 300 kN was added at several locations to analyse where on the cover the force will generate the highest shear and axial forces, and the highest moments. There were 19 load cases, or load impact locations, in the analysis. 18 of them, starting from the bottom node and moving up node by node, are represented by a green force arrow (and thus showing its impact location) plus the blue uniform load from the weight of the cover, see Figure 4.3-32. The last load case is the blue uniform load alone as a control, and the sum of reaction forces in Figure 4.3-33 shows that the mass of the cover is added correctly.

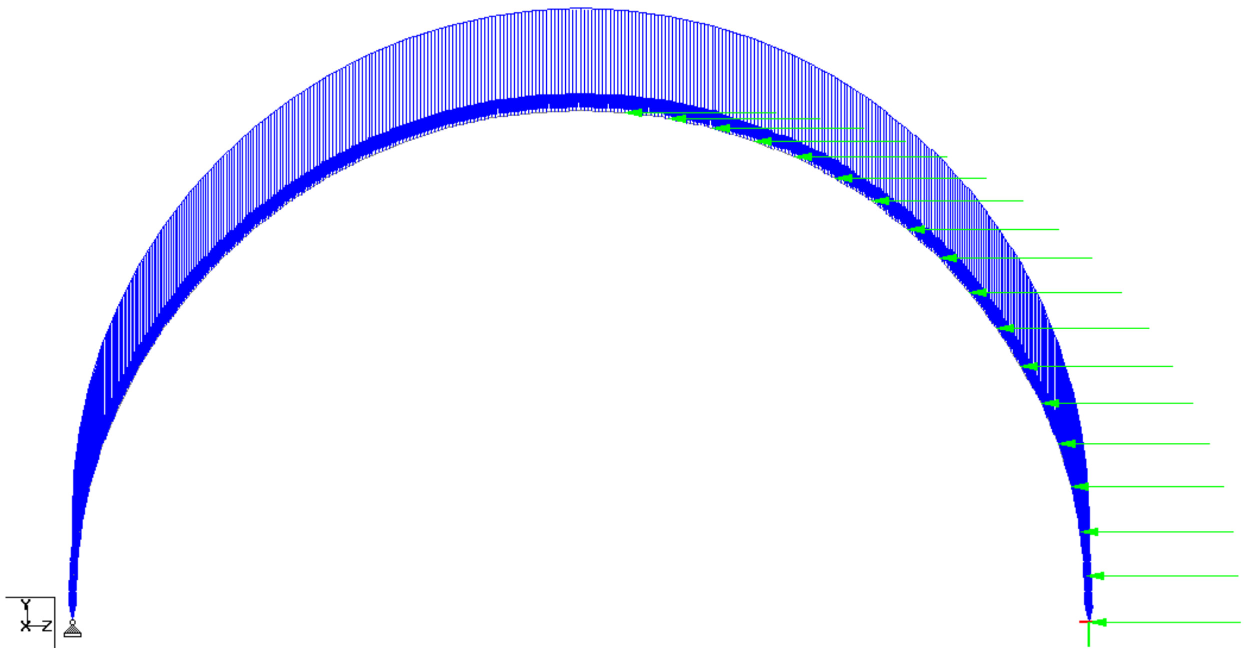

Figure 4.3-32 Forces and its locations used in the analysis. Source: ***STAAD.Pro V8i***

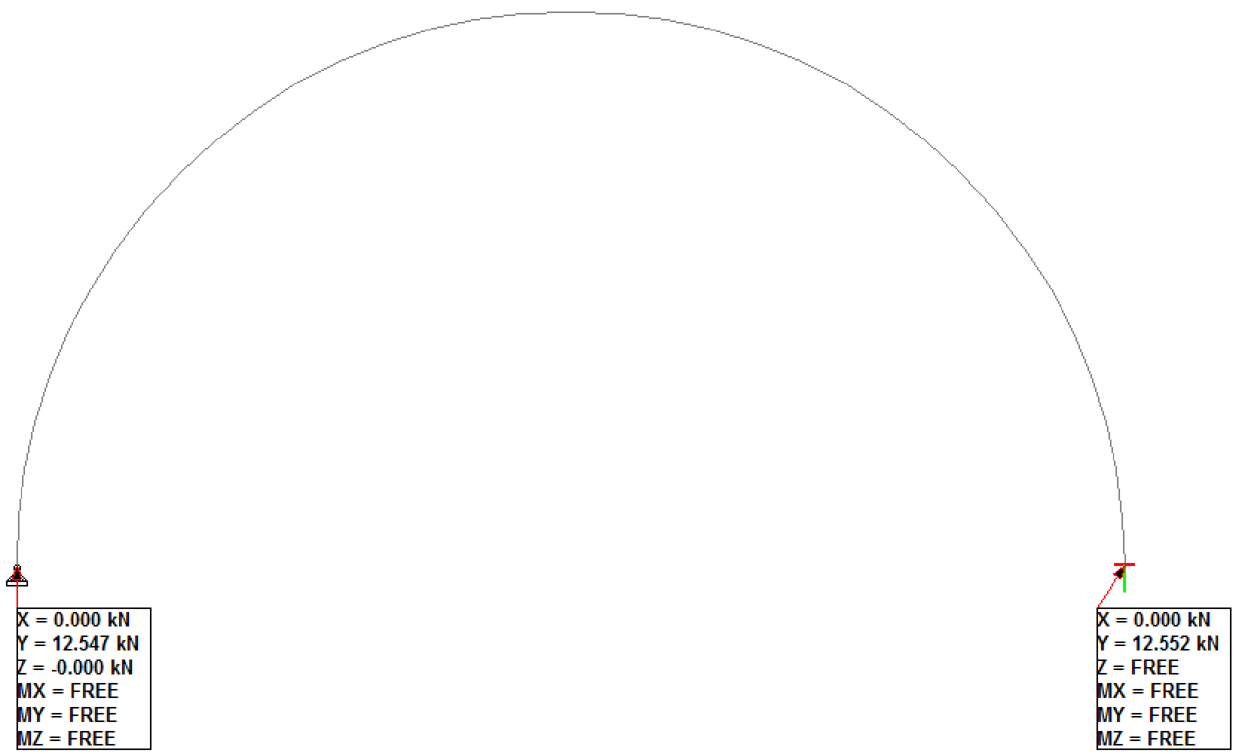

Figure 4.3-33 Reaction forces from the mass of the cover alone. Source: ***STAAD.Pro V8i***

4.4 Concrete and reinforcement design according to *Eurocode 2*

The concrete standard *NS-EN 1992-1-1:2004+NA:2008. Eurocode 2: Design of concrete structures - Part 1-1: General rules and rules for buildings* (Norsk Standard, 2004) gives design rules and guidelines for concrete structures.

The *Eurocode 2* is mainly based on design of regular horizontal beams and vertical columns and slabs etc. Due to the curved shape of the cover, or beam as it would be in this case, the actual applicability of the *Eurocode 2* design codes to this beam is questionable; but an attempt was made nevertheless.

The requirements to concrete cover of the reinforcement were calculated according to EC2 §4.4.1.1 and the Table NA.4.4N in EC2.

The material data is calculated in accordance to EC2 §3.1.3, EC2 §3.1.6, EC2 §3.2 and Table NA.E.1N in EC2.

Longitudinal reinforcement requirements are calculated in accordance with EC2 §9.2.1.1.

Moment capacity calculations are in accordance with EC2 §6.1 and *Reinforced Concrete Design to Eurocode 2* (Mosley, Bungey, & Hulse, 2012).

Requirements to shear reinforcement are calculated in accordance with EC2 §9.2.2.

Shear force capacity is calculated in accordance with EC2 §6.2.2.

The axial force capacity is usually calculated as part of the moment capacity calculations, specifically as second order moments due to forces on curved columns or columns with geometrical deviations. This is usually done using MN-diagrams, EC2 §5.8.3 and EC2 §5.8.8.2. In addition, the booklet *Betongkonstruksjoner: Formler og Diagrammer: NS-EN 1992-1-1* (Høgskolen i Bergen, Institutt for bygg og jordskiftefag, 2011) was used.

4.5 Dropped object test on the concrete protection cover

The *NORSOK standard U-001* (Norwegian Technology Centre (NTS), 2002) defines impact requirements that simulate impacts from drill pipes dropped over board and onto the protection cover. The cover to be tested in this impact test is an arch shaped spool or pipeline cover.

4.5.1 Description

A heavy object will be dropped onto the cover from a specific height to create the impact energies of 5 kJ, 20 kJ, 30 kJ and 50kJ. It is important to use correct impact area for the given impact energy, specifically 100 mm, 500 mm, 500 mm and 700 mm accordingly. Objects falling through water will eventually fall at a terminal velocity due to the buoyancy and restraining force, or drag force, equaling the downwards gravitational pull. In the *Subsea Dropped Objects* document by DROPS Online (DROPS online, 2010), the terminal velocity for drill pipes are given as 6 m/s. The aim was to have the object fall slightly faster than this, to be on the safe side. This is accounted for in the weight and height calculations of the dropped objects, see in Appendix D Impact Calculations. Assuming free fall in vacuum, this results in a necessary drop height of approximately 3,7 m.

An initial test will be performed outside on gravel at Multiblokk AS locations using the 1400 kg and 700 mm diameter object, which shall simulate the 50 kJ energy impact. The result of this test will either give the go ahead signal to move onto the next test in the laboratories of the University of Stavanger, or give clues as to what needs to be revised and done differently before proceeding with the next test. At the UiS laboratory, the cover will be submersed in water to simulate damping effects from the water and the general conditions more correctly. The cover will be placed on big bags of sand and rock to protect the basin and to simulate the ground conditions more correctly.

As a simplification to creating a full size cover, which would have been incredibly costly at this initial design stage in a master thesis, drain pipes kindly provided by Multiblokk AS was cut into halves and used for this test. This alternative is less costly and will be an acceptable simplification for the purpose of the thesis and the impact test. One of the assumptions in regards to this method is that this half circle represents the majority of the structural strength of the cover, and that the rest of the volume, the mud mats and trawl deflectors, on the cover mostly add weight to the cover, and that the addition of structural strength from these parts are limited or negligible.

What these added trawl deflectors will do, however, is to increase the area of the cover on the seabed, which will make the geotechnical assessments easier. But in regards to the dropped object test, the increased area will most likely result in that the cover is not pushed as much down into the sand or seabed. Thus, more of the impact energy will have to be absorbed by the cover internally, as opposed to by the ground by sinking into it. Thus, depending on the softness of the ground, this effect can be considered not conservative.

The half drain pipes are not overtrawlable, even though that is the requirement stated in *NORSOK standard U-001* (Norwegian Technology Centre (NTS), 2002), but they are adequately similar in shape to the designed protection cover. This impact test will not be affected by the fact that the cover is not overtrawlable, but the area of the "legs" of the cover might be considered not conservative, as described above.

4.5.2 Qualification process

All items of permanent equipment, such as protection covers, that have not previously been qualified for use, must be verified through necessary analyses and tests that show whether or not the equipment has the needed strength and is fit for use. The reason for the dropped object test on the concrete protection cover is to verify that it can withstand the impact energy requirements in the *NORSOK standard U-001* (Norwegian Technology Centre (NTS), 2002). According to *NORSOK standard U-001*, the impact requirements are:

Table 4.5.2-1 Impact energies from dropped objects (Norwegian Technology Centre (NTS), 2002)

Group	Impact energy, kJ	Impact area	Object diameter, mm
Multi well structures	50	Point load	700
	5	Point load	100
Other structures	20	Point load	500
	5	Point load	100

In addition, the impact requirement of 30 kJ with an object diameter of 500 mm will be tested. This is in reality not a dropped object requirement, as explained earlier, but a coming revision of the trawl gear impact requirements in the same standard.

4.5.2.1 Qualification method

The qualification method to be used for this thesis is impact testing of the concrete cover, backed up by a simple finite element analysis in *Ansys® Workbench, Release 14.5*. As a simplification, half drain pipes of inner diameter 2000 mm and thickness 215 mm will be used. The pipes are reinforced with 8 oval bars of Ø12 mm steel for the first test, and then 12 double bars of Ø12 mm steel for the second test.

The various dropped objects are made in a slightly different manner to each other. The heavy object of 1400 kg is made by filling up a reinforced concrete pipe of diameter Ø700 mm with concrete. The two objects of diameter Ø500 mm are made by filling up two steel pipes of diameter Ø500 mm with concrete. The 140 kg object is made using two parts, one Ø100 mm diameter pipe for impact, and one Ø300 mm diameter concrete block to decrease necessary height. On the bottom of the objects, which is where they will impact the covers, steel plates of approximately 10 mm thickness with correct impact diameters are fastened.

The various impact energies, object diameters, weight of objects, drop heights and impact velocities have been calibrated to each other to yield the desired test conditions, see Appendix D Impact Calculations.

The deflection and deformation of the protection cover will be recorded during the test. This will be done by cameras and simple measuring devices placed beneath the covers.

The impact and damages to the cover will be recorded on video and photos.

4.5.2.2 Verification criteria

The verification criteria for the impact test are that the dropped object shall not penetrate the protection cover and thus damage the equipment inside. According to *NORSOK standard U-001*, 'impact loads from dropped objects shall be treated as a PLS condition' (Norwegian Technology Centre (NTS), 2002). This means that the cover is to be considered in the Progressive Collapse Limit State (PLS), which means that plastic deformation of the cover is acceptable, but that complete penetration or breakdown of the structural integrity of the cover is not acceptable. In addition, due to the tension on the underside of the top of the cover, cracking and possibly concrete chunks coming loose is expected to happen. The amount of concrete that has broken loose from the roof inside the cover will have to be assessed in each case to decide whether or not it could damage the structure underneath.

In addition, the deflection of the cover and how much it is pushed down into the ground, will be monitored by measuring devices and cameras. The minimum clearance from object to the inner roof and walls of the cover shall not be exceeded. The minimum clearance requirement in similar projects, are typically in the area of 300 mm, which, for a 16" pipe (diameter 406,4 mm), leaves a maximum deflection on the roof of the cover of 293,6 mm when the inner radius of the cover is 1000 mm. Including the horizontal movement of spools of approximately 800 mm and necessary clearance, the cover is left with an allowed maximum deflection of approximately 193,6 mm.

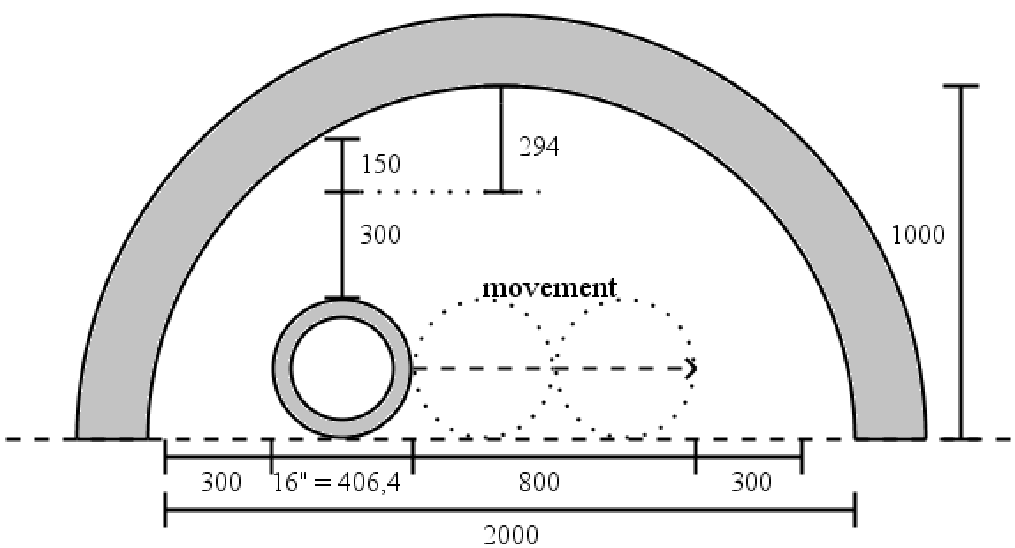

Figure 4.5.2-34 Vertical and horizontal movement and clearance of a 16" pipe inside protection cover.

4.5.2.3 Finite Element Analysis

A simple Finite Element Analysis of the impact will be performed in *Ansys® Workbench, Release 14.5*, using the Explicit Dynamics system and the Autodyn solver, to compare to the result from the tests. The result from the analysis will however be a guideline at best, due to the difficulty of modeling the impact together with the effects of water. Such an analysis has not been performed before in Subsea 7, and it would be difficult to say whether or not the analyses were representative.

For more info about the finite element analysis, see chapter 4.1 Finite Element Analysis using *Ansys® Workbench, Release 14.5*.

4.5.3 Equipment

The following chapter is a summary and explanation of the equipment used in the dropped object tests. The equipment varies somewhat between the initial test at Multiblokk AS and the tests at the University of Stavanger.

4.5.3.1 Concrete Protection Cover

The protection covers that will be tested are basic, tunnel shaped arch covers. As a simplification, stock drain pipes cut into halves was provided by Multiblokk AS. The specific drain pipe to be used is called IG-Rør Armert Falsrør, Basal.

ig-rør armert falsrør, Basal

Varenr.	DN innv.	Lengde i mm	Vekt i kg	Godstykkelse i mm/m	Maks overdekning i m	Maks avvinkling i mm/m.	Info.	Pris per l.m.	Pris
5460	2000	1500	5700	215	0,5 - 6	10	NB!*	12667	19000,-
54601	2000	1500	5700	215	0,5 - 8	10	NB!*	14667	22000,-
54602	2000	1500	5700	215	0,5 - 3	10		11334	17000,-

Figure 4.5.3-35 Material data for drainage pipe supplied by Multiblokk AS
Source: http://www.skjeveland.no/skjaeveland/avlopsror-og-deler/ig-ror-og-deler-basal/ig-ror-armert-falsror-basal, downloaded 3/3-2015

According to the product catalog, see Figure 4.5.3-35 and Chapter 6.4 in the Basal Standard (Basal AS, 2009), the data of the inner diameter of this pipe is 2000 mm (+/- 15 mm), the length is 1500 mm (+ 30 mm, - 10 mm), the thickness is 215 mm (+/- 5%) and the weight is 5700 kg (when cut in half it is 2850 kg). This is enough inner space for cover of a 16" pipeline, included motion of the pipeline as well as clearance.

The reinforcement used in the first test at Multiblokk AS' premises was 8 oval bars of diameter Ø12 mm with a center distance of about 163 mm. For the second test at UiS laboratories, the amount of reinforced used was increased to 12 double bars of diameter Ø12 mm with a center distance of about 100 mm, resulting in a total of 24 bars. The distance between the double reinforcement rings was 153 mm.

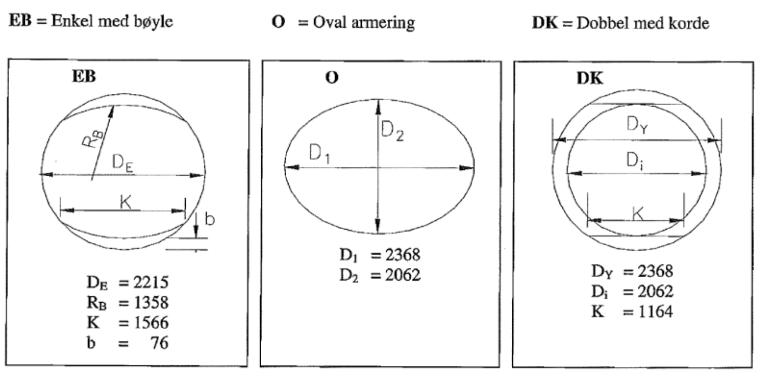

Figure 4.5.3-36 Reinforcement data: O = Oval reinforcement, DK = Double reinforcement Source: (Basal AS, 2009)

Multiblokk AS uses a special dry-casting method for their products. This results in 'zero slump, and the forms can be stripped as soon as the concrete has been consolidated' (ConcreteNetwork.com). This method enables easier mass production of products, but does, according to Multiblokk AS, suffer somewhat in strength tests compared to regular wet-cast concrete, making them slightly more brittle.

Figure 4.5.3-37 The protection covers provided by Multiblokk AS.

4.5.3.2 Concrete material data

The concrete material used by Multiblokk AS is in accordance with the concrete standard *NS-EN 206-1:2000*. There are some small differences between material data and requirements between this standard and the *Eurocode 2*, but the *NS-EN 206-1:2000* standard was not available at the time of writing, and thus it was decided to give indicative material data from *Eurocode 2* for the same material strength B40.

According to Chapter 6.4 in the *Basal Standard* (Basal AS, 2009), the minimum durability class of the concrete used in the covers is M40 and maximum water to binder-ratio (v/c+Σkp) = 0,40.

According to Table NA.E.1N in the *Eurocode 2* (Norsk Standard, 2004), the expected minimum concrete strength class is B40, based on the durability class of M40.

Further, according to Table 3.1 of the *Eurocode 2*, some of the strength and deformation characteristics of the concrete are therefore:

Table 4.5.3-1 Material data for B40 concrete from EC2 Table 3.1

Concrete strength class B40		**Explanation**
f_{ck} (MPa)	40	Characteristic compressive cylinder strength of concrete at 28 days
$f_{ck,cube}$ (MPa)	50	Characteristic compressive cylinder strength of concrete at 28 days
f_{cm} (MPa)	48	Mean value of concrete cylinder compressive strength
f_{ctm} (MPa)	3,5	Mean value of axial tensile strength of concrete
$f_{ctk,\ 0,05}$ (MPa)	2,5	5 % fractile
$f_{ctk,\ 0,95}$ (MPa)	4,6	95 % fractile
E_{cm} (GPa)	35	Secant modulus of elasticity of concrete
ε_{c1} (‰)	2,3	Compressive strain in the concrete at the peak stress f_c
ε_{cu1} (‰)	3,5	Ultimate compressive strain in the concrete, 1
ε_{c2} (‰)	2,0	Compressive strain in the concrete, 2
ε_{cu2} (‰)	3,5	Ultimate compressive strain in the concrete, 2
η	2,0	
ε_{c3} (‰)	1,75	Compressive strain in the concrete, 3
ε_{cu3} (‰)	3,5	Ultimate compressive strain in the concrete, 3

See the *Eurocode 2* (Norsk Standard, 2004) for more details about the material.

4.5.3.3 Dropped objects

The dropped objects used in the test have been made using different methods. For use in the initial test at Multiblokk AS, only the 1400 kg object for the 50 kJ test was made. This object broke during the test. For the tests at the University of Stavanger laboratories, the 1400 kg object from the first test had to be remade, and in addition, the rest of the objects 550 kg, 850 kg and 140 kg were also created. See the full calculations in in Appendix D Impact Calculations.

4.5.3.3.1 1400 kg object

The 1400 kg object was made by filling a reinforced 700 mm outer diameter drain pipe with concrete. The total height of the object was calculated to be 1,51 m using concrete density of 2400 kg/m^3.

$$Needed\ object\ height, h = \frac{1400kg}{2400\frac{kg}{m^3} * \pi(\frac{0,7m}{2})^2} = 1,51m$$

On the bottom of the object a steel plate was placed in order to achieve even distribution of the forces from the impact. Onto this plate several reinforcement bars that point upwards into the object were welded on, making sure that the plate stuck to the object properly and that the impact energies were absorbed upwards into the object as well as on the impact plate.

A wire to hook into the release mechanism was fastened with a rebar inside the object and cast into place.

Figure 4.5.3-38 The 50 kJ impact object of approximately 1400 kg and diameter 700 mm.

Figure 4.5.3-39 The impact plate of the 1400 kg object.

4.5.3.3.2 550 kg and 850 kg objects

The 550 kg and the 850 kg objects were made using a diameter Ø500 mm steel pipe kindly provided by the Subsea 7 base at Dusavik as walls and formwork of the object cut into the necessary heights. The objects were made by pouring concrete into the steel pipe up to the calculated height. As with the 1400 kg object, impact plates with vertical reinforcement bars are fastened to the bottom of the objects.

The height calculations are as follows, assuming a density of concrete of 2400 kg/m^3 and of steel of 7850 kg/m^3.

Data of diameter Ø500 mm steel pipe from Dusavik Base:

$$Outer\ radius = \frac{500mm}{2} = 250mm$$

$$Measured\ wall\ thickness = 19mm$$

$$Inner\ radius = 250mm - 19mm = 231mm$$

Needed height for object mass 550 kg:

$$mass\ of\ steel\ pr.\ meter = (\pi * 250mm^2 - \pi * 231mm^2) * 7850\frac{kg}{m^3} = 225{,}38\frac{kg}{m}$$

$$mass\ of\ concrete\ pr.\ meter = (\pi * 231mm^2) * 2400\frac{kg}{m^3} = 402{,}33\frac{kg}{m}$$

$$\left(225{,}38\frac{kg}{m} + 402{,}33\frac{kg}{m}\right) * needed\ height = 550\ kg * m$$

$$needed\ height = \frac{550kg}{\left(225{,}38\frac{kg}{m} + 402{,}33\frac{kg}{m}\right)} = 0{,}876m$$

The needed pipe and object height of the 550 kg object are therefore approximately 880 mm. The same calculations for the 850 kg object, which can be viewed in the appendices, yielded a necessary object height of 1350 mm.

Figure 4.5.3-40 The reinforcement inside the objects.

Figure 4.5.3-41 The 30 kJ and 20 kJ impact objects of approximately 850 kg and 550 kg and diameter 500 mm.

4.5.3.3.3 140 kg object

The object of 140 kg was made in a slightly different manner due to the impossible height needed when pouring concrete into the Ø100 mm steel pipe that was found on Subsea 7's Dusavik base alone. It was decided to use a protruding diameter of Ø100 mm as the impact area, and expand the diameter to Ø300 mm above it to limit the needed object height. The Ø300 mm part of the object was made using a ventilation duct of the same size as formwork. It is assumed that the weight added by the ventilation pipe can be neglected. The Ø100 mm pipe found at the Dusavik base will be inserted about 200 mm into the Ø300 mm object, leaving about 150 mm to protrude from the wider part. The protruding part of the pipe will also be filled with concrete to limit the chance of buckling of the pipe walls. An impact plate of diameter Ø100 mm was added to the bottom of the protruding pipe. The necessary object height of the Ø300 mm part is calculated from:

Data of Ø100 mm steel pipe from Dusavik Base:

$$Outer\ radius = \frac{100mm}{2} = 50mm$$

$$Wall\ thickness = 10mm$$

$$Inner\ radius = 50mm - 10mm = 40mm$$

Needed height for object mass 140 kg:

$$mass\ of\ steel\ pr.\ meter = (\pi * 50mm^2 - \pi * 40mm^2) * 7850\frac{kg}{m^3} = 22{,}19\frac{kg}{m}$$

$$mass\ of\ concrete\ pr.\ meter = (\pi * 40mm^2) * 2400\frac{kg}{m^3} = 12{,}06\frac{kg}{m}$$

$$mass\ of\ 200\ mm\ of\ this\ pipe\ size = \left(22{,}19\frac{kg}{m} + 12{,}06\frac{kg}{m}\right) * 200mm = 6{,}85kg$$

$$remaining\ mass = 140kg - 6{,}85kg = 133{,}15kg$$

$$Needed\ height\ of\ Ø300mm\ part = \frac{133{,}15kg}{2400\frac{kg}{m^3} * \left(\pi * \left(\frac{300mm}{2}\right)^2\right)} = 0{,}78\,m$$

The concrete column part of diameter Ø300 mm of the 140 kg object will need to be 780 mm high.

Figure 4.5.3-42 The reinforcement inside the 5 kJ object.

Figure 4.5.3-43 The 5 kJ impact object of approximately 140 kg and impact diameter 100mm.

4.5.3.4 Deflection measuring devices

The deflection measuring devices used in the first test at Multiblokk AS' premises were tested as a proof of concept before the full scale test at the laboratories of the University of Stavanger. Due to the potential of crushing of whatever equipment that was placed beneath the cover, a decision to use cheap and replaceable equipment was made.

Four different methods of measuring were used:

- A telescope magnet that could easily be retracted, but would stop once it was no longer pushed back. The telescope staff was placed in an upright position beneath the cover to measure the maximum deflection of the cover, and also the amount of deflection retraction caused by the tension in the reinforcing bars.
- A metal rod with a sharp tip being pushed down by the cover deflection into oasis foam used for gardening was placed in an upright position beneath the cover. Like the telescope staff, this method will also yield the maximum deflection as well as the deflection retraction by the reinforcement.
- A simple ruler was placed in front of the cover and the deflection could easily be recorded from this. The maximum and end deflection was also filmed by a front facing camera.
- The depth between the water surface and the top of the cover was measured using a ruler when the cover was submerged in the basin.

For the first test at Multiblokk premises, the telescope magnet, metal rod into oasis foam and the ruler was used successfully. The magnet method was used for the 5 kJ and 20 kJ impacts, but was destroyed while lifting the cover out of the basin. After that, the deflection was measured using the depth between water surface and top of the cover. This would essentially give the same approximate result as measured from underneath, because the measuring itself was difficult under water and underneath the midpoint of the cover. A camera was also set up in front of the cover underneath the water, but the sand and silt from the sand bags whirled up into the water and severely limited the sight under water, rendering the recordings useless.

Figure 4.5.3-44 Deflection measuring devices used during the test.

4.5.3.5 Equipment used during the test at Multiblokk AS' premises

During the initial drop test at Multiblokk AS' premises, the following equipment was used.

The test was performed outside on gravel. The object was lifted and dropped from a Manitou Maniscopic Telehandler lift. As can be seen in Figure 4.5.3-45, a simple lifting rig consisting of a roundsling, a shackle and a quick release mechanism was used. A rope with a heavy object at the end was used to control that the drop height was correct.

The quick release mechanism that was used during this drop test was a SH-16 Pelican hook, also called Slip Hook, produced by Kjættingfabrikken AS. The breaking force of the hook was in the documentation of the hook given as 275 kN, equaling a mass of 28 tons in gravity, thus having more than enough strength for this test.

$$Breaking\ force = \frac{275kN}{9{,}81\frac{m}{s^2}} = 28\ 042{,}2kg$$

The object was hooked onto the nether part of the hook, and was released under pressure by pulling the security ring upwards and off. This was done from a safe distance by fastening a rope to the trigger on the slip hook. To ensure easier pulling and release of the object, the trigger rope was led through a pulley block with minimal friction.

Figure 4.5.3-45 The Manitou Maniscopic Telehandler lift and general test set-up.

Figure 4.5.3-46 The SH-16 Pelican hook used during the test.

Slipphake – varmforsinket / Pelican hooks – hot dip galv.

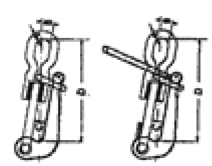

Varenr. Item no.	Type Code	Prøvekraft Proof force kN	Bruddkraft Breaking force kN	Mål i mm/Dim mm A	B	C	D	Kg
0601701	SH-16	157	275	16	27	21	205	1,6
3	SHR-16	157	275	16	27	21	205	1,7

Figure 4.5.3-47 Documentation for the SH-16 Pelican hook. Source: www.framlink.no/upload/files/pdf/1150465193_gruppe_9_s51-55.pdf, downloaded 15/2-2015

4.5.3.6 Equipment used during the test at the University of Stavanger

During the drop tests performed at the University of Stavanger, the following equipment was used.

The test was performed inside in the basin in the new laboratories. The objects, covers and protection sand bags were moved, placed and removed using a 5 ton overhead crane and forklift. Old car tires and pallets were used as protection of walls and the floor as well. The Figure 4.5.3-48 shows the test system before filling the basin with water. As can be seen in Figure 4.5.3-49, a similar quick release system was rigged for this test as well, using a 2 ton HK4 Pelican Slip Hook[1]. A rope with a shackle at the end was used to control that the drop height was correct for each case.

The object was hooked onto the nether part of the hook, and was released under pressure by pulling the security ring upwards and off. This was done from a safe distance by fastening a rope to the trigger on the slip hook. To ensure easier pulling and release of the object, the trigger rope was led through a pulley block with minimal friction.

The Figure 4.5.3-50 and Figure 4.5.3-51 shows the test setups for the 5 kJ and 50 kJ impact tests.

---

[1] Article nr. 0831042 from web page http://john-dahle.no/johndahle/index.asp?produkter/2889263/2/0/Usertifisert jernvare - Slipphake/0, downloaded 15/3-2015

Figure 4.5.3-48 The cover, protection sand bags and other equipment to protect the basin.

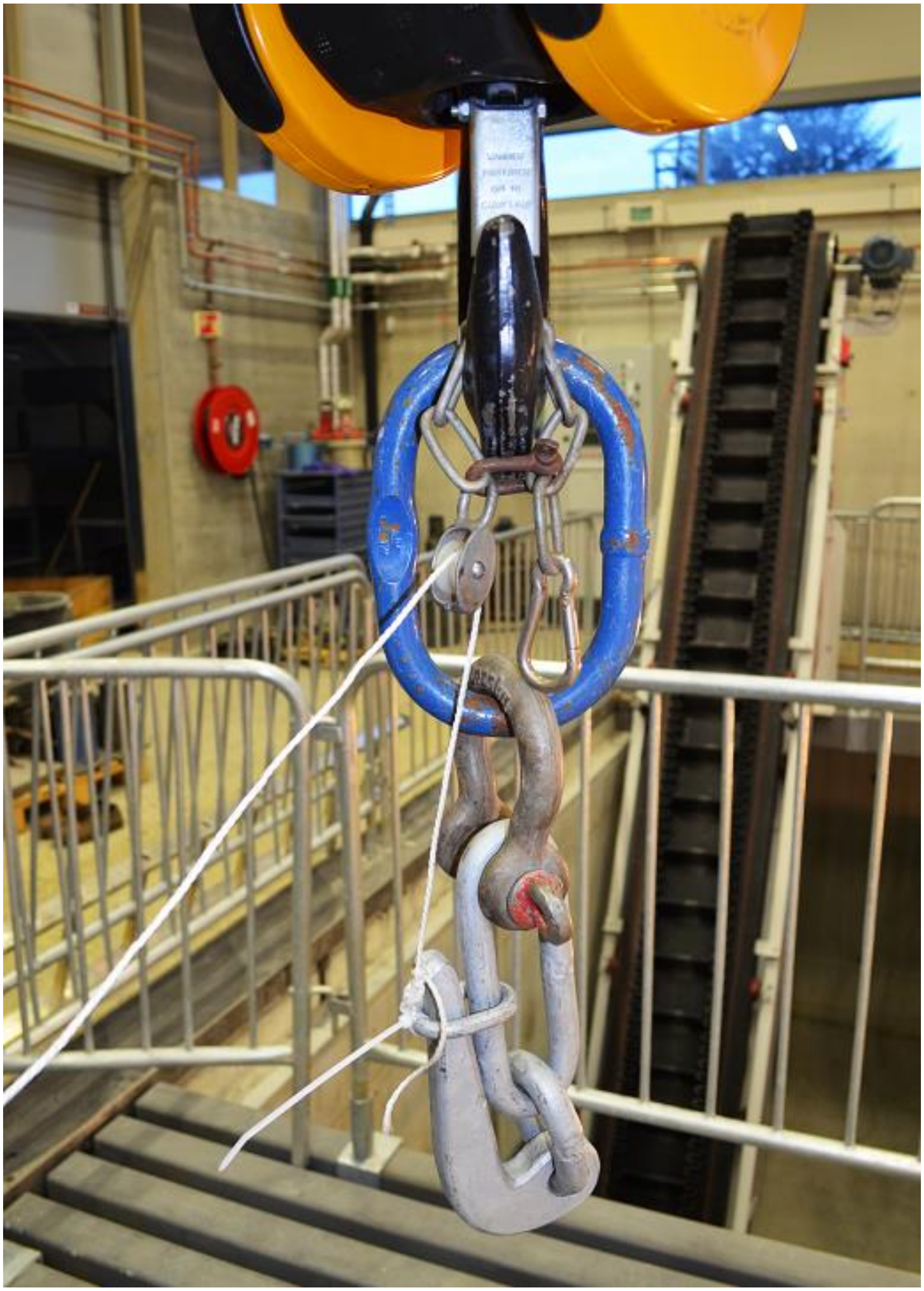

Figure 4.5.3-49 The quick release system used during the tests.

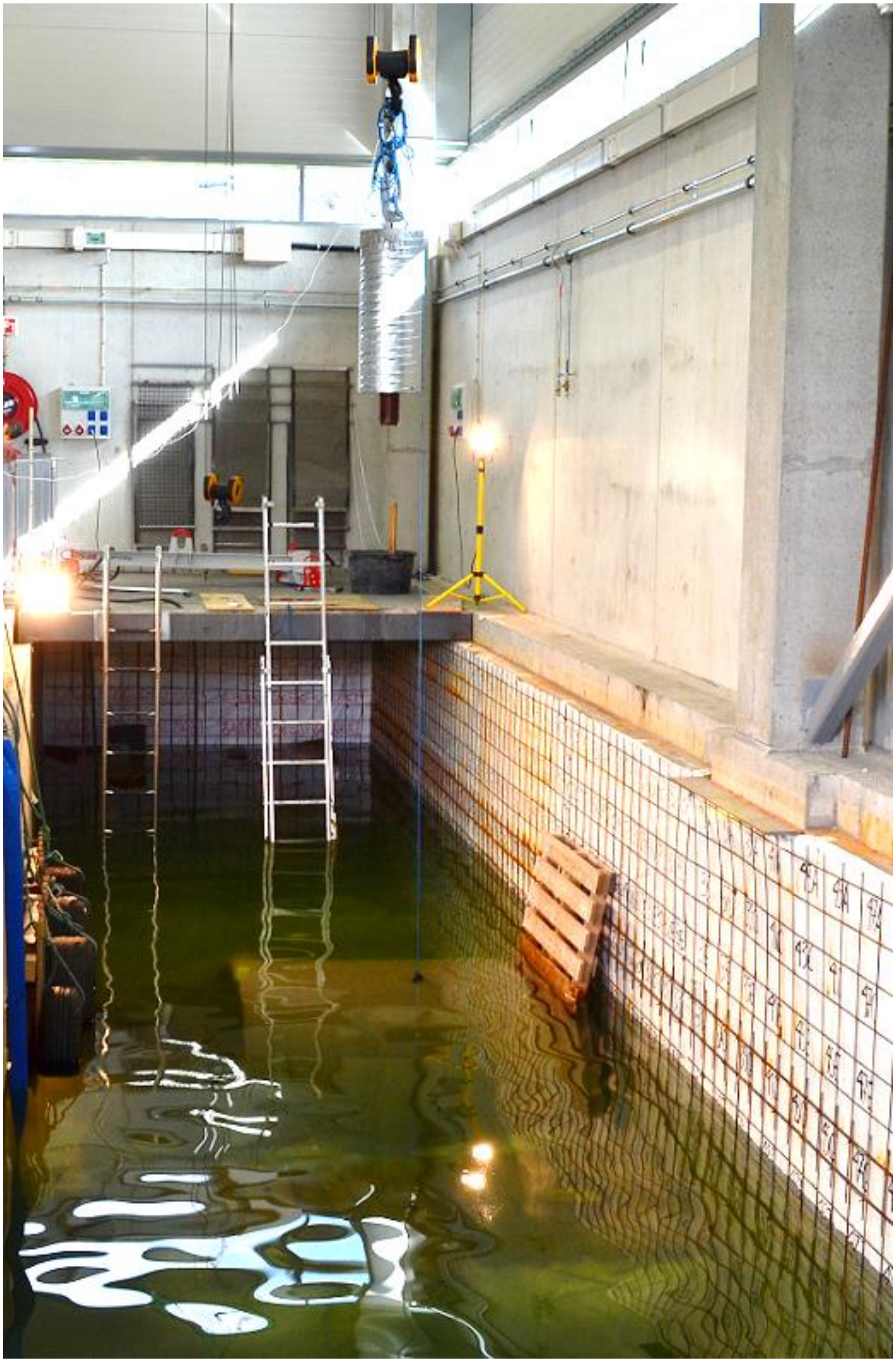

Figure 4.5.3-50 The test set-up of the 5 kJ drop test.

Figure 4.5.3-51 The test set-up of the 50 kJ drop test.

4.5.4 Summary of the impact test method

4.5.4.1 General

To qualify the concrete protection cover for dropped object impact energies according to *NORSOK standard U-001* (Norwegian Technology Centre (NTS), 2002), the dropped object impact tests shall be performed on the concrete covers.

Devices for measuring the deflection during impact shall be present during the test. Several cameras shall be present to record the impact. They will be used to document the deflections found by the deflection measuring devices as well as the damages to the covers.

The covers tested were arch shaped spool or pipeline covers. For simplicity's sake, three drain pipes provided by Multiblokk AS were cut in half and used as a representation of the protection cover, as discussed earlier. Some variations in amount of reinforcement were made between the two tests, as described earlier.

Four different impact energies shall be tested, 5 kJ, 20 kJ, 30 kJ and 50 kJ. The objects shall have the following impact diameters: 100 mm, 500 mm, 500 mm and 700 mm.

The drop height will be adjusted on test site to account for the actual weight of the object, see Table 4.5.4-1. This will give a speed of the falling object at slightly above 6 m/s, which is approximately the terminal velocity of a drill pipe sinking in water (DROPS online, 2010), see further weight, height and speed calculations in the in Appendix D Impact Calculations.

Table 4.5.4-1 Overview of the impact tests that shall be performed.

Impact energy	Diameter	Weight	Drop height	Type	Material used
5 kJ	100 mm	140 kg	3,64 m	Dropped object	Concrete inside steel pipes of various cross sections.
20 kJ	500 mm	550 kg	3,71 m	Dropped object	Concrete inside steel pipe
30 kJ	500 mm	850 kg	3,60 m	Trawl impact	Concrete inside steel pipe
50 kJ	700 mm	1400 kg	3,64 m	Dropped object	Concrete inside concrete drain pipe

4.5.4.2 Test set-up

The first test was performed at Multiblokk AS' premises. It consisted of only one cover and one dropped object energy and load, the 50 kJ impact with the 1400 kg object. The test was performed outside on gravel, as a worst case scenario (hard ground and no dampening effects from the water). The load was hoisted to approximately 3,6 m directly above the cover and was released by pulling a rope, triggering a quick release slip hook.

The second test was performed in the laboratories at the University of Stavanger. This test consisted of three drain pipes cut into six halves, and the four dropped objects of various sizes. The covers were placed in a 3 m x 3 m x 25 m concrete basin on top of big bags of sand, stone and silt. This was done to protect the floor of the basin and to give a better representation of the conditions on the seabed. Water was filled up to approximately 10 cm above the cover. This is to simulate the effect of the cover in interaction with the water. The speed of the cover is calibrated to simulate terminal velocity in water. The objects were hoisted up using a 5 ton overhead crane. The objects were placed above the covers and released by pulling a rope, triggering a quick release slip hook.

4.5.4.3 Test procedure

The test procedure can be summarized in the following steps:

- Place big bags of sand in basin to support cover and to protect floor
- Place cover into the basin
- Secure the walls and surrounding floor from being impacted by the dropped object
- Fill the basin with water until it reaches 10 cm over the top of the cover
- Install and position the deflection measuring devices and cameras
- Confirmation of correct test set-up for the protection covers
- Confirmation of impact energy, impact diameter and drop height
- Place object above the center and mid-span of the cover
- Check and adjust that the impact object is in center by raising the object 1m and lowering it back down to the cover again
- Raise the impact object to the specified drop height, determined by object weight
- Let impact object hang until stabilized
- Risk of debris from cover – clear test site
- Release impact object by pulling rope and triggering the quick release mechanism
- Impact!
- Read off the deflection measuring device prior to moving cover. Fill in results in registration tables.
- Remove cover or drain water for inspection and documentation of both sides.
- Document damage by photos and comments.

5 Results

The results from the various analyses and tests will be presented in this chapter.

5.1 Finite Element Analysis using *Ansys® Workbench, Release 14.5*

As explained earlier, the finite element analysis of the cover was performed for two different cases; the first being the static analysis load due to the trawl board overpull load, and the second being the dynamic analysis simulating the dropped object tests.

Ansys® Workbench, Release 14.5 is able to output deformations and stresses in the protection cover and reinforcement, but forces for the design according to *Eurocode 2* will have to be output from *STAAD.Pro V8i*.

5.1.1 Trawl board overpull – Static Structural

The trawl board overpull analysis was performed at twelve different locations on the cover. The loads were applied in positive Z-direction at the roll supported side. The results from the twelve analyses are presented in Table 5.1.1-1 below. The results are also presented as bar graphs to illustrate the differences between the different impact locations.

The deformation in X-direction is ignored due to the negligibly small values due to restriction in both supports.

The reaction forces for the cover reveal a problem with the stability of the system due to the relatively low weight of the cover compared to the tipping moment created by the trawl force. At the lowest impact locations Outer 1, there is a negative vertical reaction force component of about 14 kN, for Outer 2 the force has increased to about 55 kN, for Outer 3 it is approximately 90 kN and for the top load case Outer 4, the force is approximately 120 kN. These reaction forces are the same for the equivalent heights for the other load cases as well. This means that there is a tipping moment about the pinned support, and that the mass of the cover is not enough alone to hold the cover in equilibrium, and thus the reaction force is needed to hold the cover down. See chapter 5.2 for calculations on the mass and tipping moment.

Table 5.1.1-1 The stress and deformation results from the trawl board overpull finite element analysis in *Ansys® Workbench, Release 14.5*.

Maximum values	Outer 1	Outer 2	Outer 3	Outer 4
Equivalent Stress (von-Mises) (MPa)	26,72	22,65	19,90	18,22
Total Deformation (mm)	14,95	11,40	8,79	7,24
Directional Deformation Y (mm)	4,77	3,94	3,22	2,69
Directional Deformation Z (mm)	14,85	11,35	8,76	7,22
Reinforcement Axial Stress Compression (MPa)	124,38	106,00	93,36	85,50
Reinforcement Axial Stress Tension (MPa)	107,07	89,72	76,87	67,72
	Left 1	Left 2	Left 3	Left 4
Equivalent Stress (von-Mises) (MPa)	25,74	21,96	19,30	17,55
Total Deformation (mm)	14,38	11,13	8,69	7,21
Directional Deformation Y (mm)	4,67	3,86	3,17	2,66
Directional Deformation Z (mm)	14,28	11,07	8,66	7,19
Reinforcement Axial Stress Compression (MPa)	121,53	104,32	91,91	83,75
Reinforcement Axial Stress Tension (MPa)	105,99	89,14	76,44	67,42
	Mid 1	Mid 2	Mid 3	Mid 4
Equivalent Stress (von-Mises) (MPa)	24,82	21,35	18,73	16,90
Total Deformation (mm)	13,66	10,74	8,51	7,13
Directional Deformation Y (mm)	4,48	3,72	3,07	2,60
Directional Deformation Z (mm)	13,57	10,68	8,47	7,10
Reinforcement Axial Stress Compression (MPa)	119,66	103,46	91,14	82,81
Reinforcement Axial Stress Tension (MPa)	103,97	87,98	75,46	66,60

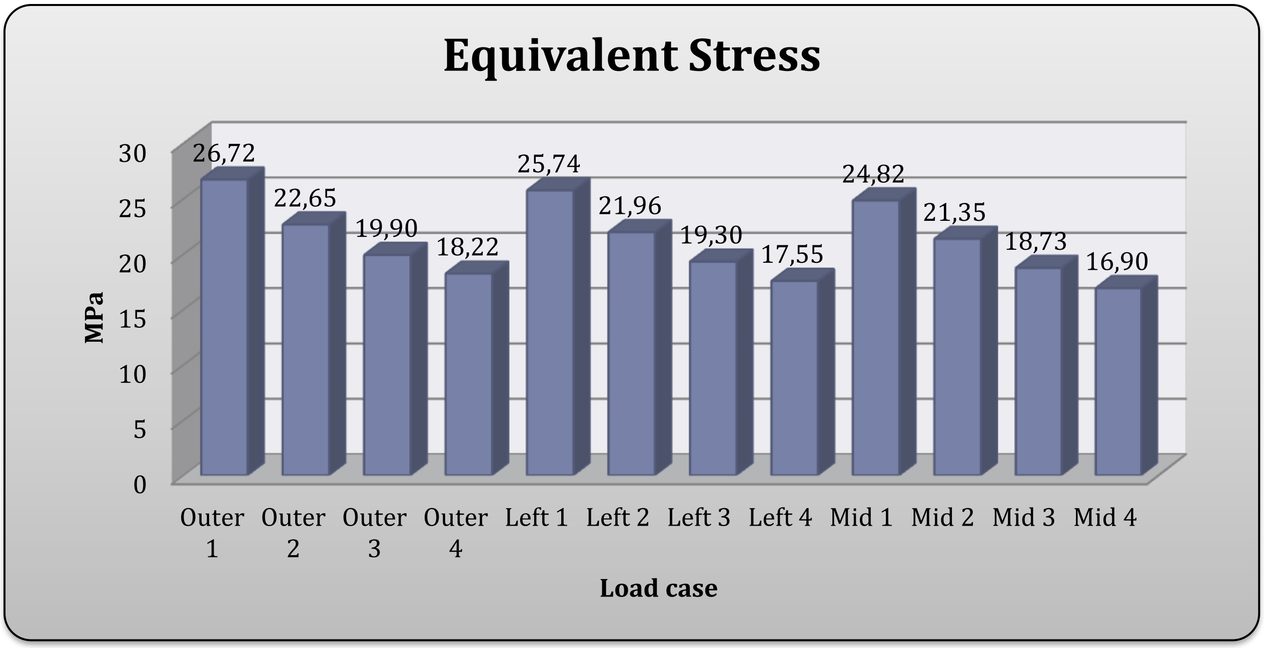

Figure 5.1.1-1 Equivalent stress results from the static trawl board overpull analyses.

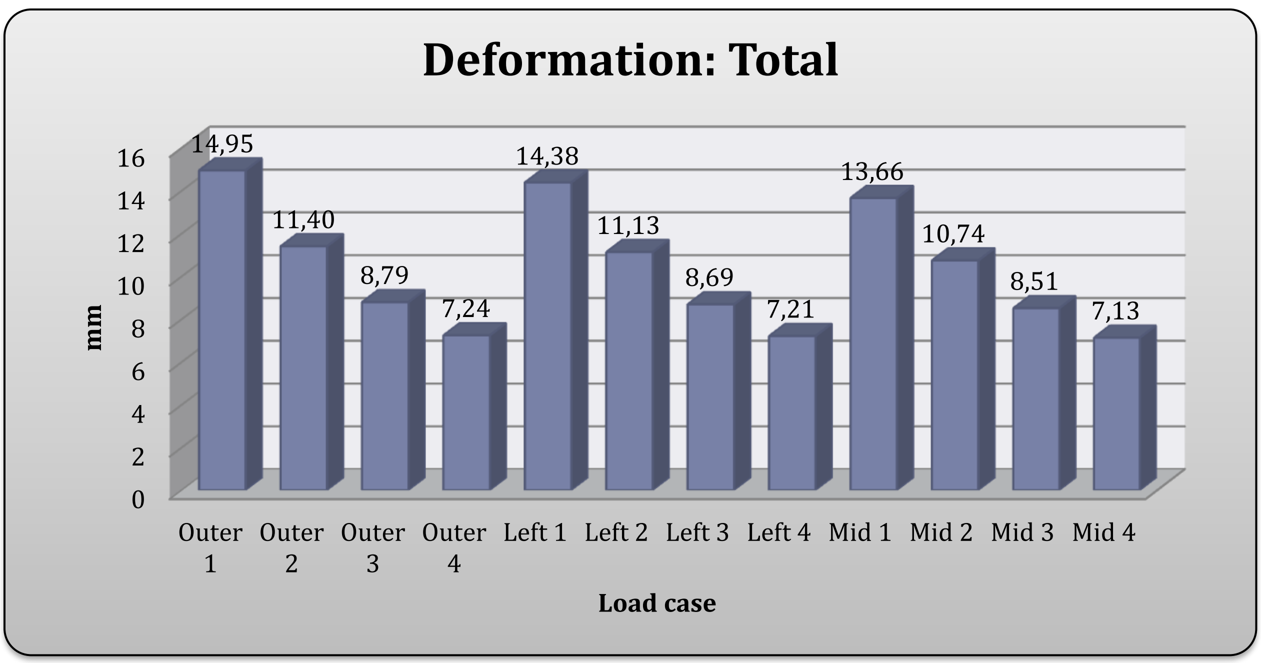

Figure 5.1.1-2 Total deformation results from the static trawl board overpull analyses.

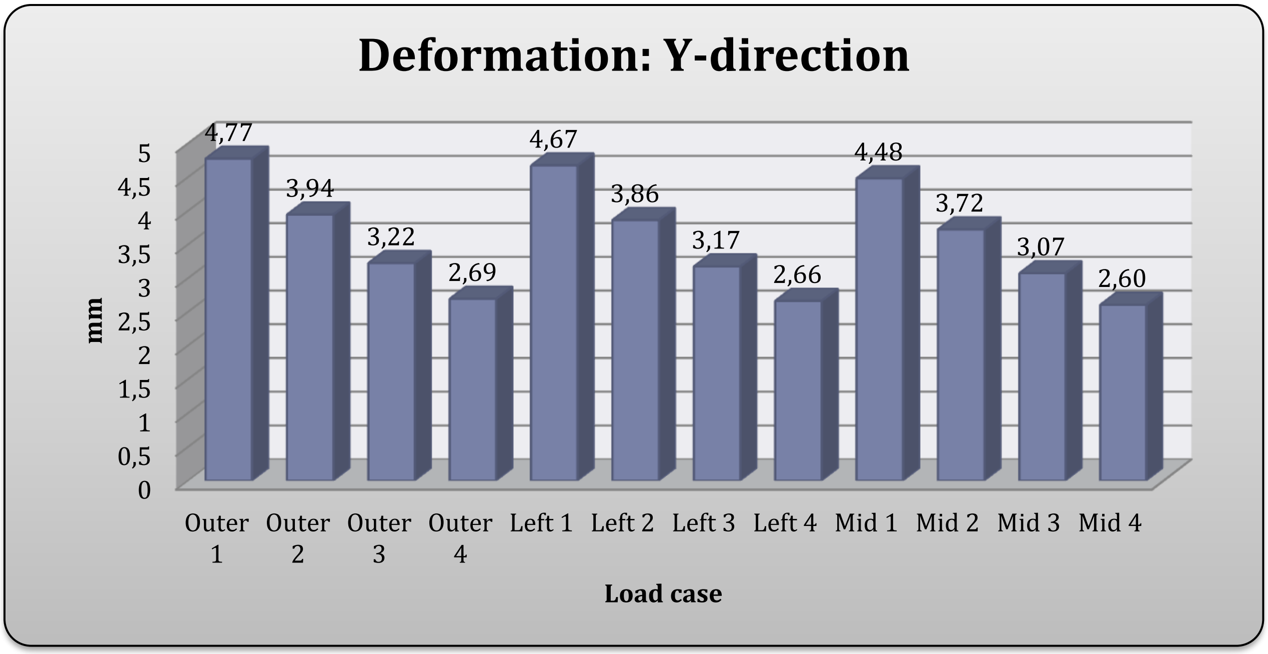

Figure 5.1.1-3 Deformation in Y-direction results from the static trawl board overpull analyses.

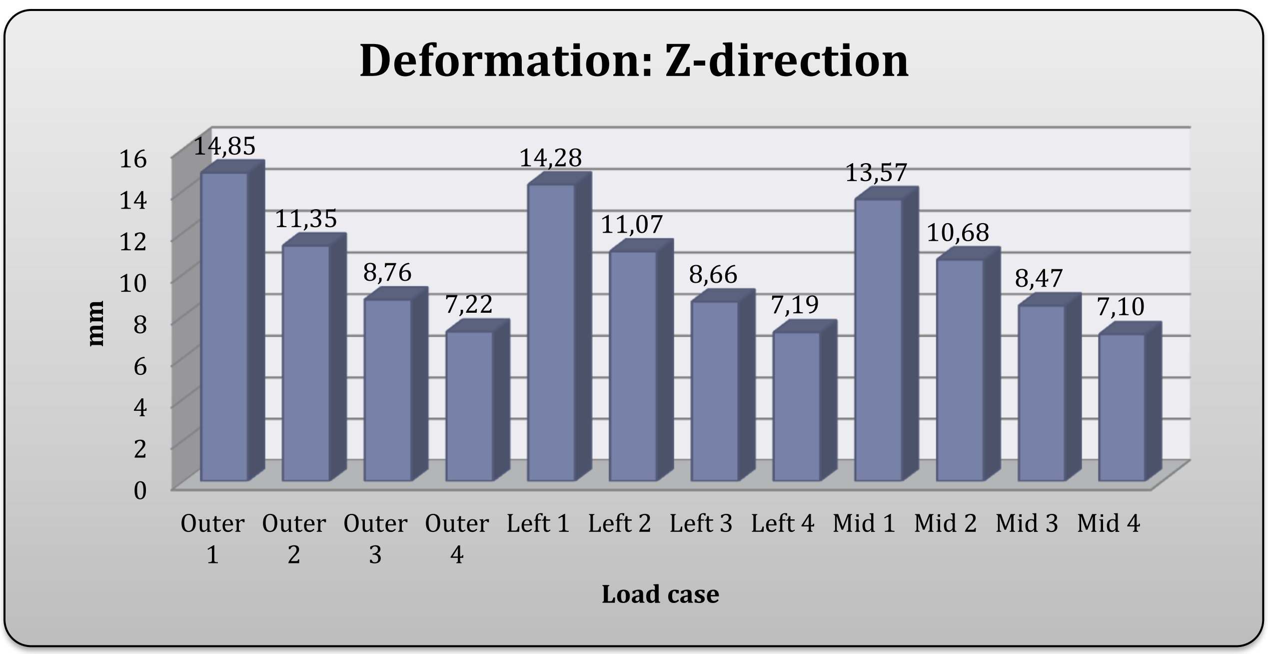

Figure 5.1.1-4 Deformation in Z-direction results from the static trawl board overpull analyses.

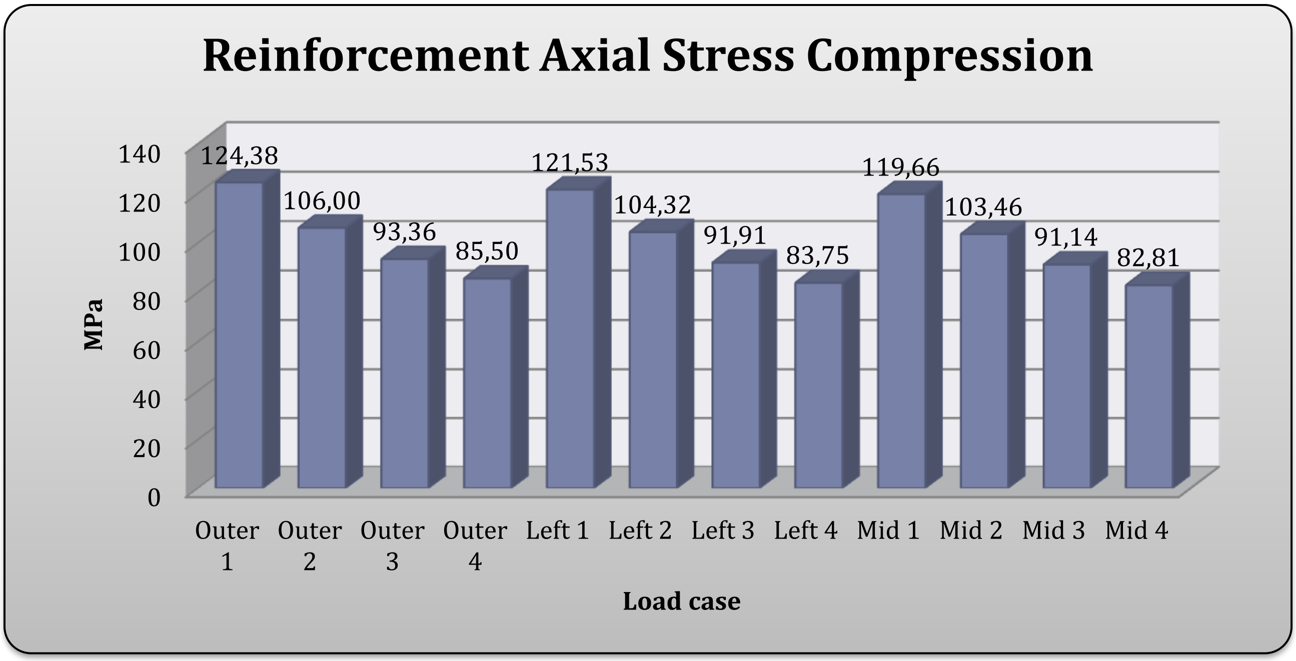

Figure 5.1.1-5 Axial compression stresses in reinforcement from the trawl board overpull analyses.

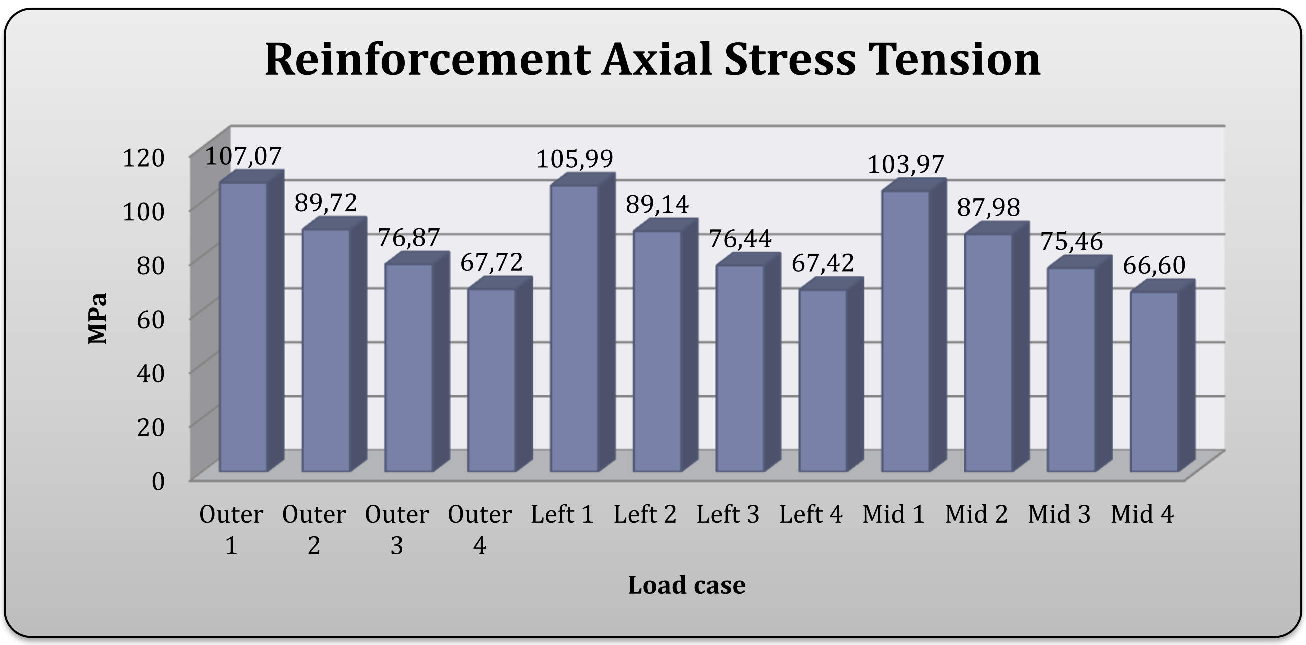

Figure 5.1.1-6 Axial compression stresses in reinforcement from the trawl board overpull analyses.

These results show that the load case called "Outer 1", which is impact from the trawl load at the lowest part of the corner of the cover, is the load case that will inflict most damage due to high stresses and the deflection on the cover. The Outer 1 load case has the highest values of deformations and stresses in all the different results. The result plots from this load case can be seen in the figures below. The rest of the plots from the other load cases can be seen in Appendix A Results from the Trawl board analysis in *Ansys® Workbench, Release 14.5*.

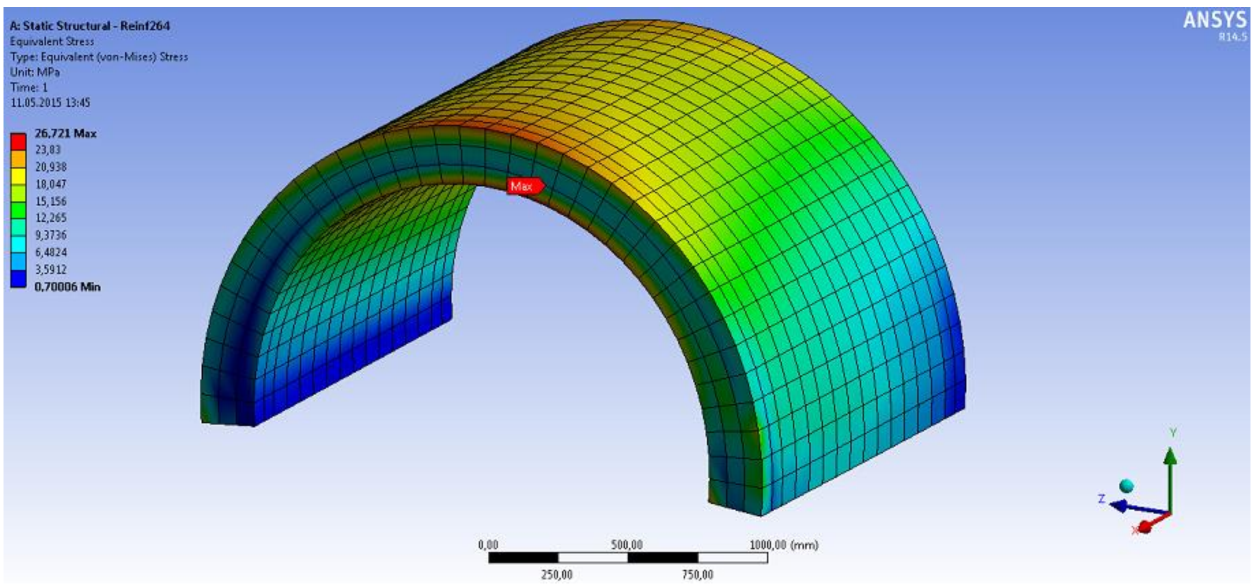

Figure 5.1.1-7 Equivalent stress plot of the Outer 1 load case. Source: ***Ansys® Workbench, Release 14.5***

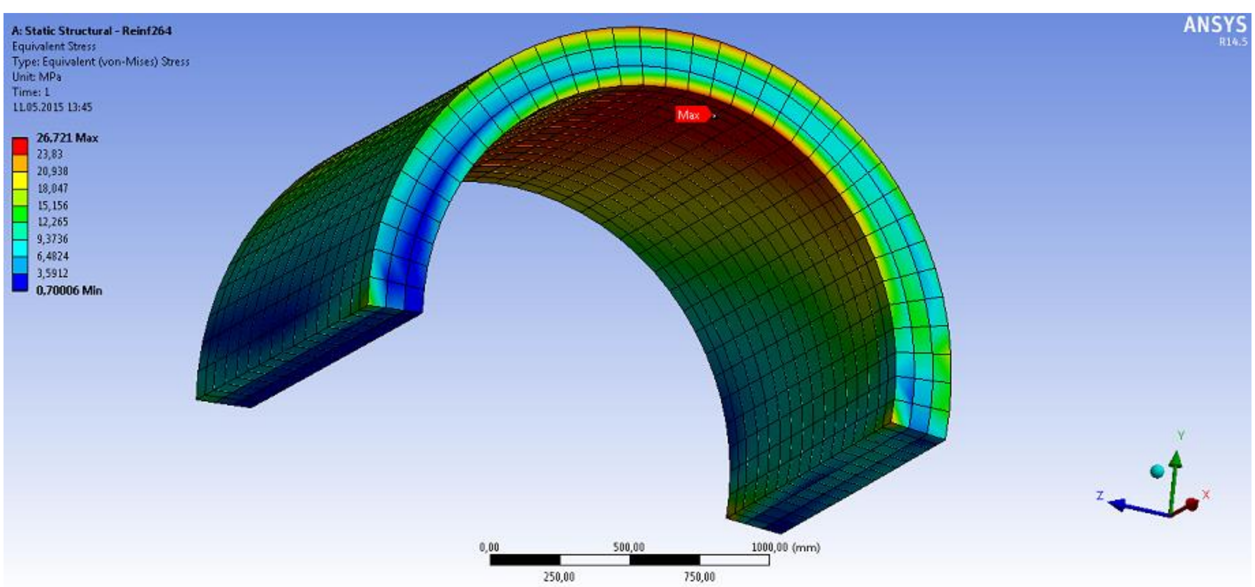

Figure 5.1.1-8 Equivalent stress plot of the Outer 1 load case. Source: ***Ansys® Workbench, Release 14.5***

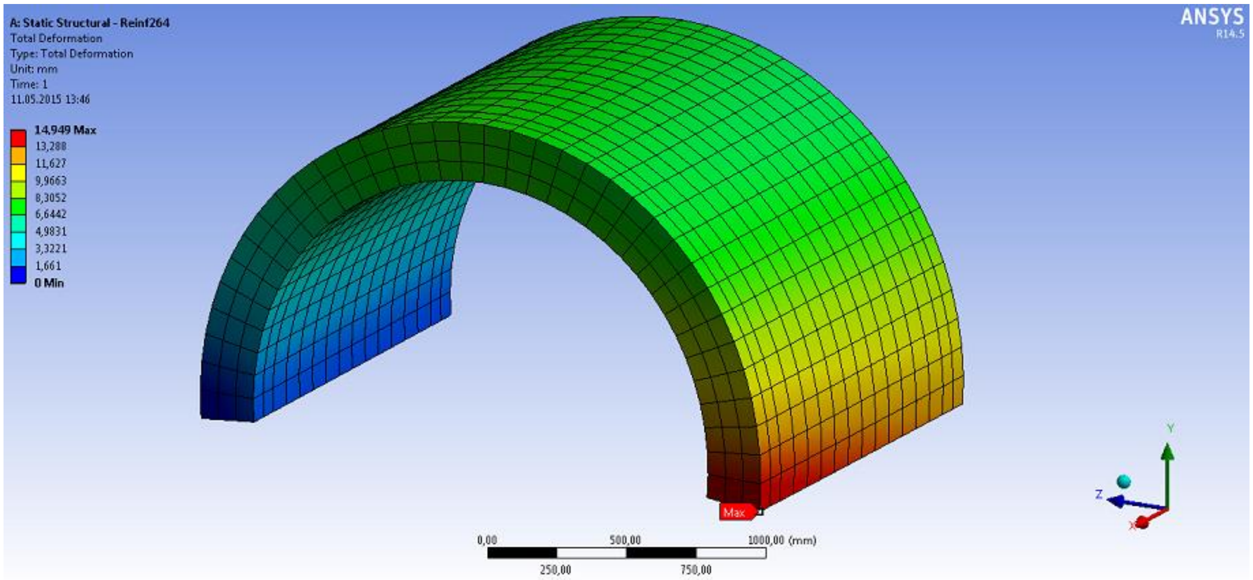

Figure 5.1.1-9 Total deformation plot for the Outer 1 load case.
Source: ***Ansys® Workbench, Release 14.5***

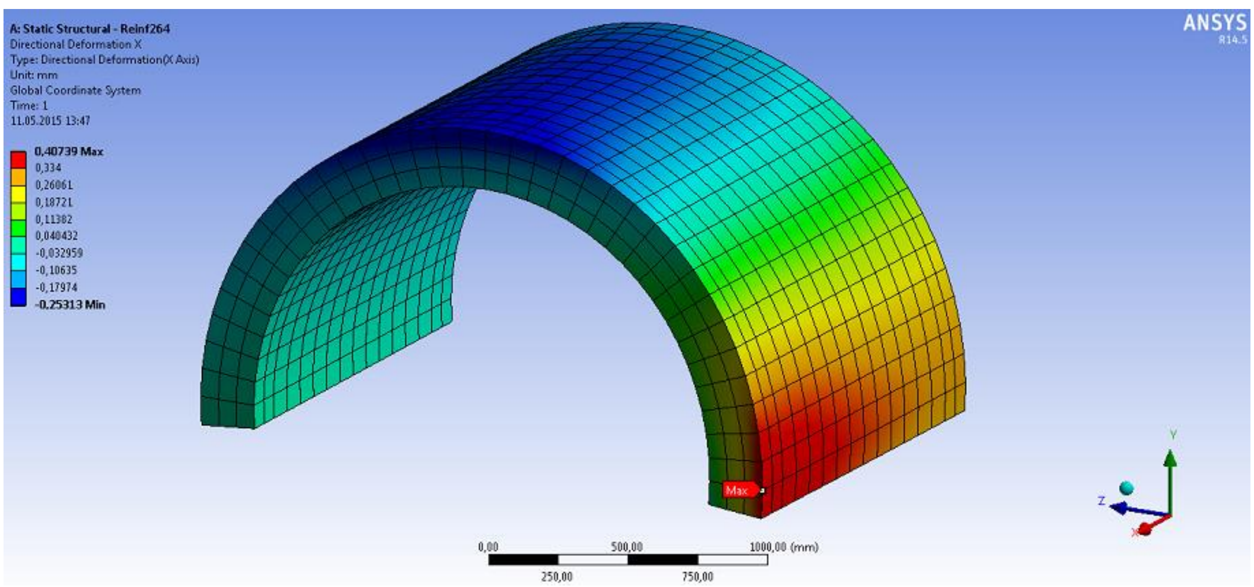

Figure 5.1.1-10 Deformation in X-direction plot for the Outer 1 load case.
Source: ***Ansys® Workbench, Release 14.5***

The plot of the deformation in the X-direction show a maximum deformation of 0,40 mm. The model is constrained in the X-direction in its supports in order to have a stable model, which means that this deformation in the X-direction is a result of a twisting motion on the cover because of the impact point of the cover. The result is however small and rather insignificant, and was thus not recorded in this thesis. This observation was similar for the rest of the load cases, and the deformation in X-direction was negligible there as well.

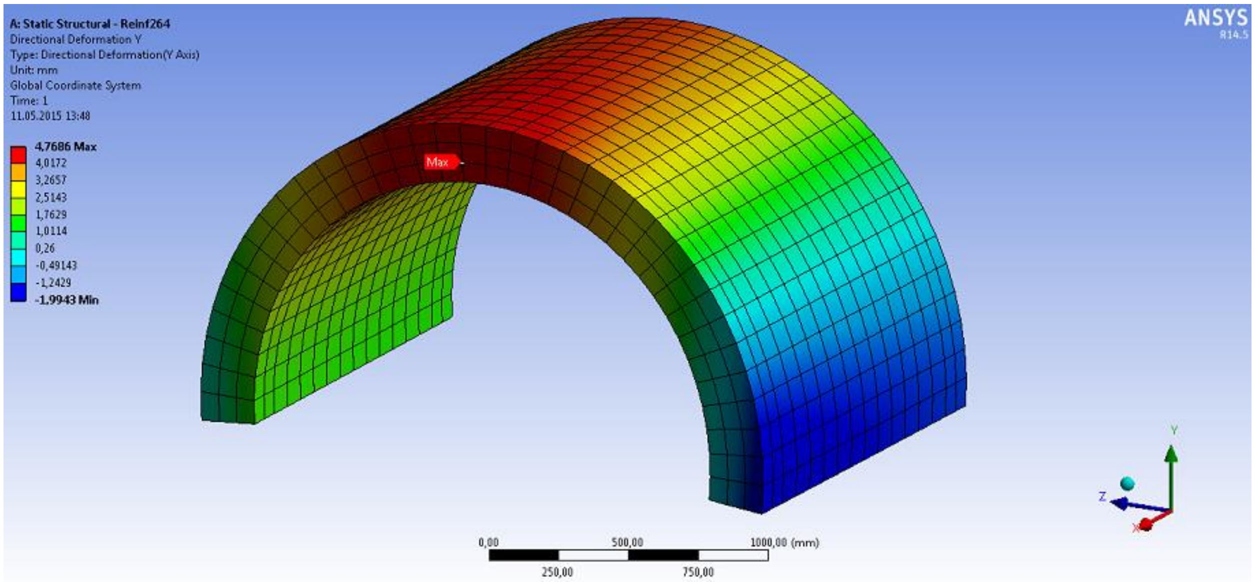

Figure 5.1.1-11 Deformation in Y-direction plot for the Outer 1 load case.
Source: ***Ansys® Workbench, Release 14.5***

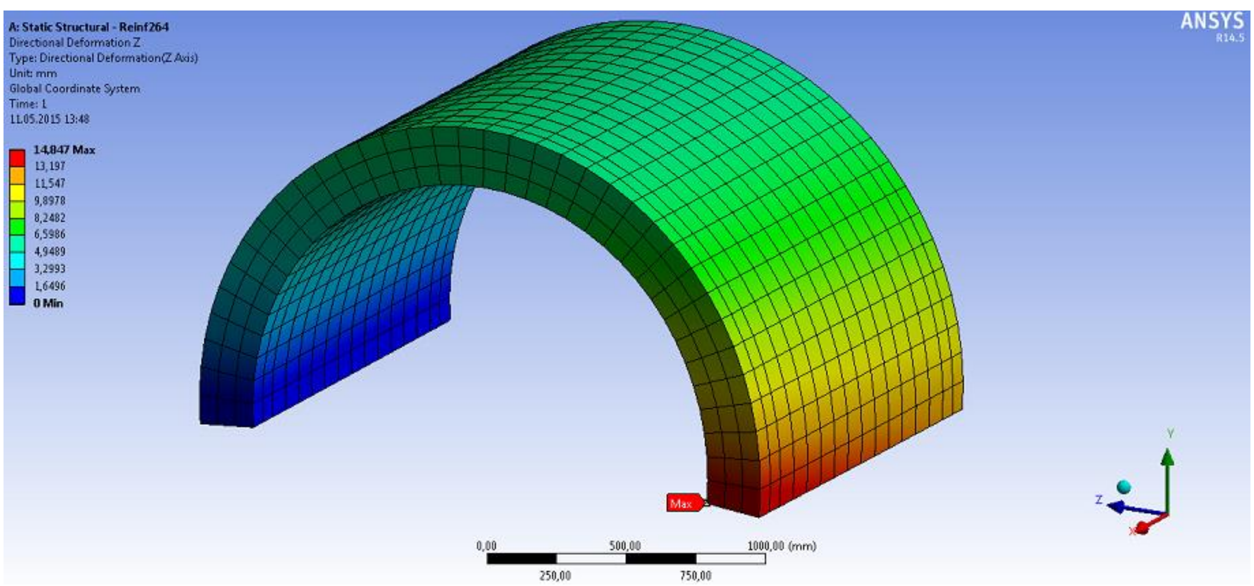

Figure 5.1.1-12 Deformation in Z-direction plot for the Outer 1 load case.
Source: ***Ansys® Workbench, Release 14.5***

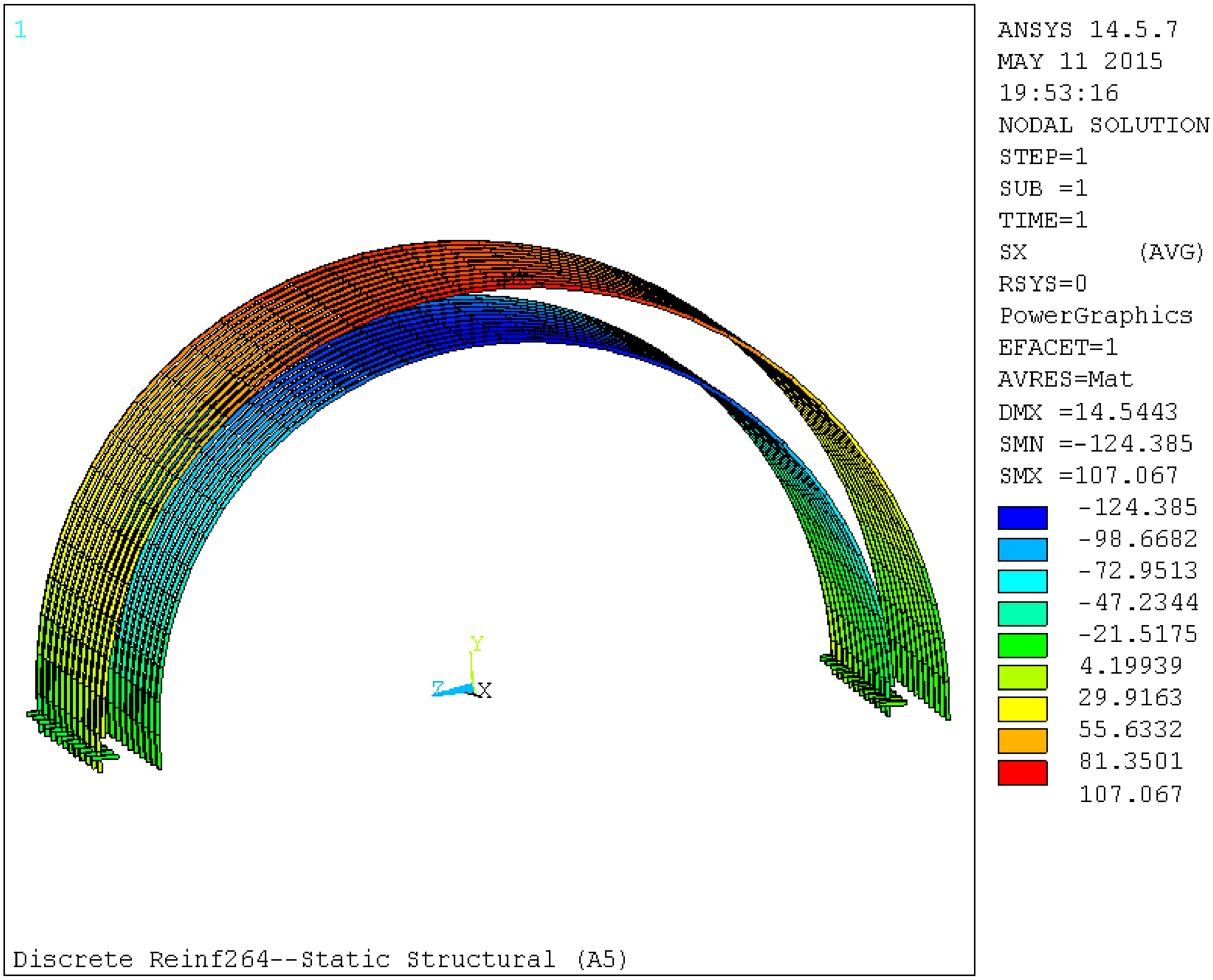

Figure 5.1.1-13 Plot of the stresses in reinforcement elements for the Outer 1 load case.
Source: ***Ansys® Workbench, Release 14.5***

In the stress plots of the reinforcement, the negative values, blue, mean compression, while the positive values, red, mean tension.

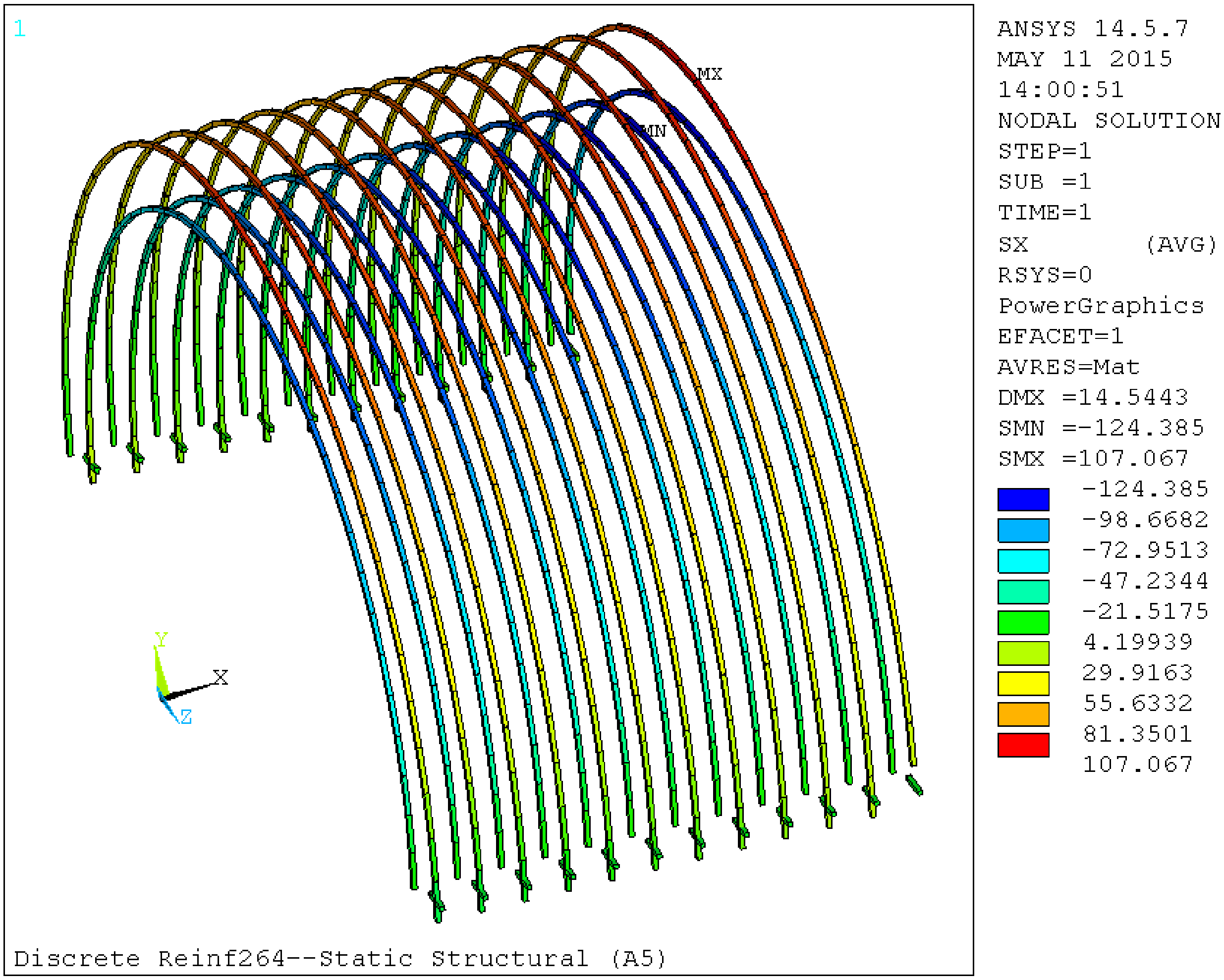

Figure 5.1.1-14 Plot of the stresses in reinforcement elements for the Outer 1 load case.
Source: *Ansys® Workbench, Release 14.5*

5.1.2 Dropped object impact test – Explicit Dynamics

The dropped object dynamic analysis was performed for four different dropped objects and impact energies. The results from the analyses are presented in Table 5.1.2-1 below. The results are also presented as bar graphs to illustrate the differences between the different impacts.

As expected, the 50 kJ impact results in the most damage, deformation and highest stresses on the cover. The resulting plots from this load case will be presented below. The rest of the plots can be seen in Appendix B Results from the Dropped object analysis *in Ansys® Workbench, Release 14.5*.

Table 5.1.2-1 The stress and deformation results from the dynamic dropped object analysis in *Ansys® Workbench, Release 14.5*.

Maximum values	**5 kJ**	**20 kJ**	**30 kJ**	**50 kJ**
Total Cover Deformation (mm)	3,44	15,23	28,50	59,37
Directional Deformation X (mm)	0,34	1,23	1,51	1,88
Directional Deformation Y (mm)	3,44	15,23	28,50	59,37
Directional Deformation Z (mm)	2,63	12,72	25,17	49,31
Equivalent Stress (von-Mises) (MPa)	15,63	33,37	39,07	42,53
Reinforcement Stress (User Defined Result) (MPa)	299,93	364,87	374,97	385,59

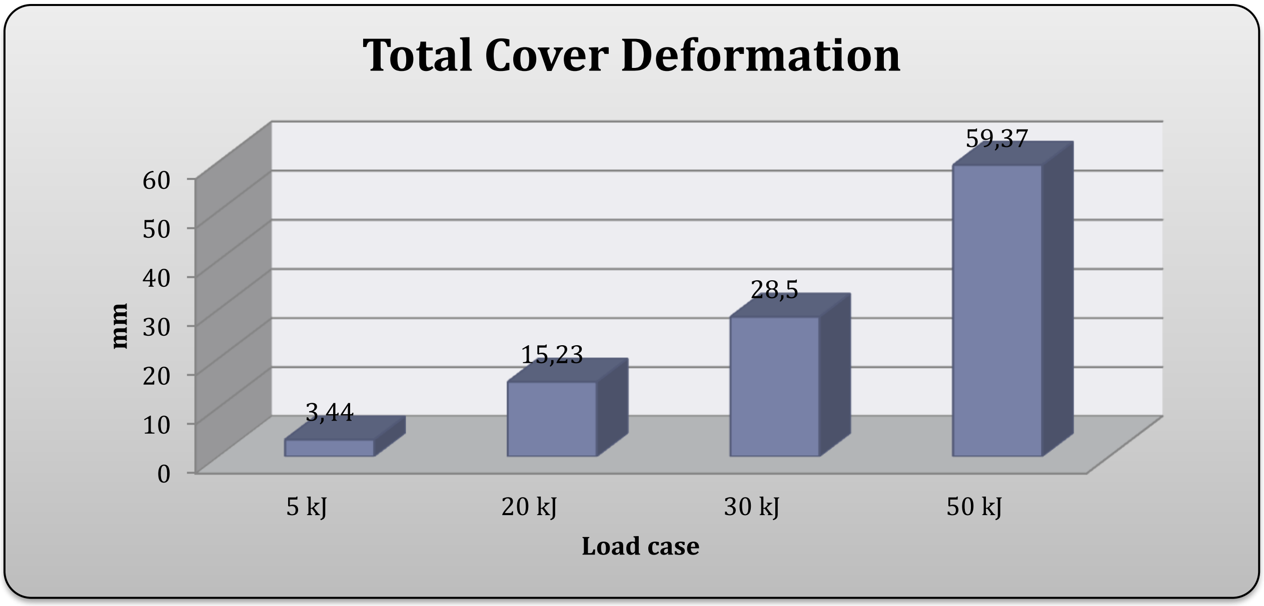

Figure 5.1.2-15 Total deformation results from the dynamic dropped object analysis.

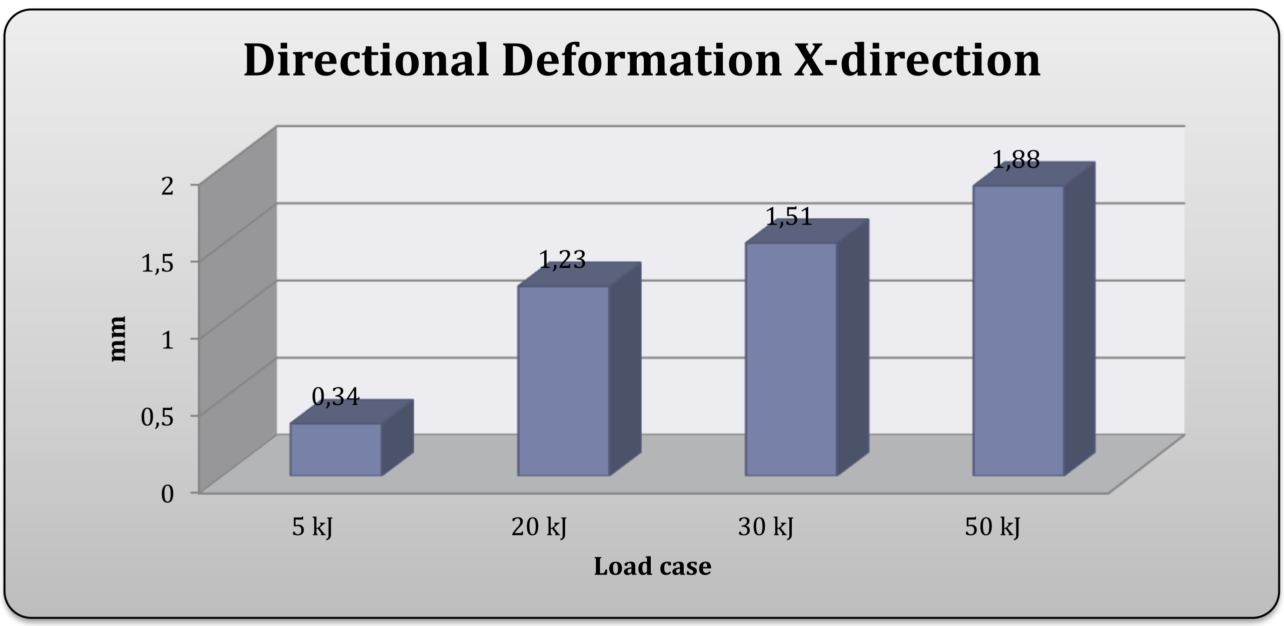

Figure 5.1.2-16 Deformation in X-direction results from the dynamic dropped object analysis.

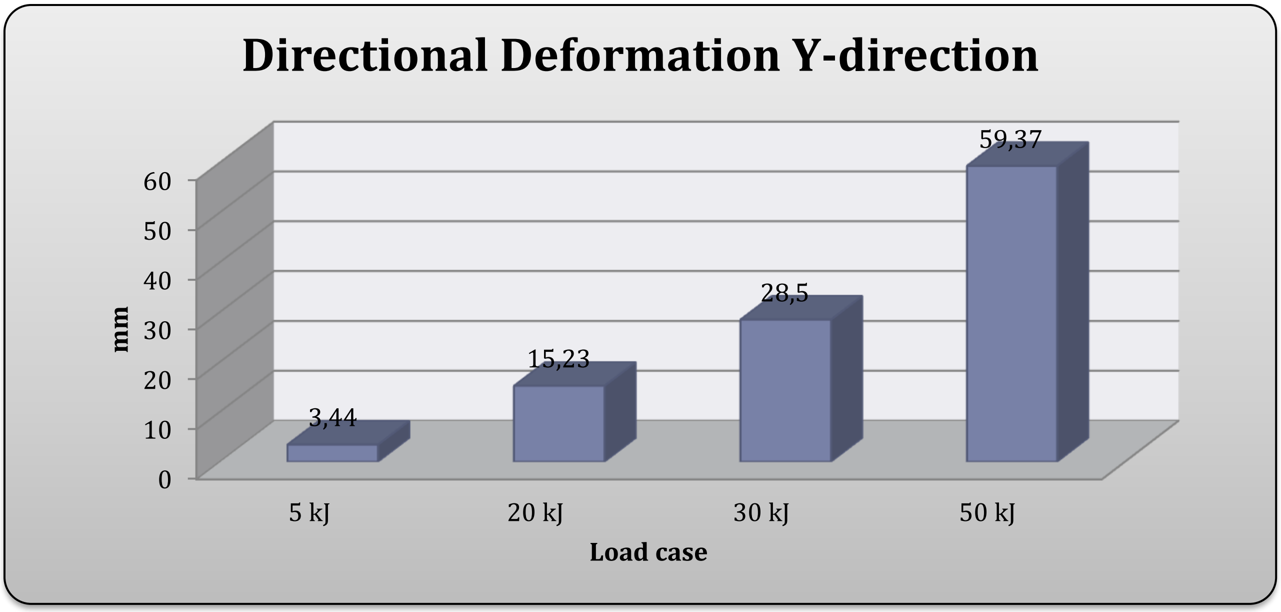

Figure 5.1.2-17 Deformation in Y-direction results from the dynamic dropped object analysis.

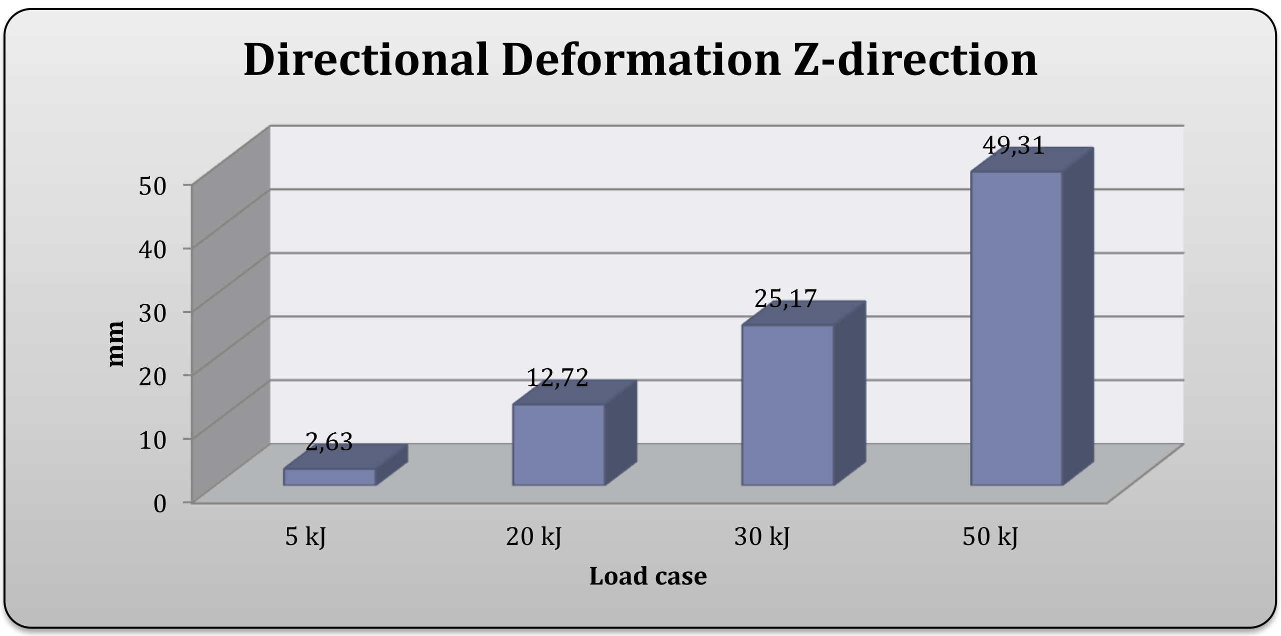

Figure 5.1.2-18 Deformation in Z-direction results from the dynamic dropped object analysis.

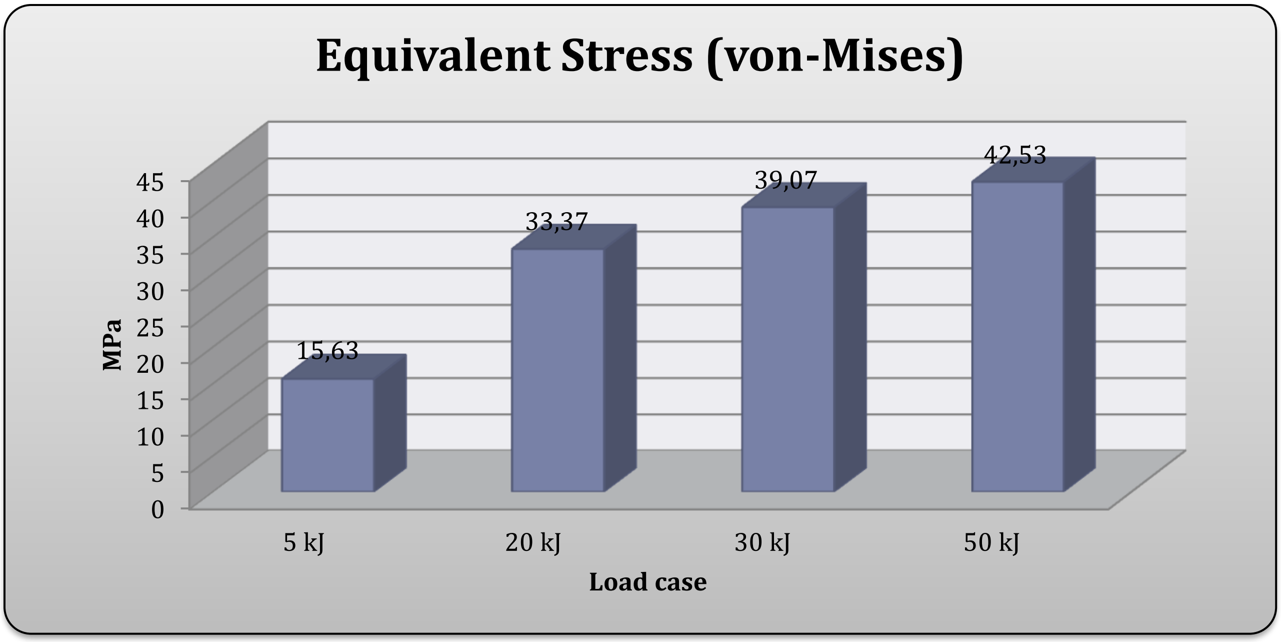

Figure 5.1.2-19 Equivalent stress results from the dynamic dropped object analysis.

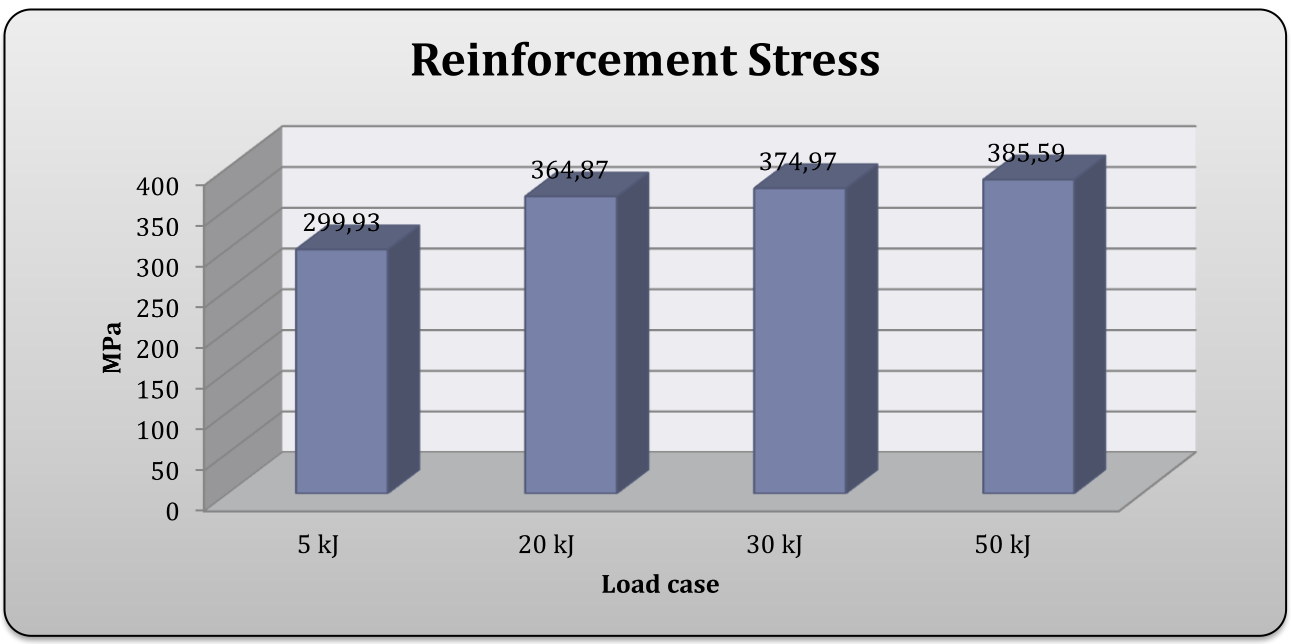

Figure 5.1.2-20 Reinforcement stress results from the dynamic dropped object analysis.

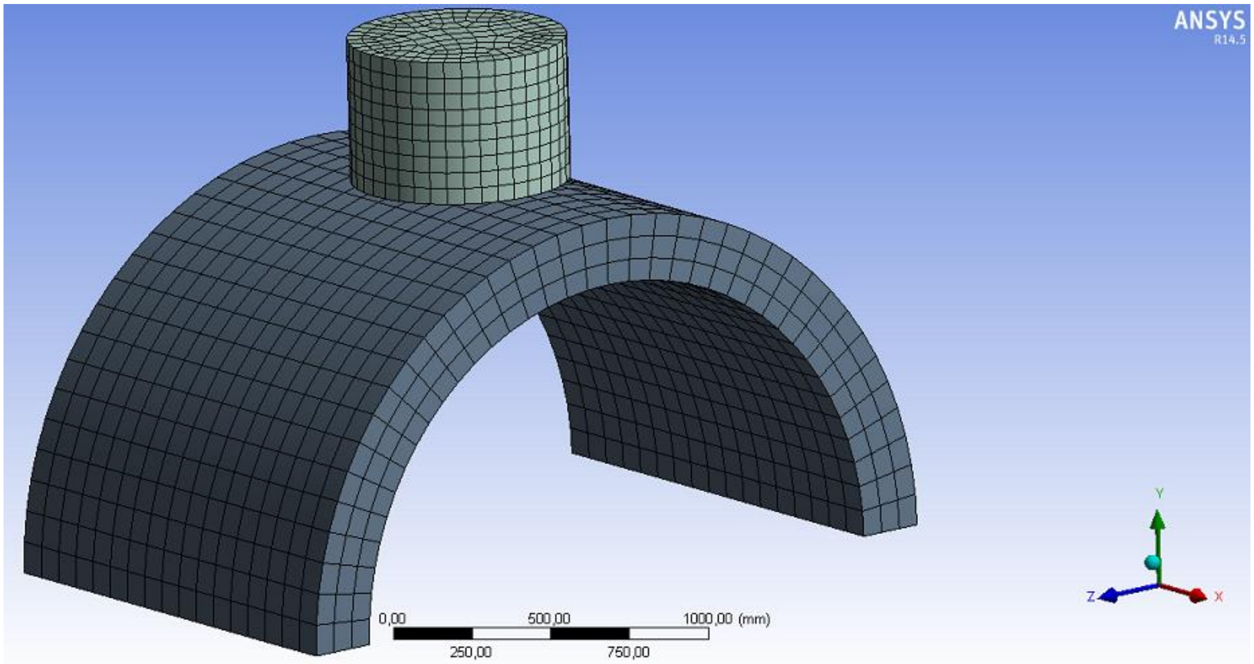

Figure 5.1.2-21 The mesh used in the 50 kJ dropped object simulation.
Source: ***Ansys® Workbench, Release 14.5***

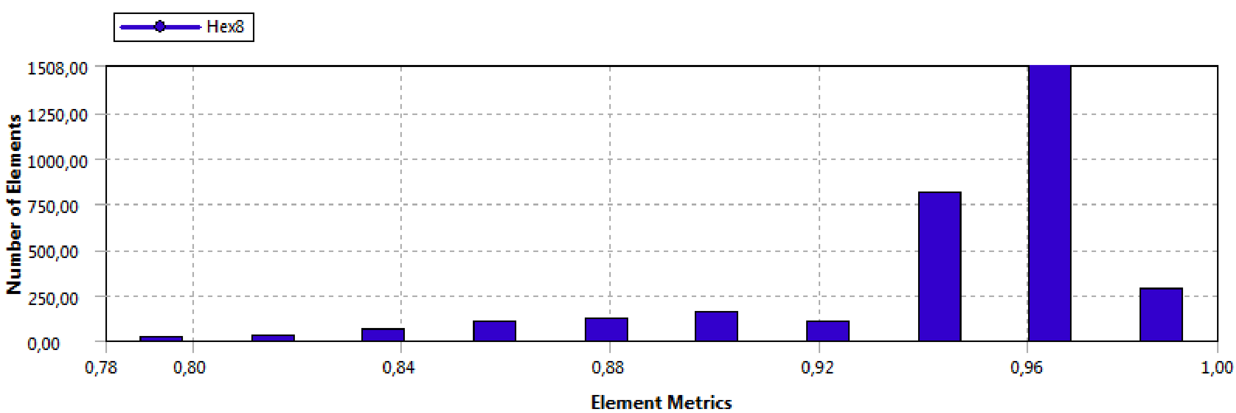

Figure 5.1.2-22 The mesh metrics from the 50 kJ impact in the dropped object simulation.
Source: ***Ansys® Workbench, Release 14.5***

The energy summary in Figure 5.1.2-24 shows that all the kinetic energy has been absorbed by the cover and been transformed to internal energy. The summary shows that some stabilizing hourglass energy has been added to the system, but it is within the acceptable limits.

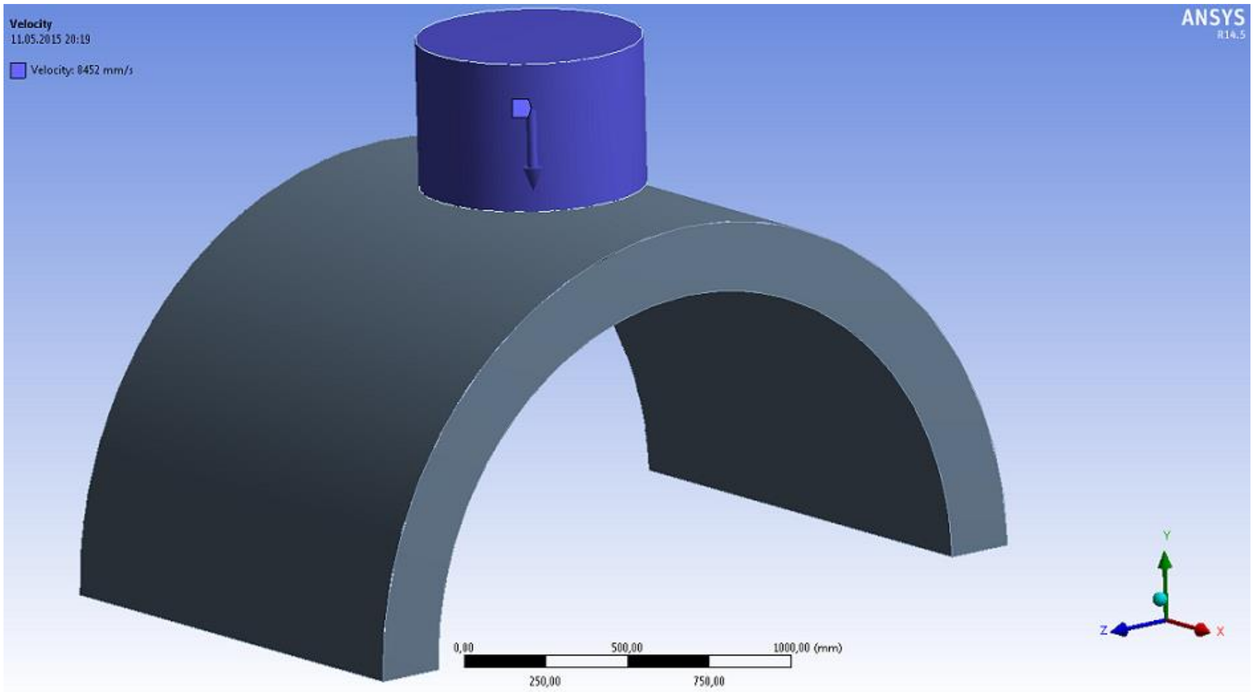

Figure 5.1.2-23 The velocity (8452 mm/s) of the object used in the 50 kJ dropped object simulation.
Source: *Ansys® Workbench, Release 14.5*

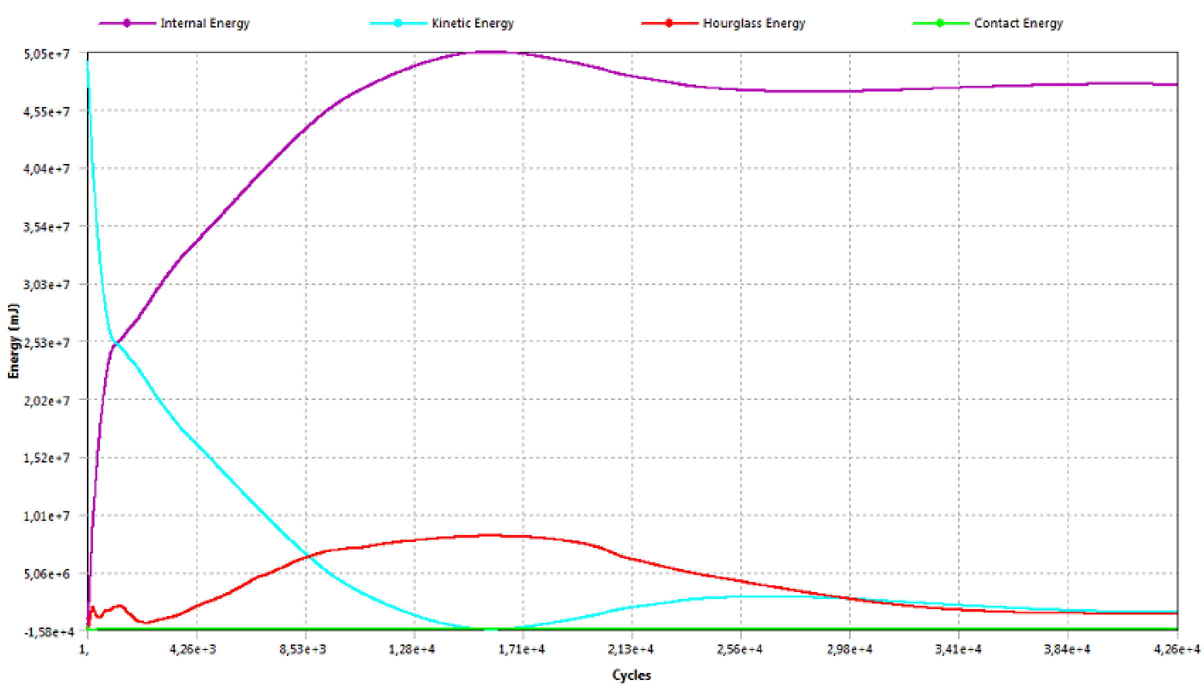

Figure 5.1.2-24 The energy summary of the 50 kJ dropped object simulation.
Source: *Ansys® Workbench, Release 14.5*

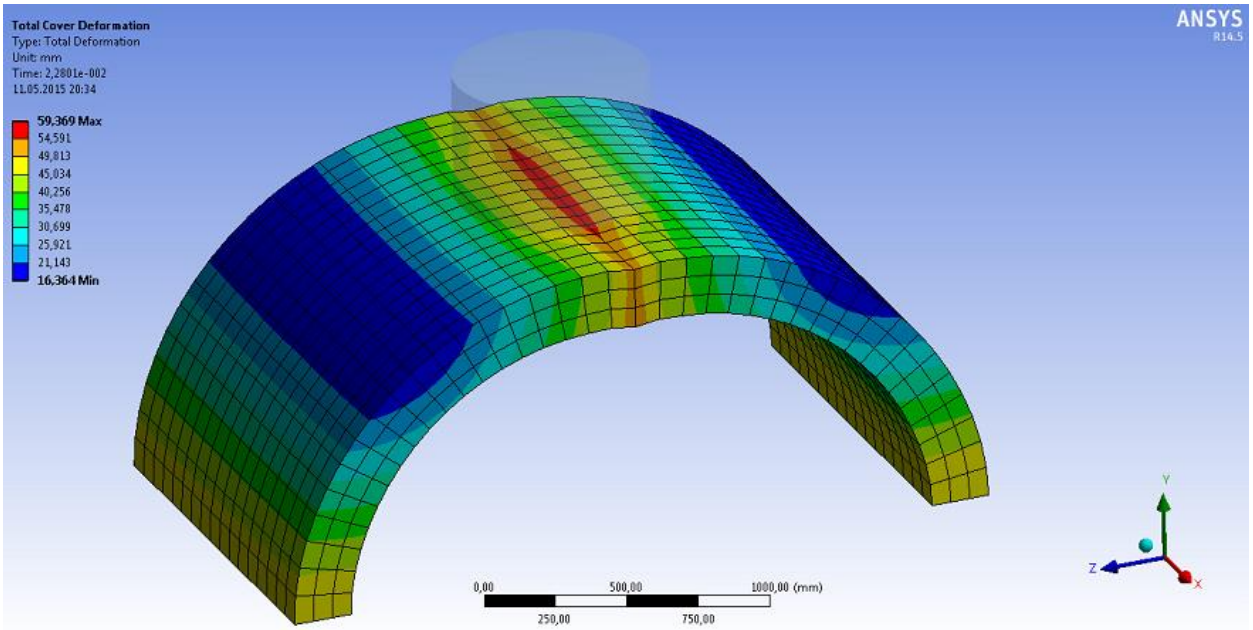

Figure 5.1.2-25 The total deformation of the cover due to the 50 kJ impact seen from above. Source: ***Ansys® Workbench, Release 14.5***

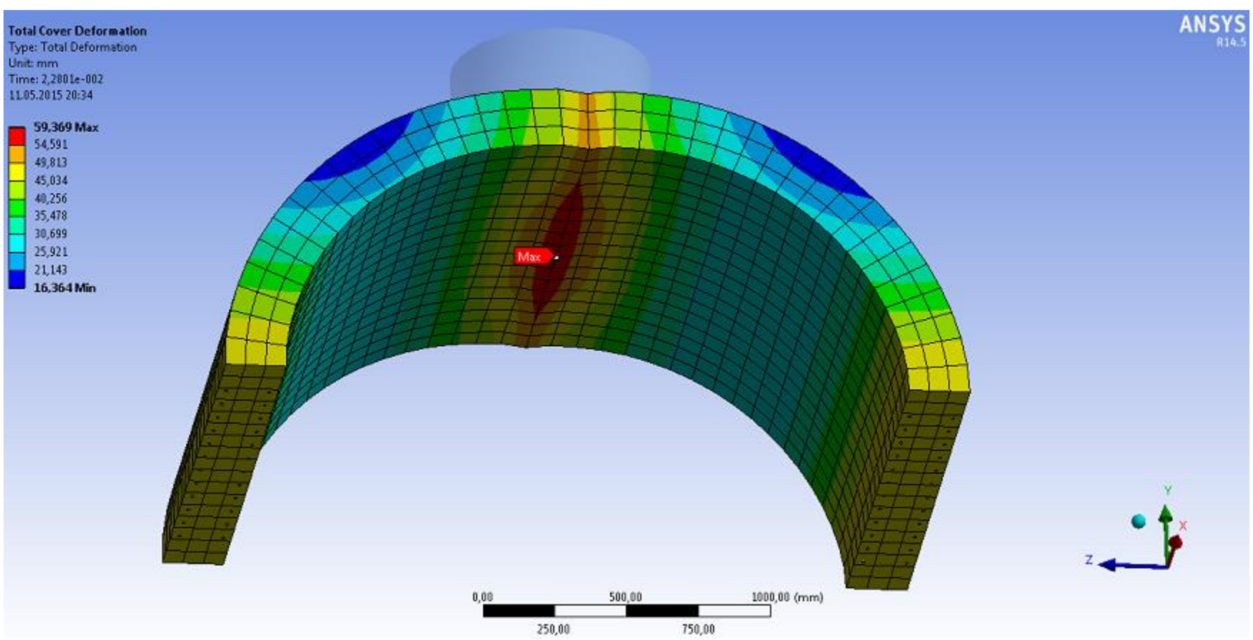

Figure 5.1.2-26 The total deformation of the cover due to the 50 kJ impact seen from underneath. Source: ***Ansys® Workbench, Release 14.5***

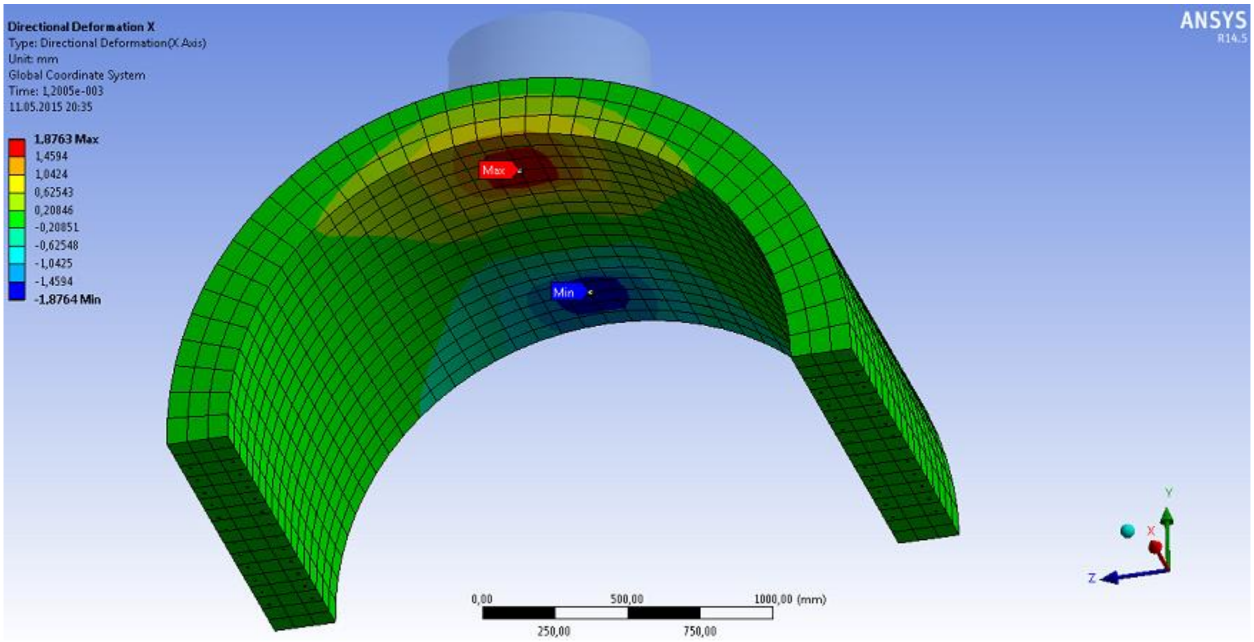

Figure 5.1.2-27 The deformation of the cover in X-direction due to the 50 kJ impact.
Source: ***Ansys® Workbench, Release 14.5***

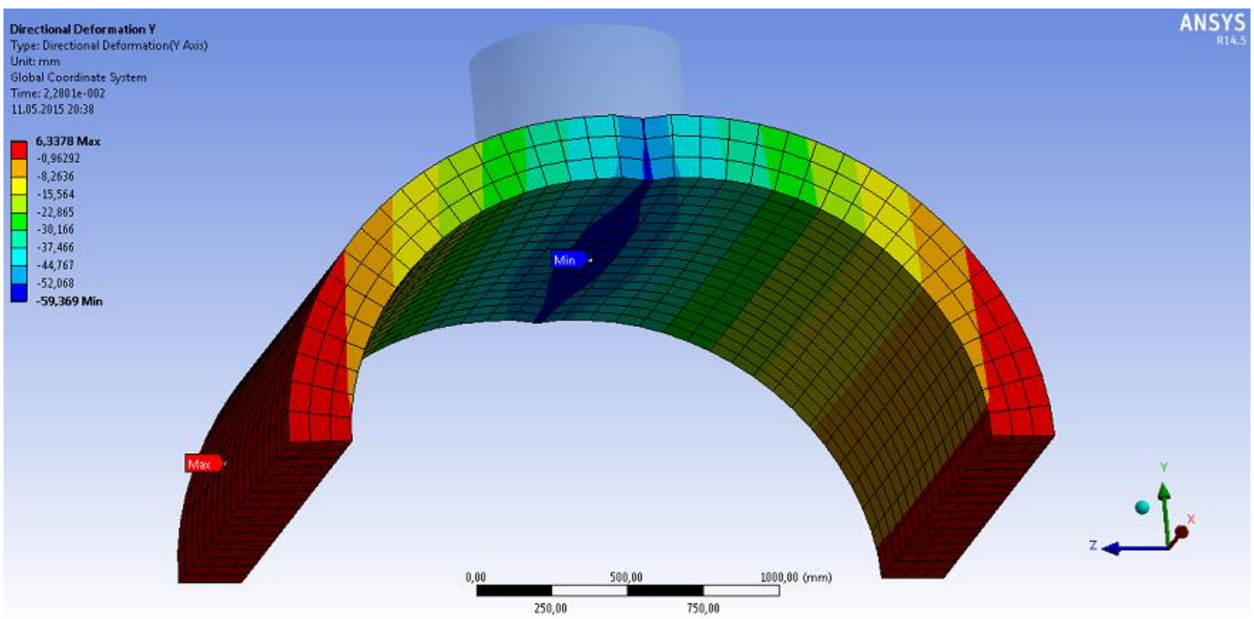

Figure 5.1.2-28 The deformation of the cover in Y-direction due to the 50 kJ impact.
Source: ***Ansys® Workbench, Release 14.5***

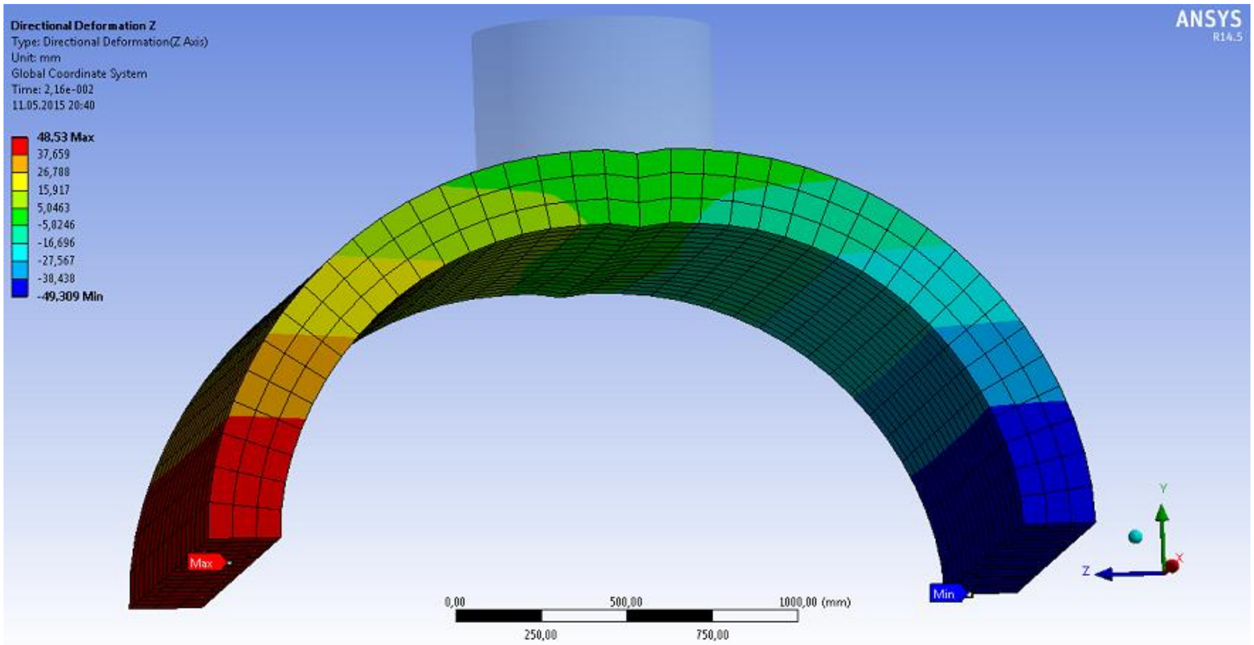

Figure 5.1.2-29 The deformation of the cover in Z-direction due to the 50 kJ impact.
Source: ***Ansys® Workbench, Release 14.5***

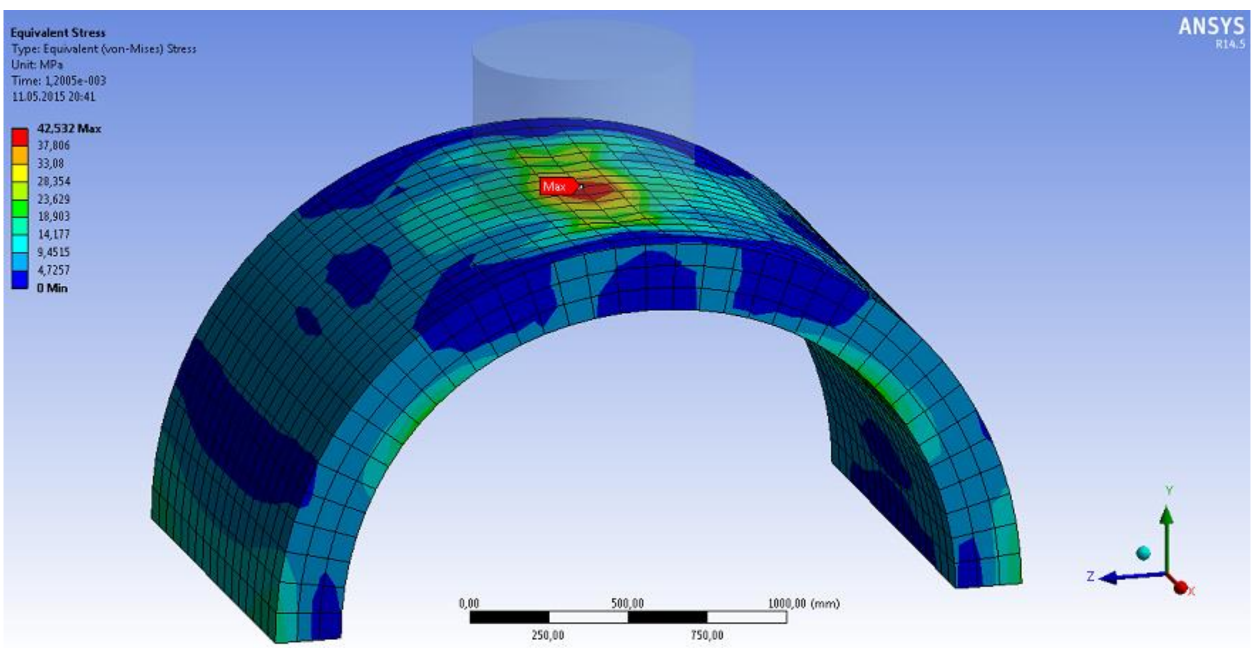

Figure 5.1.2-30 The maximum stresses in the cover due to the 50 kJ impact.
Source: ***Ansys® Workbench, Release 14.5***

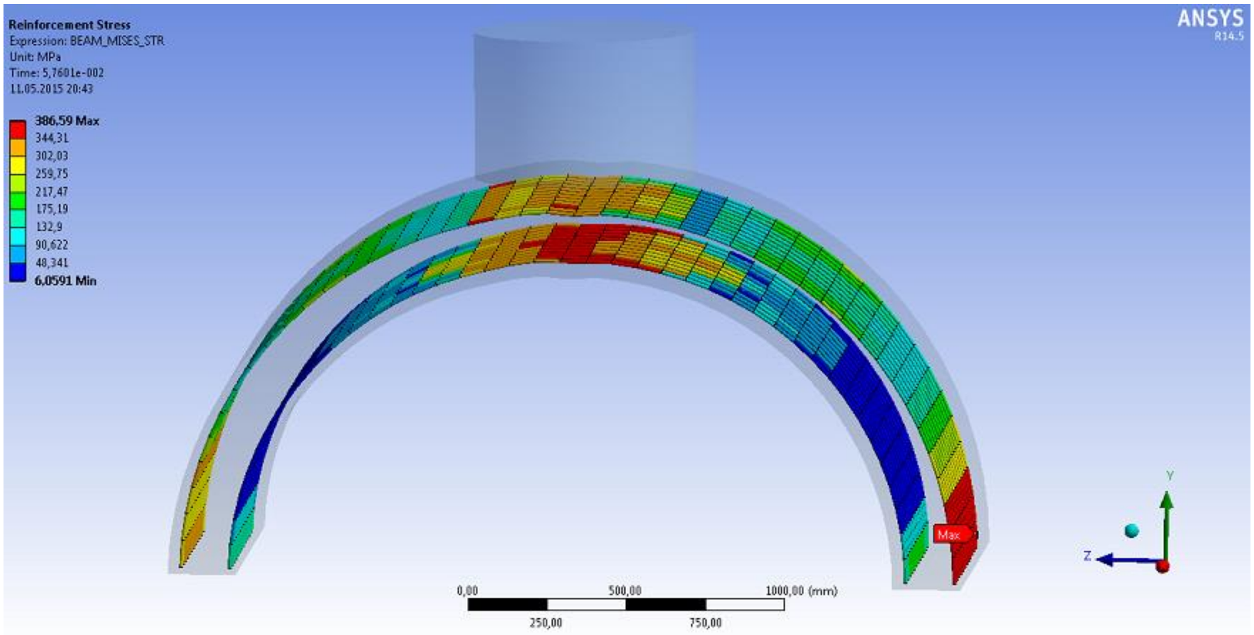

Figure 5.1.2-31 The maximum stresses in the reinforcement due to the 50 kJ impact.
Source: *Ansys® Workbench, Release 14.5*

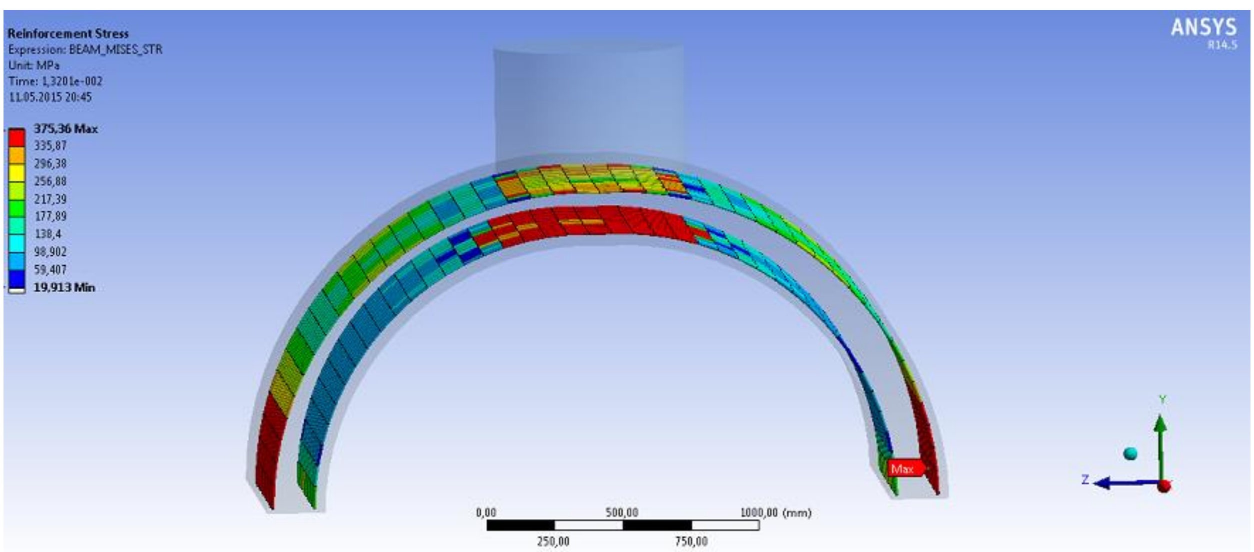

Figure 5.1.2-32 Stresses in the reinforcement momentarily after impact of the 50 kJ impact.
Source: *Ansys® Workbench, Release 14.5*

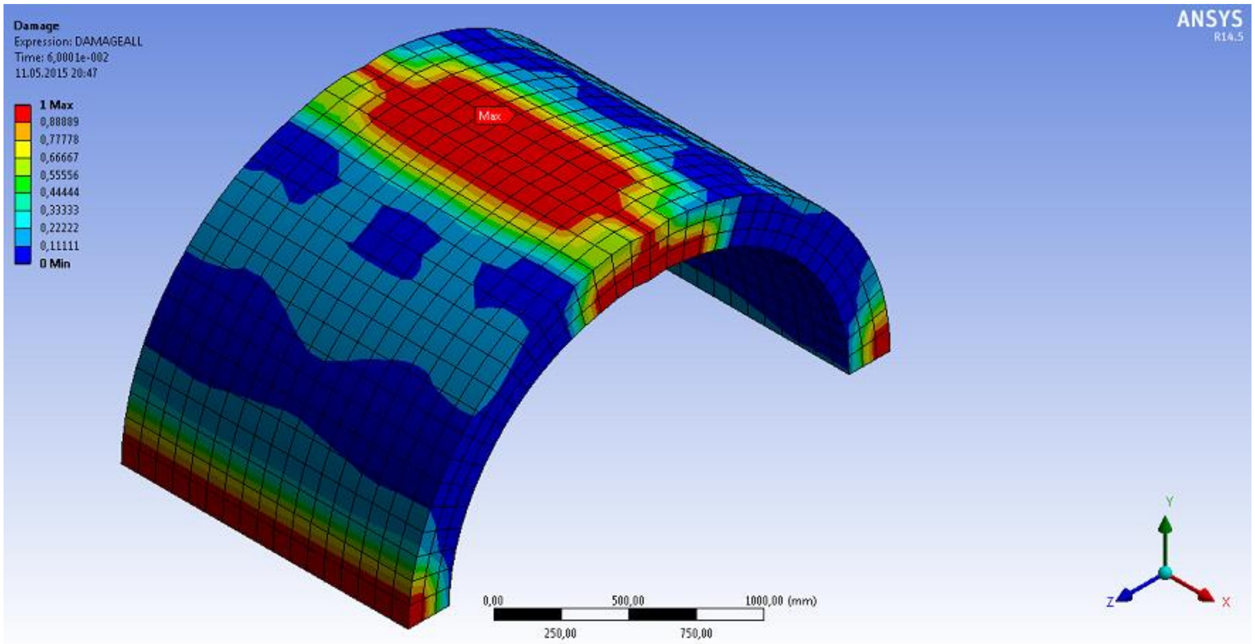

Figure 5.1.2-33 The damage on the concrete material as described in paragraph 4.1.2.3.2.4 after the 50 kJ impact. The color red and value 1 means fully fractured material.
Source: ***Ansys® Workbench, Release 14.5***

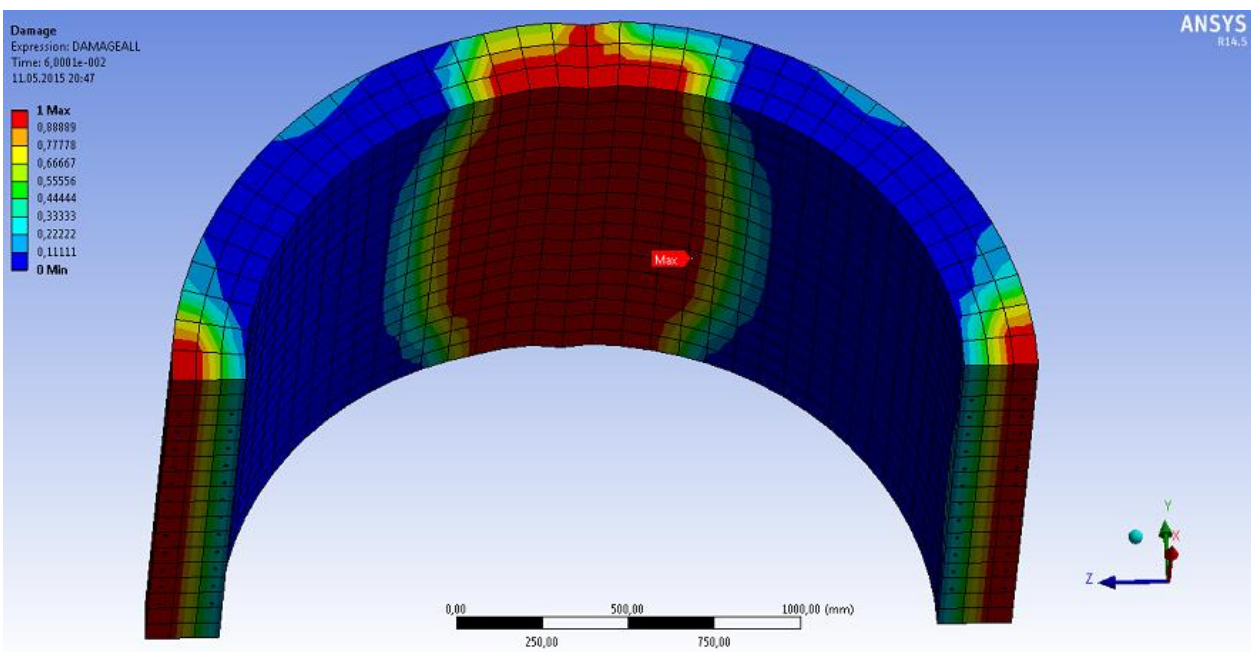

Figure 5.1.2-34 The damage on the concrete material as described in paragraph 4.1.2.3.2.4 after the 50 kJ impact. Source: ***Ansys® Workbench, Release 14.5***

5.2 Stability Calculations

As explained shortly in chapter 5.1.1, the reaction forces in the analyses show that the mass of the 1,5m long protection cover is not enough to be stable on its own upon impact from the trawl force.

Calculations on the stability of the cover was performed, assuming a simply supported system of static equilibrium equal to that of the model in *Ansys® Workbench, Release 14.5*. An assumption of impact height = 0,5 m from the ground on the cover is made. It would also be possible to assume that the supports were in reality in the middle of the legs, or trawl deflectors, for a positive effect, but it was decided to keep the supporting conditions equal to the finite element analysis for comparison of the results. Note also the fact that these calculations include the effects of buoyancy and its effective reduction of mass, which the finite element analysis does not include. For the complete set of calculations, see Appendix C Stability Calculations.

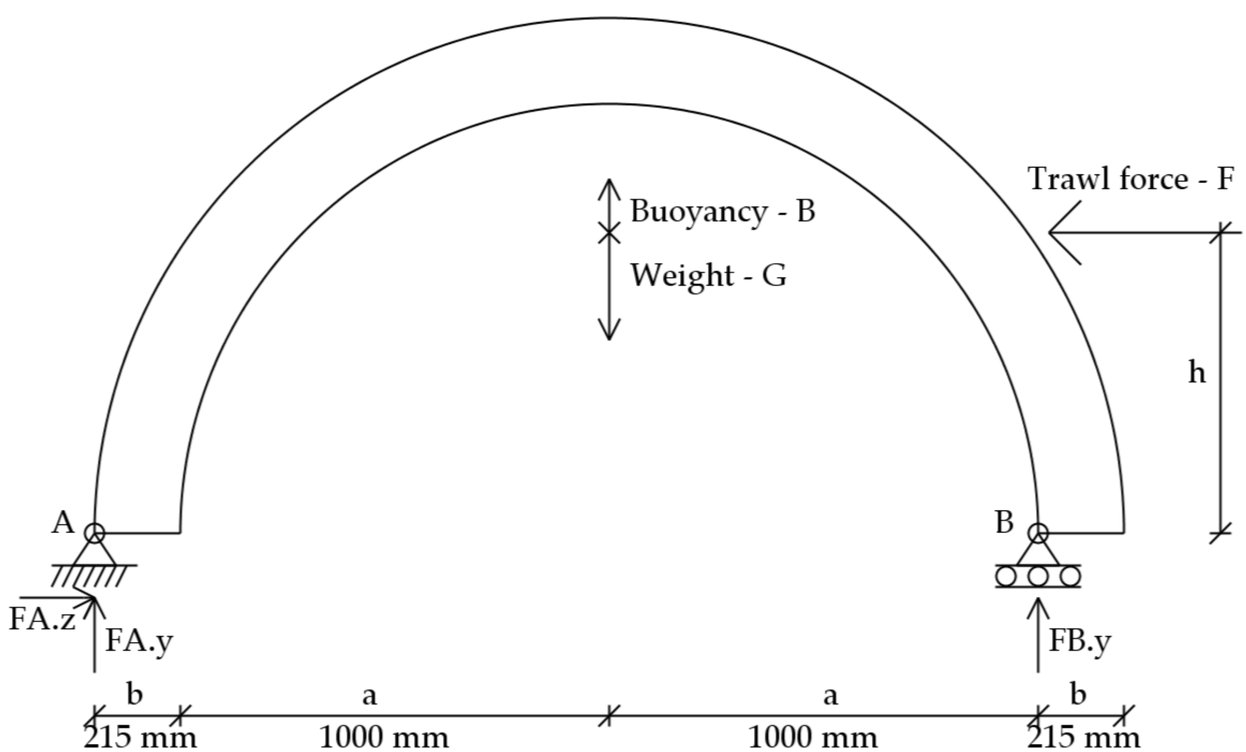

Figure 5.2-35 The system of static equilibrium set up to investigate the stability issue.

The calculations show that for the cover of 1,5 m length the negative reaction force in the F_B is approximately -59 kN, which is relatable to the reaction forces from the finite element analysis in chapter 5.1.1. This would mean that for this cover to be stable on its own when the impact height of the force is 0,5 m, an added mass of approximately 6 tons would need to be added. At this point, the cover weighs approximately 2,7 tons with an effective weight of 1,5 tons including buoyancy.

The next assessment takes into account the positive effect from the trawl board deflectors, see Figure 5.2-36. The deflectors have been modeled in *Ansys® Workbench, Release 14.5* and distances and volumes have been found from the model. The pinned support is moved, as the new tipping point is moved to the tip of the deflector, and the roll support is kept at the same position. This increases the mass of the cover by about 1,2 tons, and increases the distance between the supports.

The resulting negative reaction force F_B is approximately -41 kN. The trawl deflectors and the added mass has had a positive effect, but not enough for the cover to be stable on its own. Still approximately 4,2 tons of effective mass is needed for it to be stable. At this point, the cover weighs approximately 3,8 tons with an effective weight of 2,2 tons including buoyancy.

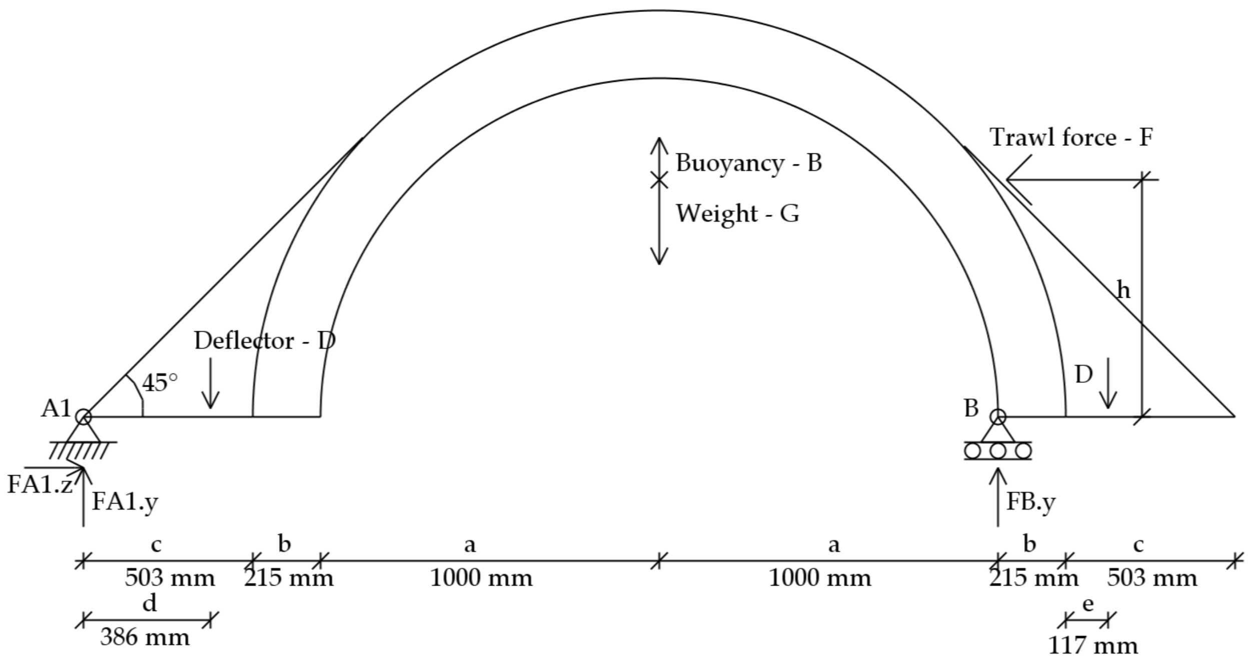

Figure 5.2-36 The system of static equilibrium including the trawl deflectors set up to investigate the stability issue.

Thus, in a real situation, the cover will need to be longer in the X-direction than 1,5 m. The typical length for GRP protection covers is in the area of 5 m to 8 m, depending on several factors. As the cover analysed is only 1,5 m, there is no question of why the reaction force in the roll support is negative and is holding down the cover; it simply weighs far too little in comparison to the magnitude of the trawl force.

By assuming the length of the cover is 6,5 m, and still including the trawl deflectors and impact height 0,5 m, the vertical reaction force F_B turns to a positive 3,8 kN. This means that the cover has approximately 380 kg of mass more than needed to be in equilibrium due to the trawl force. The mass of the cover is at this point, assuming a massive structure of concrete, 16,6 tons, with an effective weight of 9,5 tons including buoyancy.

5.3 2D model in *STAAD.Pro V8i*

The analysis of the simple 2D beam model in *STAAD.Pro V8i* resulted in the following summary of maximum shear forces F_y, axial forces F_x and bending moments M_z.

All | Summary | Envelope

	Beam	L/C	Node	Fx kN	Fy kN	Fz kN	Mx kNm	My kNm	Mz kNm
Max Fx	13	18 LOAD CA	14	**337.026**	-2.986	0.000	0.000	0.000	201.072
Min Fx	36	18 LOAD CA	37	**-137.456**	5.668	0.000	0.000	0.000	0.549
Max Fy	36	1 LOAD CAS	37	24.202	**299.257**	0.000	0.000	0.000	29.051
Min Fy	1	1 LOAD CAS	3	25.736	**-299.129**	-0.000	-0.000	-0.000	29.045
Max Fz	1	1 LOAD CAS	2	26.436	-299.096	**0.000**	0.000	0.000	0.000
Min Fz	1	1 LOAD CAS	2	26.436	-299.096	**0.000**	0.000	0.000	0.000
Max Mx	1	1 LOAD CAS	2	26.436	-299.096	0.000	**0.000**	0.000	0.000
Min Mx	1	1 LOAD CAS	2	26.436	-299.096	0.000	**0.000**	0.000	0.000
Max My	1	1 LOAD CAS	2	26.436	-299.096	0.000	0.000	**0.000**	0.000
Min My	1	1 LOAD CAS	2	26.436	-299.096	0.000	0.000	**0.000**	0.000
Max Mz	18	1 LOAD CAS	20	299.745	-12.363	-0.000	-0.000	-0.000	**327.047**
Min Mz	18	19 LOAD CA	20	-0.000	-0.003	-0.000	-0.000	-0.000	**-5.053**

Figure 5.3-37 Summary of the shear forces, axial forces and moments from *STAAD.Pro V8i*

Table 5.3-1 The relevant maximum shear forces, axial forces and moments from Figure 5.3-37

	Force or moment	Load case	Beam	Figure
Axial - Fx	Max: 337,026 kN	18 (at the top)	13 (upper left)	Figure 5.3-38
	Min: -137,456 kN		36 (lower right)	
Shear - Fy	Max: 299,257 kN	1 (at the bottom)	36 (lower left)	Figure 5.3-39
	Min: 299,129 kN		1 (lower right)	
Moment - Mz	Max: 327,047 kNm	1 (at the bottom)	18 (top beam)	Figure 5.3-40

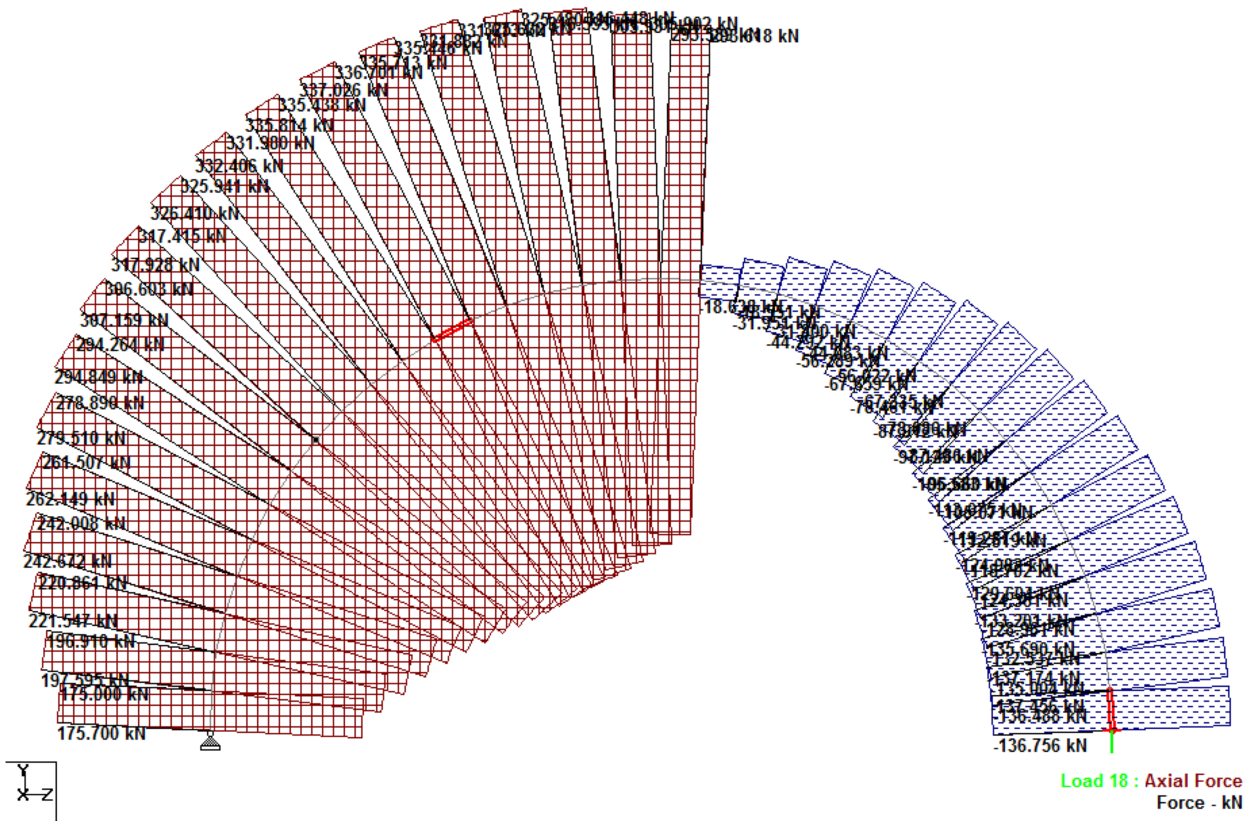

Figure 5.3-38 The distribution of axial forces in load case 18 (impact at the top). The beams with maximum and minimum axial forces are marked red. Source: *STAAD.Pro V8i*

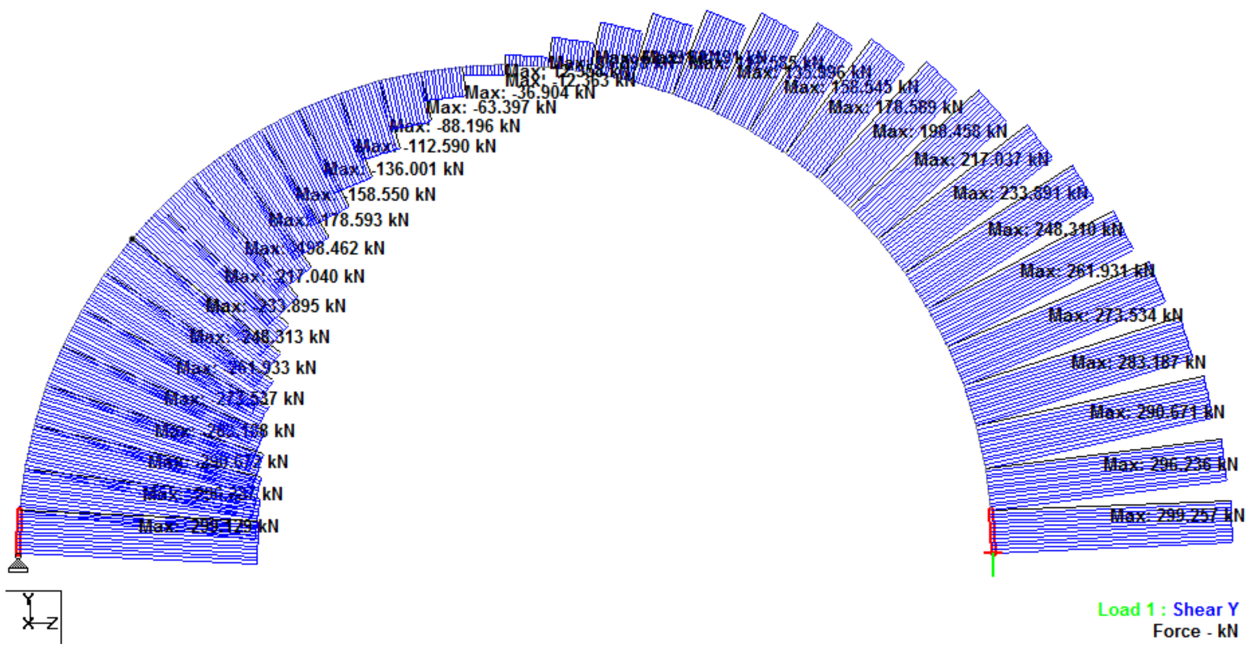

Figure 5.3-39 The distribution of shear forces in load case 1 (impact at the bottom). The beams with maximum and minimum shear forces are marked red. Source: *STAAD.Pro V8i*

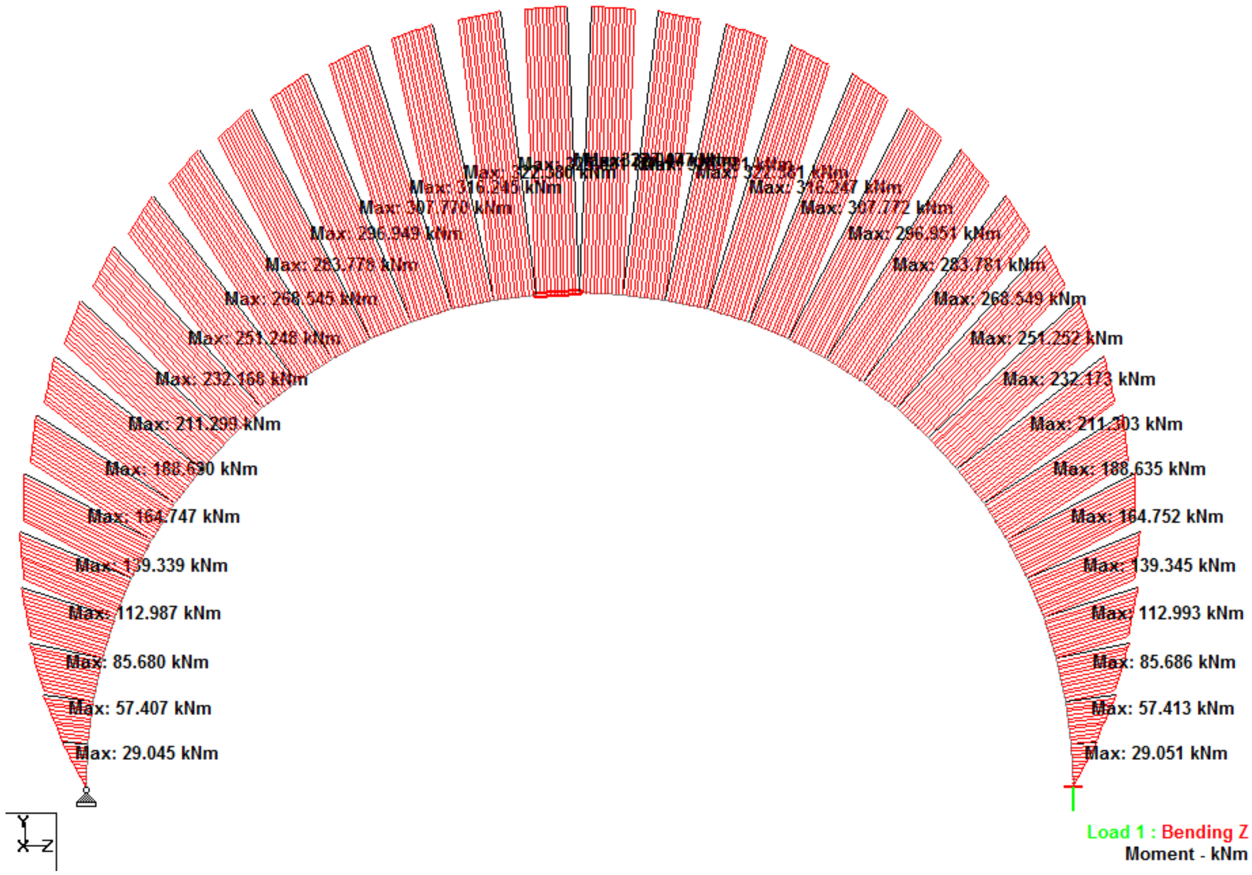

Figure 5.3-40 The distribution of moments in load case 1 (impact at the bottom). The beam with the maximum moment is marked red. Source: *STAAD.Pro V8i*

The *STAAD.Pro V8i* model also confirms the approximate location of maximum stress at the top left side, on the opposite side of the applied force. The values of the stress are not included as the sections of the beams are not representable of the protection cover. The location of the maximum point is however fairly similar to the load cases from the finite element analysis, as this one also moves from the centre to the left the higher up on the cover the load impacts.

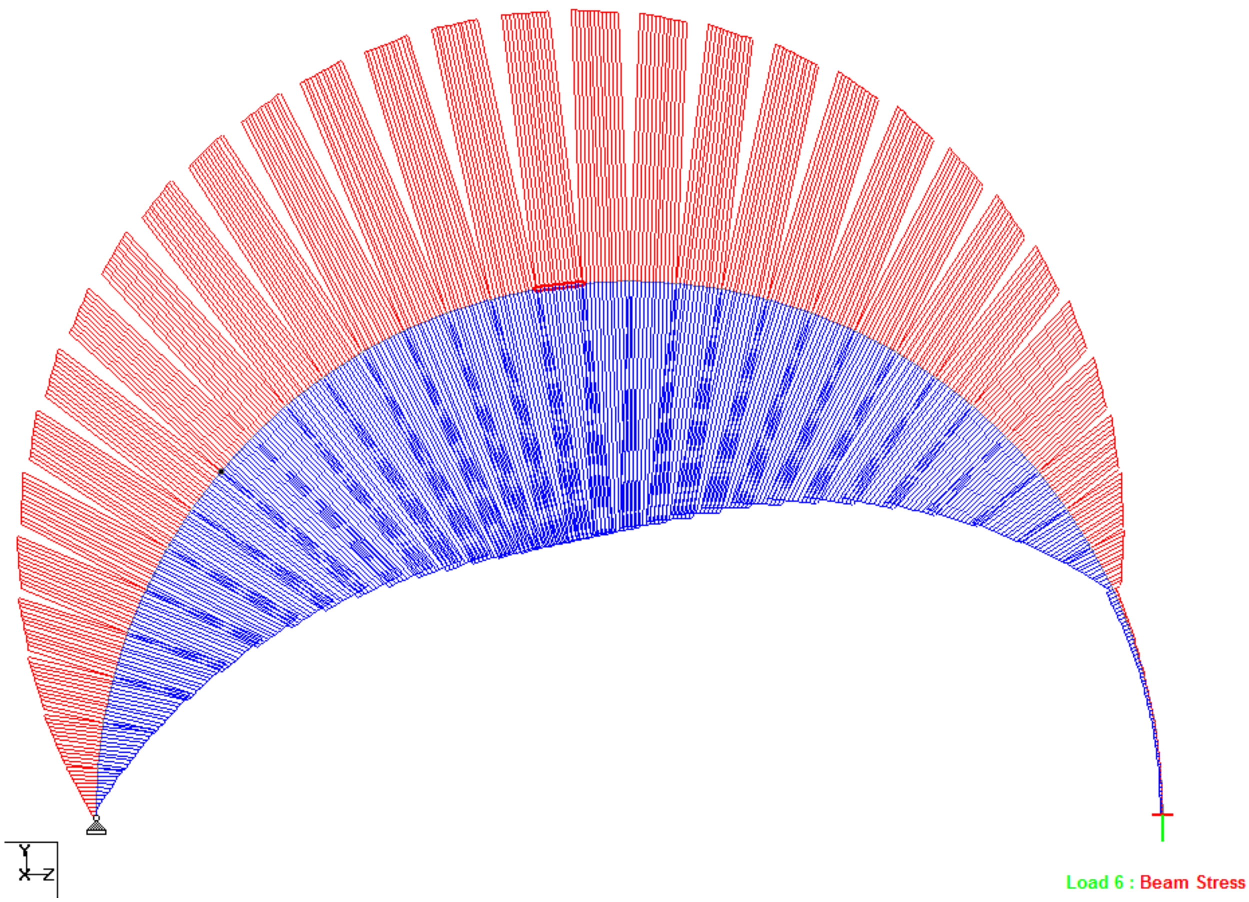

Figure 5.3-41 Stress distribution of the beam model. Location of max stress is located in red beam. Source: *STAAD.Pro V8i*

Figure 5.3-42 Reaction forces for Load Case 1 (impact at the bottom) are as expected. Source: *STAAD.Pro V8i*

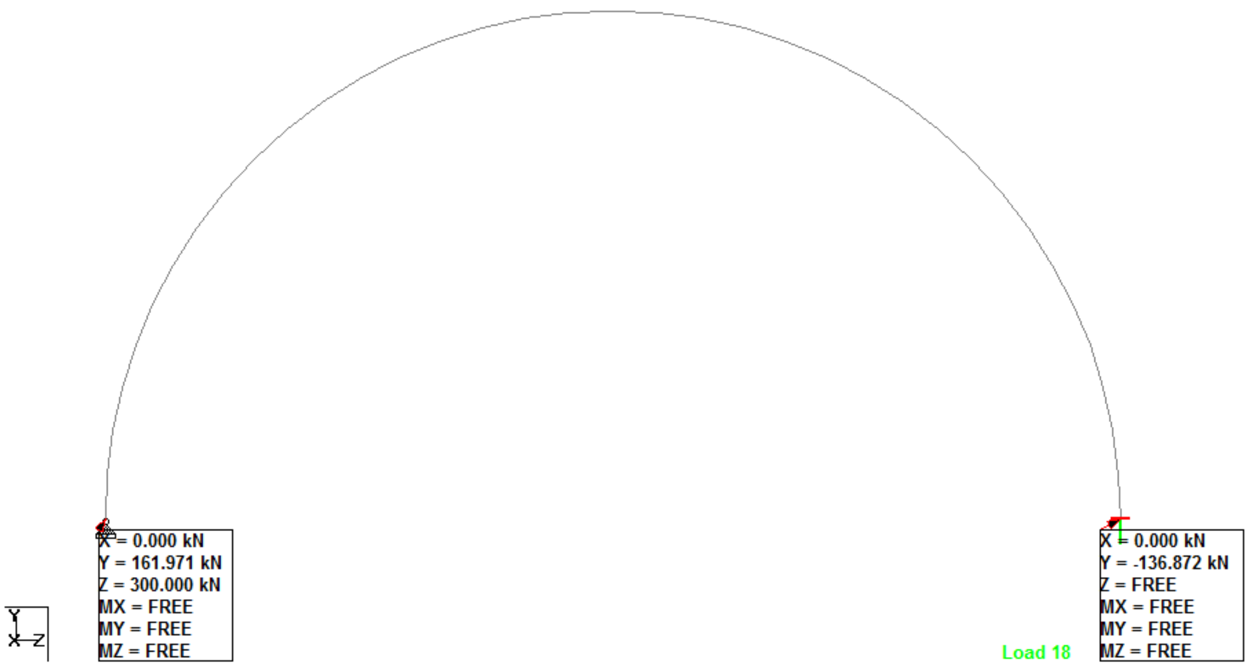

Figure 5.3-43 Reaction forces for Load Case 18 (impact at the top) is as expected in regards to negative reaction force due to tipping moment. Source: *STAAD.Pro V8i*

5.4 Concrete and reinforcement design according to *Eurocode 2*

The following is a summary of the results from the attempt at design of the cover according to the *Eurocode 2* design code (Norsk Standard, 2004). For the complete set of calculations, see Appendix E Concrete and reinforcement design calculations according *to Eurocode 2*.

5.4.1 Cover, material data and design loads from STAAD.Pro V8i

The calculations are based on the cover being 1,5 m long, without trawl deflectors. The strength class of the concrete is set to B40 and reinforcement B500NC is assumed. The design force of F = 300 kN is from *NORSOK standard U-001*. From *STAAD.Pro V8i*, the design forces and moments are

M_{Ed} = 327 kNm V_{Ed} = 299 kN N_{Ed} = 337 kN

5.4.2 Concrete cover of reinforcement requirements

The requirements to concrete cover of the reinforcement are given in EC2 §4.4.1 (Norsk Standard, 2004). The minimum concrete cover of the reinforcement is defined as a minimum cover c_{min} plus an allowance for deviation Δc_{dev}. According to EC2 NA.4.4.1.3, the deviation Δc_{dev} shall be 10 mm, but can be reduced to 5 mm if the final cover of the reinforcement is measured with high accuracy.

According to EC2 Table NA.4.4N , the durability class of permanently submerged concrete is XS2, which results in $c_{min,dur}$ = 40mm, and this gives a minimum concrete cover of the reinforcement

$$c_{nom} = c_{min} + \Delta c_{dev} = 50\ mm$$

When the height of the beam is 215 mm, this leads to and effective height d of the cover

$$d' = 50\ mm + \frac{12\ mm}{2} = 56\ mm$$

$$d = 215\ mm - d' = 159\ mm$$

The concrete cover of the reinforcement for the cover assessed in the thesis has cover c = 31 mm, and effective height d = 178 mm.

5.4.3 Material data requirements

According to EC2 Table NA.E.1N, the expected minimum strength class of M40 concrete is B40. This should give a characteristic strength of f_{ck} = 40 MPa from EC2 Table 3.1.

The yield strength of the reinforcement shall be in the area f_{yk} = 400 to 600 MPa.

The safety material factor for concrete is, according to EC2 Table 2.1N, γ_c = 1,5 and for reinforcement steel it is γ_s = 1,15.

This means that the design material compression strength for the B40 concrete is

$$f_{cd} = \frac{\alpha_{cc} * f_{ck}}{\gamma_c} = \frac{0{,}85 * 40\ MPa}{1{,}5} = 22{,}66\ MPa$$

The material tensile strength is

$$f_{ctd} = \frac{\alpha_{ct} * f_{ctk,0,05}}{\gamma_c} = \frac{0{,}85 * 2{,}5\ MPa}{1{,}5} = 1{,}41\ MPa$$

The material strength of the reinforcement steel is, if we assume B500NC and f_{yk} = 500 MPa

$$f_{yd} = \frac{f_{yk}}{\gamma_s} = \frac{500\ MPa}{1{,}15} = 434{,}78\ MPa$$

5.4.4 Longitudinal reinforcement requirements

According to EC2 §9.2.1.1 (1), the minimum requirements to amount of reinforcement are:

$$A_{s,min} = max\left\{0{,}26 * \frac{f_{ctm}}{f_{yk}} * b_t * d\ ; 0{,}0013 * b_t * d\right\} = 434{,}07\ mm^2$$

The maximum amount of reinforcement is, according to EC2 §9.2.1.1 (3),

$$A_{s,max} = 0{,}004 * A_c = 0{,}04 * b * h = 12900\ mm^2$$

5.4.5 Moment capacity

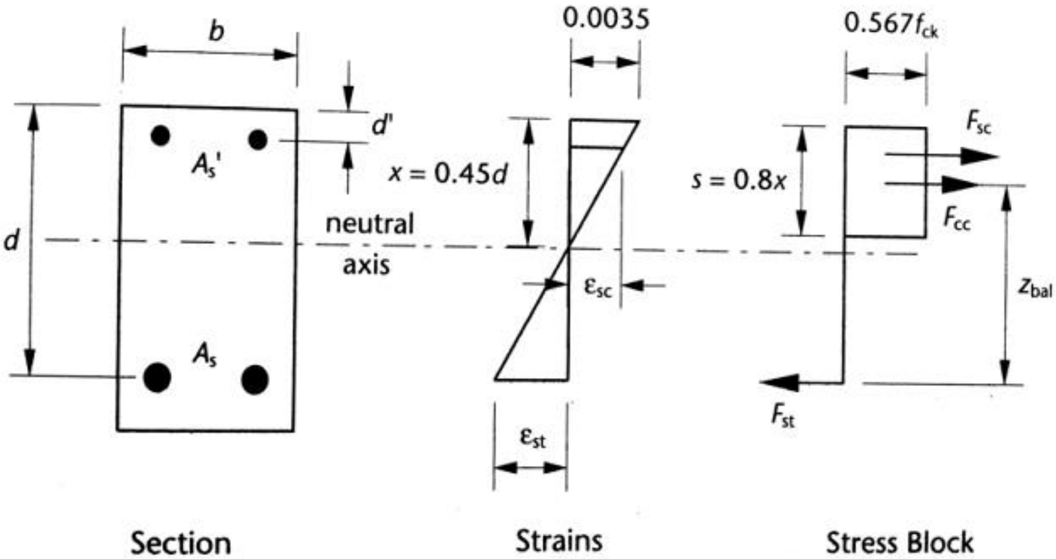

Figure 5.4.5-44 Beam section with both tensile and compression reinforcement. Source: (Mosley, Bungey, & Hulse, 2012)

The moment capacity is calculated using the method presented in *Reinforced Concrete Design to Eurocode 2* (Mosley, Bungey, & Hulse, 2012).

A simple test of moment capacity according to page 73 of (Mosley, Bungey, & Hulse, 2012), results in the capacity (assuming only tensile reinforcement)

$$M_{cd} = 0{,}167 * f_{ck} * b * d^2 = 253{,}3\ kNm$$

and for the cover assessed in the thesis (with less concrete cover c and larger effective height d) the moment capacity is

$$M_{cd} = 0{,}167 * f_{ck} * b * d^2 = 317{,}4\ kNm$$

Both are lower than the M_{Ed}, and the cover will need both tensile and compression reinforcement. The method described in Chapter 4.5 of (Mosley, Bungey, & Hulse, 2012) is used for the calculation of the necessary tension reinforcement A_s and compression reinforcement A'_s, see calculations in Appendix E Concrete and reinforcement design calculations according *to Eurocode 2*.

The resulting necessary amounts of reinforcement due to M_{Ed} are:

$$A'_s = \frac{M_{Ed} - 0.167 * f_{ck} * b * d^2}{f_{sc} * (d - d')} = 1650\ mm^2$$

$$A_s = \frac{0.167 * f_{ck} * b * d^2}{0.87 * f_{yk} * z_{bal}} + A'_s * \frac{f_{sc}}{0.87 * f_{yk}} = 6112\ mm^2$$

These amounts are higher than the reinforcement requirements $A_{s.min}$ and lower than $A_{s.max}$.

With reinforcement bars of diameter ø = 12 mm, this would lead to

$$\frac{A'_s}{\pi * (6\ mm)^2} = 14{,}6 = 15\ bars$$

$$\frac{A_s}{\pi * (6\ mm)^2} = 54{,}0 = 54\ bars$$

The resulting moment capacity from this amount of reinforcement is calculated using the method from *Betongkonstruksjoner – Formler og diagrammer – NS-EN 1992-1-1* (Høgskolen i Bergen, Institutt for bygg og jordskiftefag, 2011).

Including the effects of both tensile and compression reinforcement, the moment capacity M_{Rd} is

$$M_{Rd} = M_{Rd} + \Delta M$$

$$M_{Rd} = 0{,}8 * b * x * f_{cd} * \left(d - \frac{0{,}8 * x}{2}\right) + A'_s * f_{yd} * h' = 327{,}0\ kNm$$

$$M_{Rd} \geq M_{Ed}$$

5.4.6 Shear reinforcement requirements

The requirements to minimum and maximum shear reinforcement are given in EC2 §9.2.2, see the complete calculations in Appendix E Concrete and reinforcement design calculations according *to Eurocode 2*.

The minimum ratio of shear reinforcement ρ_w is, assuming $\alpha = 90°$

$$\rho_w = \max\left(0{,}1 * \frac{\sqrt{f_{ck}}}{f_{yk}} ; \frac{A_{sw}}{s * b * \sin(\alpha)}\right) = 0{,}00126$$

The minimum distance between shear reinforcement s_{min} is

$$s_{min} = \frac{A_{sw}}{b * \rho_{w.min}} = 59{,}6\ mm$$

The largest distance s_{max} allowed between shear reinforcement due to shear force V_{Ed} is

$$s_{max} = \frac{A_{sw} * z * f_{yd} * \cot(\theta)}{V_{Ed}} = 64{,}6\ mm$$

where $\theta = 20°$.

The maximum longitudinal spacing between shear assemblies should not exceed $s_{I.max}$

$$s_{I.max} = 0{,}6 * h' * (1 + \cot(\alpha)) = 61{,}8\ mm$$

A distance s = 60 mm between shear reinforcement bars was thus chosen for the shear design.

5.4.7 Shear force capacity

The formula for design shear force capacity without shear reinforcement $V_{Rd,c}$, which is the case of this cover or beam, is given in in EC2 §6.2.2.

$$V_{Rd,c} = \left[C_{Rd,c} * k * \left(100 * \rho_l * f_{ck}\right)^{1/3} + k_1 * \sigma_{cp}\right] * b * d = 242{,}9\ kN$$

with a minimum of

$$V_{Rd,c,min} = \left(v_{min} + k_1 * \sigma_{cp}\right) * b_w * d = 186{,}7\ kN$$

The shear force capacity $V_{Rd,c}$ = 242,9 kN is smaller than the maximum occurring shear force V_{Ed} = 299,2 kN, and the cover does therefore need extra shear reinforcement.

The maximum allowed shear capacity $V_{Rd,max}$ utilizing shear reinforcement and the strut inclination method outlined in EC2 §6.2.2 is

$$V_{Rd,max} = \alpha_{cw} * b * z * v_1 * \frac{f_{cd}}{\cot(\theta) + \tan(\theta)} = 824{,}4\ kN$$

Trying with highest strut angle θ = 21,8° allowed, and s = 60 mm, the shear capacity $V_{Rd,s}$ is not enough. A new strut angle θ = 20° is used to get the shear capacity

$$V_{Rd,s} = \frac{A_{sw}}{s} * z * f_{ywd} * \cot(\theta) = 322{,}2\ kN$$

The shear capacity $V_{Rd,s}$ = 322,2 kN is larger than the occurring shear force V_{Ed} = 299,2 kN when the distance s between every instance of shear reinforcement is 60 mm.

5.4.8 Axial force capacity as moment capacity including second order effects

The method of assessing the axial force is mainly based upon vertical columns with geometrical deviations being affected by an axial force N_{Ed} and thus creating nominal second order moments, according to EC2 §5.8.3. The applicability of this method to this cover is questionable, but an attempt was made nonetheless.

The simplified criteria for second order effects include the use of MN-diagrams based on the geometry of the beam. The ratio h'/h = 0,479 indicated that the cover has an odd shape, and the *Betongkonstruksjoner: Formler og Diagrammer: NS-EN 1992-1-1* (Høgskolen i Bergen, Institutt for bygg og jordskiftefag, 2011) did not have an applicable MN-diagram. The MN-diagram for h'/h = 0,6 was used instead and yielded m_{kap} = 0,25, which lead to the slightly too high moment capacity

$$M_{Rd} = m_{kap} * f_{cd} * A_c * h = 392{,}9\ kNm$$

which corresponds quite well with the M_{Rd} = 327 kNm found previously.

The second order effects can be ignored if normalized slenderness ratio $\lambda_n < \lambda_{n,lim}$

$$\lambda_n = \lambda * \sqrt{\frac{n}{1 + 2 * K_a * \omega}} = 10{,}04$$

$$\lambda_n = 13 * A_\varphi = 13$$

$\lambda_n < \lambda_{n,lim}$ and thus the second order effects can be neglected.

In Appendix E Concrete and reinforcement design calculations according *to Eurocode 2*, the full calculations for the inclusion of second order effects can be seen. Note that the calculations include many assumptions such as normal geometrical deviation of a column, that the arched beam is straight and has an additional curvature which gives a second order moment, and that the creep coefficient calculations can be found in the same way used for regular beams and columns (EC2 Figure 3.1).

The calculations result in a slightly higher moment including 2. order effects

$$M_{Ed.2.order} = 345\ kNm$$

which is now more than M_{Rd} and additional reinforcement A_s and A'_s is needed

$$A'_s = 2056\ mm^2 \ \rightarrow 19\ bars$$

$$A_s = 6517\ mm^2 \ \rightarrow 58\ bars$$

5.5 Dropped object test on the concrete protection cover

The following is a summary of the results from the full scale dropped object impact tests performed on the concrete protection cover. See Appendix F for the Impact Test Sheets that was recorded during the tests. See Appendix G Frame-by-Frame of dropped object tests for pictures from the tests.

5.5.1 Test overview

Table 5.5.1-1 shows an overview of the drop tests that were performed and their specific data such as measured weight of the object, calculated necessary heights and impact velocities.

Table 5.5.1-1 Dropped object test overview.

Test ID	1.1	2.1	2.2	3.1	4.1	5.1
Test Location	Multiblokk	UiS	UiS	UiS	UiS	UiS
Inner Diameter (mm)	2000	2000	2000	2000	2000	2000
Thickness (mm)	215	215	215	215	215	215
Reinforcement	Oval reinforcement 8 bars Ø12 mm C163,57 mm	Double reinforcement 2 x 12 bars Ø12 mm, C100 mm				
Impact Test (kJ)	50	5	5	20	30	50
Impact Diameter (mm)	700	100	100	500	500	700
Drop Load (kg)	1400	140	140	550	850	1400
Drop Height (m)	3,64	3,64	3,71	3,71	3,60	3,64
Measured Mass (kg)	1350	171,6	171,6	576,6	883,3	1279,5
Calculated Height (m)	3,77	2,97	2,97	3,53	3,46	3,98
Impact velocity (m/s)	8,61	7,63	7,63	8,33	8,24	8,84

5.5.2 Test ID 1.1 – 50 kJ – Multiblokk AS' premises

The first test was performed on March the 9th 2015 at Multiblokk AS' premises. The test was set up outside on gravel. The weather was dry with some wind. The object was lifted using a Manitou Maniscopic Telehandler lift, and released using a Pelican slip hook that was triggered by rope from a safe distance.

Figure 5.5.2-45 Overview of Test ID 1.1 – 50 kJ

The measured impact diameter of the object was 700 mm. The measured mass was 1350 kg, which led to a slightly higher needed drop height than anticipated due to lower mass.

$$Needed\ drop\ height = \frac{50\ 000\ J}{1350\ kg * 9{,}81\ \frac{m}{s^2}} = 3{,}77\ m$$

The 50 kJ impact led to extensive cracking and crushing of the concrete. Large cracks extended over the entire cover. Several large chunks of the cover were knocked loose and broke off during the impact, both on top of the cover and underneath. This was especially evident on the inside of the cover underneath the impact area, where the cover experienced heavy tensile strain. The cover kept its structural integrity intact and did not collapse, much due to the reinforcing steel bars. Without the reinforcement, based on the damage on the cover, it is likely that it would have completely collapsed.

The deflection measurements, along with the camera recordings, show that after reaching the maximum deflection, the tension in the reinforcement bars slightly "pull the cover back together", meaning that the final vertical deflection is less than the maximum deflection. The same is the case for horizontal deflection, or width expansion, which is also slightly pulled back together again. Another factor to this is that the object eventually fell off the cover after impact, thus removing some of the force holding down the cover deflection.

The measured deflections underneath the cover were:

Table 5.5.2-1 Measured deflections underneath the cover after Test ID 1.1 – 50 kJ

Device	Telescope	Telescope (mid)	Oasis	Ruler
Height to top, Start	508 mm	541 mm		
Height to top, End	435 mm	454 mm		
End deflection	**73 mm**	**87 mm**		
Space between cover and telescope staff	14 mm	13 mm		
Max deflection	**87 mm**	**100 mm**	**73 mm**	**75 mm**

The cover showed too much cracking and crushing with the 8 bars of Ø12 mm reinforcement and it was recommended, based on the results of the test to up the amount of reinforcement for the next covers, preferably with double reinforcement.

It is worth noting that the pipes used in the tests are not made for this type of impact load. They are pressure tested as a regular requirement, and are not made to withstand impacts of this magnitude. The fact that the covers are made using the dry-casting method also leads to the concrete being slightly more brittle than if wet-cast.

Figure 5.5.2-46 Deformation and cracking of Test ID 1.1 – 50 kJ

Figure 5.5.2-47 Cracking and crushing of Test ID 1.1 – 50 kJ

Figure 5.5.2-48 Cracking and crushing underneath the cover of Test ID 1.1 – 50 kJ

Figure 5.5.2-49 Chunks of concrete fell off and bared the reinforcement of Test ID 1.1 – 50 kJ

Figure 5.5.2-50 Widening of the legs of the concrete cover after Test ID 1.1 – 50 kJ.

5.5.3 Test ID 2.1 and ID 2.2 – 5 kJ – UiS Laboratories

The two 5 kJ tests were performed at April 27th 2015 in the basin in the laboratory of the University of Stavanger. The measured impact diameter of the object was 100 mm. The measured mass of the object was 171,6 kg. This resulted in a slightly lower drop height than anticipated to generate the impact energy of 5 kJ.

$$Needed\ drop\ height = \frac{5\ 000\ J}{171{,}6\ kg * 9{,}81\ \frac{m}{s^2}} = 2{,}97\ m$$

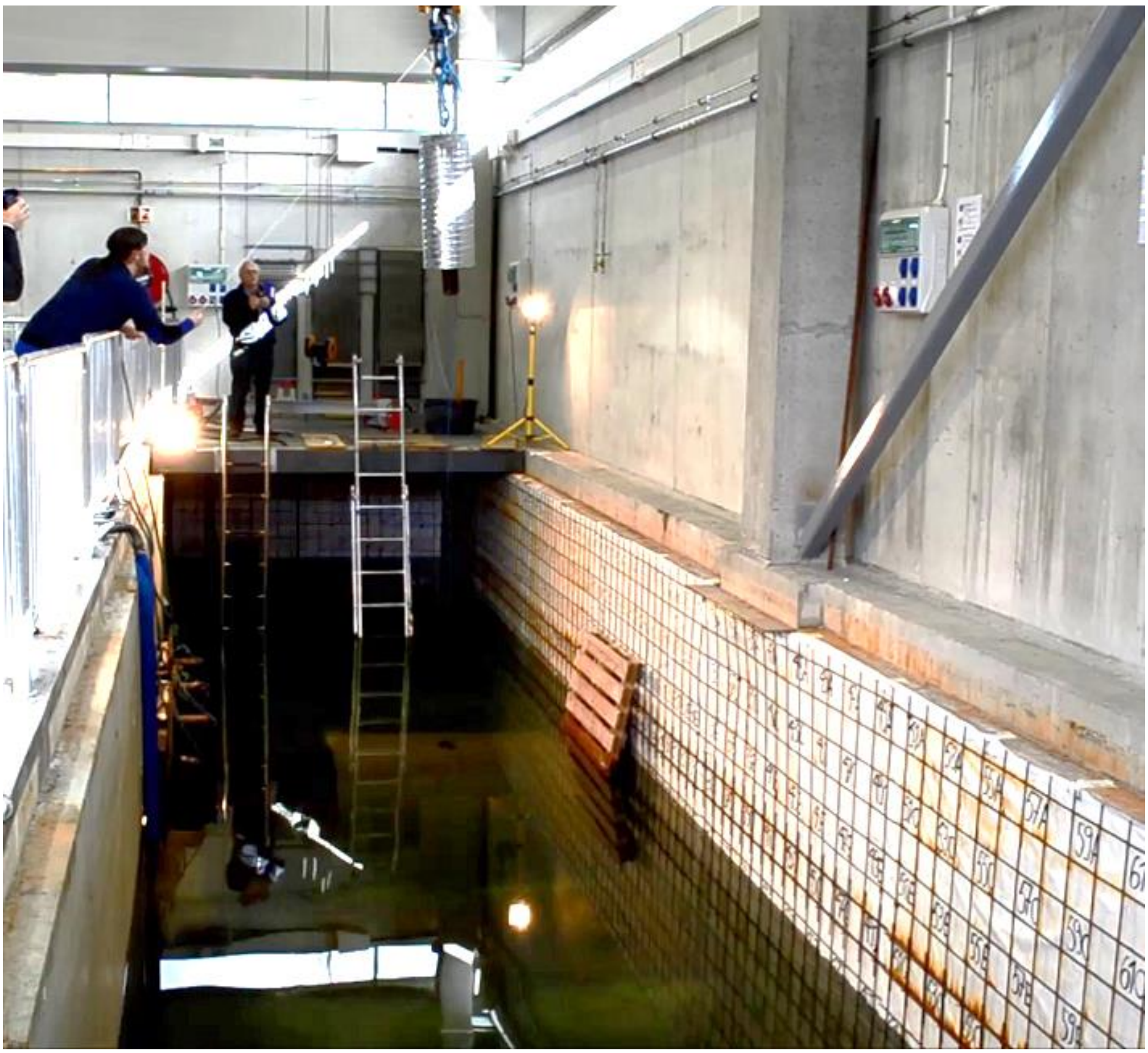

Figure 5.5.3-51 Overview of Test ID 2.1 – 5 kJ

The 5 kJ impact test was performed twice; the first drop on the midpoint of the cover, the second drop at the approximate midpoint between the edge and the midpoint of the cover. During the first test, the pull on the release mechanism gave the object a slight movement, which made the object land slightly askew. The second object was released with less sideways movement, and landed more straight, but still slightly askew.

There was no measurable vertical deflection of the cover from the measuring devices underneath the cover. The original length of the measuring device underneath the cover was 43 cm, and it was unchanged after the two impacts.

The impacts left only two impact marks of approximate 8 by 8 cm area and 1 cm depth each. No visible cracks from the impact areas were observed.

The inner height and width of the cover was measured after its removal from the basin. The height was measured to 99 cm and the width to 200 cm.

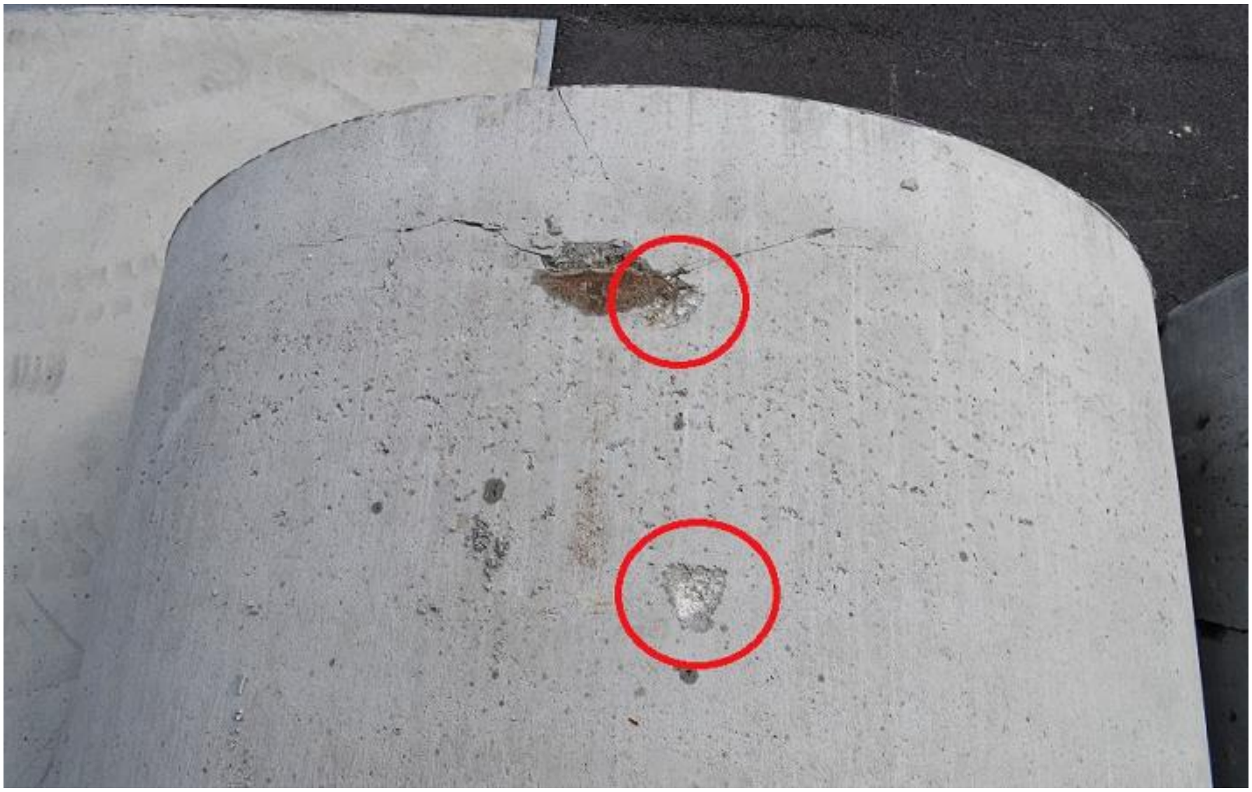

Figure 5.5.3-52 The two impact marks in the red circles from Test ID 2.1 and 2.2 – 5 kJ

Figure 5.5.3-53 Close-up of the impact from Test ID 2.1 – 5 kJ

5.5.4 Test ID 3.1 – 20 kJ – UiS Laboratories

The 20 kJ test was performed at April 27th 2015 in the basin in the laboratory of the University of Stavanger. The measured impact diameter of the object was 500 mm. The measured mass of the object was 576,6 kg. This resulted in a slightly lower drop height than anticipated to generate the impact energy of 20 kJ.

$$Needed\ drop\ height = \frac{20\ 000\ J}{576{,}6\ kg * 9{,}81\ \frac{m}{s^2}} = 3{,}53\ m$$

Figure 5.5.4-54 Overview of Test ID 3.1 – 20 kJ

Due to the limited damage on the covers from the 5 kJ impacts, it was decided to perform the 20 kJ impact on the same cover as the 5 kJ impacts for the sake of efficiency.

As with the 5 kJ impacts, the horizontal component of the pull on the release mechanism made the object fall and land slightly askew forward this time as well.

The measuring device placed beneath the cover was measured to an original height of 43 cm and a height of 39 cm after the impact, resulting in a deflection of 4 cm.

The impact left a clearly visible impact mark due to the object landing slightly askew. The mark was approximately 5 cm long, 16 cm wide and 1,5 cm deep at the most. The rest of the impact area is visible by slight colouring from the rusty surface of the impact plate.

The 20 kJ impact led to some cracking of the concrete cover. The skewed landing sent most of the impact energy forward, which left an approximately 3 mm wide crack in the top front. This crack extends from the front edge of the cover to the impact areas on the top of and underneath the cover, where it connects to cracks in the lateral direction; see Figure 5.5.4-56. The cracks in the lateral direction (Z-direction in the finite element models) are widest near the impact area, where they are in the area of 1-2 mm wide, and shrink outwards from the impact area, see Figure 5.5.4-55. Underneath the cover, the lateral crack in front was 3 mm wide at the most, Figure 5.5.4-57. Some mild flaking of the concrete could be observed underneath the cover in the form of small, loose chunks of concrete. The impact also resulted in cracks in the vertical direction (Y-direction in the finite element models), from the bottom of the cover around the midpoint of the length of the cover, which stretched up to the impact area. These cracks appear inside the cover on both sides, but only outside on the right side, see Figure 5.5.4-58, Figure 5.5.4-59 and Figure 5.5.4-60. At the bottom, were the cracks were widest; they were approximately 1-2 mm wide.

The inner height and width of the cover was measured after its removal from the basin. The height was measured to 99 cm and the width to 200 cm.

Figure 5.5.4-55 Crack pattern around impact area of Test ID 3.1 – 20 kJ

Figure 5.5.4-56 Crack in the top front of the cover after Test ID 3.1 – 20 kJ

Figure 5.5.4-57 Crack underneath the front of the cover after Test ID 3.1 – 20 kJ

Figure 5.5.4-58 Vertical crack on one side of the cover after Test ID 3.1 – 20 kJ

Figure 5.5.4-59 Vertical crack on the right outside of the cover after Test ID 3.1 – 20 kJ

Figure 5.5.4-60 Vertical crack on the inside on right side the cover after Test ID 3.1 – 20 kJ

5.5.5 Test ID 4.1 – 30 kJ – UiS Laboratories

The 30 kJ test was performed at April 27th 2015 in the basin in the laboratory of the University of Stavanger. The measured impact diameter of the object was 500 mm. The measured mass of the object was 883,3 kg. This resulted in a slightly lower necessary drop height than anticipated to generate 30 kJ of impact energy.

$$Needed\ drop\ height = \frac{30\ 000\ J}{883{,}3\ kg * 9{,}81\ \frac{m}{s^2}} = 3{,}46\ m$$

Figure 5.5.5-61 Overview of Test ID 4.1 – 30 kJ

Due to the damage on the cover used for the 5 kJ tests and the 20 kJ test, a new cover was used in the 30 kJ test.

The video recording shows no evidence of horizontal movement and rotation due to the horizontal component of the pull during the fall of the object, but the impact mark clearly shows that this object landed slightly askew as well.

The measuring device placed beneath the cover broke during removal of the first cover. A new method to gain a deflection measurement of fairly equal accuracy and quality was used. This method was to simply measure the original depth from the water surface to the top of the cover. Two measurements were taken; one in the middle point between the impact area and the front, and one between the impact area and the back of the cover. The measured depths were:

Table 5.5.5-1 Measured deflections from water surface to top of cover after Test ID 4.1 – 30 kJ

Measured Depths	Before	After	Result
Front	21,5 cm	26,5 cm	5 cm
Back	24 cm	26 cm	2 cm

This shows that the object landed slightly askew forward, and thus pushed the front of the cover furthest down into the supporting sand bags.

The impact left a clearly visible impact mark of approximately 10 mm depth, due to the object landing slightly askew forward. The rest of the diameter of the impact object can be observed by the colouring from the rusty surface of the impact plate.

The 30 kJ impact led to rather severe cracking of the concrete cover. The skewed landing sent most of the impact energy forward, which left an approximately 6 mm wide crack in the top front. This crack extends from the front edge of the cover to the extensive web of cracks (of approximately 0,5 mm width on top) around the impact area on the top of and underneath the cover. Underneath the cover, an extensive and fairly symmetric web of cracks of width in the range between 4 mm and 0,5 mm can be observed. In addition, some concrete chunks almost came loose in front of the cover, underneath the impact area.

The cover cracked vertically on the right side from the bottom up to the web of cracks in the impact area. On the bottom outside of the cover, this crack is approximately 10 mm wide, and on the bottom inside, it is approximately 9 mm wide. This crack narrows as it moves upwards to join in the web of cracks around the impact area.

The inner height and width of the cover was measured after its removal from the basin. The height was measured to 98,5 cm and the width to 202 cm.

Figure 5.5.5-62 Cracks outside on the right side of the cover after Test ID 4.1 – 30 kJ

Figure 5.5.5-63 Cracks on the front of the arch after Test ID 4.1 – 30 kJ

Figure 5.5.5-64 Cracks and impact mark on top of the cover after Test ID 4.1 – 30 kJ

Figure 5.5.5-65 Web of cracks underneath the cover after Test ID 4.1 – 30 kJ

Figure 5.5.5-66 Vertical crack on the right side underneath the cover after Test ID 4.1 – 30 kJ

Figure 5.5.5-67 Vertical crack on the right outside of the cover after Test ID 4.1 – 30 kJ

5.5.6 Test ID 5.1 – 50 kJ – UiS Laboratories

The 50 kJ test was performed at April 28th 2015 in the basin in the laboratory of the University of Stavanger. The measured impact diameter of the object was 700 mm. The measured mass of the object was 1279,5 kg. This resulted in a slightly higher necessary drop height than anticipated to generate 50 kJ of impact energy.

$$Needed\ drop\ height = \frac{50\ 000\ J}{1279{,}5\ kg * 9{,}81\ \frac{m}{s^2}} = 3{,}98\ m$$

Figure 5.5.6-68 Overview of Test ID 5.1 – 50 kJ

A new cover was placed in the basin for this test.

The amount of weight hanging in the release mechanism minimized the horizontal movement from the pull of the release mechanism, which made the object fall and land flatly on the cover.

The depth measurements from the water surface to the top of the cover before and after the impact were:

Table 5.5.6-1 Measured deflections from water surface to top of cover after Test ID 5.1 – 50 kJ

Measured Depths	Before	After	Result
Front	19 cm	26 cm	7 cm
Back	19 cm	26,5 cm	7,5 cm

This shows that the object landed fairly even, and pushed the cover evenly down into the supporting sand bags.

The impact did not leave a local indentation, as was the case for the previous impacts. Instead, this impact left an even impact mark visible by the colour rub-off from the rusty surface of the impact plate. The even landing sent less of the energy forward, but spread it more evenly on the whole cover. This resulted in narrower and less severe cracks, but more cracking on the cover overall.

For instance, the crack in the top front is approximately 2 mm wide. In addition, the cover has cracked several places on the arch with fairly symmetric spacing between. These cracks can be followed from the front of the cover and all the way to the back of the cover. At their widest, these cracks are measured to a wideness from 1,5 mm to 0,2 mm. Further, a symmetric and extensive web of cracks can be seen underneath the impact area, stretching out to large parts of the cover. These cracks are typically in the area of 0,5 mm to 1,5 mm wide.

No vertical crack along the side of the cover can be observed, as opposed to the 20 kJ and 30 kJ impacts. The inner height and width of the cover was measured after its removal from the basin. The height was measured to 97,5 cm and the width to 202 cm.

Figure 5.5.6-69 Front view of cover after Test ID 5.1 – 50 kJ

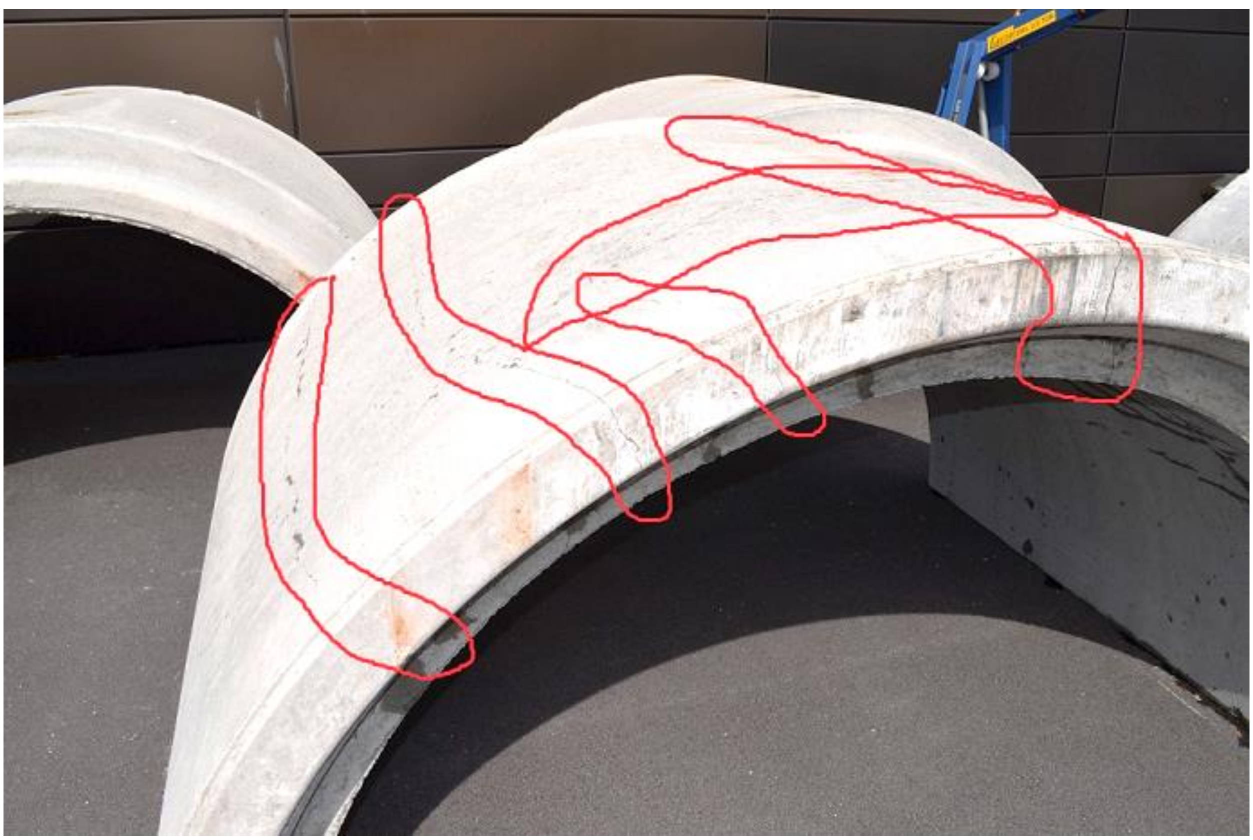

Figure 5.5.6-70 Cracks along the length of the cover marked by red after Test ID 5.1 – 50 kJ

Figure 5.5.6-71 Crack in the top front of the cover after Test ID 5.1 – 50 kJ

Figure 5.5.6-72 Web of cracks underneath the cover after Test ID 5.1 – 50 kJ

Figure 5.5.6-73 Left side underneath the cover after Test ID 5.1 – 50 kJ

Figure 5.5.6-74 Right side underneath the cover after Test ID 5.1 – 50 kJ

Figure 5.5.6-75 Top of the cover after impact of Test ID 5.1 – 50 kJ

5.5.7 Sand bag supports

The big bags filled with rock, sand and silt were placed with as even heights as possible in the basin, and the covers were placed as evenly as possible on the four inner sand bags. The outer bags were used as protection of the floor from the falling object. After all the impacts were done, the water in the basin was drained and the sand bags that the covers had been placed upon to protect the concrete floor of the basin, as well as to give a more representative result in regards to the actual sea bed conditions (which of course may vary, but in the very least are not concrete or packed gravel), was revealed.

It was revealed that much of the measured deflection of the covers in the basin came from the legs of the cover being pushed down into the sand bags. The covers had dug valleys into the sand bags which were clearly visible after draining the water. The valleys in the sand bags were measured at several points, but due to the interspersed uncertainty of the heights and movement of the sand bags and the placement of the covers, these numbers cover a great span of different heights.

Table 5.5.7-1 Measured heights of the valleys in the big bags after all drop tests

Sand bag	Valley height measurements (cm)	Average (cm)
Left, front	7, 13, 12, 7, 16	11
Left, back	15, 12, 14, 5, 12	11,6
Right, front	9, 10, 6, 7, 5	7,4
Right, back	9, 5, 10, 5, 7	7,2

Figure 5.5.7-76 Overview of placement of big bags. Valleys are clearly visible on both sides.

Figure 5.5.7-77 Close-up of the valley on the front left bag.

Figure 5.5.7-78 Typical measurement of the right back bag.

5.5.8 Test summary

None of the covers were penetrated by the dropped objects.

The test of the oval reinforced cover saw several large chunks of concrete fall down from the roof inside. No chunks of concrete came loose on the doubly reinforced covers.

The covers experienced different cracking patterns depending on the object and its landing. Test ID 1.1 saw large cracks and more or less complete break-offs of concrete, as well as a lot of crushing of concrete around the impact area. Test ID 2.1 and 2.2 left nothing but two small impact marks on the cover. Test ID 3.1 and 4.1 landed askew forward and saw severe cracking patterns in front and on the side of the covers. Test ID 5.1 landed straight and left less severe cracks than the previous tests, but more cracking on the cover overall. The cracks started on one end of the cover and stretched all the way to the other end.

The measured deflections, including sinking into the ground or support, of the covers:

Table 5.5.8-1 The measured deflections from the impact tests.

Test ID	Measured deflections
Test ID 1.1 - 50 kJ	73 mm to 100 mm
Test ID 2.1 and 2.2 - 5 kJ	0 mm
Test ID 3.1 - 20 kJ	40 mm
Test ID 4.1 - 30 kJ	50 mm in front
	20 mm in back
Test ID 1.1 - 50 kJ	70 mm in front
	75 mm in back

The measured height and width inside cover after removal from basin and placed outside:

Table 5.5.8-2 The measured inner heights and widths of the covers after removal from basin

Measured height and width inside cover		
Cover / Impact test	**Inner height**	**Inner width**
Test ID 1.1 – 50 kJ	---	---
Test ID 2.1, 2.2 and 3.1 – 5 kJ and 20 kJ	99 cm	200 cm
Test ID 4.1 – 30 kJ	98,5 cm	202 cm
Test ID 5.1 – 50 kJ	97,5 cm	202 cm

6 Discussion

This chapter will discuss the results obtained from the various analyses and tests. At the end of this chapter, suggestions for the next iteration of the cover design will be presented based on the results and the discussion.

6.1 Finite Element Analysis using *Ansys® Workbench, Release 14.5*

6.1.1 Trawl board overpull – Static Structural

6.1.1.1 General

The goal of the finite element analysis of the trawl board load requirement was to determine whether or not the given geometry of the protection cover could withstand the impact from the trawl gear. The criteria of a successful test listed in chapter 2 Technology Qualification, is that the cover is not allowed to be penetrated, have large amounts of concrete debris knocked off from the roof, or to deform so much that the required clearance to roof and walls are compromised. In addition, the stresses in the cover and reinforcement should not exceed the design stresses, and the cover should be stable on its own on the ground during impact of the trawl load.

As has been mentioned in chapter 4.1.1 Modelling of concrete and reinforcement, the modeling of the concrete material behavior is a complex process due to the material's brittleness, weakness to tension, cracking etc. Thus, the first and one of the most important assumptions that should be pointed out, is that all of these analyses, are based on simplified models and ideal representations of a complicated real world situation.

The effects of rock dumping are not included in this model due to the premise of the thesis being to investigate the applicability of concrete protection covers where rock-dumping is impossible.

The hydrodynamic dampening effects of the water surrounding the cover has not been included in the model. It is probable that this would have a slight limiting effect on the deflections and movements of the cover. The hydrodynamic forces from currents and waves are not included in the model as well, nor the effect of buoyancy on the weight of the cover.

The seabed has not been modeled, as this would have meant the need to regenerate the mesh after the model and reinforcement were properly generated and working. To include the seabed would mean new support conditions, where friction between the cover and the seabed has a restraining effect on deformations, as well as a dampening effect in vertical direction. Depending on several factors, this could have resulted in the finite element software not being able to converge the solution and finish the calculations. Therefore, it was decided to keep the model simple without adding more uncertainties.

In regards to the reinforcement, the Reinf264 elements and the slightly faulty generation of these, specifically the cross of reinforcement elements and the two missing elements at the bottom, although the error is fairly conspicuous in the model, the effect of it is most likely quite insignificant. Most of the maximum stresses and deformations are not located near the errors, and are relatively low on the bottom where these errors in the reinforcement are located.

In addition, it is important to remember that the horizontal reinforcement bar connecting the inner and outer rings of reinforcement in the cover supplied by Multiblokk AS for the dropped object test has not been included in this model. This shows that there are several ways to enhance the strength of the protection cover, and that this model of the protection cover has used quite small amount of reinforcement as opposed how it could be done in a real situation.

6.1.1.2 Results from analyses

The results from the finite element analysis of the static trawl board model was based on the reinforced concrete model of the protection cover with a simple support situation and the 300 kN design trawl board overpull load applied on twelve different locations on the cover. The load was applied in a matrix formation of three locations from the midpoint to the edge of the cover, and in four different heights, where 1 is at the bottom and 4 at the top. The load was applied as slightly conservative nodal forces as opposed to having the load evenly spread over an area on the cover, which is the more realistic approach. As explained earlier, this was not possible due to the selection and command process needed for the generation of reinforcement elements.

The results from theses analyses have a clear trend based on the impact area of the force. The results presented in Table 5.1.1-1 and Figure 5.1.1-1 to Figure 5.1.1-6 show that when the force is applied on the bottom, the protection cover experiences the highest stresses, both in the concrete cover and the reinforcement, as well as the largest deformations in all directions. The reason for this is possibly due to the arched shape of the cover, the roll support on the side where the force was applied, and the moment the force generates. The stresses and deformations decrease as the load impacts higher up on the cover, or essentially nearer the pinned support and are thus generating less moment. The impact location with highest stresses and largest deformations was the Outer 1 load case, where the load is applied in the lower left corner of the cover. The further away from the corner the load is applied, in other words nearer the midpoint of the cover, the more the stresses and deformations decrease. One of the reasons for this could be the added twisting motion of the cover that the experiences when the load is applied off-center. This effect is limited though, as both supports are restrained in the X-direction to keep the model stable, but it will have some effect on the model even after restricting the supports.

In a real situation, the protection covers will be placed next to each other in a long chain. It is probable that this will somewhat affect and limit movement in X-direction on the whole cover, depending on the overlap details between the covers, instead of only in the supports of the model, and thus also possibly limit the twisting effect from the trawl load impact in the corner. The load could also possibly be shared by two covers instead of only one.

The design compression stress of the concrete is f_{cd} = 22,6 MPa and the design tensile strength is f_{ctd} = 1,41 MPa, but it is assumed that the reinforcement steel with a design yield strength of f_{yd} = 434,7 MPa will take the tension stress. According to Figure 4.5.2-34, the allowed vertical deformation in negative Y-direction is 294 mm and approximately 193,6 mm from the walls in horizontal Z-direction.

As can be seen from Table 5.1.1-1, several of the bottom load cases result in stresses higher than the f_{cd}, both tension (which is on top of the cover due to the bending of the cover) and compression (which is underneath the cover, also because of the way the cover is bended by the force). This may indicate that the cover will experience cracking in the areas of tension and possibly crushing, cracking and flaking in the area of compression. The loads that impact higher up on the cover, especially position 3 and 4, generate stresses that are lower and within the design limit f_{cd}.

In regards to stresses in the reinforcement, the maximum compression stress recorded is from the Outer 1 load case at 124,4 MPa and 107,1 MPa for tension stress. These, and all the other load cases, result in reinforcement stresses way below the design yield strength f_{yd}. From Figure 5.1.1-13, it can be seen that the tension stress is colored red and appears on the top of the outer reinforcement circle, and that the compression stress is plotted blue and appear on the inner circle of reinforcement. The stresses at the bottom are fairly small, and it can thus be assumed that the faulty reinforcement at the bottom of the cover is a more or less negligible error. From the stress plots it can be seen that the stresses increase fairly linearly from the bottom on one side of the cover up to the maximum at the top, and down to a similar amount of stress on the other side. It is also notable that the further up on the cover the trawl load impacts (from load cases 1 at the bottom to 4 almost at the top) the points of maximum stresses move from the mid to the left side, away from the impact side of the cover. At the same time, the maximum stresses decrease as the load is moved from bottom to the top load location.

The maximum deformations can be found for load case Outer 1 as well. The total deformation is 14,95 mm at the most, in the same corner of the cover as where the load is applied, see Figure 5.1.1-9. This is directly over the roll support, which makes sense, as there is no restriction in Z-direction in this support.

The plot of deformation in X-direction is included for the Outer 1 load case, even though the values are small due to the restraint in the supports, see Figure 5.1.1-10. It describes the twisting motion in the X-direction caused by the off-center load location. The maximum deformation in X-direction is in these models 0,4 mm, and it may be assumed that these are negligible in the bigger picture of the model.

The deformation in Y-direction for Outer 1 load case is displayed in Figure 5.1.1-11. This shows a clear picture of how the cover deforms when impacted. The color red is the maximum deformation and is located on the middle of the cover at the top, and suggests that the top of the cover is pushed up a maximum of 4,8 mm. This is a plausible result from having the load pushed in from the side. As the width of the cover decreases, the height of the cover must increase due to the shape of the protection cover. The Y-direction plot clearly shows that this is happening. In addition, there are some negative values (blue color) on the right side of the cover. This can be explained by the supports, which are pinned in the corners and does not hinder rotation, and that, by following the same logic as above, when the cover is pushed together sideways and up vertically in the middle, the legs of the cover will rotate slightly in the supports. Because the left side is supported on the outside, it is logical that the green color on the inside means that the inside has been rotated and moved slightly upwards (by approximately 1 mm), and the blue on the right outside, where the support is on the inside, has been rotated the other way approximately 2 mm down at the maximum.

The deformation in Z-direction, or the same direction as the trawl load is applied is important to consider as well. The maximum deformation in Z-direction was also found for the load case Outer 1, where the element with the maximum deformation is located on the inner side of the corner at the same side where the load was applied. At this point the maximum deflection in Z-direction was approximately 14,8 mm. From the plot in Figure 5.1.1-12 it can be seen that this corner is the most affected, and that the deformation in the Z-direction decreases seemingly linearly from the roll support to the pinned support.

It should be noted that on the right inside of the cover, over the roll support, the protection cover experience some fairly low stresses that should not have been there. Figure 5.1.1-8 shows that there are stresses of color green above the inner corner, where there should have been more or less zero stress, or blue color. The reason for this stress could be the low mass of cover and that the support is forcing the cover to stay down, and thus causing the forced stress that is visible in the plot. This is evident in the reaction forces for the Outer 1 load case, see Figure 6.1.1-1 below, where a negative vertical force of -14,6 kN holds the cover down. This means that under impact from the trawl force, the cover is not stable, and it may suggest that the cover could be moved, tipped over or capsized by the trawl force. The further up the trawl force impacts, the larger the tipping moment about the pinned support is, and the larger the negative vertical reaction force in the roll support is. The load cases at height number 4 results in negative support forces of about -120 kN, see Figure 6.1.1-2. This would mean that in order to counteract the tipping moment about the pinned support using weight along, the cover would need an approximate added mass of 12,2 tons. A further assessment of this problem will follow in the next chapter.

As can be seen from all of the result plots in Appendix A Results from the Trawl board analysis in *Ansys® Workbench, Release 14.5*, the pattern of highest stress underneath the cover at the top, moving from the middle to the left the further up on the cover the trawl load impacts can be seen on all of the simulations. This is the case for both the stresses in the cover and in the reinforcement. A pattern in regards to the deformations can be seen for all of the simulations as well. The deformations in Y direction for the various load cases all show the same pattern of deformations in positive Y-direction at the top of the cover. The vertical deflection is quite similar for the three various positions, but decrease as the load impacts higher up on the cover. In the Z-direction, the same pattern can be seen as well. The deflection on the roll supported side, where the maximum point is located, is quite similar for all the locations (differing only approximately 1 mm), but decrease rapidly as the load impacts further up on the cover.

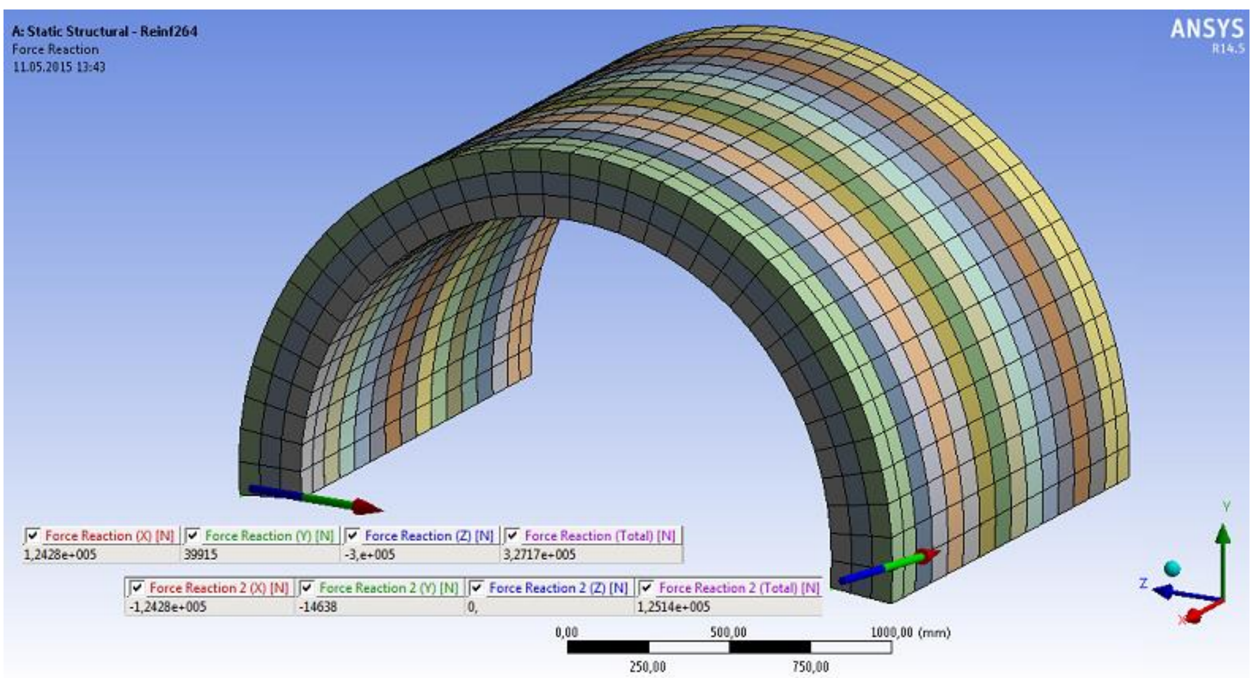

Figure 6.1.1-1 Reaction forces from the Outer 1 load case. Source: *Ansys® Workbench, Release 14.5*

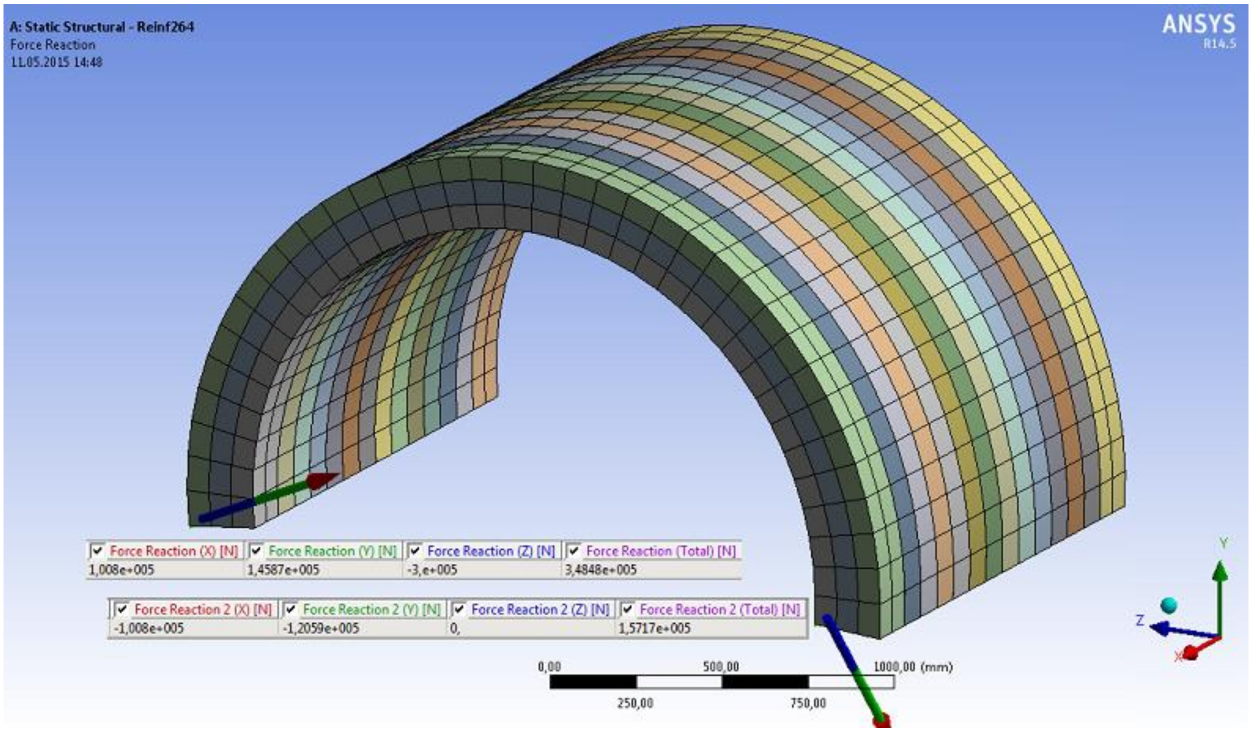

Figure 6.1.1-2 Reaction forces from the Outer 4 load case. Source: *Ansys® Workbench, Release 14.5*

Table 6.1.1-1 Summary of reaction forces in Outer 1 and Outer 4 load cases

Support forces	Pinned support (left) [N]	Roll support (right) [N]
Outer 1 load case		
Total	327170	125140
X	124280	-124280
Y	39915	-14638
Z	-300000	0
Outer 4 load case		
Total	348480	157170
X	100800	-100800
Y	145870	-120590
Z	-300000	0

The stress results may indicate that the cover will experience some slight cracking, possibly both from crushing underneath and tension on the top of the cover. The stress values are however not outrageously high above the design stress limits, and it is unlikely that the cover would flake off large pieces of concrete that could damage the pipeline beneath. The possible cracking may however mean that water will make its way into the reinforcement and reduce the lifetime of the cover due to corrosion.

The stress values for the reinforcement are well below the design yield level. This means that the reinforcement is deforming in the elastic range, and it is likely that after the trawl load has passed, the reinforcement will push the cover back out and down again, although not necessarily completely back to prior state, as the elastically strained portion of the reinforcement tries to revert back to a more or less zero tension state.

The maximum deformations recorded for load case outer 1 is 4,8 mm positive in the vertical direction, and is thus in no danger of deforming downwards into the clearance area. For a 16" pipe, the negative deflection could have been up to approximately 294 mm before exceeding the allowed deformation. The maximum deformation in positive Z-direction is 14,8 mm for the Outer 1 load case. This is also well within the clearance requirement of approximately 193,6 mm which is left on the right side of the cover in Figure 4.5.2-34, taking into account the approximate movement of a spool pipeline of about 800 mm.

6.1.2 Dropped Object Impact Test – Explicit Dynamics

6.1.2.1 General

The goal of the dynamic finite element analysis of the dropped object requirement was to compare it to the full scale drop tests. A dynamic analysis of such span had not been performed before by Subsea 7, and there were thus no previous analyses to compare the behavior of the model and the results with. That being said, from the looks of it, and taking into account the assumptions and boundary conditions applied, the model seems to behave pretty well and close to the reality. The criteria of the dropped object test is that the cover shall not be penetrated by the objects, that the deflection of the cover shall not exceed the 294 mm in vertical direction. The cover is allowed to deform, crack and crush due to the accidental limit state, but large amounts of concrete are not allowed to fall from the roof of the cover and potentially damage delicate equipment underneath. This is not measurable in the model, but the Damage result will give a plot of where the protection cover is likely to crack and be damaged.

The same precautions about concrete material behavior as described previously must be assumed for this model, although the concrete material data used in the dynamic analysis is based on another source, and the dynamic behavior of the concrete material is more thoroughly described, possibly from testing, see the source of the material in Figure 4.1.2-5. The analysis is based on simplified models and ideal representations of a very complicated real world situation. The material strength of the concrete used in the analysis is 35 MPa, which is slightly lower than the minimum 40 MPa which is required by the *Eurocode 2*, and what was used in the concrete cover used in the full scale dropped objects test where the material quality was minimum 40 MPa.

The effects of rock-dumping are not included in this model due to that the premise of the thesis is to investigate the applicability of concrete protection covers where rock-dumping is not possible.

The hydrodynamic dampening effects of the water surrounding the cover have not been included in the model. It is probable that this would have a slight dampening effect on the deflections and movements of the cover. The hydrodynamic forces from currents and waves are not included in the model either, nor the effect of buoyancy on the weight of the cover.

The seabed has not been modeled, but supports under the legs of the cover restricting movement in vertical Y-direction are assumed. Essentially, both of the flat undersides of the legs of the cover are roll supported. This is a simplification of the real situation where the cover is placed upon the seabed. It is fair to assume that the cover will be pushed somewhat into the ground, as the dropped object test showed, but this effect is not included in the model, and all vertical deformation in the model come thus from deformation of the cover. This could have been achieved by modelling a floor upon which the cover was placed. It would then be possible to assign seabed material data to the floor which would allow for pushing the cover down into it. It would then also be possible to add the effect of friction between the cover and the seabed, which would both dampen the deformation of the cover in the Z-direction and dampen the oscillating movement present in the model after impact.

In regards to the reinforcement used in the model, the explicit dynamics uses a simpler method of reinforcing, where the software automatically converts line bodies to reinforcement bars. Thus, the errors experienced in the trawl load analyses were easily avoided, and nicely looking and working double reinforcement arches were achieved. The horizontal bar between the inner and outer reinforcement ring could have been fairly easily implemented into this model, but it was decided to keep the two models as similar to each other as possible. But this also means that the 3D model has slightly lower strength, especially in regards to the tension underneath the top to the cover, than the covers used in the full scale test partly due to the missing reinforcement bar.

6.1.2.2 Results from analyses

The results from the dropped object finite element analyses was based on the reinforced model of the protection cover with a two roll supports situation, which would allow the cover to deform equally on both sides, which can be assumed is nearer a real situation than having one leg pin supported and thus limiting movement in z-direction. Four different objects were used to simulate the four required impact energies of 5 kJ, 20 kJ, 30 kJ and 50 kJ. The load was placed directly on top of the cover and was given a velocity corresponding to the weight of the object to achieve the wanted kinetic impact energy.

The results from the analyses show a clear trend in regards to amount of impact energy that the cover was subjected to. The higher the energy, the more deformation, stresses and damage the cover is exposed to, and as expected, the 50 kJ impact was by far the most damaging and deforming load case. As can be seen from the Figure 5.1.2-15 to Figure 5.1.2-20, the deformations increase rapidly and fairly linearly (with some exceptions), while the stresses increase more slowly and appear to be converging towards a maximum stress level. This seems to be the case for both stresses in the concrete and in the reinforcement. This may indicate that the model implements the effect of stress redistribution as the materials reach the plastic strain state.

The Figure 5.1.2-24 shows the energy summary of the 50 kJ impact and shows that the amount of hourglass energy needed in the model is fairly low; somewhere between 5 % and 10 % of the maximum kinetic energy. More than 10 % hourglass energy is not recommended, and for the purpose of this thesis, such a result would arguably be within allowed limits.

The maximum total deformation for the analyses is approximately 59,4 mm for the 50 kJ impact. The maximum point is located in the middle, on the underside of the cover, almost directly under the impact area of the object, see Figure 5.1.2-25 and Figure 5.1.2-26.

The deformation in X-direction shows a plot of a maximum (1,87 mm) and, minimum (-1,87) on both sides of the object between the impact area and the edges, see Figure 5.1.2-27. This indicates that, as the object impacts the mid span of the length of the cover, the midpoint is pushed down, and the two sides are pulled slightly towards the center of the cover. One side is pulled in positive X-direction, and the other in negative X-direction. The equally large maximum and minimum deformations indicate that the cover is impacted symmetrically about its center axis. The same pattern is recognizable on all four load cases, but as Table 5.1.2-1 indicates, the deformation values decrease as the impact energy decreases.

The deformation in Y-direction is possibly the most important plot in these analyses. It depicts the vertical deformation of the cover and shows the point of maximum deformation, which can be found in the middle, underneath the protection cover. For the 50 kJ impact, the maximum is approximately 59,3 mm in negative Y-direction directly underneath the impact object. Figure 5.1.2-17 shows the vertical deformation of the cover for all load cases, and the pattern mentioned above is clear here as well. The lower the impact energy is, the lower the maximum vertical deformation is. The three lowest impact energies seem to have a fairly linear relationship, but the 50 kJ seem to have increased slightly more than expected, as it has doubled the deformation from the 30 kJ impact without doubling the impact energy. The plot also shows that the red areas on the nether parts of the legs, the cover is pushed slightly upwards due to rotation, but more on the problem this created later.

The deformation in Z-direction has a clear connection to the vertical deformation, as can be seen by comparing the Figure 5.1.2-17 and Figure 5.1.2-18. The same deformation connection is described for the static system, and means essentially that as the top mid of the cover is pushed down, the sides or legs of the cover must be pushed out. The plot of the deformation in Z-direction for 50 kJ in Figure 5.1.2-29 shows that both sides of the cover are pushed fairly symmetrically out to approximately 49 mm on each side. The same pattern is clear for the other magnitudes as well, but with smaller deformations.

The stresses in the concrete cover reaches its maximum of 42,5 MPa during the 50 kJ impact, see Figure 5.1.2-30. This is well above the design material strength f_{cd} = 22,6 MPa (or actually slightly lower due to that the material used in the model has a characteristic material strength of 35 MPa instead of 40 MPa). The maximum stress is located directly below the center of the object, and the area around is quite heavily affected as well. This may indicate that the cover will experience quite some damage in this area, from cracking or crushing. The stresses of the other load cases, which can be seen in Appendix B Results from the Dropped object analysis *in Ansys® Workbench, Release 14.5*, follow the same pattern with maximum underneath the object, but with a slightly more spread distribution for the two lowest energies. The stress levels for all but the 5 kJ impact experience stresses above the design material strength f_{cd}.

The stresses in the reinforcement reach a maximum during the 50 kJ impact as well at 385,6 MPa. The steel material was given a yield limit of 355 MPa in the bilinear isotropic hardening material data. This means that after reaching this level of stress, the reinforcement will start to strain plastically, and thus redistribute the stresses to neighboring regions, and thus avoiding stress peaks at plastically affected areas. The stresses in Figure 5.1.2-20 indicates that this is the reason that the stresses do not increase as rapidly as the deformations, but seem to converge towards a value of stress higher than what was achieved in these analyses. The stress levels and redistributions may indicate that the red reinforcement elements in Figure 5.1.2-31 and Figure 5.1.2-32 are plastically strained, as the stresses are above 355 MPa.

The damage results ranges from 0 to 1, where 0 means that the material is intact, and 1 means fully fractured. The damage model uses the cumulative damage model in *Ansys® Workbench, Release 14.5*, and uses the factor to reduce the elastic module and yield strength of the damaged material. The fully damaged material has some residual strength in compression, but none in tension (ANSYS, Inc.). The color red in the plot indicates a value of 1 and fully fractured material. The plot of the 50 kJ reveal that there are extensive damage to the cover in the middle, both on top and especially underneath, where the concrete is experiencing tensile strain. The plots in Figure 5.1.2-33 and Figure 5.1.2-34 show that the outer corners on the bottom of both sides are fully fractured as well. These results are however a bit illogical and not expected, but fairly easy to explain. As with the static model of the cover, the supporting legs of the cover want to rotate when impacted. In this case, when the cover is pushed down in the middle, the outside of the legs want to rotate upwards. This is however not allowed by the supporting conditions, as the entire undersides of the legs are restrained from deformation in Y-direction. This means that the support holds back the rotation, and that on the outside of the cover, tension stresses in the concrete are created, which the concrete has very little strength against. This hindering of the rotations thus fully fractures the corners of the cover in the damage model. In hindsight, it is possible that supporting the cover with roll supports on the lines of the two inner corners would have been a better option, and would have given more realistic damage results without the damage in the corners.

For the same reason as described above, there can be observed high stresses on the outside of the covers, both in the concrete and in the reinforcement, which is where the maximum stresses are located for the 50 kJ and 30 kJ impact. The high stresses in these locations are most likely due to restricting the rotation motion and thus forcing high tension stresses to appear in these areas. The expected location of the maximum stresses is somewhere underneath the dropped object.

As can be seen from all the resulting values and plots in Appendix B Results from the Dropped object analysis *in Ansys® Workbench, Release 14.5*, the maximum deflections and deformations of the protection cover are well within the criterion of maximum 294 mm vertical deformation from the top. As the cover is impacted it widens, and the criterion of maximum deformation of approximately 196 mm in the opposite direction is not exceeded. The spool or pipeline underneath should still be protected, as the cover does not show any signs of penetration from the objects.

The stresses in the cover and reinforcement are quite high at some points, but the dropped object requirement is considered in the accidental limit state, and irreversible plastic deformation of the cover and reinforcement is allowed as long as the cover does not exceed the deformation criteria above and does not leave the product underneath uncovered and unprotected. The results can therefore be assumed well within the requirements to the dropped object test.

6.2 Stability Calculations

The stability issue due to the tipping moment created by the trawl impact load that was discovered in the stress plots and reaction forces indicated that the mass of the protection cover was too small for the cover to be stable on its own when impacted by the trawl load. In the analyses, the cover has a mass of approximately 2560 kg. The effective mass of the cover is 1542 kg including buoyancy.

The goal of this analysis was to give a rough estimate of how long the cover will need to be in order to be heavy enough not to be affected by the trawl load.

The first analysis of the cover, modeled as it is in the finite element analyses, and by assuming that the trawl load impacts at an height 0,50 m from the ground (higher impact will need more mass to be stable) revealed that the negative reaction force in the roll support that was holding the cover down was -59,4 kN and that the extra effective mass needed to keep the cover stable is approximately 6,0 tons.

In order for the cover to be overtrawlable without rock-dumping, some changes need to be made to the design of the cover. One of the requirements for overtrawlability is that no angle on the structure shall be steeper than 58°. A possibility to satisfy this requirement is to implement so called trawl deflectors on each side of the cover. These are assumed to be 45°, and were designed in *Ansys® Workbench, Release 14.5* to get details such as extra width, added mass, center of gravity etc. The deflectors are assumed added along the outer curve of the cover and extend about 500 mm out on both sides. The added effective mass per deflector is 326 kg for the 1,5 m long protection cover. The deflectors effectively change the tipping point of the cover with a positive effect in regards to needed weight. The wider, or calmer angled, the deflector is, the more positive effect is has on both added weight and the tipping moment; but at the same time, the more difficult to handle on land or boat the cover gets.

The addition of deflectors on both sides, while changing the pinned support to the new corner of the left deflector, and keeping the roll support at the same location, resulted in a negative reaction force of 41,5 kN which translates to the cover still needing 4,2 tons of effective mass in order to counteract the tipping moment from the trawl force when impacting at 0,5 m height. Impact higher up will increase the needed weight.

The length of the cover and deflectors were then extended to 6,5 m long in the X-direction. This is in the area of normal length for the protection covers. The total mass of the cover was now 16,6 tons, and the effective mass in the sea was calculated to 9,5 tons. The assessment of the tipping moment resulted in a positive reaction force of 3,8 kN, which translates to the cover having an excess of approximately 380 kg from being in equilibrium with the trawl force impact at 0,5 m height. Positive reaction force downwards indicates that the cover is heavy enough on its own to be stable when impacted by the trawl force - at least in this simplified assessment of the problem. In a real situation, several covers will be connected to each other in a long chain, and depending on the overlap details, the neighboring covers could also help with keeping the cover stable when impacted by the trawl board.

This simple assessment gives an indication that getting the cover heavy enough within reasonable cover lengths is possible, and backs up the arguments for the reaction forces and forced stresses in the corners from the finite element analyses of the trawl board impact.

A tipping moment assessment should be performed for wave and current forces as well, but this unfortunately falls outside the scope of this thesis. An indication of whether or not the effective weight found from these calculations are enough to withstand the hydrodynamic forces can be based on the values from a report by Subsea 7 (Subsea 7, 2014), where a 2D CFD analysis was performed and resulted in the required submerged weight of 6,0 tons for the 10-year requirement and 9,0 tons for the 100-year requirement for a cover of similar shape, but slightly smaller radius of the arch, see chapter 3.4 On-bottom stability requirements. This could indicate that the effective weight of the protection cover will need to be somewhat higher than 9,5 tons in order to be stable from the hydrodynamic forces due to its slightly bigger cross-section.

6.3 2D model in *STAAD.Pro V8i*

The analysis of the 2D model of the cover created in *STAAD.Pro V8i* was performed to be able to output the maximum design shear and axial forces and the bending moments occurring in the cover after being impacted by the trawl board load as a single point load in different locations on the cover.

The radius of the cover was chosen as the centerline of the 3D model of the protection cover, and is likewise simply supported. Weight of the cover was added as an evenly distributed load. The trawl board overpull design load is to be considered in the Ultimate Limit State, and safety load factors should be applied to the loads. However, the trawl board overpull load is already a design load, which includes the safety load factor. The weight of the cover is however not design load and should have included a safety factor. In this case, however, when the cover is pushed together and up in the middle, it is plausible that the added weight from the load factor would have had a non-conservative effect on the result. In addition, the safety factor for the weight of the cover has not been included in the finite element analyses either, and it would be inconsistent to use the factor in this analysis. This way, the results are more comparable between the analyses.

Although unlikely, the model includes the conservative possibility that the trawl board impacts the cover with full design force in both the supported bottom node as well as in the top node of the cover. It is more likely that the trawl board impacts further up on the cover based on the typical shapes of trawl boards, see Figure 3.2.1-3. The top and bottom locations, or load cases, ended up being the two load cases which resulted in the maximum forces. The maximum axial force of F_X = 337 kN occurs on one of the the upper left beams when the trawl force impacts all the way at the top of the cover. Both the maximum and minimum shear of F_Y = 299 kN occur in the two bottom beams on both sides when the trawl board force impacts all the way down on the cover, essentially directly into the roll support in the direction that is not constrained. The maximum bending moment M_Z = 327 kNm occurs in the top of the cover when the trawl force is applied on the bottom in the roll supported node. This behavior makes sense, as it is much the same behavior seen in simply supported beams loaded by a point load, where the maximum shear is located in both ends, close to zero shear in the middle and with the maximum moment located in the middle;

except that this beam is curved and thus the distributions of forces and moments look a bit different.

The results from this analysis, which can be seen in Table 5.3-1 and Figure 5.3-37 to Figure 5.3-43, will be used in the concrete and reinforcement design according to *Eurocode 2*.

6.4 Concrete and reinforcement design according to *Eurocode 2*

The goal with these calculations, which can be read in its entirety in Appendix E Concrete and reinforcement design calculations according *to Eurocode 2*, was to attempt to design the protection cover using the rules and regulations in the *Eurocode 2* standard. The applicability of the codes to this problem was a bit questionable, however, as the *Eurocode 2* is mainly based on buildings, and in that case most likely regular horizontal beams and vertical columns. This cover, or "beam", is curved, and most likely does not fit entirely into the assumptions made in the standard. This was especially the case for axial force capacity of the cover, which is calculated by finding the geometrical deviations of the column and adding the axial force to the design moment as second order moments. It is hard to imagine the applicability of this to the case from *STAAD.Pro V8i* above, but an attempt was made nonetheless. Shear force and bending moment design were a bit more straightforward, as they consider the design forces or moments in a section in the beam, and the relation between the standard and this case is a bit clearer.

In regards to material data and quality, the Norwegian Annex to the *Eurocode 2* states that the concrete of the cover, which is to be completely submerged, falls under the exposure class XS2 and needs to have a durability class of minimum M40, which corresponds to a strength class of minimum B40. The covers analyzed in the finite element models have strengths of B40 for the trawl board load, and B35 for the dropped object analysis. The cover tested for the dropped object test has a minimum strength class of B40 as well.

The exposure class leads to the minimum concrete cover of the reinforcement c_{min} = 50 mm. The covers in the finite element analyses have a concrete cover of the reinforcement of approximately 31 mm, which is based on the cover supplied for drop testing by Multiblokk

AS. 31 mm is too little reinforcement cover, but by increasing the cover to 50 mm, the inner and outer bar of reinforcement gets closer together. This takes away a lot of the bending moment resistance in the cover by reducing the effective height between the edge of the beam and the center of the tension reinforcement, as well as the distance between the reinforcement bars. The calculations are based on the cross section from the cover used with the necessary concrete cover of 50 mm, except where explicitly written otherwise, such as simple capacity tests of the cover used in the other analyses.

The amount of tension and compression reinforcement needed for the given cross section and placement of reinforcement to withstand the design moment M_{Ed} = 327 kNm, was A'_s = 1650 mm^2, or 15 bars of compression reinforcement (inner reinforcement ring), and A_s = 6112 mm^2, or 54 bars of tension reinforcement for the cover (outer reinforcement ring), when the length is 1500 mm and height is 215 mm. This would result in only 27 mm of center distance between the reinforcement bars in the outer circle. This is an impractical solution and it should be investigated whether altering the geometry of the cover could be a better solution. By increasing the height of the beam (thickness of the cover), for instance at the top, where the design moments are found, the effective height between the reinforcement could be increased and the need for tension reinforcement could be drastically reduced. As was indicated by the dropped object tests, the roof of the cover could easily have been made thicker by reducing the inner height of the cover, without exceeding the clearance requirements from vertical deformation. Making the cover thicker would also most likely increase the strength of the cover and increase its resistance to dropped objects.

The cover assessed throughout the thesis has no shear reinforcement, only longitudinal tension and compression reinforcement. The analysis in *STAAD.Pro V8i* indicates that, at impact from the trawl board, large shear forces will appear in the cover. The calculation of the shear capacity in the cover without reinforcement indicates that the shear capacity in the cover itself is too small to resist the design shear force V_{Ed} = 299 kN, and that extra shear reinforcement is needed. However, by including the added thickness to the cover provided by the trawl deflectors, and assuming that these are reinforced as well, and by taking into account that the beam will have to be approximately 6,5 m instead of 1,5 m long (it is a bit unclear whether or not the formula is meant for "beams" of such odd shapes as the cover is), the shear force capacity of the cover can be increased a lot and thus possibly avoiding the requirement of extra shear reinforcement. On the other hand, adding some shear reinforcement would probably assist in creating a self-bearing structure when the length and width of the protection cover is increased. If the thicknesses and thus effective heights are increased, the shear capacity would also increase, but at the same time generate more weight that the self-bearing structure would need to be able to handle.

The problem of making sure that the structure is self-bearing as also relevant in regards to lifting operations on the cover, where the lifting points most likely would be extra reinforced local points on the cover. When the cover weighs more than 16 tons in the air, the cover must be able to bear its own weight. In addition, as the weight and size increases, the cover quickly becomes more difficult to handle safely. The lift design of the cover was however not possible to include in the scope of the thesis due to time limitations.

The applicability of the calculations of moment capacity including axial force and its second order effects are of questionable nature. They are mainly based on vertical columns that are experiencing second order effects from the geometrical deviation of the column, as well as due to curvature deflection from the axial force etc. The fact that the cover, or beam, or in this case column, is curved, is not taken properly into account in these calculations. In addition, many assumptions in regards to several different factors needed to be made in order to complete the calculations.

The axial force calculations revealed that the second order effects could be ignored, based on the comparison of the slenderness ratio to the limit for the slenderness ratio. This is also based on the slightly odd shape of the column, or cover, which would be affected by any changes to the thicknesses or length of the cover.

Although the calculations should be disregarded because of the questionable applicability, the calculations were performed nevertheless; if only as a test. The second order effects resulted in a small increase in the design moment, and thus the need for slightly increased amount of longitudinal reinforcement.

6.5 Dropped object test on the concrete protection cover

6.5.1 Results

The full scale dropped object test was performed effectively and with great success over two days with help from everyone involved. The goal of the test was to determine whether or not the protection cover with the given size, thickness and amount of reinforcement would be able to withstand the dropped object requirements from *NORSOK standard U-001*. The results of each test are presented in chapter 5.5 Dropped object test on the concrete protection cover, and the drops can be viewed in the picture-by-picture images in Appendix G Frame-by-Frame of dropped object tests.

Six drop tests were performed in total. The first and initial drop test of the 50 kJ requirement was performed outside on gravel and was used as a guidance for the five next drop tests. The first test was performed on a cover of the same size, length 1500 mm, thickness 215 mm and inner diameter of 1000 mm, but with less reinforcement: only eight Ø12 mm oval reinforcement bars. The test resulted in severe damage on the cover, but it did not completely collapse nor was it penetrated by the object, and would still have been of some protection to the pipeline because of the reinforcement holding the cover together. The cover was however severely damaged, and several large cracks almost separated one part of the cover from the other, see Figure 5.5.2-46 and Figure 5.5.2-47. In addition, several of the reinforcement bars were bared as large chunks of concrete came off from the underside of the roof of the cover. This would have resulted in quick initiation of corrosion of the reinforcement. As can be seen in Figure 5.5.2-48 and Figure 5.5.2-49, the amount of concrete coming loose was a bit too much, and some of this could have possibly damaged the spool or pipeline if delicate parts of it were located underneath the affected cover. Although not collapsing entirely, the damage on the cover was still too much, and could have possibly damaged the equipment underneath; the test was not approved according to the criteria. A decision was made to up the amount of reinforcement in the cover before the next tests.

The vertical deformation of the top of the cover was measured with several different measuring devices in order to test which would be best suitable for the next tests. The telescope magnet underneath the midpoint of the cover, which was also the method used for the next tests, measured that the maximum vertical deflection of the cover was 100 mm, but after the object fell off and the tension in the reinforcement was released, the cover retracted, or pulled itself slightly back together, and left an end deflection of 87 mm. This deformation is within the criteria for vertical deformation. On the ground where the legs of the cover were placed, clear marks that the cover had been widened, i.e. the legs pushed wider, could be observed. This is also visible on the recorded video presented as pictures in Appendix G Frame-by-Frame of dropped object tests. The new width of the cover was unfortunately not measured, but based on the video and photographic evidence, approximately 7-8 cm on each side seems reasonable, see Figure 5.5.2-50. The widening of the cover would not have compromised the horizontal deformation clearance criteria.

The next set of tests was performed submerged in the basin at the laboratories in the University of Stavanger. With the increased amount of reinforcement, 12 double bars of Ø 12 mm reinforcement, i.e. 24 bars in total, it was expected, based on the results from the initial test, that the covers would hold themselves together in a more satisfying way. The covers were placed upon big bags of sand and rock in the basin. This had two effects, first and foremost it would protect the concrete floor of the basin, and secondly it would be a more realistic support or ground condition for the cover. The seabed conditions will vary from location to location, and the sand bag supports cannot be a simulation of them all, but what can be said for certain is that it is more realistic than concrete. As was seen from the results in chapter 5.5.7 Sand bag supports, the covers were pushed down into the sand bags during the impacts. How much the individual cover was pushed down cannot be said for certain, as the bags were only accessible after all the tests were done and the water drained. The bags served their purpose well, and the concrete floor of the basin was not damaged during the tests.

It was decided to use water in the test, as this would be a more realistic scenario than in air. Water is assumed incompressible, and it is thus likely that the water on the inside of the cover will have a dampening effect on the deformations of the cover. This goes also for the water on the outside of the cover, which will have to be pushed away for the cover to expand sideways during impact. It was decided to fill the basin up only to about 10 cm over the cover and calibrate the velocity of impact to the terminal velocity in water, or slightly above to be safe. This would allow the object to hit the cover where and with the velocity intended, instead of losing aim and velocity once it hit the water above the cover.

From the beginning of the test, it was planned to record the impacts underwater from the front of the cover, as was done for the initial test. After the 5 kJ and 20 kJ tests were performed, the action camera was removed due to the fact that the sand and silt from the sand bags were whirled up into the water, and it was not possible to see anything on the recordings. For the two remaining tests, the action camera was placed in front of the camera, but over the water. For this reason it was not possible to see on video the push down and widening effect that the individual impacts had on the covers and sand bags.

The vertical deflection measuring method chosen for the tests was the telescope magnet, as the oasis was difficult to get to work under water. The ruler in front of the cover was also removed, as the action camera under water was not able to clearly record the deflections. The limitations of the chosen measuring device are worth noting: it was only able to measure the total deflection of the cover, including the inevitable push down of the cover into the sand bags. Therefore an additional measurement of the inner height and width of the covers was recorded after removal from the basin. There are a couple of uncertainties worth noting about this method. As the cover is lifted up and out of the water and the basin, a lifting sling was inserted under the cover and was lifting the cover in the middle from underneath. As this is done, it is possible that some of the deformation on the cover is reverted due to the weight of the cover and the upwards pulling force from the sling. Therefore it is possible that the measured deformations after removal from the basin are slightly smaller than the maximum deformations momentarily after the impact. In addition, it is difficult to be absolutely certain that the inner height of the cover was exactly 1000 mm, as the cover is made from a round pipe cut into two halves. Although the cut is performed to the best of abilities, there will always be some small deviations. That the height of the cover has changed is therefore difficult to say with certainty. The width of the cover of 2000 mm (with some allowed deviations here as well, see chapter 4.5.3.1 Concrete Protection Cover), is however easier to note changes in. For the two covers impacted by 30 kJ and 50 kJ there were measured about 20 mm of increased width in total. After the 20 kJ test, the measuring device broke as the cover was removed. The deflections of the top of the cover plus the push into the sand bags were measured from the top of the surface level of the water and down to the top of the cover. This measurement was performed both before and after the drop test, and will essentially give the same result as the measuring device underneath the cover. The water level in the basin was not changed during the testing.

It is also probable that the retraction of the deformation due to release of tension in the reinforcement is present in these tests as well, as recorded in the initial test and the finite element models. Due to the cover being under water, and that the action camera was not able to capture the deformations under water, it was not possible to record this effect.

The pictures of the sand bags after all the impacts, see Figure 5.5.7-76 to Figure 5.5.7-78, show that a sizeable portion of the measured deflection is due to the legs of the cover being pushed down into the sand. The protection covers need to be overtrawlable, which these are not, and the plan is to increase the surface area of the legs by adding trawl deflectors, as described earlier. It is possible that this increased area would render these tests not conservative due to the increased area that needs be pushed into the seabed. This could increase the amount of energy that has to be absorbed internally by the cover and possibly result in more damage and cracking. A solution to this could be to increase the thickness and reinforcement both in cover and the deflectors, which is also indicated necessary by the design according to *Eurocode 2*. The trawl deflectors could however end up having the opposite effect, depending on the execution of the design, and increase the strength of the cover by increasing the cross-section and amount of reinforcement. It could also be possible to thicken the cover in the top. This would allow for more distance between reinforcement, which is positive for strength in the section.

The objects were measured and weighed before the drop so that the impact height could be adjusted to yield the correct impact energy. The minimum impact velocity allowed in the tests was the terminal velocity of 6 m/s from drill pipes in water (DROPS online, 2010), and all of the weights of the object resulted in an impact velocity between 7,63 m/s and 8,84. m/s.

The five next drop tests (the 5 kJ impact was tested twice) were performed with the same outer dimensions of the cover as before, but with 2x12 Ø12 mm double reinforcement bars. As can be seen in the figures in chapter 5.5.3 to chapter 5.5.6, the impacts caused some slight damage in the form of cracks, some crushing and some deformation, but nowhere near the results from first test. The most critical damage to the covers did not come from the 50 kJ impact, but the 30 kJ impact because this landed slightly askew and most of the impact energy had to be absorbed by the front of the cover which resulted in large cracks in front. The 50 kJ landed flatly, and the energy was absorbed by the entire cover which resulted in smaller cracks in size, but more cracks on the cover overall. It is safe to say that the covers were not penetrated, and the measured deflections, included being pushed into the sand bags, did not exceed the clearance requirement. No sizeable chunks of concrete were knocked loose from the roof of the covers, and the spool or pipeline under the cover would have been safe and sound after all of the tested impacts. The protection covers passed all of the requirements and criteria for the drop test.

6.5.2 Full scale drop test results compared to results from dynamic finite element analysis

For the results from the dynamic finite element analyses, please refer to Appendix B Results from the Dropped object analysis *in Ansys® Workbench, Release 14.5*.

The 5 kJ impacts resulted in no measurable deflection in the top of the cover and left only two small impact marks and no visible cracking in the vicinity of the impact marks. Compared to the finite element analysis of the 5 kJ impact, these results makes sense. The analyzed vertical deformation is 3,4 mm on the top of the cover underneath the impact area, this is comparable to the impact marks left on the covers. The inner height of the cover is reduced by approximately 1 mm in the model and the width is increased by between 1 and 2 mm on each side. These changes are too small to be possible to record on the tested cover, especially when considering the arguments mentioned above. The damage result shows that a small area around the impact area is affected, but that no part of the cover is fully fractured, as the factor does not reach 1. This coincides with the results from the impact test.

The 20 kJ impact resulted in 4 cm measured deflection or sink down into the sand bags. The deformation in Y-direction in the finite element model show a maximum of 15,2 mm, and a widening of 12 mm in positive and negative Z-direction. The difference may indicate that most of the measured deflection was the cover being pushed into the sand bags. This theory is also backed up by the measurements of the inner height and width, which only were able to detect 1 cm deflection in the top, no widening of the inner diameter. Considering the uncertainties mentioned above, these results are not far from each other. The damage plot from the model reveals that in an ideal situation, where the object lands evenly, the cover is fully fractured in an area directly below the object on the topside and underside of the cover, as well as in a line in center from front to back of the cover. In the drop test, the object landed askew, and thus damaged the front more than the back. The web of cracks on the topside and underneath of the cover also tells the same tale. Most of it is located in the front of the cover. The model did not however, predict the vertical crack down the right side of the cover.

The 30 kJ impact resulted in a measured deflection of 50 mm in front and 20 mm in the back (in the midpoints between center and edges of the cover) including being pushed into sand, most likely due to the object landing askew forward. After removal from basin the height deflection was measured to 15 mm and the widening of 20 mm in total. The finite element model resulted in a vertical deformation in the middle of the cover of 28 mm and a widening of approximately 25 mm on both sides. These numbers are also fairly coinciding if the uncertainties mentioned above are taken into account. The deformation of the cover is most likely reverted somewhat in the lifting process. The damage on the cover in the model shows that a large area directly under the impact object is fully fractured, as well as a large field underneath from the front to the back of the cover. The object landed slightly askew in this test as well, and most of the impact energy was directed to the front of the cover which was the most damaged. Like the model, a large crack and fully fractured material appeared in the top front, as well as a large, fully fractured web underneath the top of the cover. On the top of the cover, the damages were less visible, but a web of cracks and fractured material can be observed here as well. The model was not able to predict the vertical cracking on both sides during this test. The largest crack on the cover was located on the right side of the cover. It is however important to remember that the solid element Solid185 that was used in the model does not have the crack prediction function that the legacy element Solid65 has. The model is thus not able to predict cracking, but uses a cumulative damage model instead to give a hint of where the damage will be.

The 50 kJ impact resulted in measured deflection of 70 mm in front and 75 mm in the back, including being pushed down into the sand bags. This could suggest that the object landed straight on the cover. The damage, distribution of cracks and video evidence supports this assumption. The inner deflection of height after removal from basin was measured at 25 mm and the widening at 20 mm in total. The finite element model resulted in a vertical deformation in the middle of the cover of 59 mm and horizontal widening of approximately 49 mm on both sides. The model is based on a hard floor with no allowable deformation in Y-direction, and it is logical that the deformations in the model are a bit larger than the ones seen in the tests. In addition, the arguments in regards to lifting are valid for this case as well. The damage on the model of the cover shows that a large area on the top is fully fractured for an area almost stretching from back to front, as well as the line in the middle both on the top and underneath the cover stretching from front to back. Underneath, there is a large fully fractured area from the front to the back. The fractured areas in the outer corners are most likely credited to the support conditions of the cover and restraint of rotation. The cracking patterns from this test confirm much of the predictions of the damage model. A large web of cracks both on the top and underneath the cover is clearly visible, and many of the cracks extend from the front of the cover to the back. The cracks extend further down the sides of the cover than the damage model is able to predict. This cover was not cracked vertically down the sides like the other two covers, and it is possible that this could have something to do with the even or askew landing of the object.

In summary, the concrete protection covers would have protected the pipeline from the dropped objects, and was able to absorb the impact energies without being penetrated or collapsing upon the equipment. In addition, when considering the differences in support conditions, there is a quite clear similarity between the results from the dynamic finite element analyses and the results from the drop test.

6.6 Suggestions for protection cover design based on results

Based on the results from the various analyses and tests, a few suggestions for the next iteration of the design of the cover will be given here.

One of the most important things is to add a way for the cover to be overtrawlable, and like has been suggested earlier, diagonal deflectors with an angle of for example 45 degrees could be added, see Figure 6.6-3 and Figure 6.6-4. A lower angle could be used to increase the weight of the cover and to positively affect the tipping moment calculations. Care must be taken not to make the covers too difficult to handle due to the increased weight and width, and a balance point between practicality and increase of width and weight should be found.

It would also be important to reinforce the trawl deflectors in connection with the cover, so that the reinforcement will help make the structure self-bearing. The design of the cover according to *Eurocode 2* revealed that, for the areas experiencing the maximum shear forces and moments, extra reinforcement is needed in order to make the cover withstand the forces. A thicker cross-section and distance between reinforcement bars would help increase the capacities as well.

Increasing the surface area of the legs by adding the deflectors could, as mentioned earlier, negatively affect the results from the dropped object tests, as more area would have to be pushed into the ground. This could result in that more of the energy has to be absorbed internally, which could damage the cover more severely than what the drop tests performed in this thesis showed. A mitigation to lessen the possible result of this could be to increase the thickness of the top of the cover, for example by lowering the roof somewhat. The tests have shown that there would be room for this without compromising the clearance criteria. The distance between the reinforcement bars could then be significantly increased and thus the strength of the concrete cross section is increased as well. It is however important to also remember that the new requirement for concrete cover of the reinforcement is 50 mm, as opposed to 31 mm used for the models in this thesis. Another possibility to reduce the amount of impact energy that has to be absorbed internally by the structurally bearing part of the structure is to add a layer of porous layer of weak concrete on top of the cover. The intention would be that this layer crushes first and absorbs most of the impact energy, both from dropped objects or trawl boards.

The weight of the cover needs to be increased as well. As indicated from the stability calculations, the cover will need an effective weight of approximately 9,5 tons to be stable when impacted by the trawl gear at a height of 0,5 m. This would correspond to a weight in air of 16,6 tons. A similar approximate weight is needed for the cover to be stable due to hydrodynamic forces, as indicated in chapter 3.4 On-bottom stability requirements although this will need to be assessed in a proper CFD analysis of the cover. The weight of the cover can be increased by making the cover longer, as illustrated by the stability calculations. In addition, steel clump weights can be built into the trawl deflectors to increase the weight of the cover if needed. An effective design to easily accommodate for lifting and possibly stacking of the covers should be investigated. A balance point between size of the cover, self-bearing capacity, the various requirements to strength and practicality in regards to lifting and handling should be investigated.

By making a steel frame for mass producing concrete covers of a given size, as well as finding a standardized design for the protection cover and reinforcement, could in the long run result in a cost effective solution for protection covers where rock-dumping is not possible or difficult.

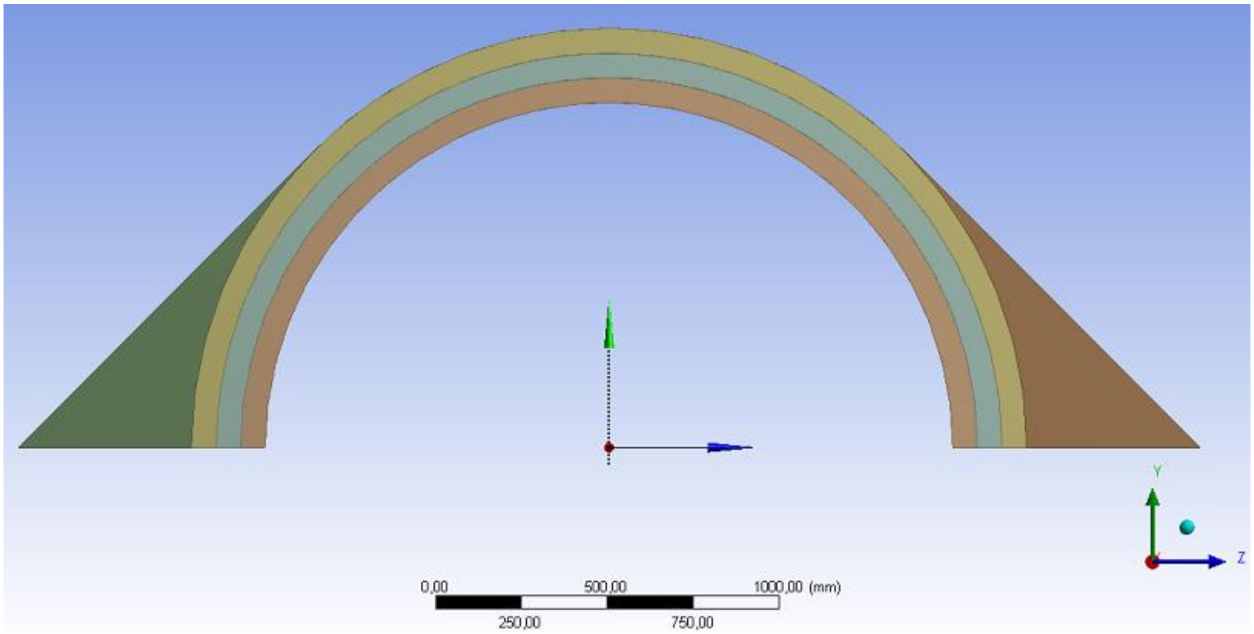

Figure 6.6-3 Example of the original cover with 45° mud mats extending the width with 500 mm on each side. Source: ***Ansys® Workbench, Release 14.5***

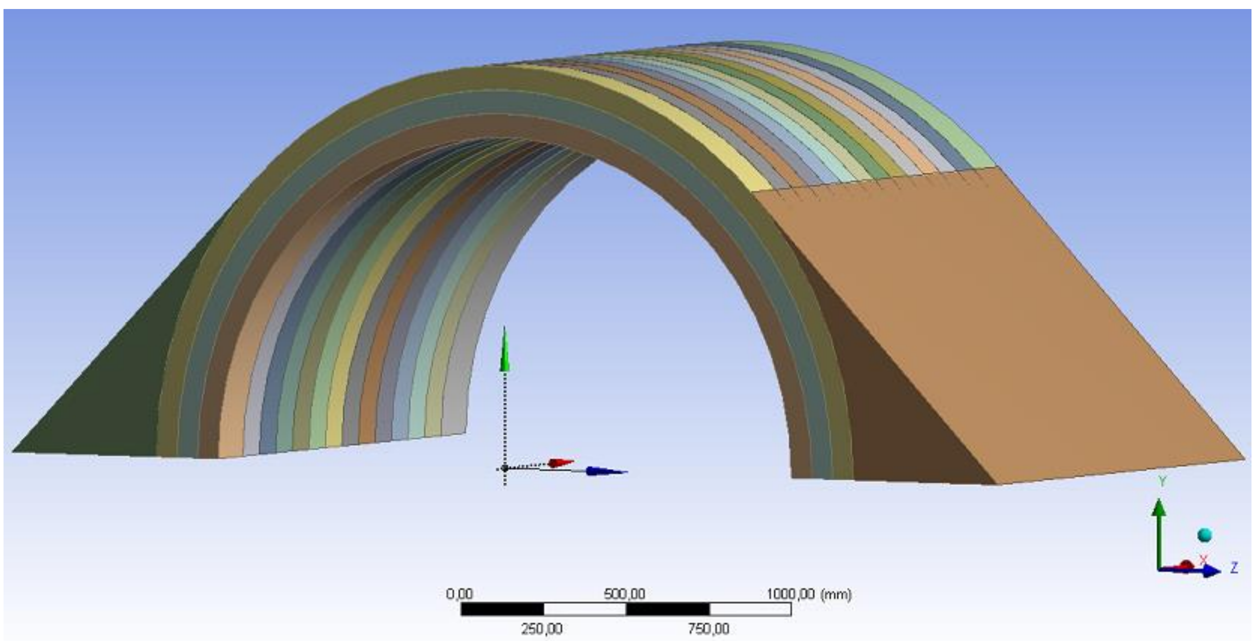

Figure 6.6-4 Example of the original cover with 45° mud mats on each side.
Source: ***Ansys® Workbench, Release 14.5***

6.7 GRP versus concrete

In the end, a small reflection about GRP covers will be included. The initial problem in the thesis was that GRP covers need a lot of ballast in order to achieve on-bottom stability, and that in some cases rock-dumping is not possible, and thus making the need for extra ballast weight even greater. This thesis has assessed whether concrete protection covers are a viable option or not, and come up with some solutions in order to create a cover with the needed weight and design in order to make it a viable alternative.

The problem is, however, that due to the versatility in regards to shapes and strength of the GRP covers, there are many solutions available for GRP covers as well. For instance, the trawl deflectors could be built into the GRP covers as well. This could be done for instance by adding stiffened plates in an angle from the seabed up to the cover. This trawl deflector could also possibly be filled with various ballast material which would rapidly increase the weight of the cover.

Increasing the strength of the GRP covers is possible by for instance building beams of reinforcing materials into the design of the cover. In addition, there are several other benefits of using GRP such as the possibility to create grated walls or roof, which does not catch waves the same way as a solid wall or roof does. This could be possible with concrete as well, but probably not as easily.

Therefore, the next step of the concrete protection cover assessment should be to refine the geometry, configuration and design based on the results from this thesis. When a working model and geometry of the concrete protection cover has been achieved, the advantages and disadvantages of the two methods should be compared. A cost-efficiency analysis between the two, possibly also including steel as an option, should be performed in order to figure which method can be used in what situations and which would be the less costly alternative. This is extremely important in an industry where cost-efficiency is a, if not the, keyword in the present.

7 Conclusion

The results from the various structural analyses of the first iteration of the protection cover design has provided quite clear indications that creating a protection cover from reinforced concrete absolutely is a viable method of protecting subsea equipment such as spools or pipelines. The cover has the necessary strength to resist impacts from trawl gear and dropped objects, and it has the stiffness to not deform more than is allowed by the requirements from both the situations.

In detail, this means that the trawl board overpull analyses in *Ansys® Workbench, Release 14.5* indicate that the cover will experience stresses that might damage the cover by for instance cracking, but the deformations are within the given criteria.

The stability calculations indicate that by making the cover longer, adding trawl deflectors and thus increasing the weight of the cover to an effective weight of approximately 9,5 tons, or 16,6 tons in air the cover will be able to be stable on the seabed when impacted by a trawl board at an height of 0,5 m.

The *Eurocode 2* gives rules and regulations in regards to the design and configuration of the cover. The minimum cover of the reinforcement shall for instance be 50 mm, and the concrete material of minimum B40 strength. The strength calculations for shear force, bending moments and axial force indicates that the cover is able to withstand the design forces and moments from the trawl board impact in its current geometry if some changes are made to the amount of reinforcement. By changing the geometry of the cover, for instance by adding trawl deflectors and increasing the thickness at the top of the cover and thus increasing the spacing between tension and compression reinforcement, the various capacities of the concrete cover can be increased even more.

The full scale dropped object tests proved that the cover in its current configuration is able to withstand the impact energy requirements in *NORSOK standard U-001* (Norwegian Technology Centre (NTS), 2002) without completely collapsing or being penetrated and thus damaging the product underneath. The concrete covers experienced some measurable deformation and large areas of the cover were cracked, especially underneath the cover where it is exposed to tension from the bending of the cover. The results coincide quite well with the results from the dropped object analysis performed in *Ansys® Workbench, Release 14.5* if the uncertainties from the tests and different supporting conditions are considered.

There are a lot of work remaining before the concrete protection cover design is finalized, but the initial signs are positive. Some design configurations need to be made; such as making the cover overtrawlable by adding trawl deflectors, but also lowering the roof and making the cover thicker in top would be wise. Finding an optimal design which accommodates lifting, possibly stacking of covers while the cover is able to carry its own weight should be focused on.

One of the benefits of the concrete protection cover is that once a design is finalized, and the creation of a casting frame is done, the actual casting of the cover should be a relatively quick and simple process. Done right, this could in the long run mean cost efficient protection covers with a competitive edge where rock-dumping is not possible.

The problem is however that many of the advantages that the concrete protection cover possesses are also able to be achieved using GRP protection covers. Trawl deflectors could for instance fairly easily be built into a GRP cover design.

Therefore it will be important to investigate the strengths and weaknesses of the protection covers made of the different materials, and compare them against each other to find out in which cases it would be beneficial to use one or the other. A cost analysis of the manufacturing, transportation, lifting, installation and various other operations needed for the two covers should be performed in order to figure out whether the use of concrete protection covers is a viable protection method for spools and pipelines that could be preferred to GRP or steel protection covers.

Based on the results from this structural assessment of the concrete protection covers, it is clear that the concrete protection covers is a feasible concept that it would be beneficial to investigate further and in more detail. Its heavy weight, high strength and the liberation from the rock-dump requirements gives the concrete protection cover a competitive edge that would be well worth exploring further.

8 Recommendations for future work

As has been mentioned earlier, the focus of this thesis has been on the structural design of the concrete protection cover. There are several other aspects to the concrete protection cover that should be investigated further in order to gain a complete picture of the viability of using concrete instead of GRP.

For instance, the geometry and design configurations of the cover should be taken further. The results provided in this thesis should give some guidance as to what needs to be improved about the cover for the next iteration of the technology qualification process. The design should also be taken to the next level of detail and focus on things like the overlap between covers, lift and reinforcement design, as well as finding the optimal balance between weight, width, angles on trawl deflectors and the cover's ability to carry its own weight.

In addition, the hydrodynamic assessment of the cover should be performed and a required effective weight should be found. This would include for example a CFD analysis of the cover and the fluid flow based on the wave and current conditions of the given location. A geotechnical assessment of the seabed conditions should be performed as well.

An economic analysis of the cost-efficiency between the concrete protection cover and its competition, GRP and steel covers, should be performed in order to figure out which would be most beneficial in cases where rock-dumping is not possible.

List of References

Anderson, T. L. (2004). *Fracture Mechanics: Fundamentals and Applications, Third Edition* (3. ed.). Boca Raton, Florida, The United States of America: CRC Press, Taylor & Francis Group.

ANSYS, Inc. (n.d.). *ANSYS® Workbench, Release 14.5, Help System.* Canonsburg, Pennsylvania, USA: ANSYS, Inc.

Atkins Boreas, Shell UK Ltd. (2009). *5075215/001/BR09002 Rev C - Updated Fishing Loads - Subsea Structure Design.* Aberdeen: Atkins Boreas.

Basal AS. (2009). *Basal Standard.* Oslo, Norway: Basal AS.

Bond, A. J., Brooker, O., Harris, A. J., Harrison, T., Moss, R. M., Narayanan, R. S., & Webster, R. (2006). *How to Design Concrete Structures using Eurocode 2.* Blackwater: The Concrete Centre.

Callister, W. D., & Rethwisch, D. G. (2010). *Materials Science and Engineering: An Introduction - Eighth Edition.* Hoboken, New Jersey, The United States of America: John Wiley & Sons, Inc.

ConcreteNetwork.com. (n.d.). *ConcreteNetwork.com*. Retrieved March 12, 2015, from Precasting Methods and Materials: http://www.concretenetwork.com/precast-concrete/wet-cast.html

Det Norske Veritas AS. (2010). *DNV-RP-F107 Risk Assessment of Pipeline Protection.* Høvik, Norway: Det Norske Veritas AS.

Det Norske Veritas AS. (2011). *DNV-RP-F109 On-Bottom Stability Design of Submarine Pipelines.* Høvik, Norway: Det Norske Veritas AS.

Det Norske Veritas AS. (2012). *DNV-OS-H102 Marine Operations, Design and Fabrication.* Høvik: Det Norske Veritas AS.

Det Norske Veritas AS. (2013). *DNV-RP-A203 Technology Qualification.* Høvik: Det Norske Veritas AS.

Det Norske Veritas AS. (2014). *DNV-RP-F111 Interference between Trawl Gear and Pipelines.* Høvik, Norway: Det Norske Veritas AS.

DROPS online. (2010, August). *Subsea DROPS - Items dropped into the sea.* (G. Reid, Ed.) Retrieved 1 26, 2015, from DROPS online- The Dropped Objects Prevention Ccheme- Global Resource Centre: http://www.dropsonline.org/index45cd.html?id=1&refID=60&refID2=133&refID3=193&contentID=193 , http://www.dropsonline.org/downloads/DROPS_SubseaDROPS.pdf

Fiskeridirektoratet. (2010, May 26). *Beskrivelse av relevante fiskeredskap og fiskeriaktivitet i Norges økonomiske sone*. Retrieved from Oljedirektoratet: http://www.npd.no/Tema/Seismikk/Relevante-fiskeredskap-og-fiskeriaktivitet-/

Fokk, T. (2005). *MT55-F05-041 - Norne Satellites - Overtrawling Study - Model Test Report.* Marintek. Trondheim: Marintek.

Gudmestad, O. T. (2015). *Marine Technology and Operations - Theory & Practice.* Southampton, Norway: WIT Press.

Høgskolen i Bergen, Institutt for bygg og jordskiftefag. (2011). *Betongkonstruksjoner: Formler og Diagrammer: NS-EN 1992-1-1.* Bergen: Høgskolen i Bergen, Institutt for bygg og jordskiftefag.

International Organization for Standardization. (2010). *BS EN ISO 13628-1:2005+A1:2010: Petroleum and natural gas industries. Design and operation of subsea production systems. General requirements and recommendations.* Geneva, Switzerland: BSI. Retrieved from https://bsol.bsigroup.com/Bibliographic/BibliographicInfoData/000000000030159563

Krogstad, H. E., & Arntsen, Ø. A. (2000, February 23). *NTNU- Department of Structural Engineering.* (Ø. A. Arntsen, Ed.) Retrieved from Wave Descriptions and Theory- Linear Wave Theory: http://folk.ntnu.no/oivarn/hercules_ntnu/LWTcourse/

Mosley, B., Bungey, J., & Hulse, R. (2012). *Reinforced Concrete Design to Eurocode 2 - Seventh Edition.* London: Palgrave Macmillan.

National Oceanic and Atmospheric Administration. (2015, January). *NOOA's National Ocean Service*. Retrieved from NOOA's National Ocean Service: Education: Currents: http://oceanservice.noaa.gov/education/tutorial_currents/welcome.html

Norsk Standard. (2004). *NS-EN 1992-1-1:2004+NA:2008. Eurocode 2: Design of concrete structures - Part 1-1: General rules and rules for buildings.* Oslo: Standard Norge.

Norwegian Technology Centre (NTS). (2002). *NORSOK Standard U-001: Subsea production systems. Rev. 3, Oct. 2002.* Oslo: Standards Norway.

Norwegian Technology Centre (NTS). (2004). *NORSOK Standard M-001: Materials selection, Rev. 4, August 2004* (4. ed.). Oslo: Norwegian Technology Centre (NTS).

Norwegian Technology Centre. (2013). *NORSOK Standard N-004: Design of steel structures. Rev. 3, Feb. 2013.* Oslo: Standards Norway.

Puig, P., Canals, M., Company, J. B., Martìn, J., Amblas, D., Lastras, G., . . . Calafat, A. M. (2012, September 05). Ploughing the deep sea floor. *Nature- International weekly journal of science*. Retrieved from http://www.nature.com/nature/journal/v489/n7415/full/nature11410.html

Subsea 7. (2014). *C127-AQ-U-RA-0005: Mariner SURF EPCI (Subsea, Umbilicals, Risers, Flowlines)- Protection Cover Design Report.* Stavanger: Subsea 7.

Subsea 7. (2014). *C127-AQ-U-XD-0021-01: Mariner SURF EPCI- GRP Cover Straight General Arrangement.* Stavanger: Subsea 7.

Subsea 7. (2015). *ST-GL-ENG-ST-021 - Engineering Standard - Structures - Subsea Protection Structure Design Guideline.* Stavanger: Subsea 7.

Appendices

A. Results from the Trawl board analysis in *Ansys® Workbench, Release 14.5*

Outer 1 load case can be seen in chapter 5.1.1 Trawl board overpull – Static Structural.

Outer 2 load case:

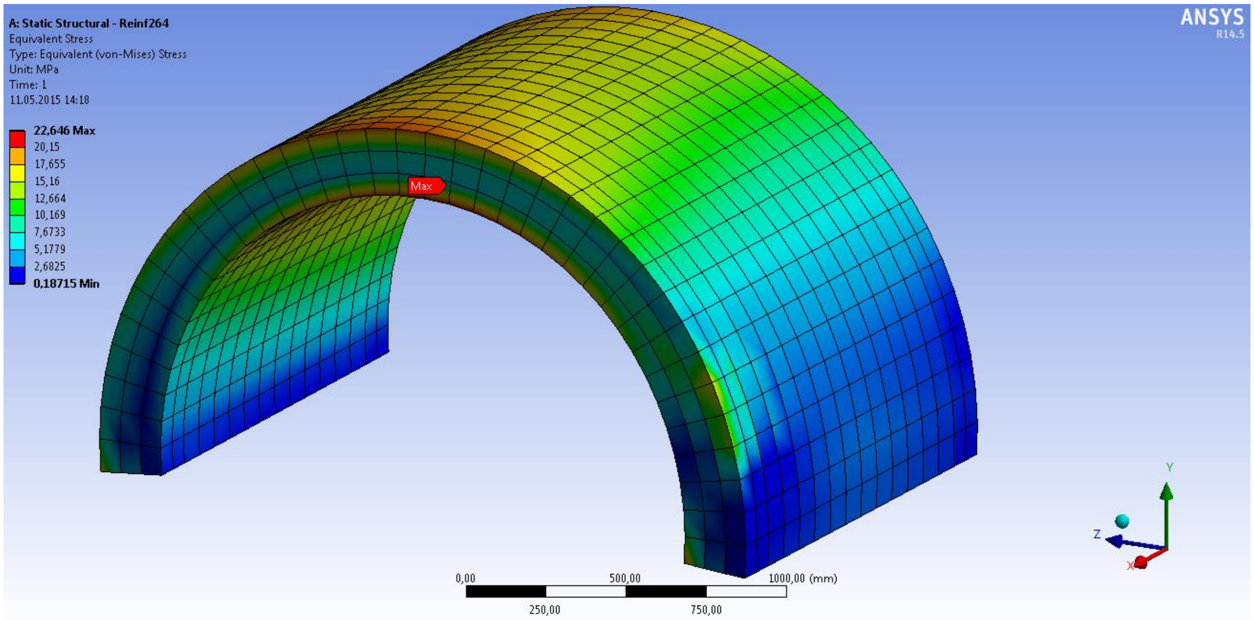

Figure A-1 Equivalent Stress – Outer 2 load case. Source: ***Ansys® Workbench, Release 14.5***

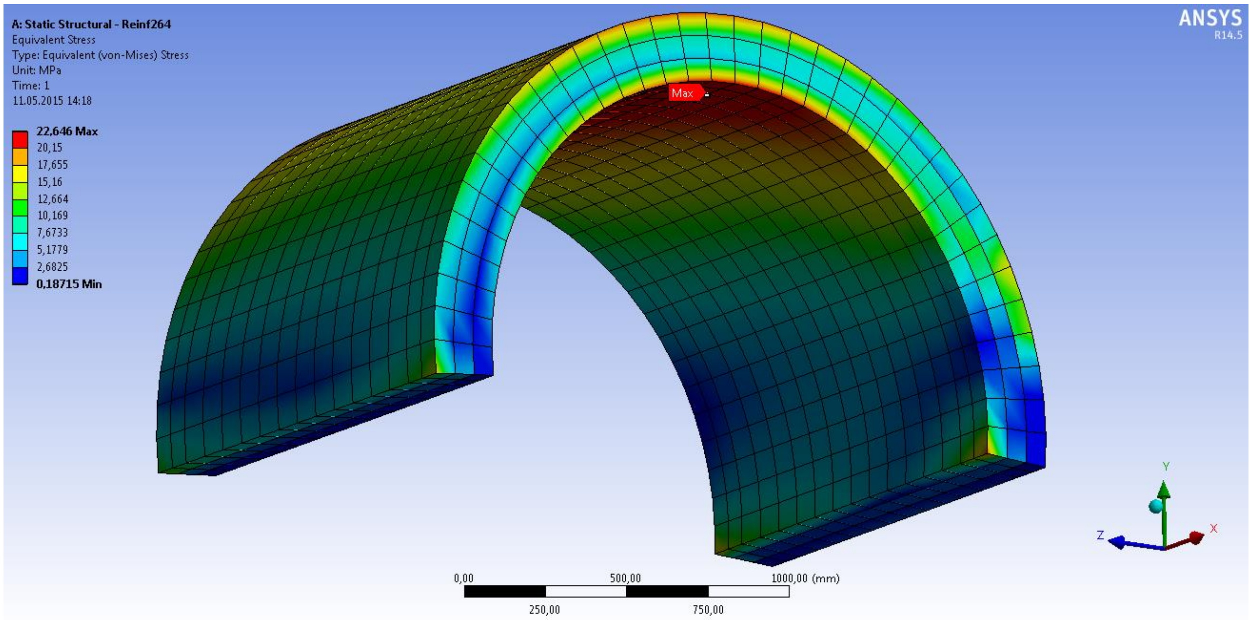

Figure A-2 Equivalent Stress – Outer 2 load case. Source: ***Ansys® Workbench, Release 14.5***

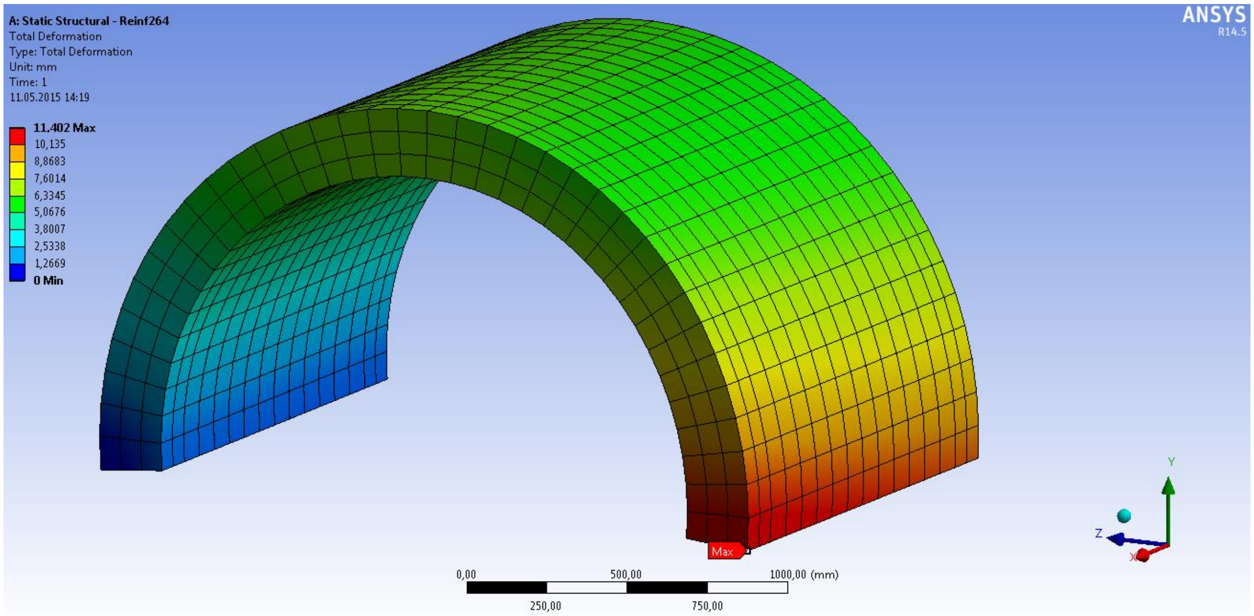

Figure A-3 Total Deformation – Outer 2 load case. Source: ***Ansys® Workbench, Release 14.5***

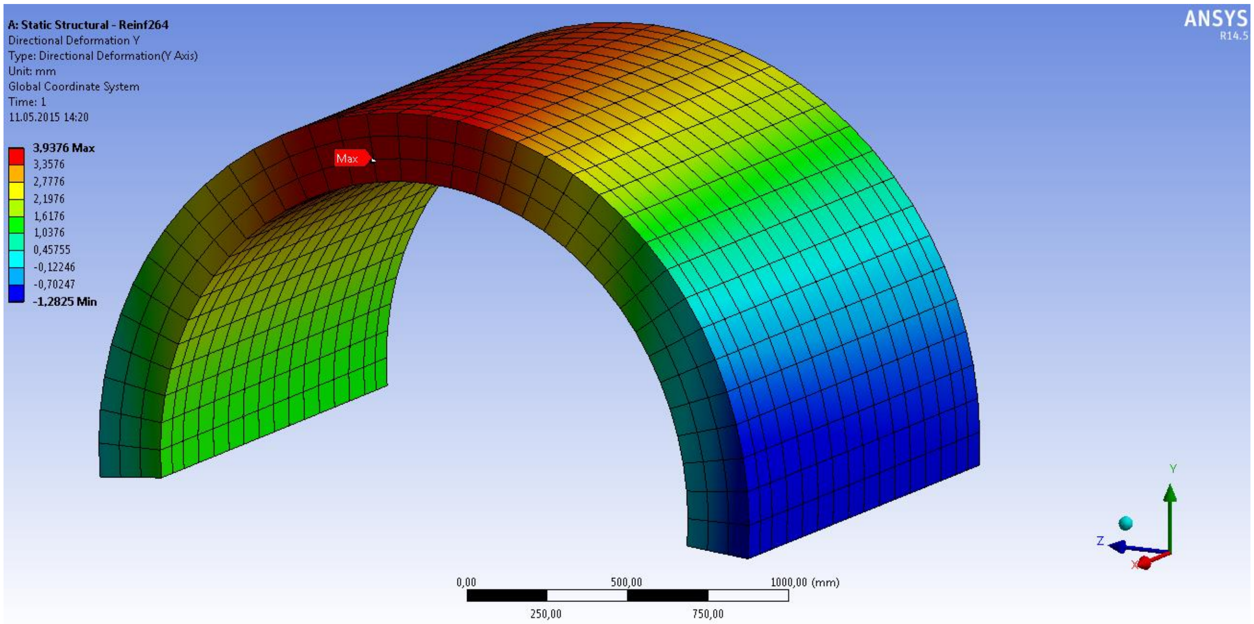

Figure A-4 Directional Deformation Y – Outer 2 load case. Source: ***Ansys® Workbench, Release 14.5***

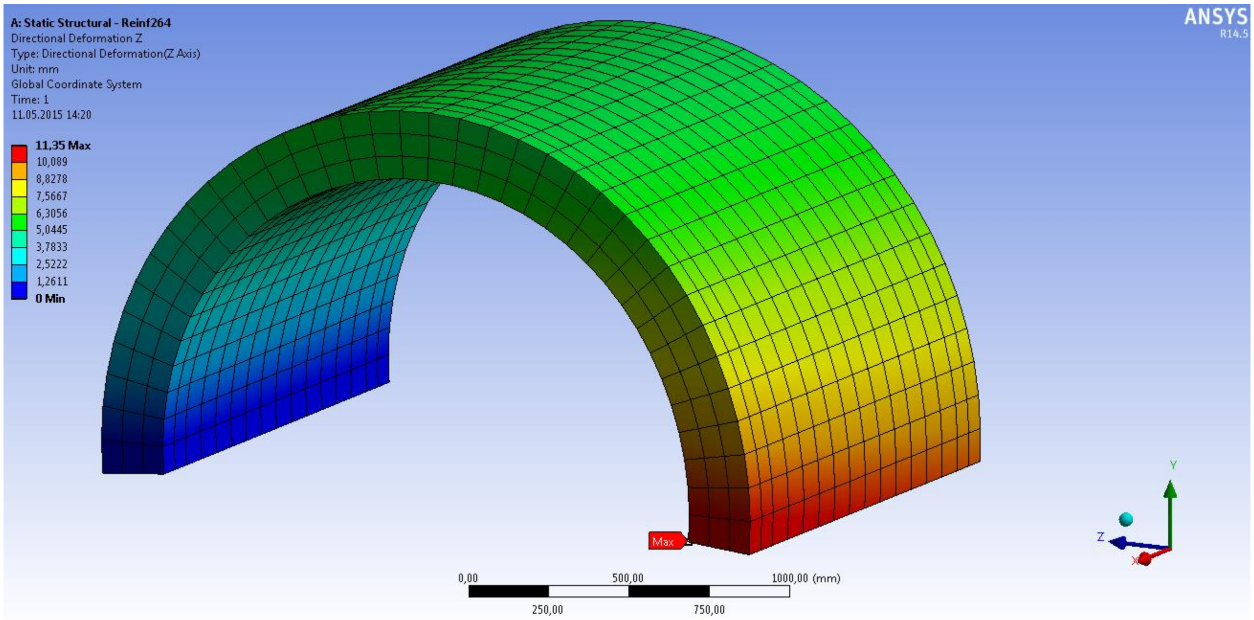

Figure A-5 Directional Deformation Z – Outer 2 load case. Source: ***Ansys® Workbench, Release 14.5***

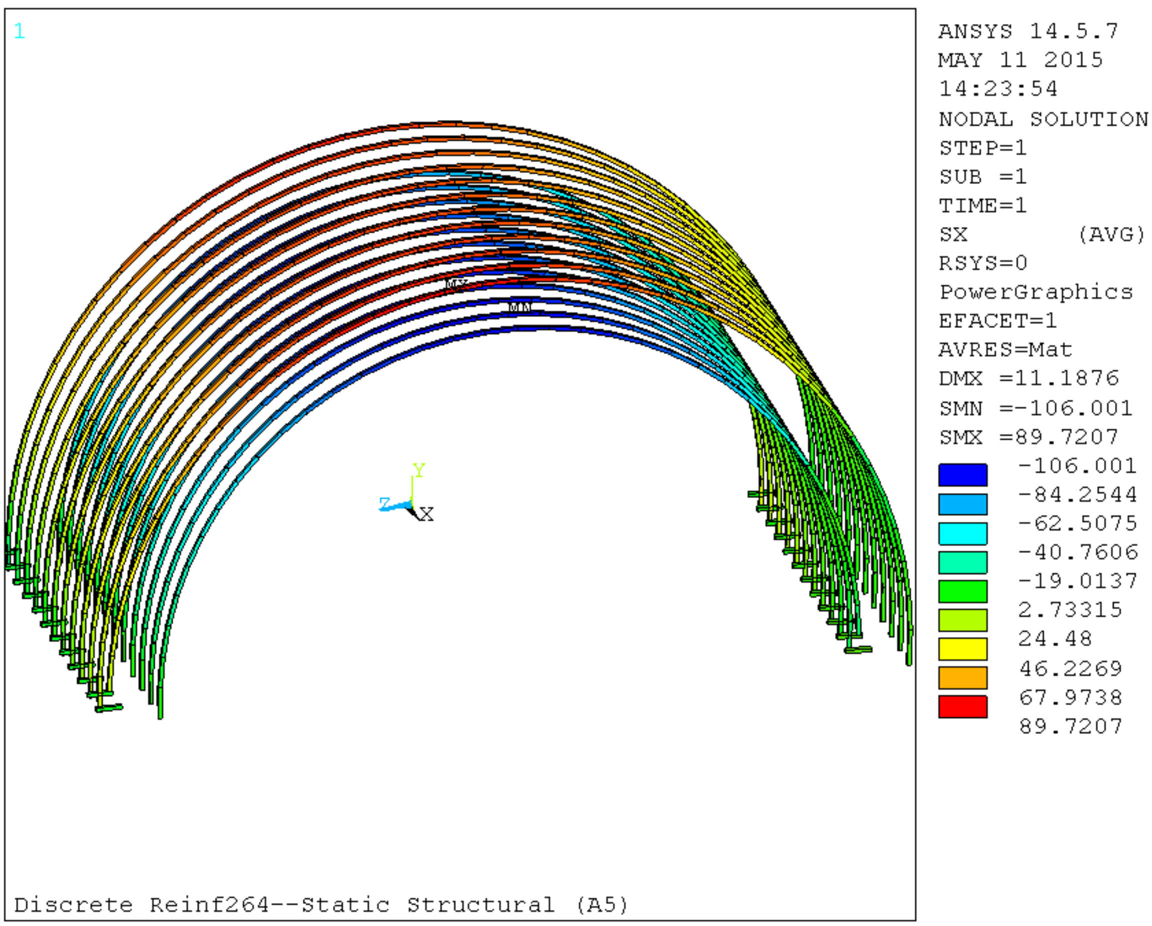

Figure A-6 Axial Stresses in Reinforcement – Outer 2 load case.
Source: ***Ansys® Workbench, Release 14.5***

Outer 3 load case:

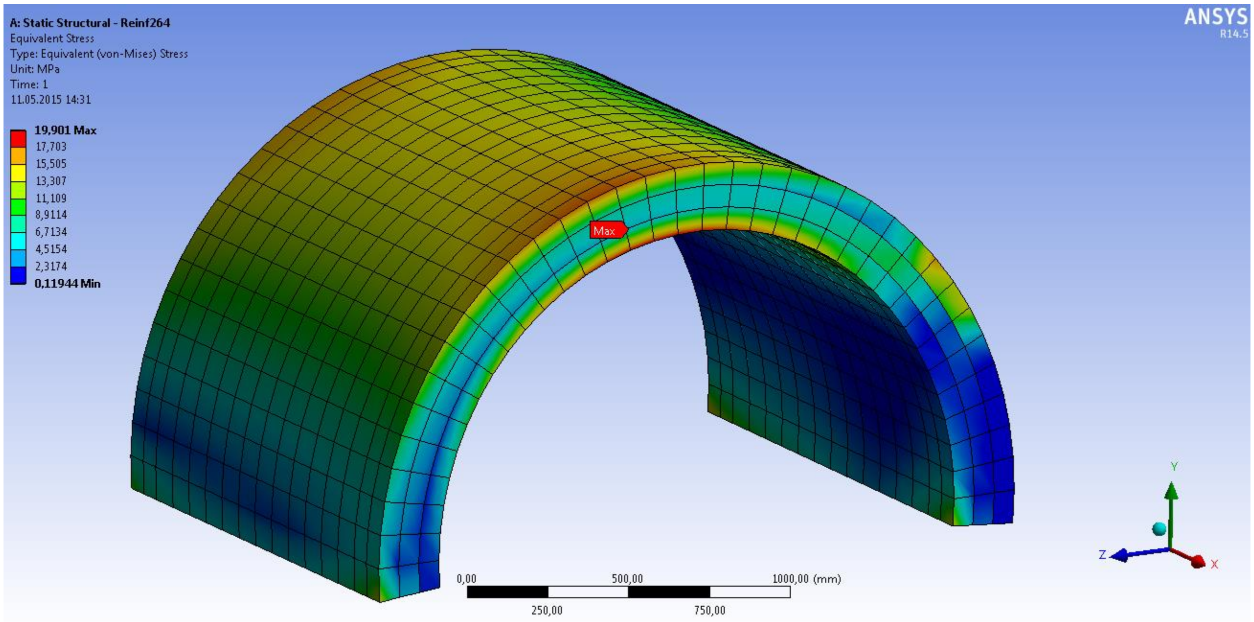

Figure A-7 Equivalent Stress – Outer 3 load case. Source: ***Ansys® Workbench, Release 14.5***

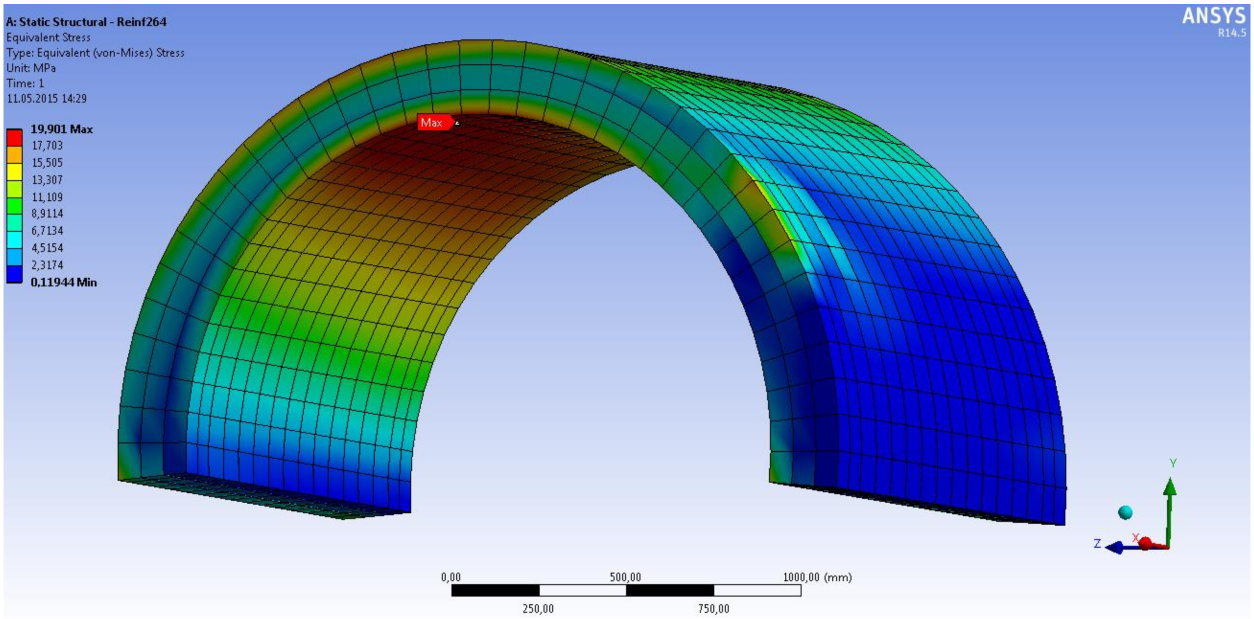

Figure A-8 Equivalent Stress – Outer 3 load case. Source: ***Ansys® Workbench, Release 14.5***

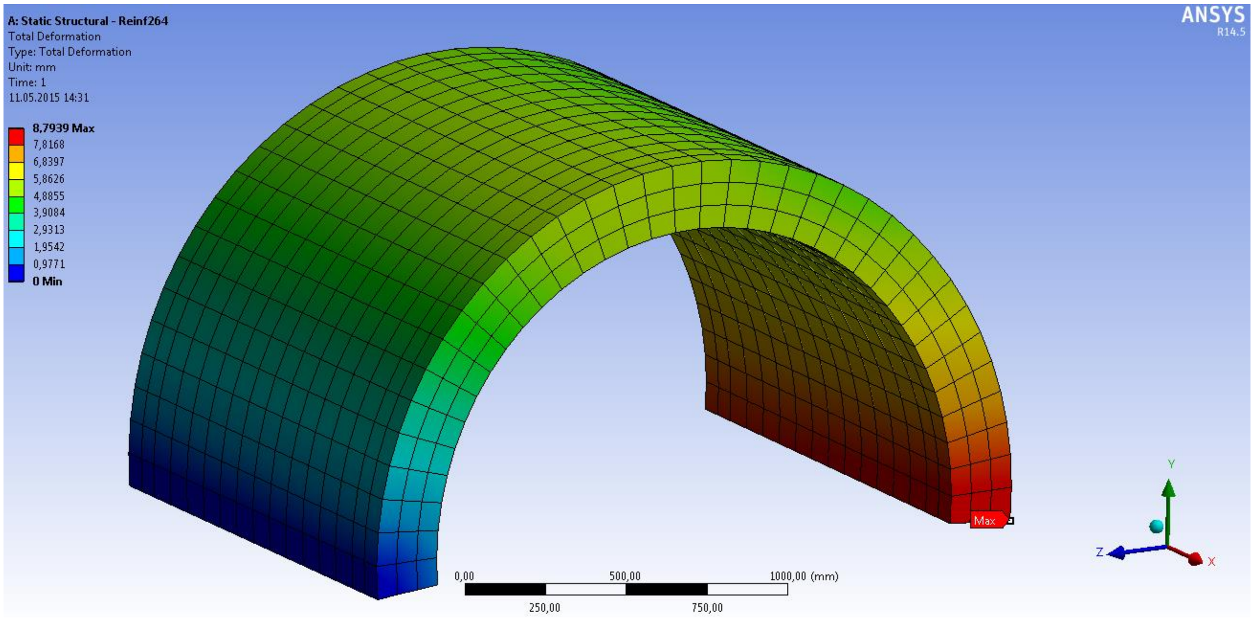

Figure A-9 Total Deformation – Outer 3 load case. Source: ***Ansys® Workbench, Release 14.5***

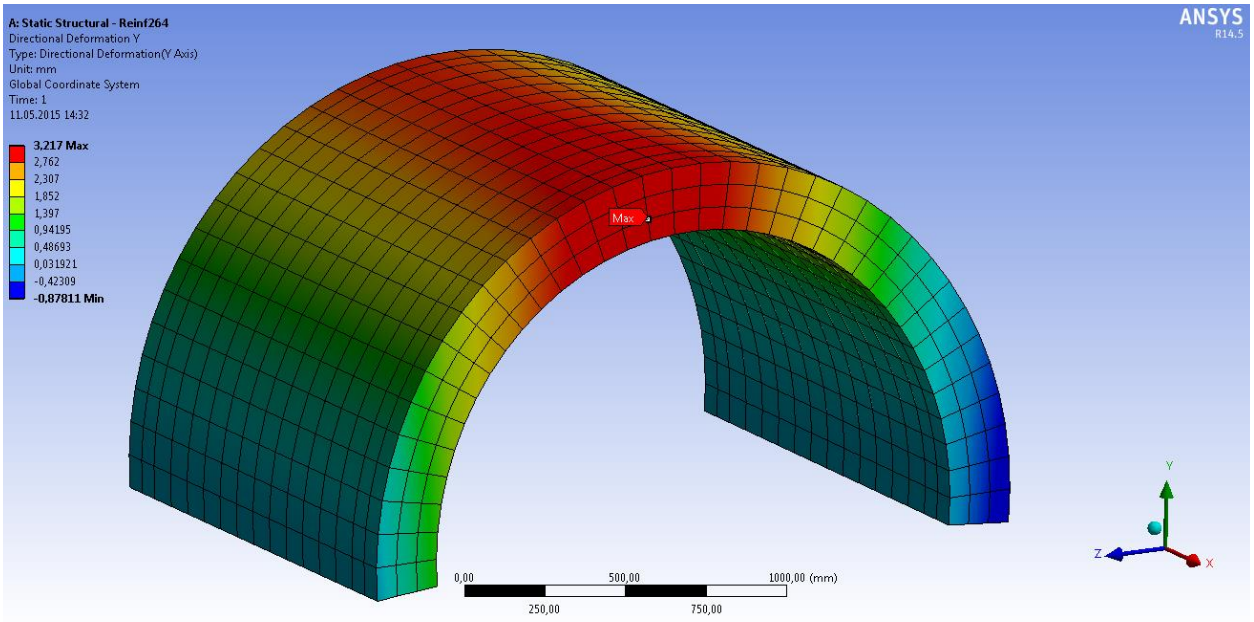

Figure A-10 Directional Deformation Y – Outer 3 load case. Source: ***Ansys® Workbench, Release 14.5***

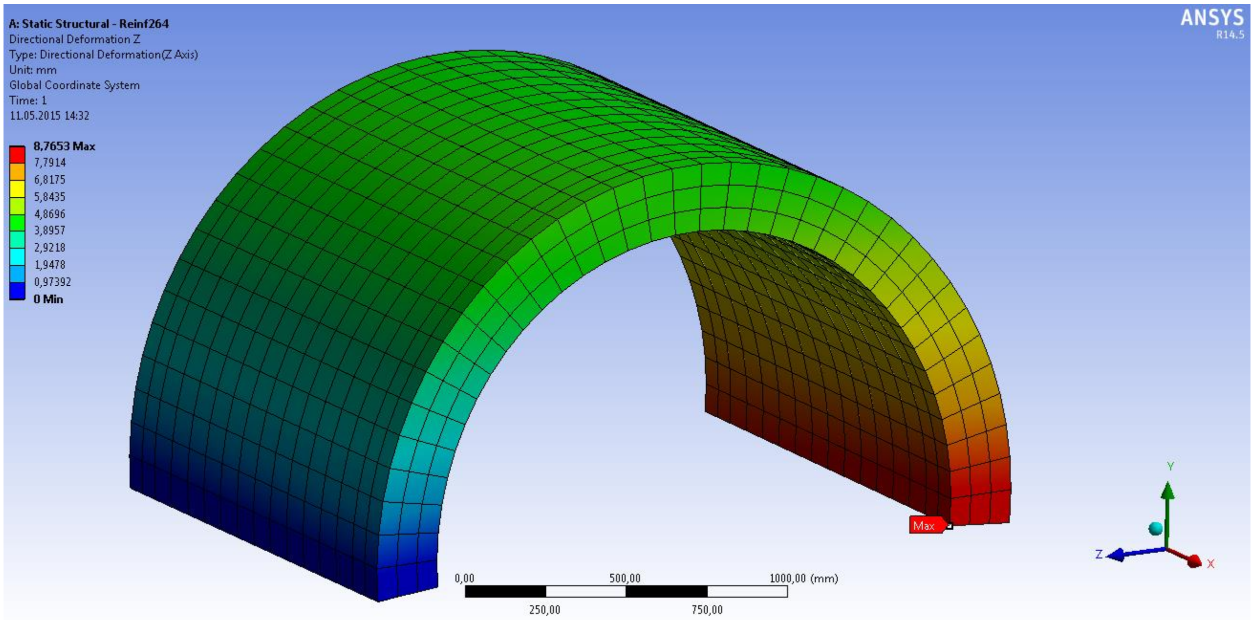

Figure A-11 Directional Deformation Z – Outer 3 load case. Source: *Ansys® Workbench, Release 14.5*

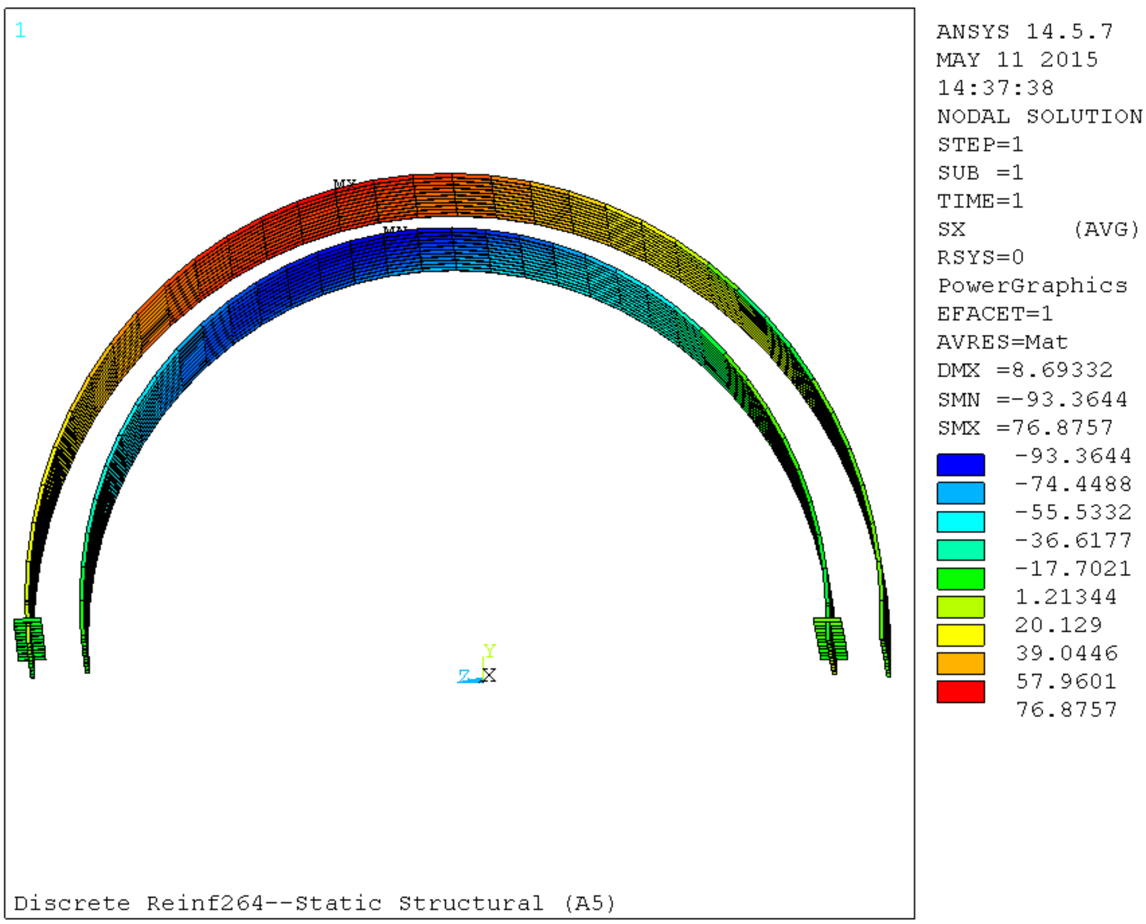

Figure A-12 Axial Stresses in Reinforcement – Outer 3 load case.
Source: *Ansys® Workbench, Release 14.5*

Outer 4 load case:

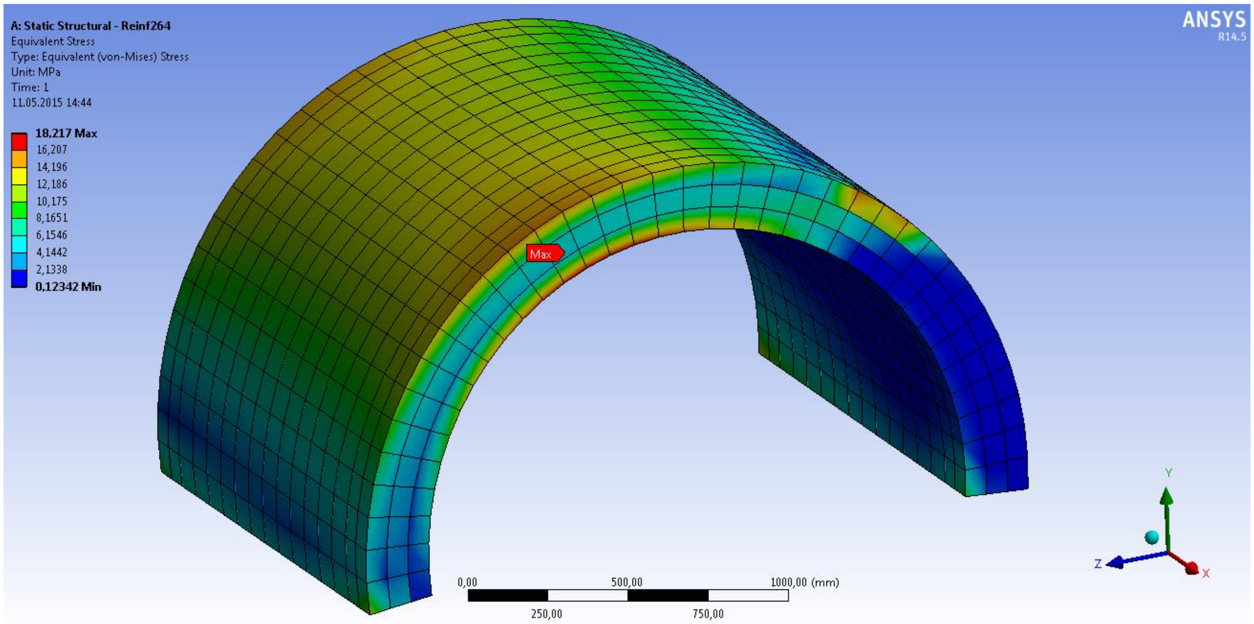

Figure A-13 Equivalent Stress – Outer 4 load case. Source: *Ansys® Workbench, Release 14.5*

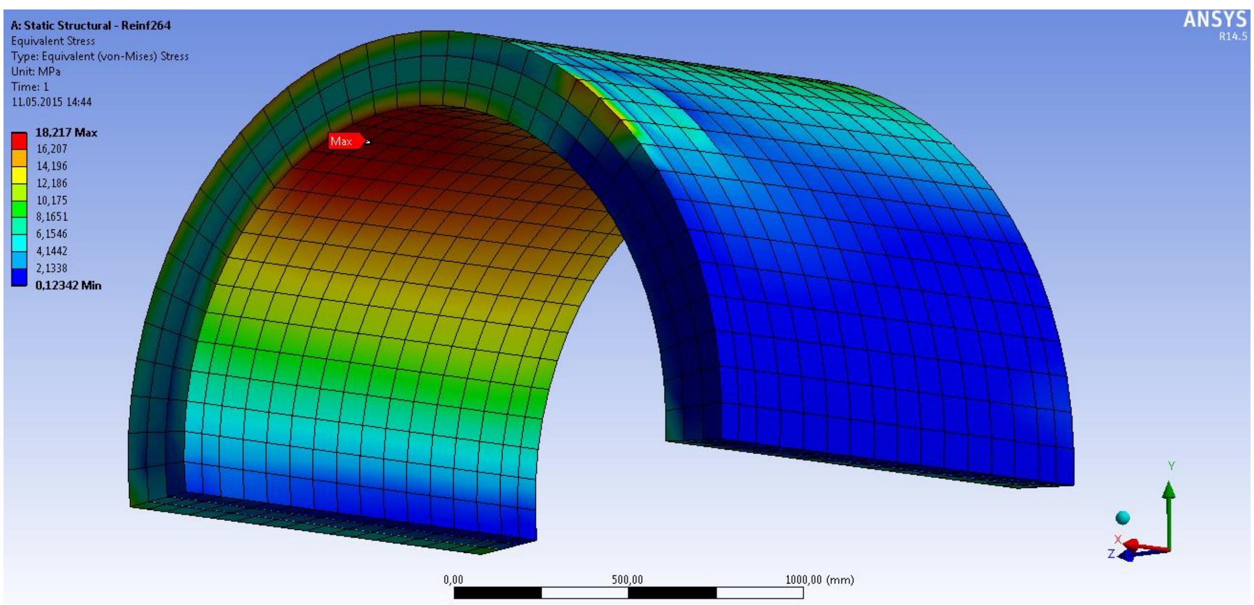

Figure A-14 Equivalent Stress – Outer 4 load case. Source: *Ansys® Workbench, Release 14.5*

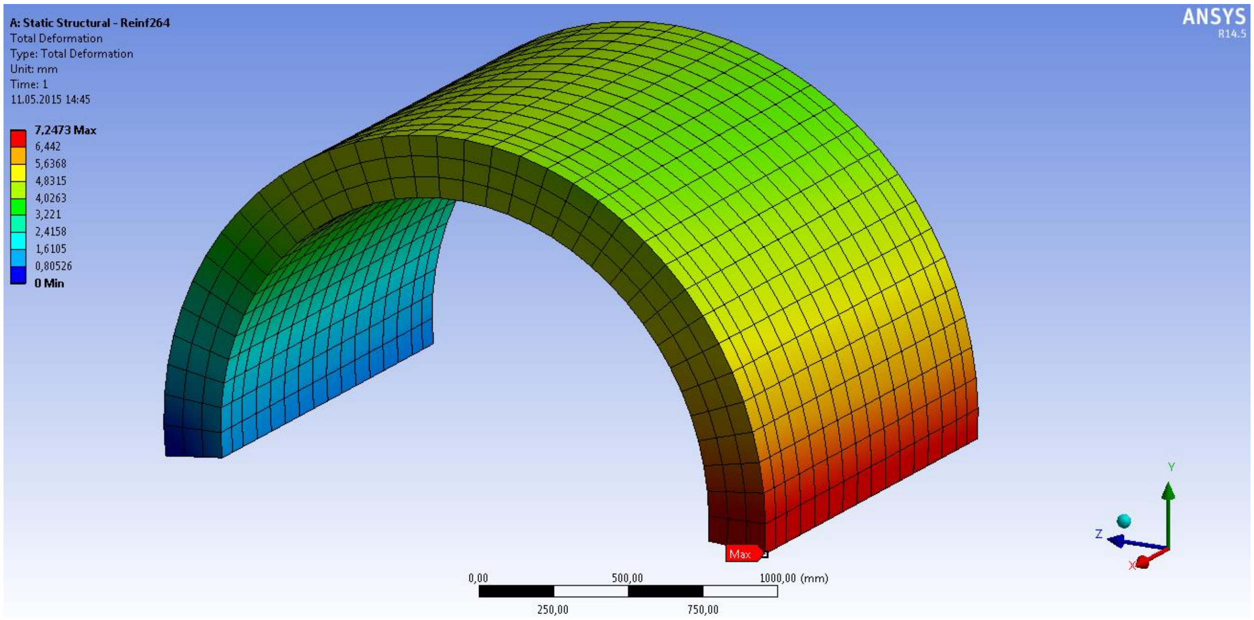

Figure A-15 Total Deformation – Outer 4 load case. Source: ***Ansys® Workbench, Release 14.5***

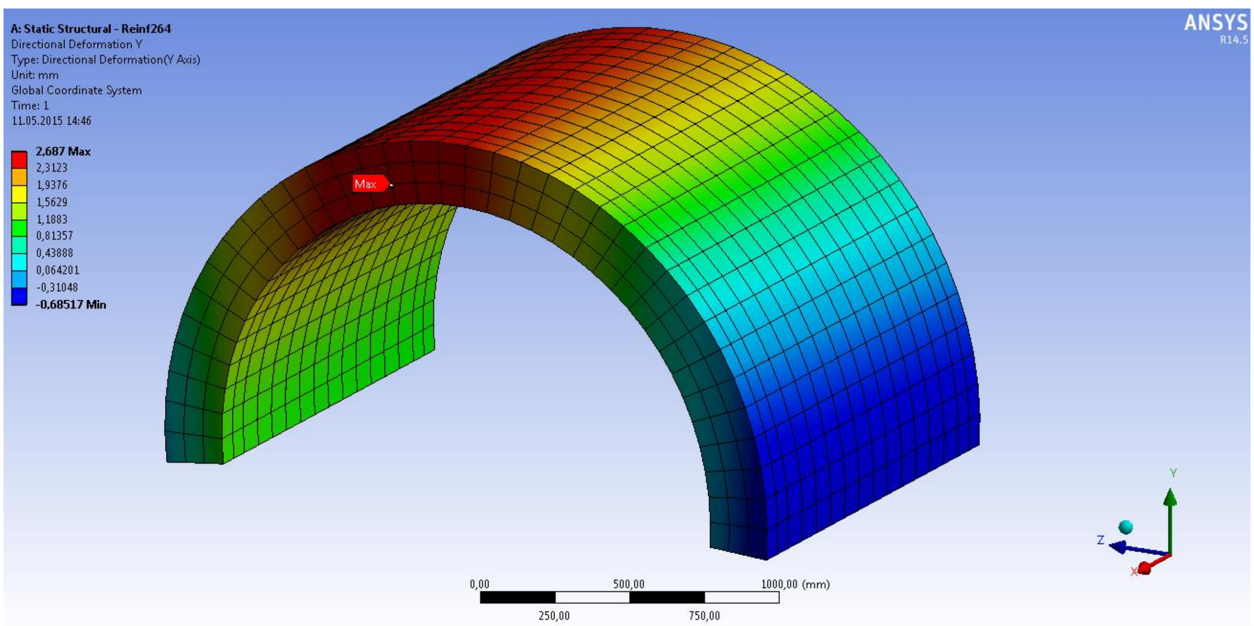

Figure A-16 Directional Deformation Y – Outer 4 load case. Source: ***Ansys® Workbench, Release 14.5***

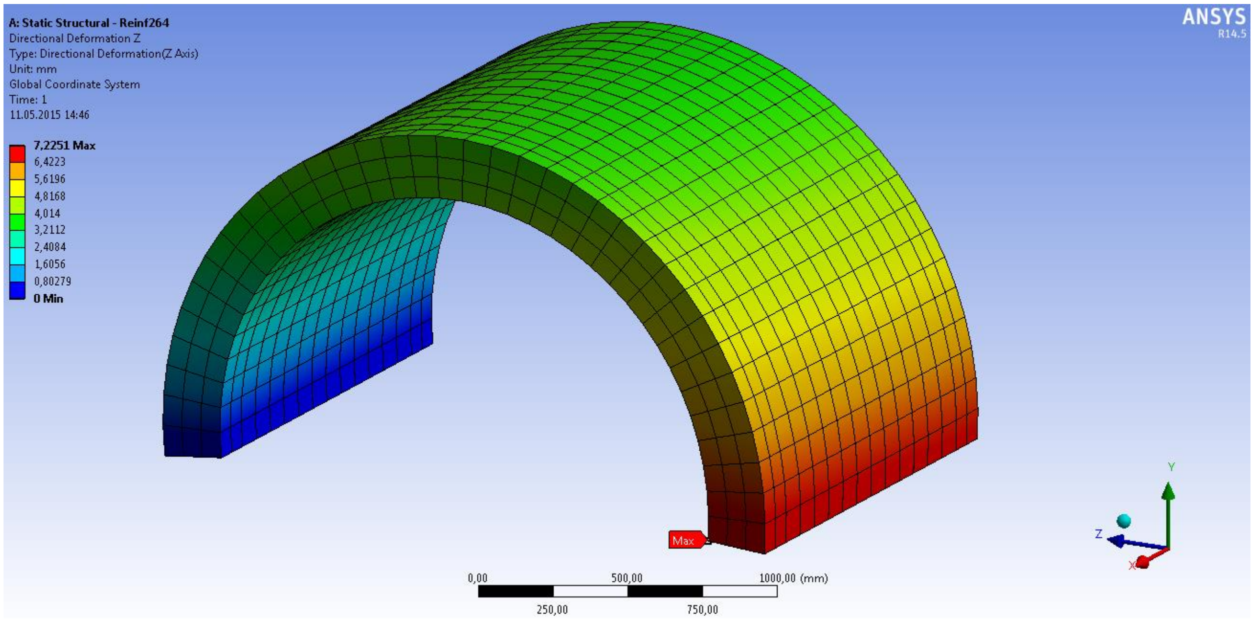

Figure A-17 Directional Deformation Z – Outer 4 load case. Source: *Ansys® Workbench, Release 14.5*

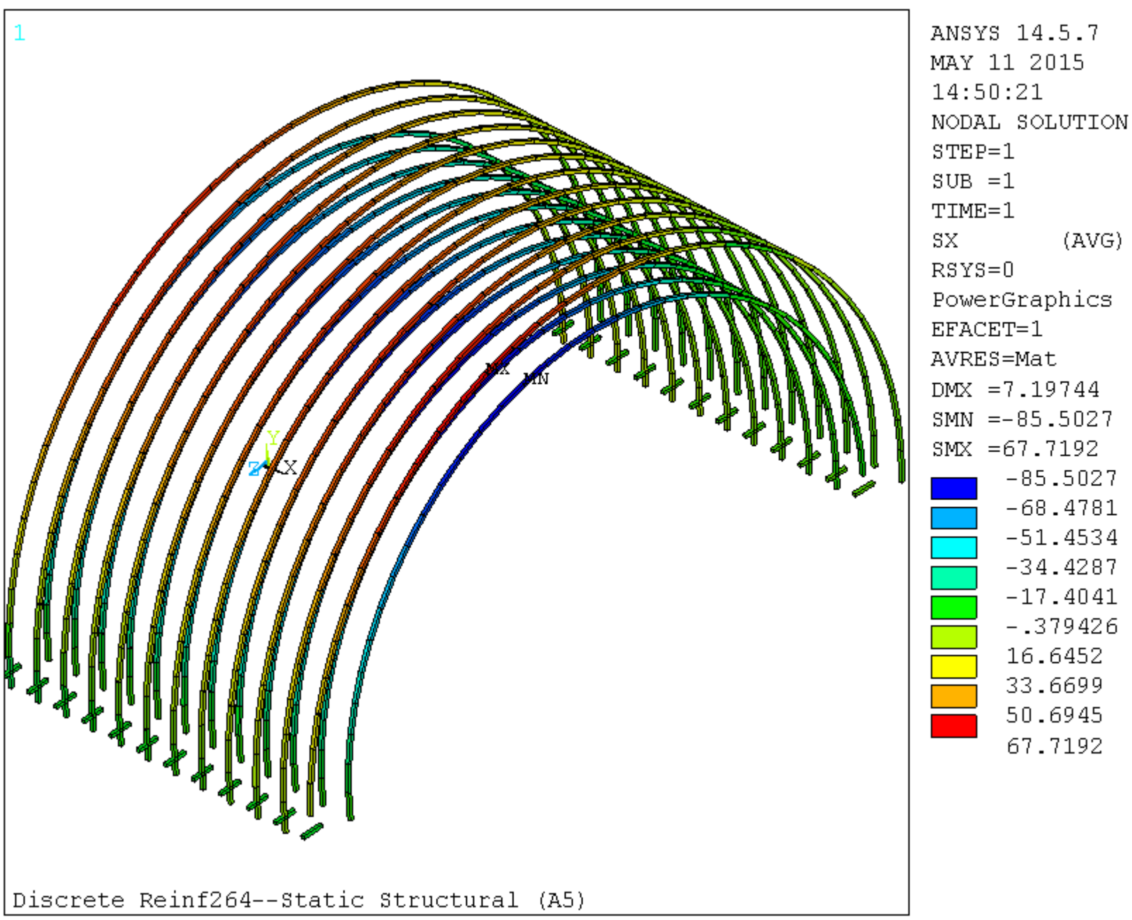

Figure A-18 Axial Stresses in Reinforcement – Outer 4 load case.
Source: *Ansys® Workbench, Release 14.5*

Left 1 load case:

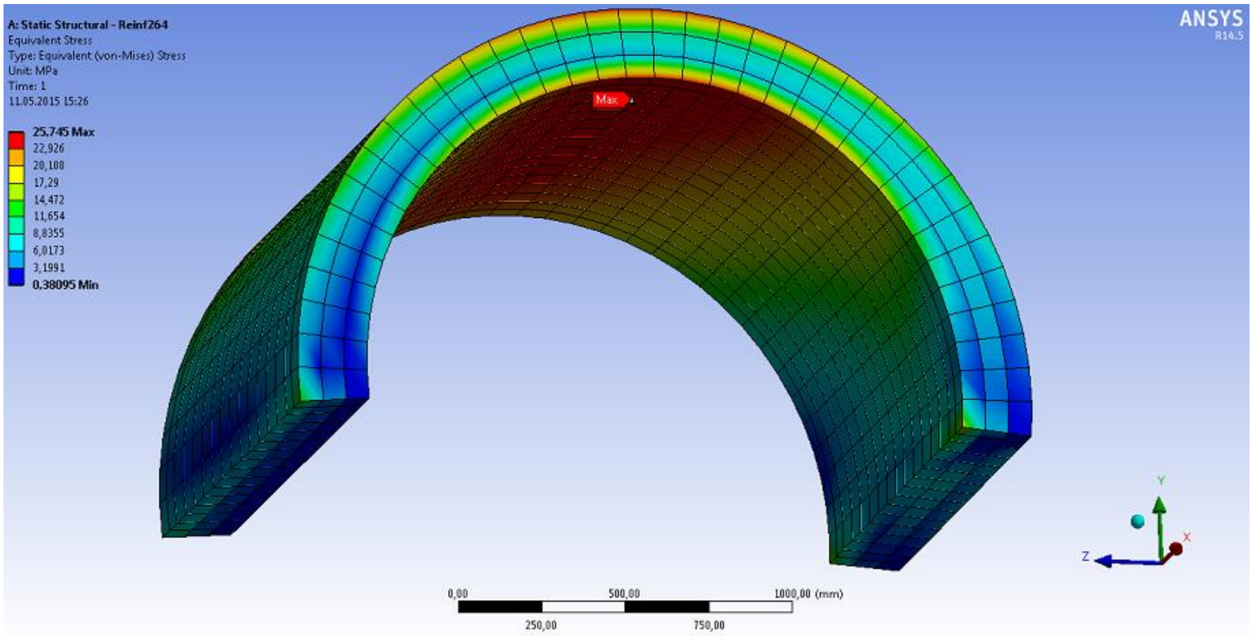

Figure A-19 Equivalent Stress – Left 1 load case. Source: *Ansys® Workbench, Release 14.5*

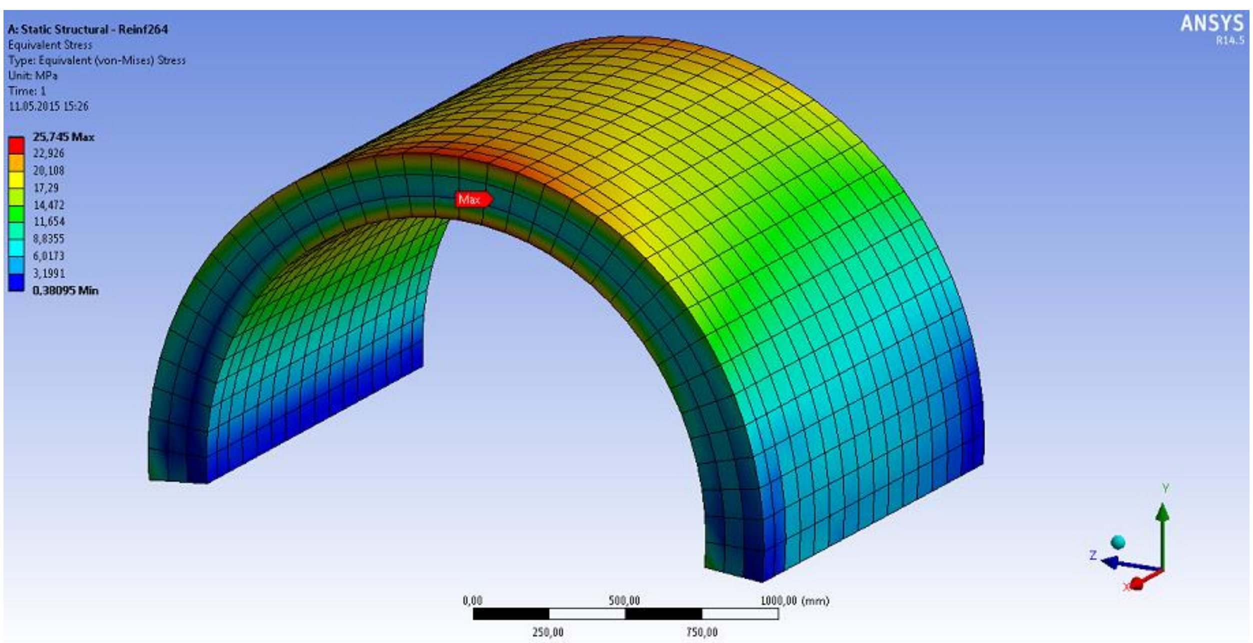

Figure A-20 Equivalent Stress – Left 1 load case. Source: *Ansys® Workbench, Release 14.5*

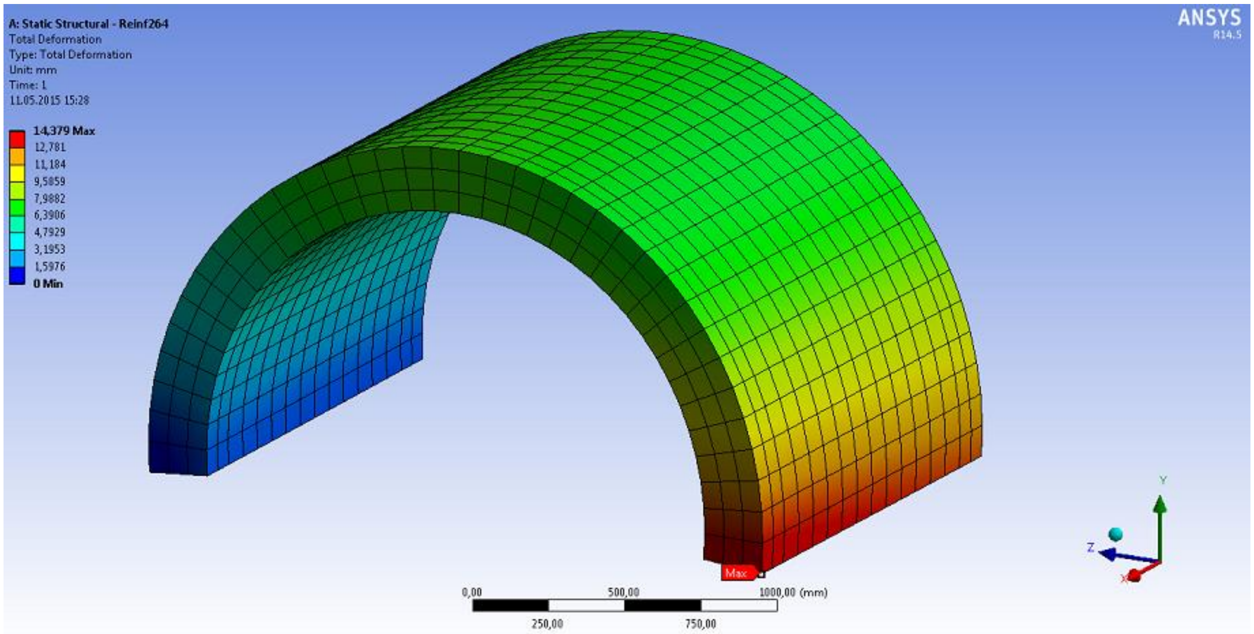

Figure A-21 Total Deformation – Left 1 load case. Source: ***Ansys® Workbench, Release 14.5***

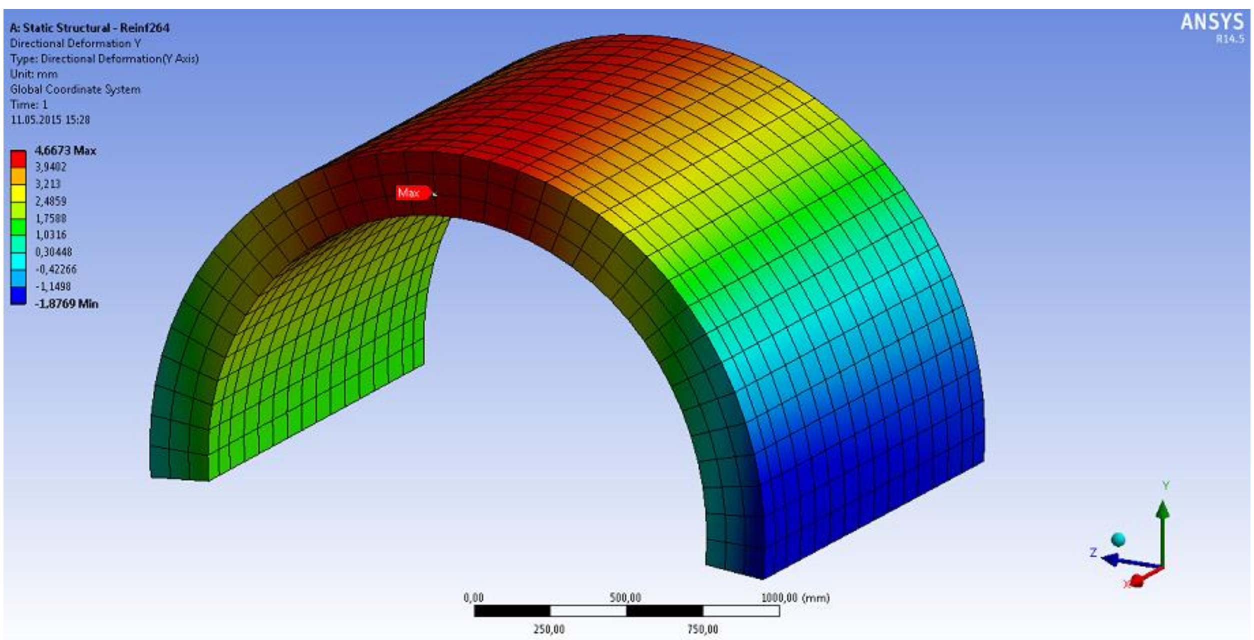

Figure A-22 Directional Deformation Y – Left 1 load case. Source: ***Ansys® Workbench, Release 14.5***

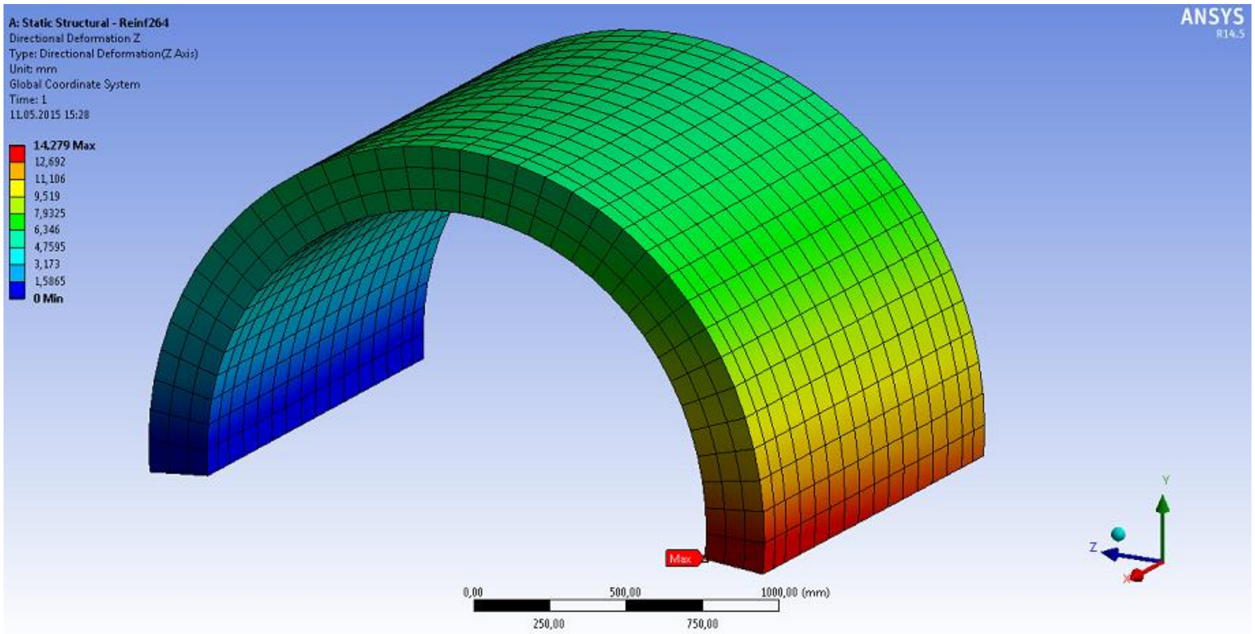

Figure A-23 Directional Deformation Z – Left 1 load case. Source: *Ansys® Workbench, Release 14.5*

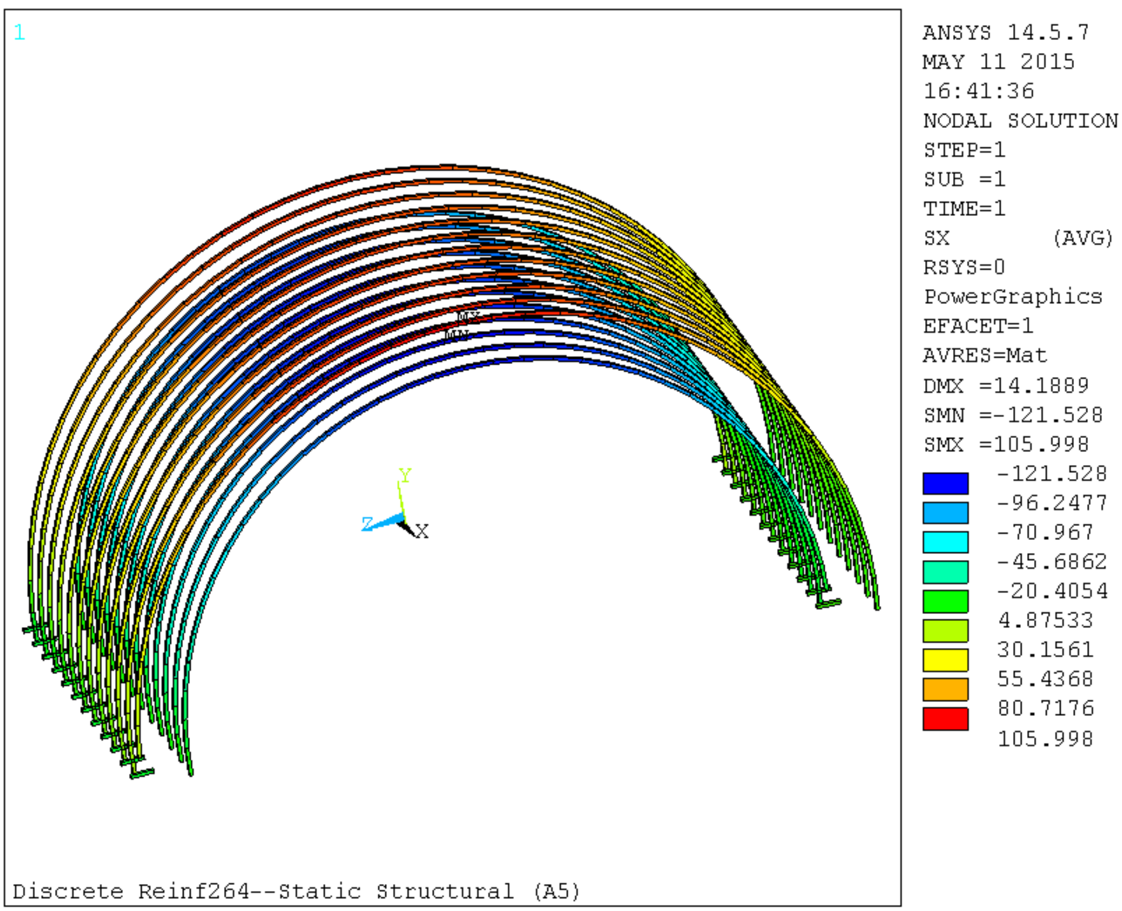

Figure A-24 Axial Stresses in Reinforcement – Left 1 load case.
Source: *Ansys® Workbench, Release 14.5*

Left 2 load case:

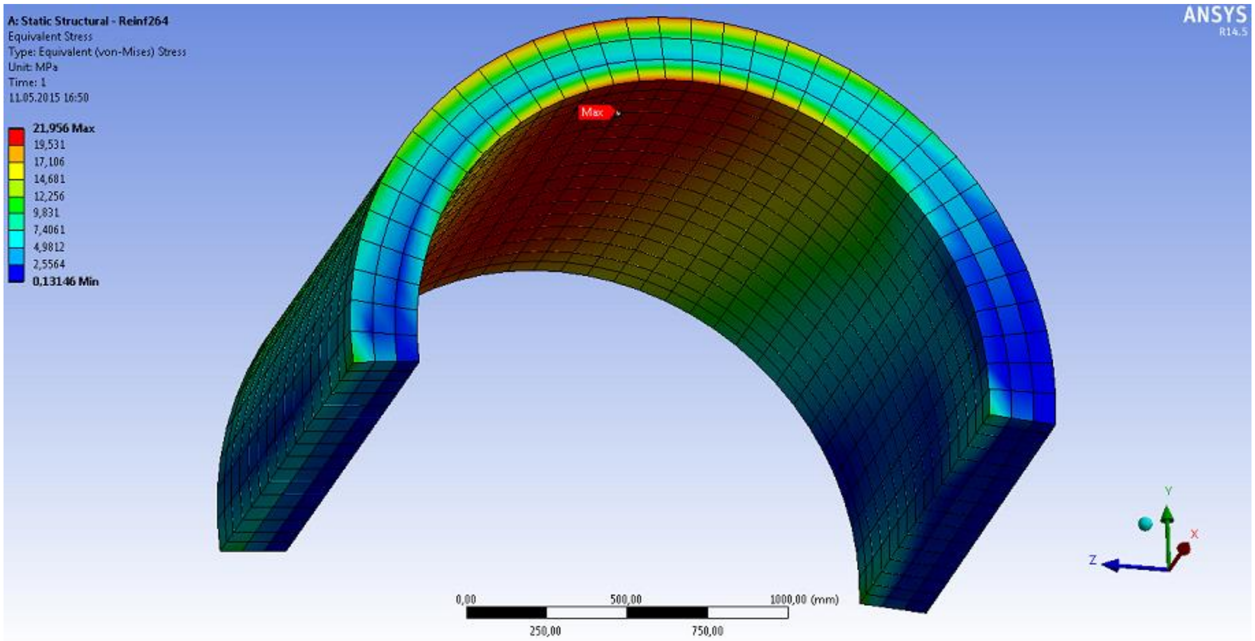

Figure A-25 Equivalent Stress – Left 2 load case. Source: *Ansys® Workbench, Release 14.5*

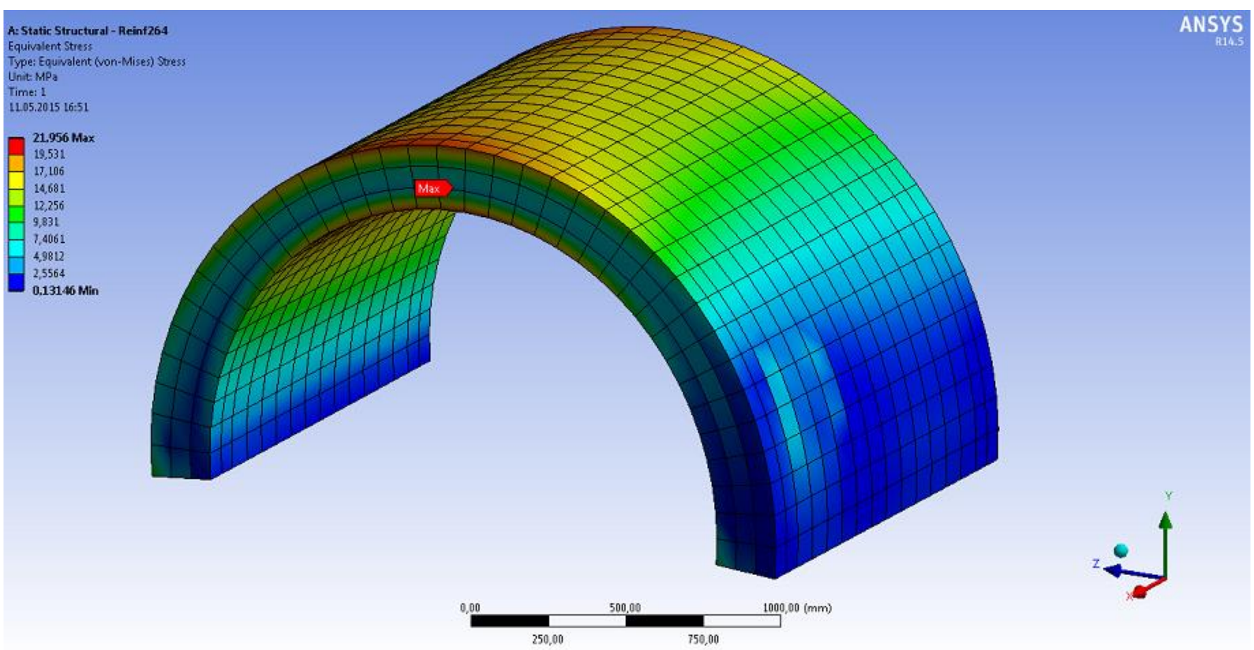

Figure A-26 Equivalent Stress – Left 2 load case. Source: *Ansys® Workbench, Release 14.5*

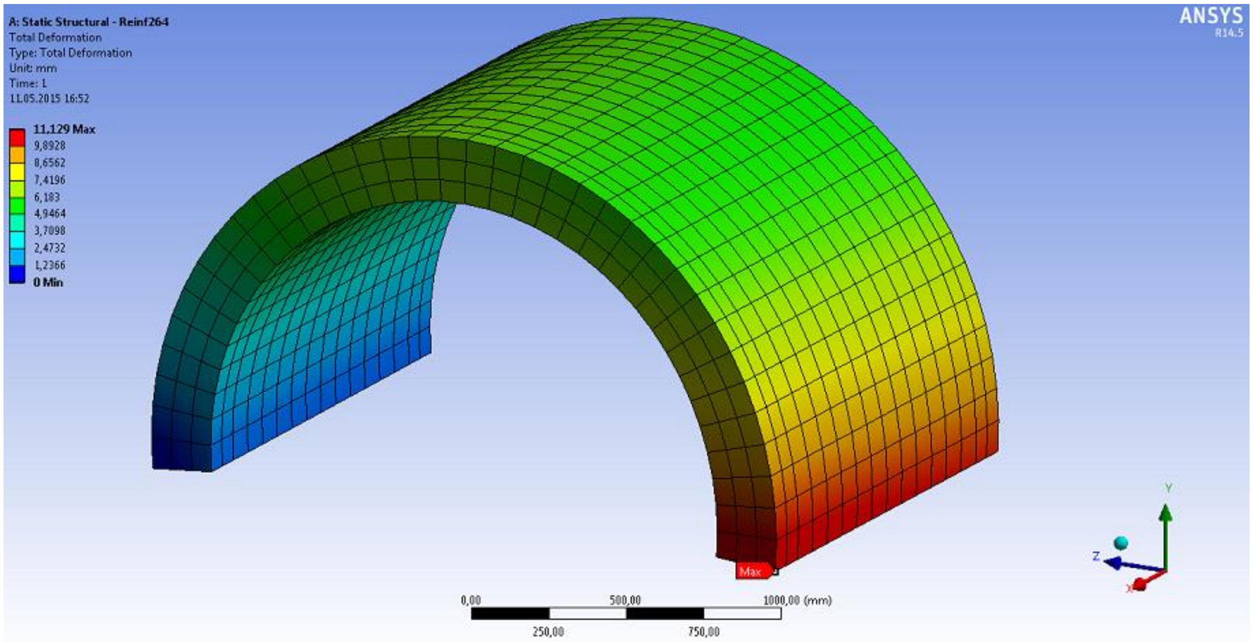

Figure A-27 Total Deformation – Left 2 load case. Source: ***Ansys® Workbench, Release 14.5***

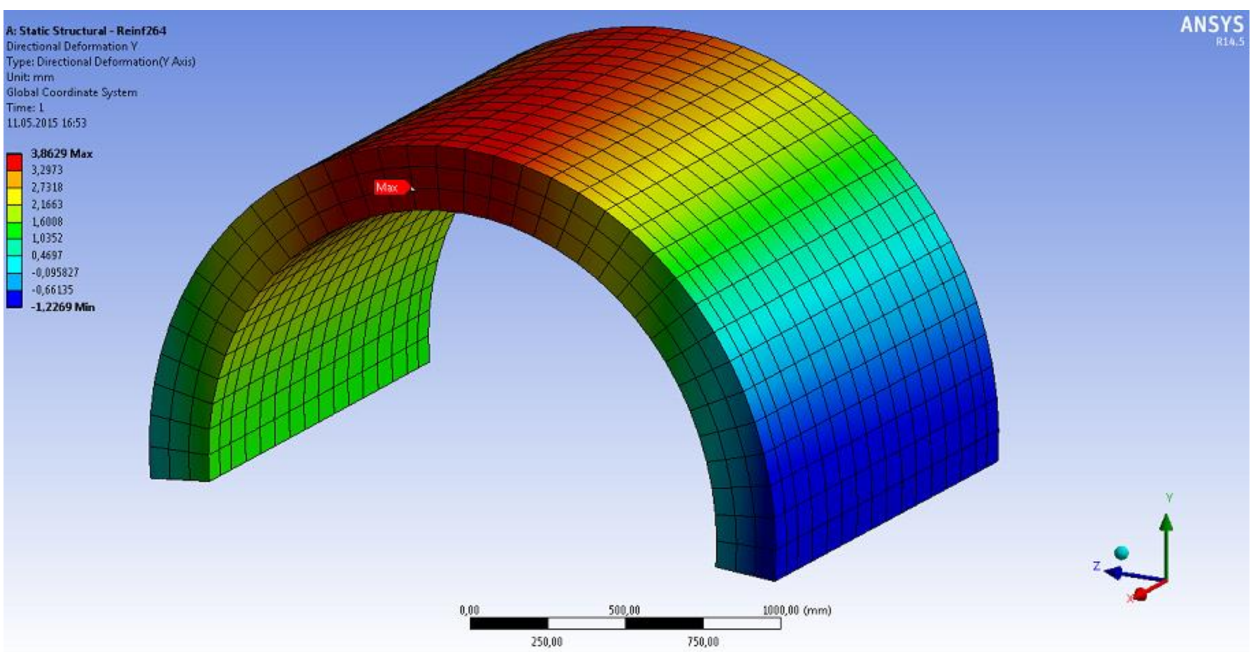

Figure A-28 Directional Deformation Y – Left 2 load case. Source: ***Ansys® Workbench, Release 14.5***

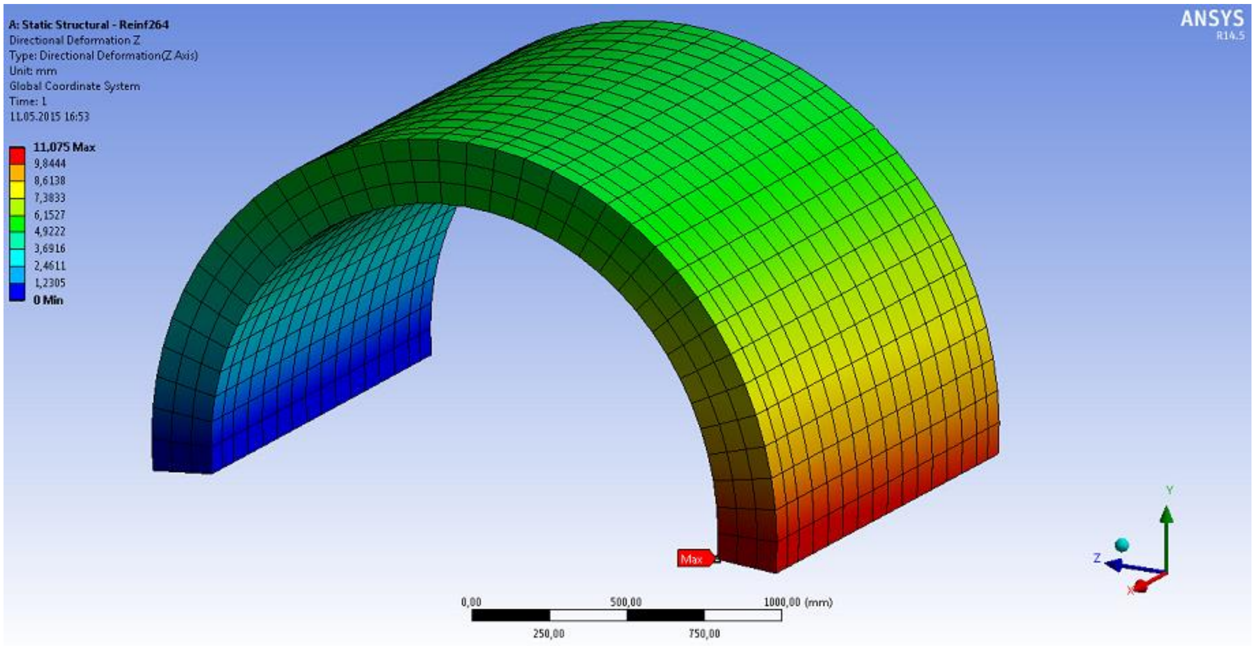

Figure A-29 Directional Deformation Z – Left 2 load case. Source: *Ansys® Workbench, Release 14.5*

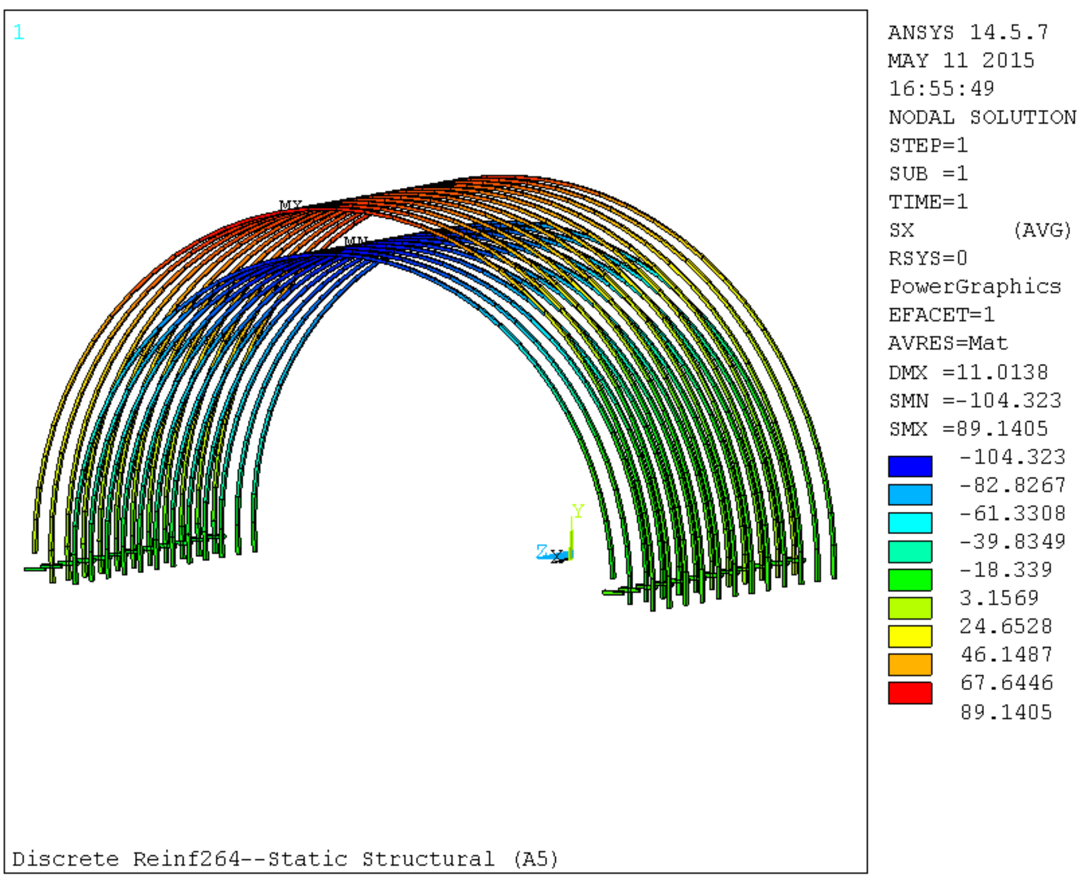

Figure A-30 Axial Stresses in Reinforcement – Left 2 load case.
Source: *Ansys® Workbench, Release 14.5*

Left 3 load case:

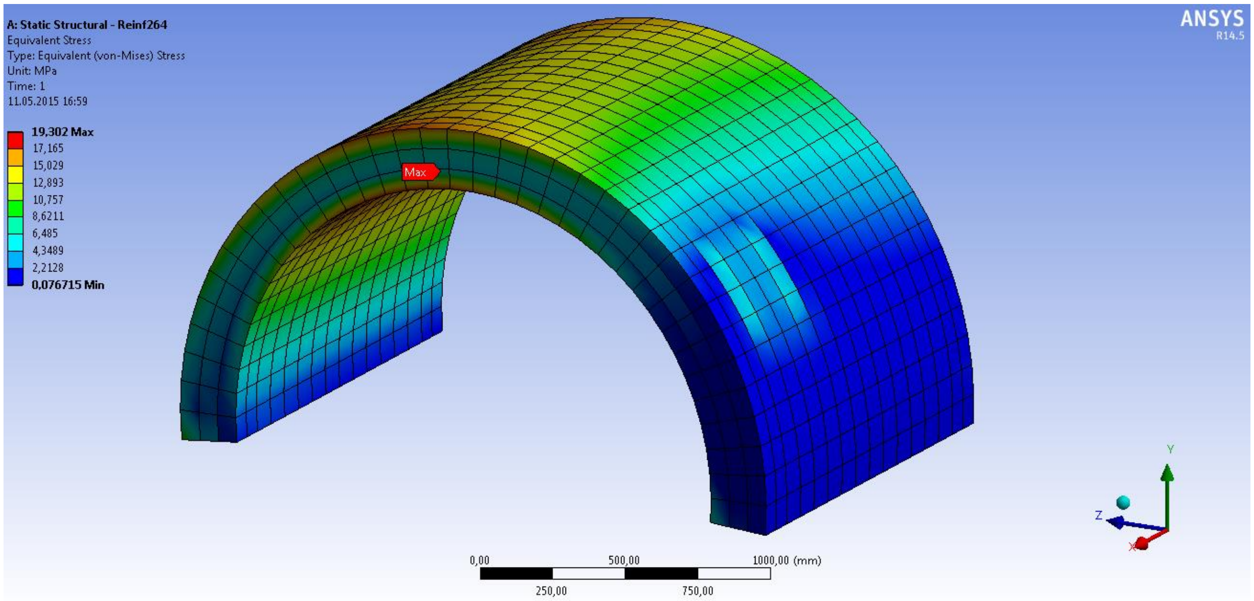

Figure A-31 Equivalent Stress – Left 3 load case. Source: ***Ansys® Workbench, Release 14.5***

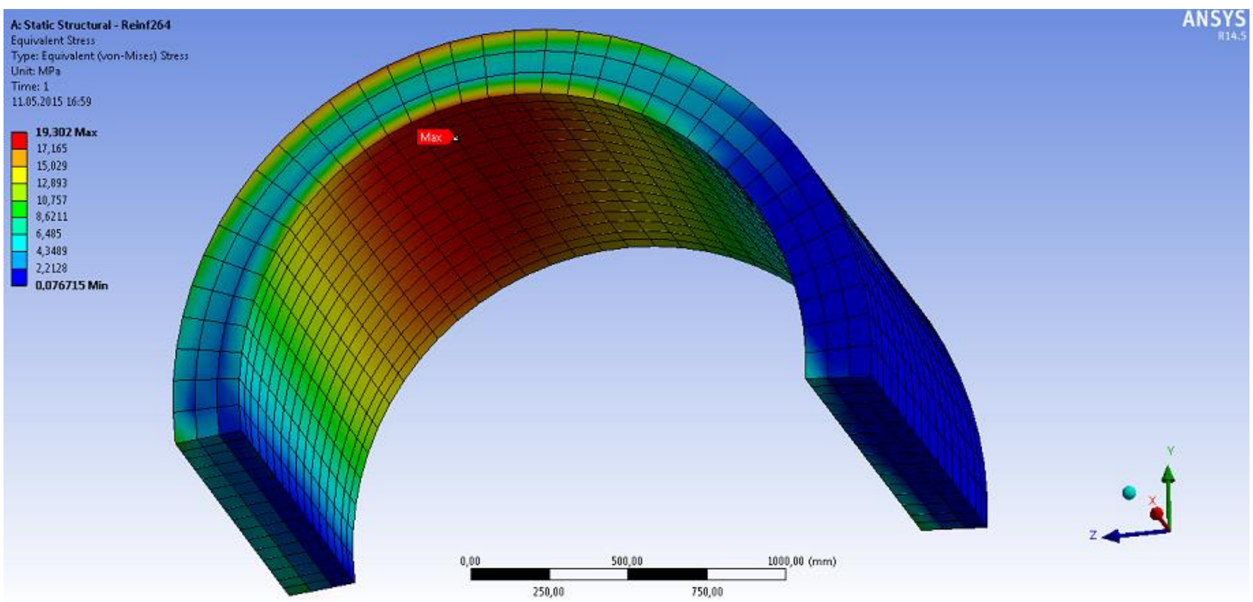

Figure A-32 Equivalent Stress – Left 3 load case. Source: ***Ansys® Workbench, Release 14.5***

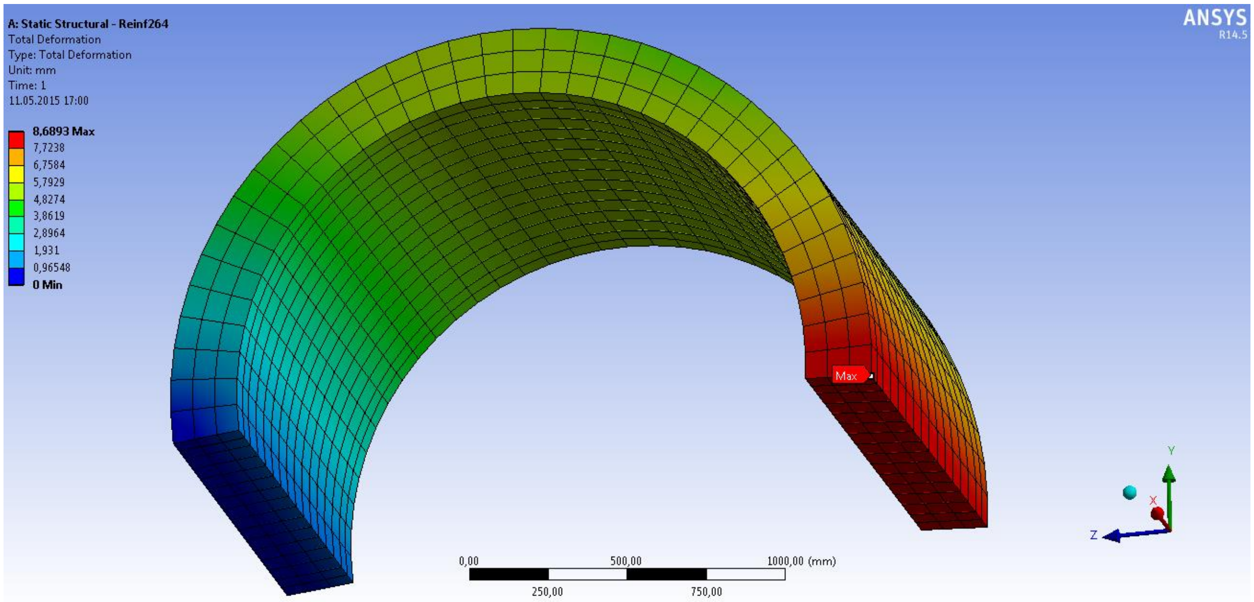

Figure A-33 Total Deformation – Left 3 load case. Source: *Ansys® Workbench, Release 14.5*

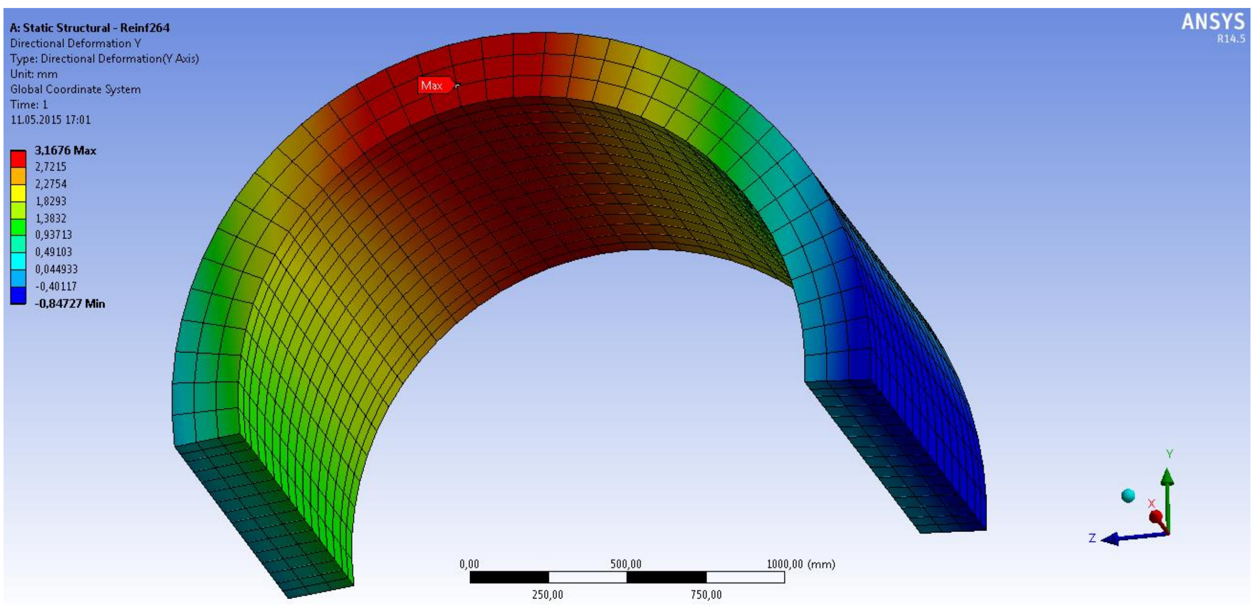

Figure A-34 Direction Deformation Y – Left 3 load case. Source: *Ansys® Workbench, Release 14.5*

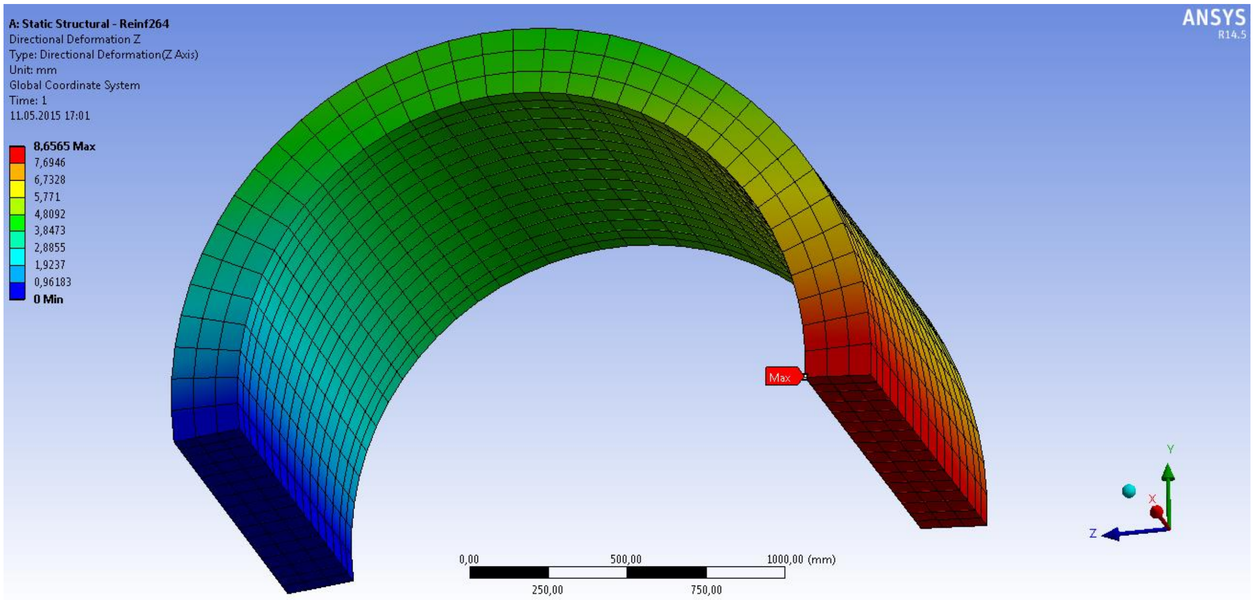

Figure A-35 Direction Deformation Z – Left 3 load case. Source: ***Ansys® Workbench, Release 14.5***

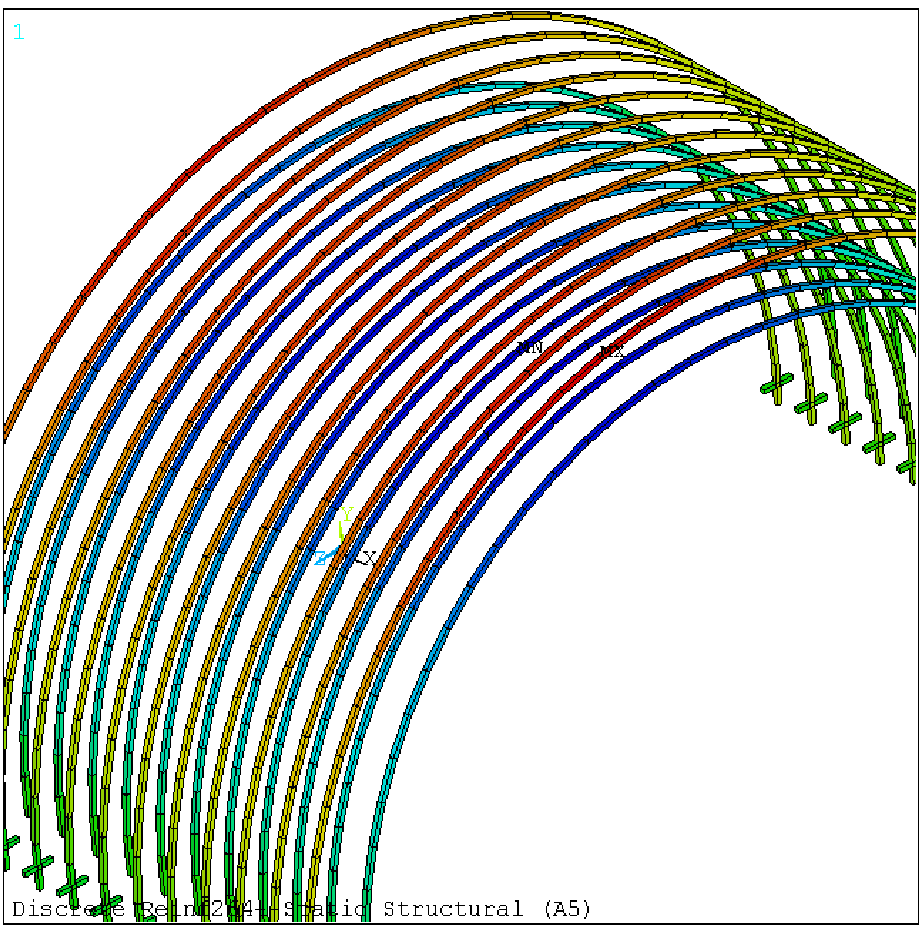

Figure A-36 Axial Stresses in Reinforcement – Left 3 load case.
Source: ***Ansys® Workbench, Release 14.5***

Left 4 load case:

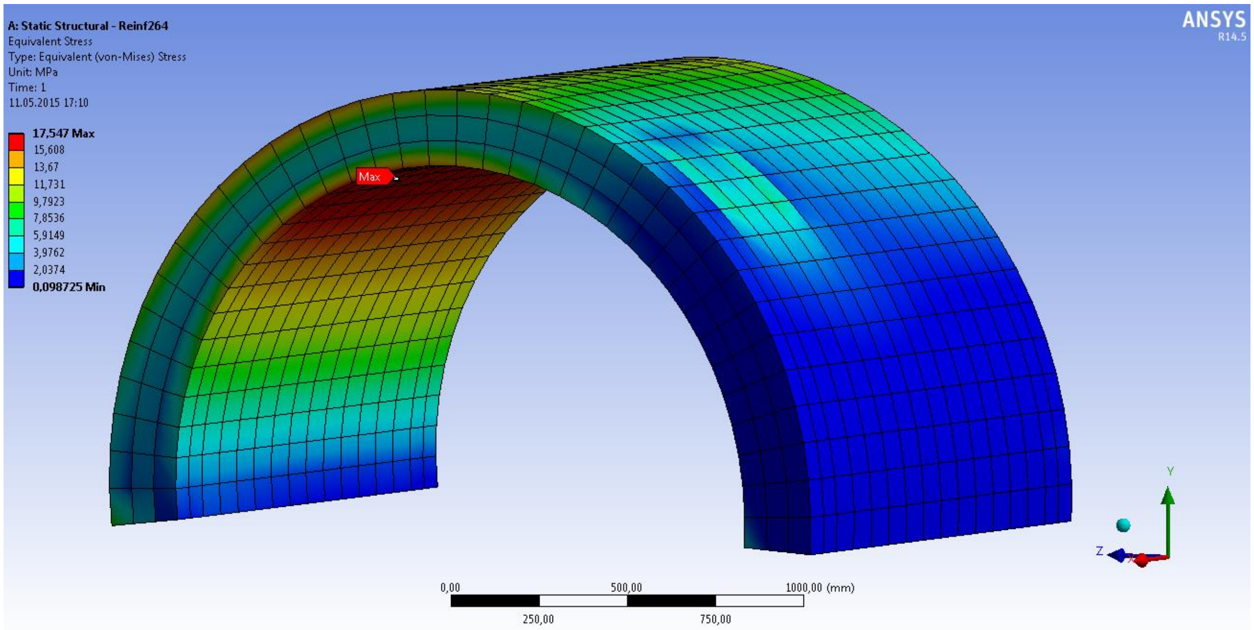

Figure A-37 Equivalent Stress – Left 4 load case. Source: ***Ansys® Workbench, Release 14.5***

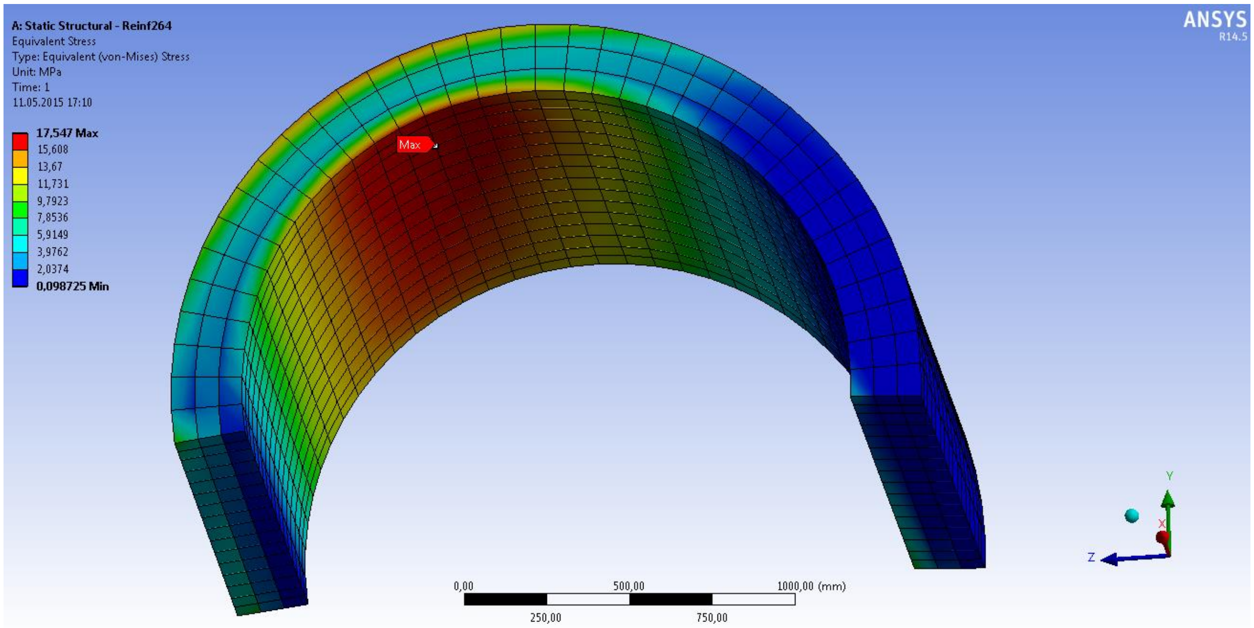

Figure A-38 Equivalent Stress – Left 4 load case. Source: ***Ansys® Workbench, Release 14.5***

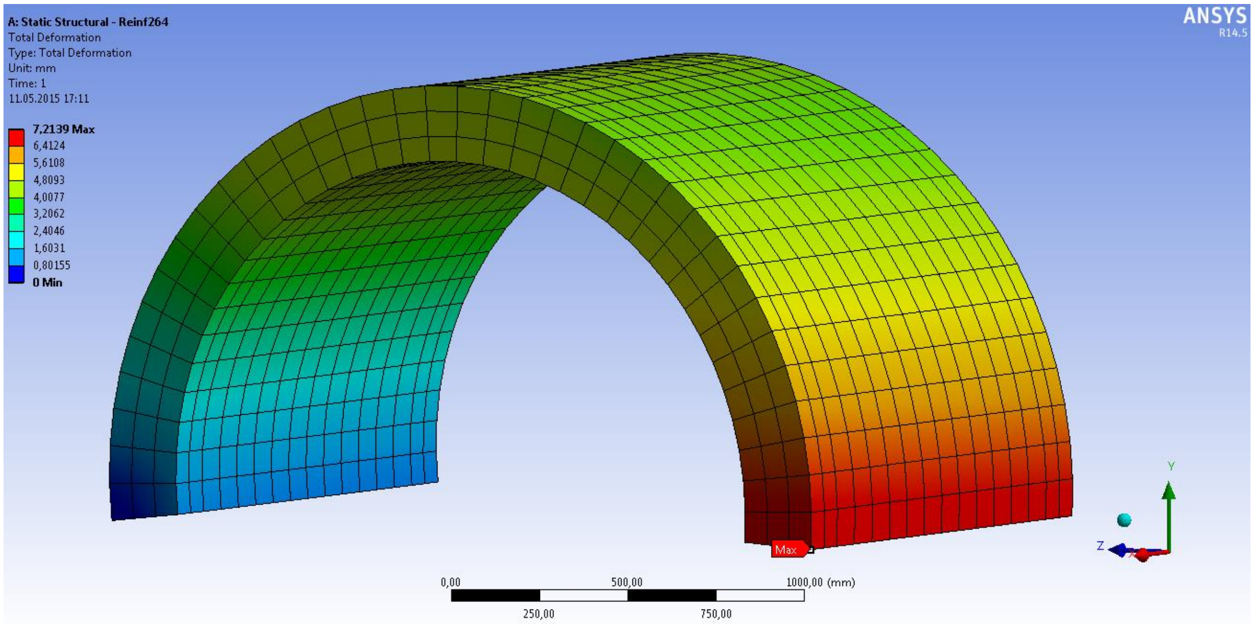

Figure A-39 Total Deformation – Left 4 load case. Source: ***Ansys® Workbench, Release 14.5***

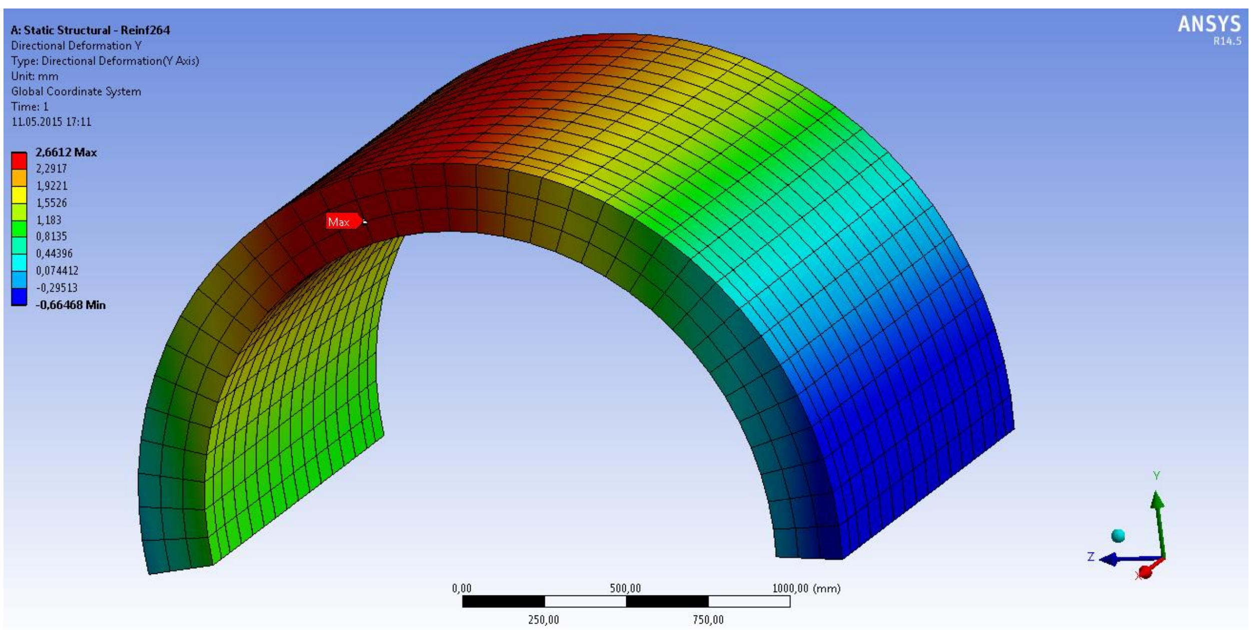

Figure A-40 Directional Deformation Y – Left 4 load case. Source: ***Ansys® Workbench, Release 14.5***

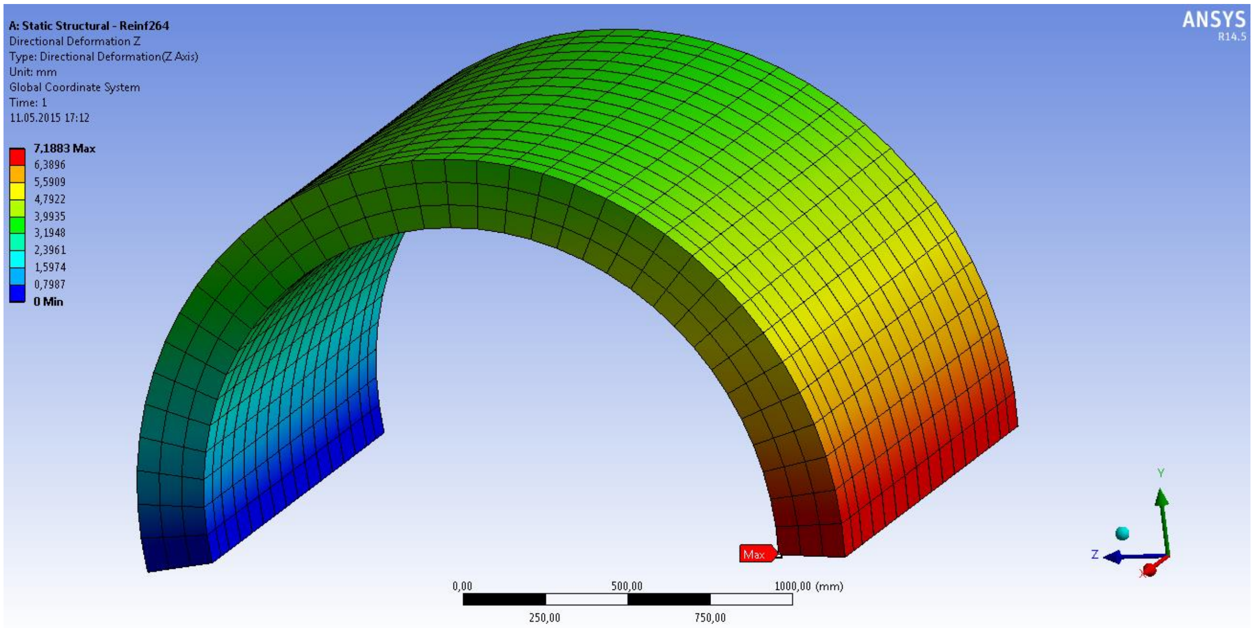

Figure A-41 Directional Deformation Z – Left 4 load case. Source: ***Ansys® Workbench, Release 14.5***

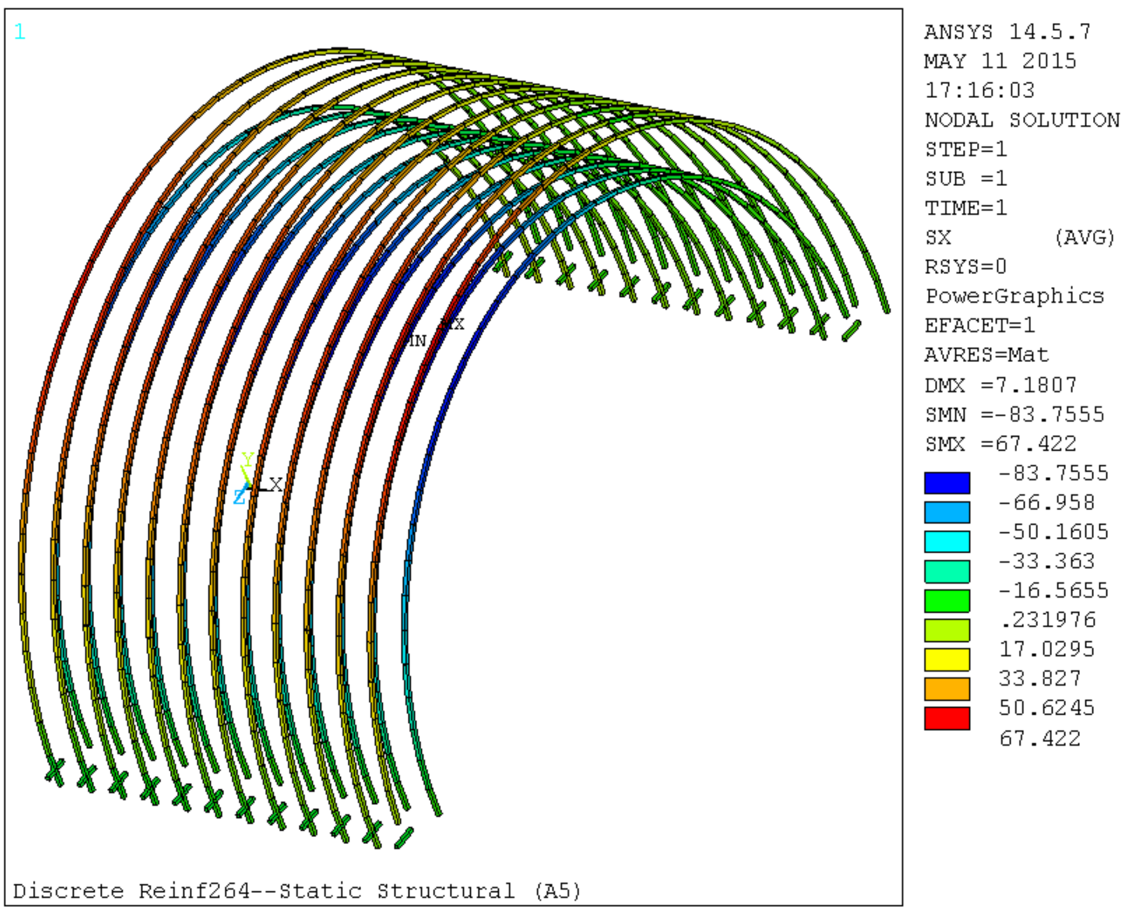

Figure A-42 Axial Stresses in Reinforcement – Left 4 load case.
Source: ***Ansys® Workbench, Release 14.5***

Mid 1 load case:

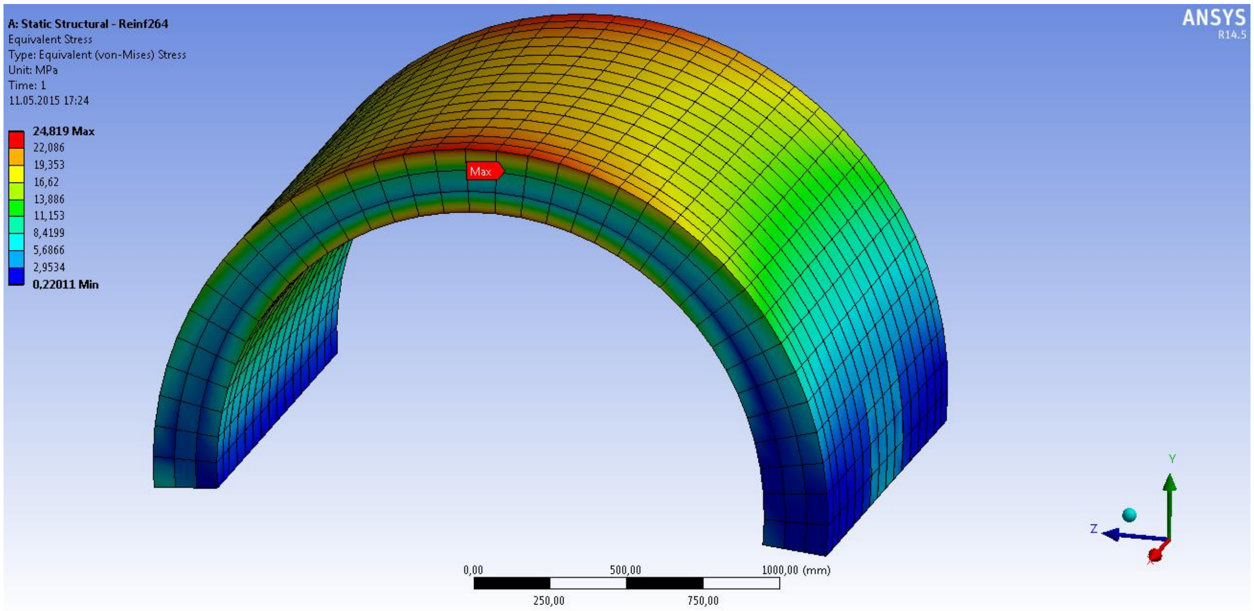

Figure A-43 Equivalent Stress – Mid 1 load case. Source: ***Ansys® Workbench, Release 14.5***

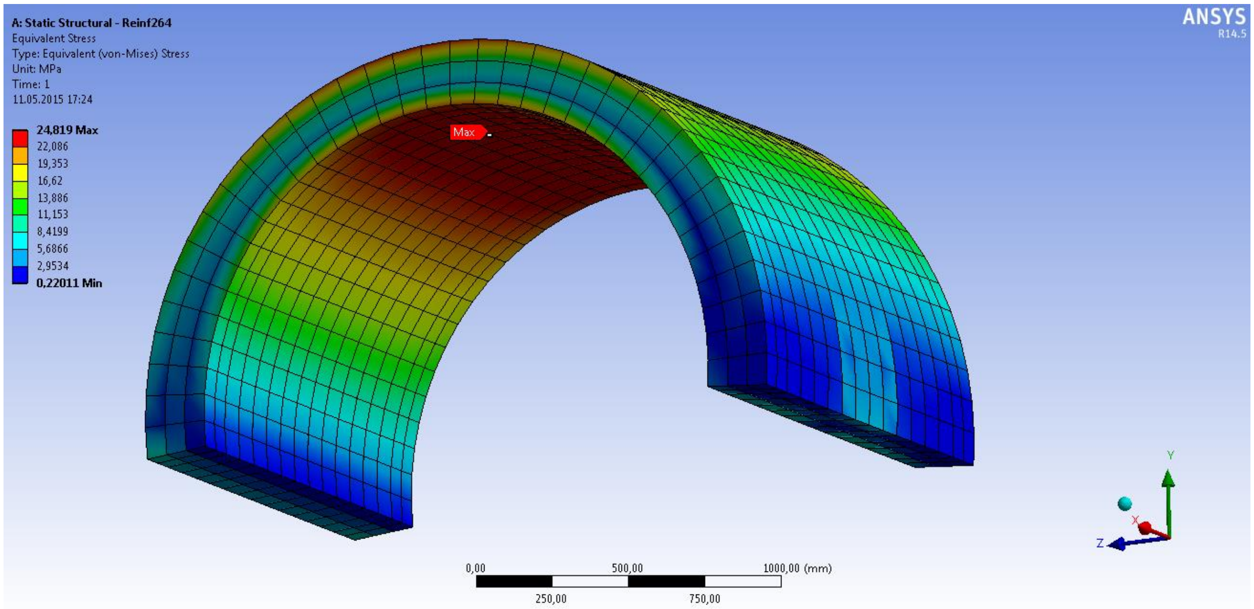

Figure A-44 Equivalent Stress – Mid 1 load case. Source: ***Ansys® Workbench, Release 14.5***

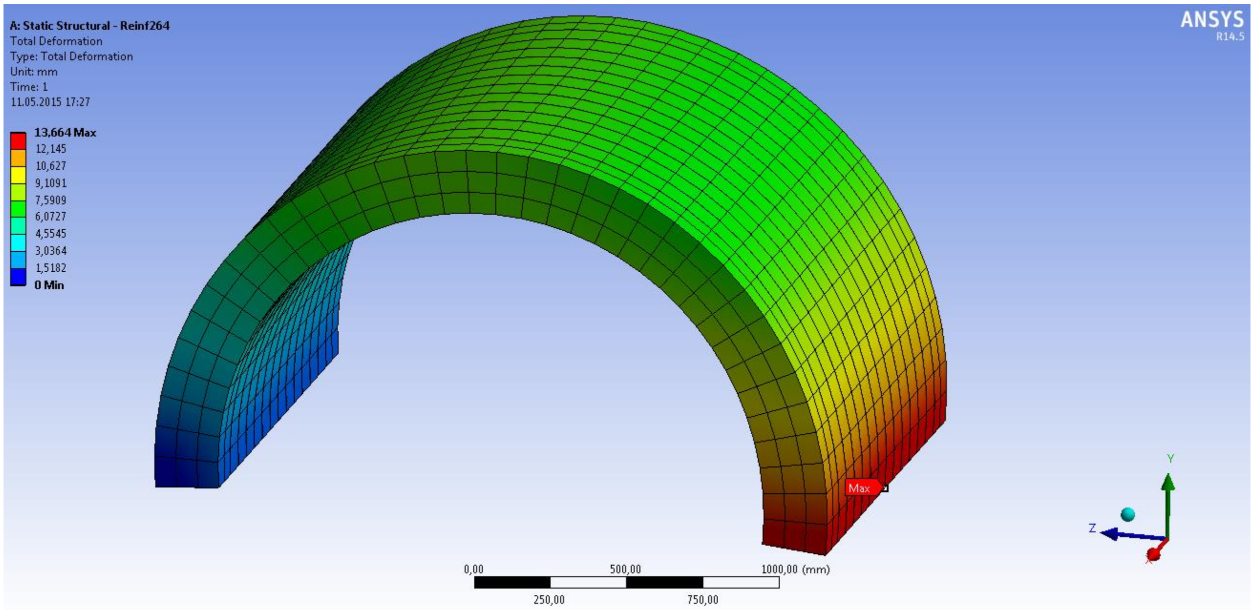

Figure A-45 Total Deformation – Mid 1 load case. Source: ***Ansys® Workbench, Release 14.5***

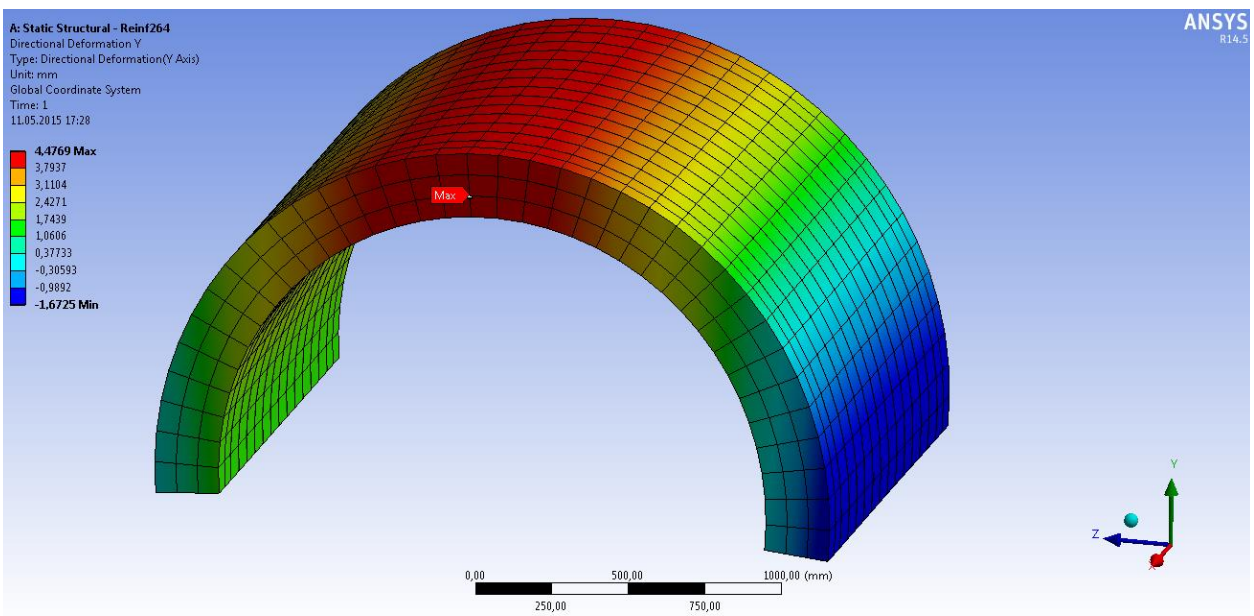

Figure A-46 Directional Deformation Y – Mid 1 load case. Source: ***Ansys® Workbench, Release 14.5***

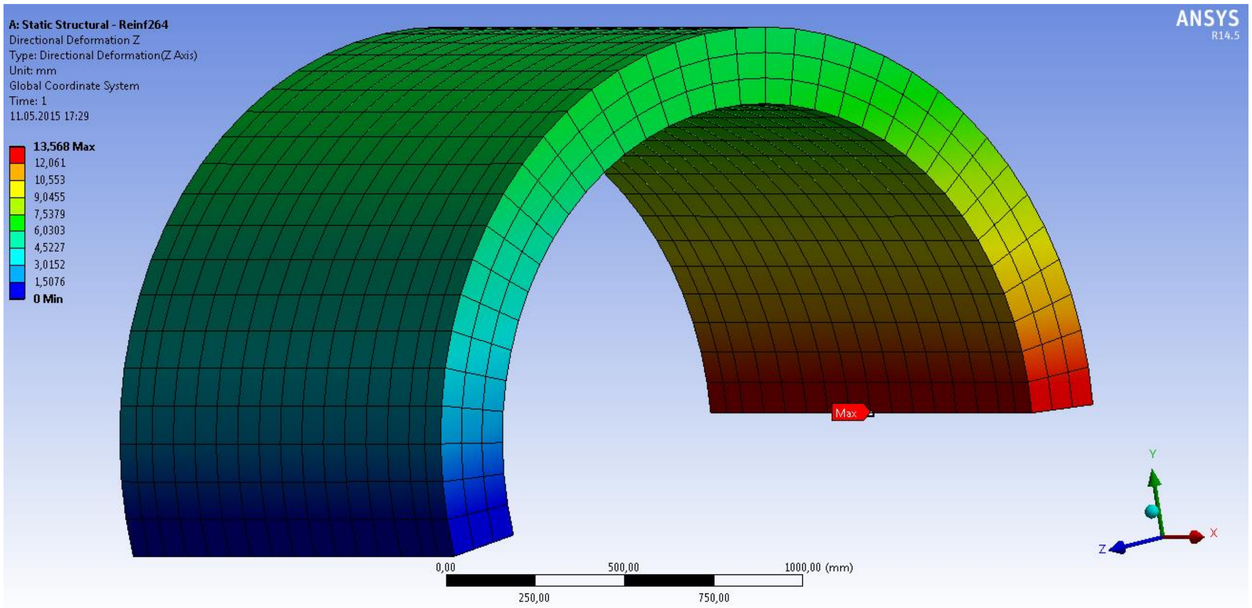

Figure A-47 Directional Deformation Z – Mid 1 load case. Source: *Ansys® Workbench, Release 14.5*

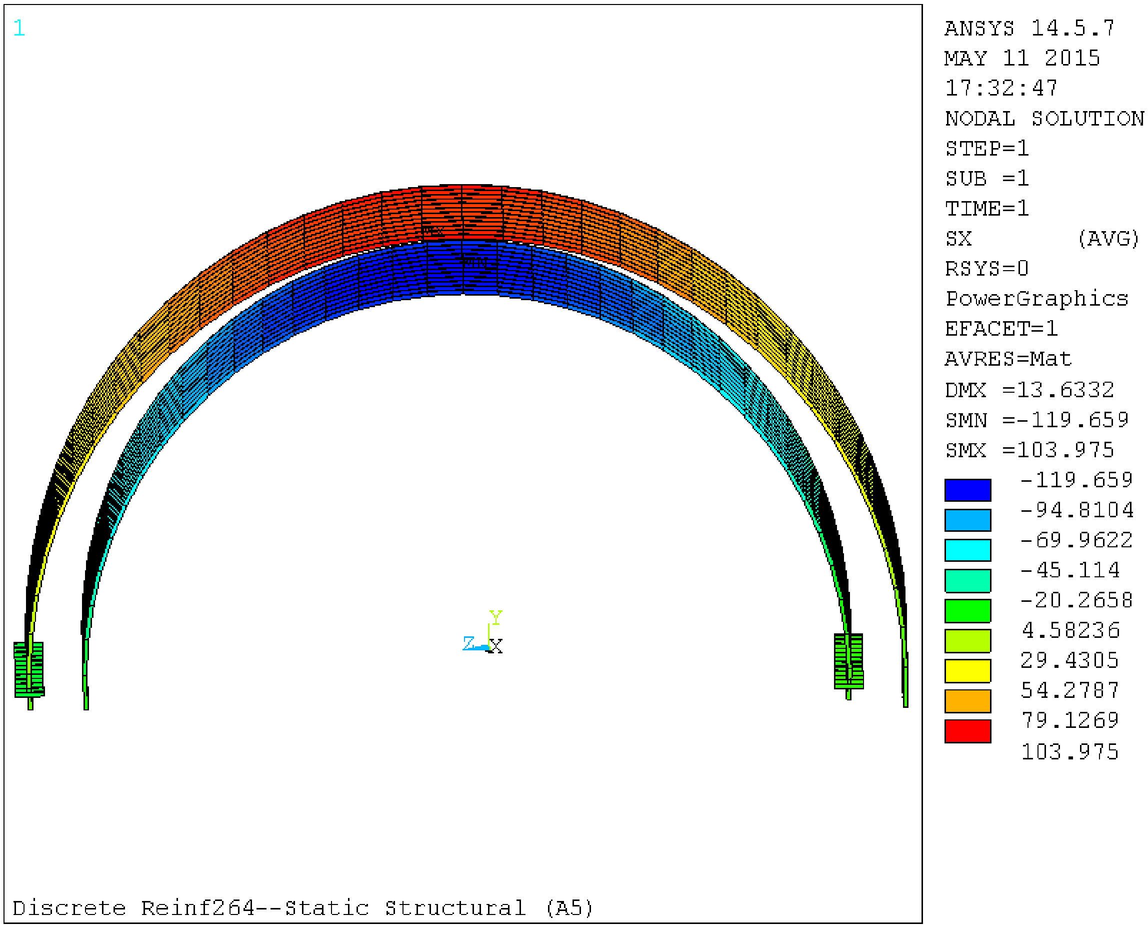

Figure A-48 Axial Stresses in Reinforcement – Mid 1 load case.
Source: *Ansys® Workbench, Release 14.5*

Mid 2 load case:

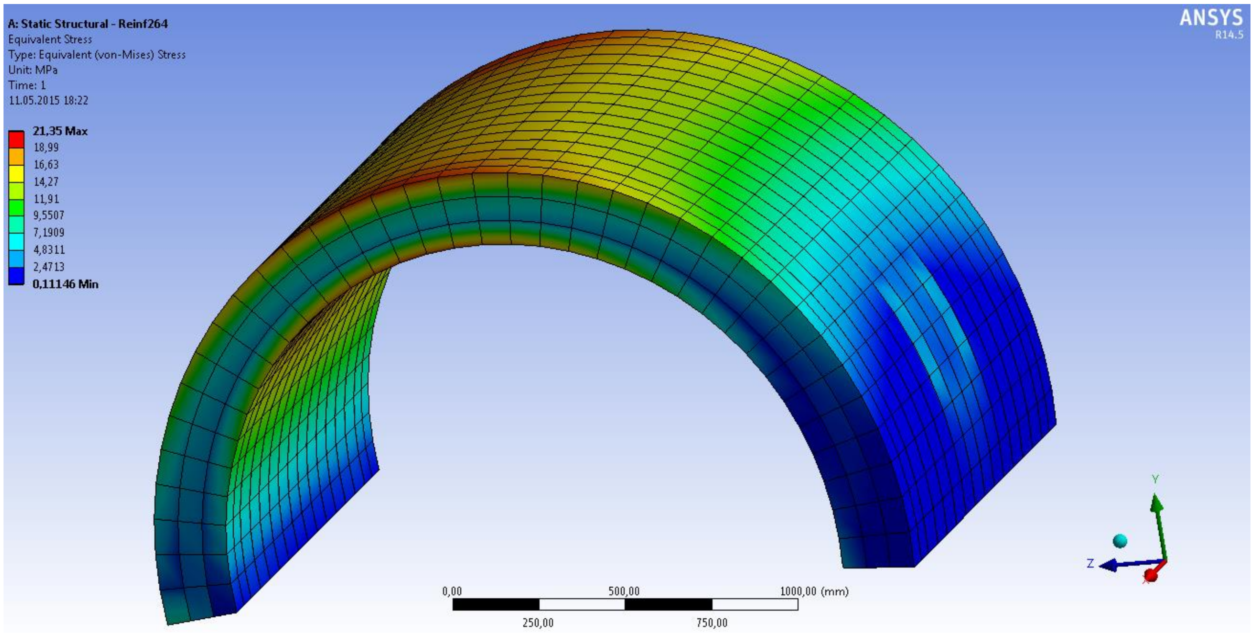

Figure A-49 Equivalent Stress – Mid 2 load case. Source: *Ansys® Workbench, Release 14.5*

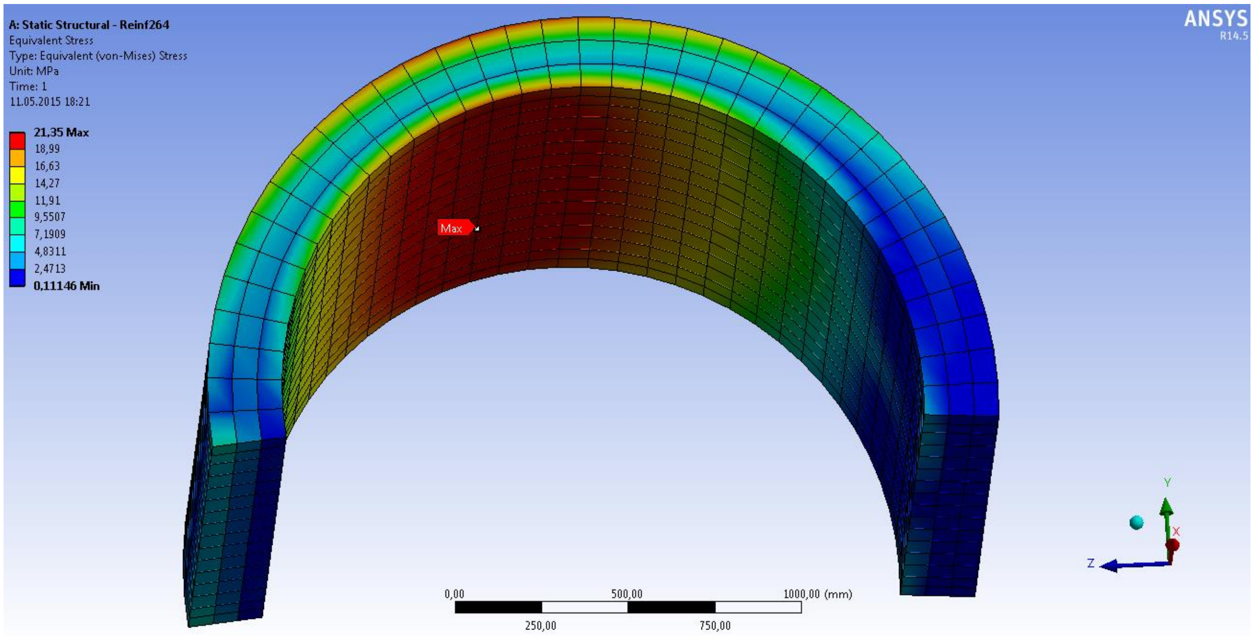

Figure A-50 Equivalent Stress – Mid 2 load case. Source: *Ansys® Workbench, Release 14.5*

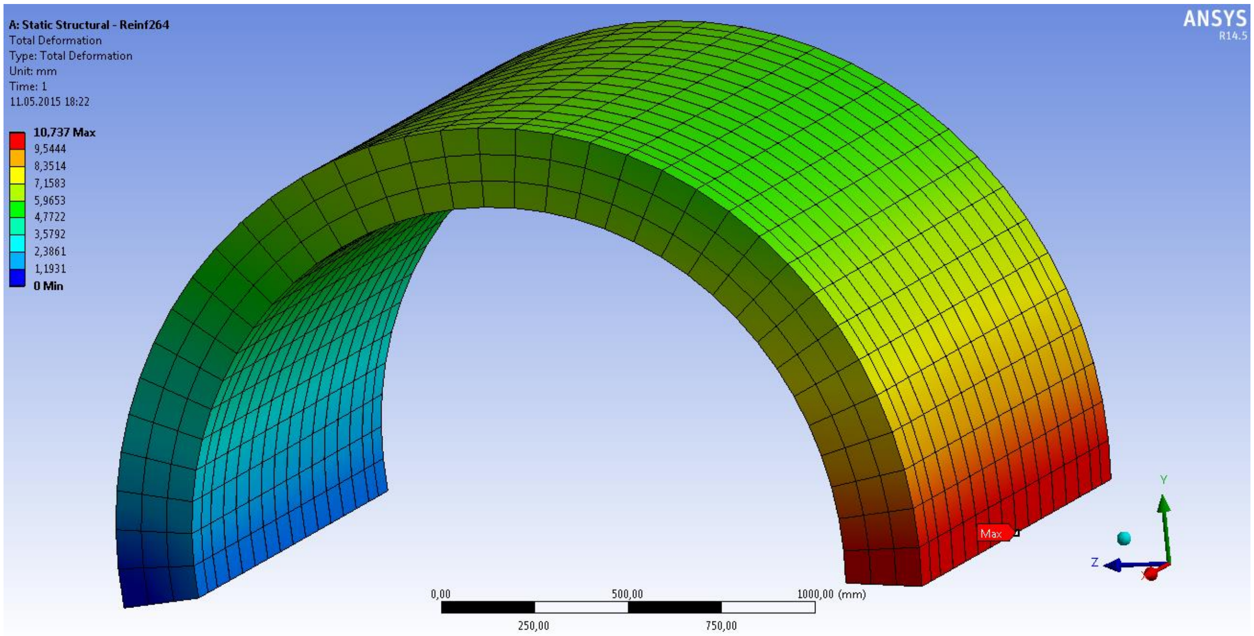

Figure A-51 Total Deformation – Mid 2 load case. Source: ***Ansys® Workbench, Release 14.5***

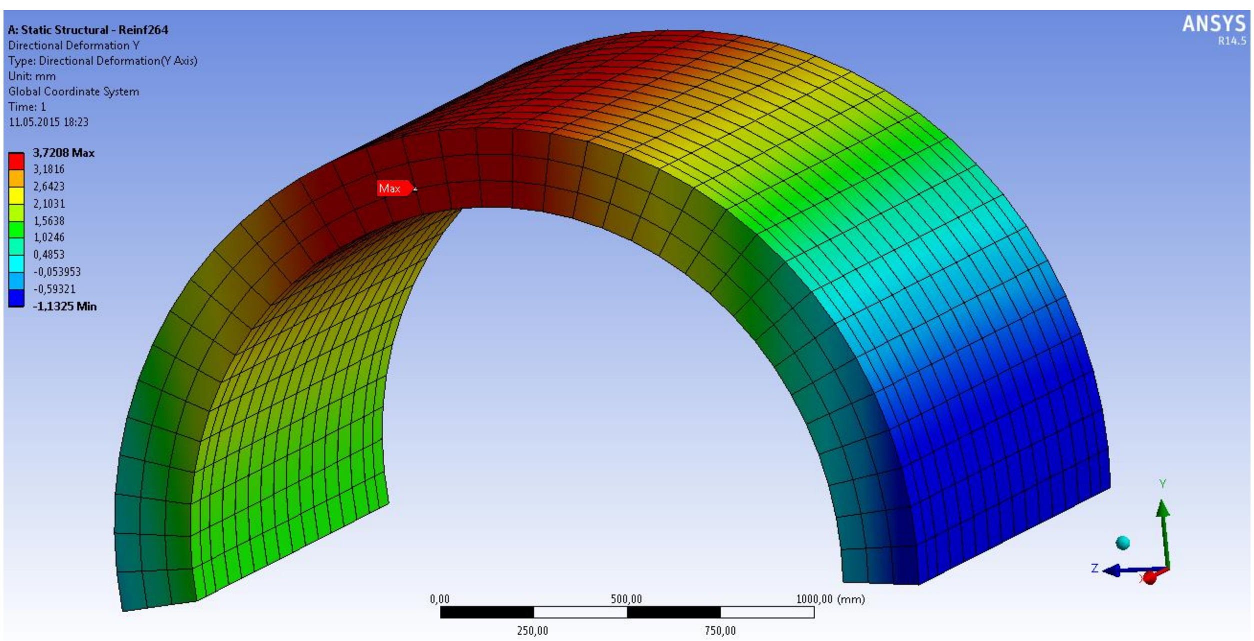

Figure A-52 Directional Deformation Y – Mid 2 load case. Source: ***Ansys® Workbench, Release 14.5***

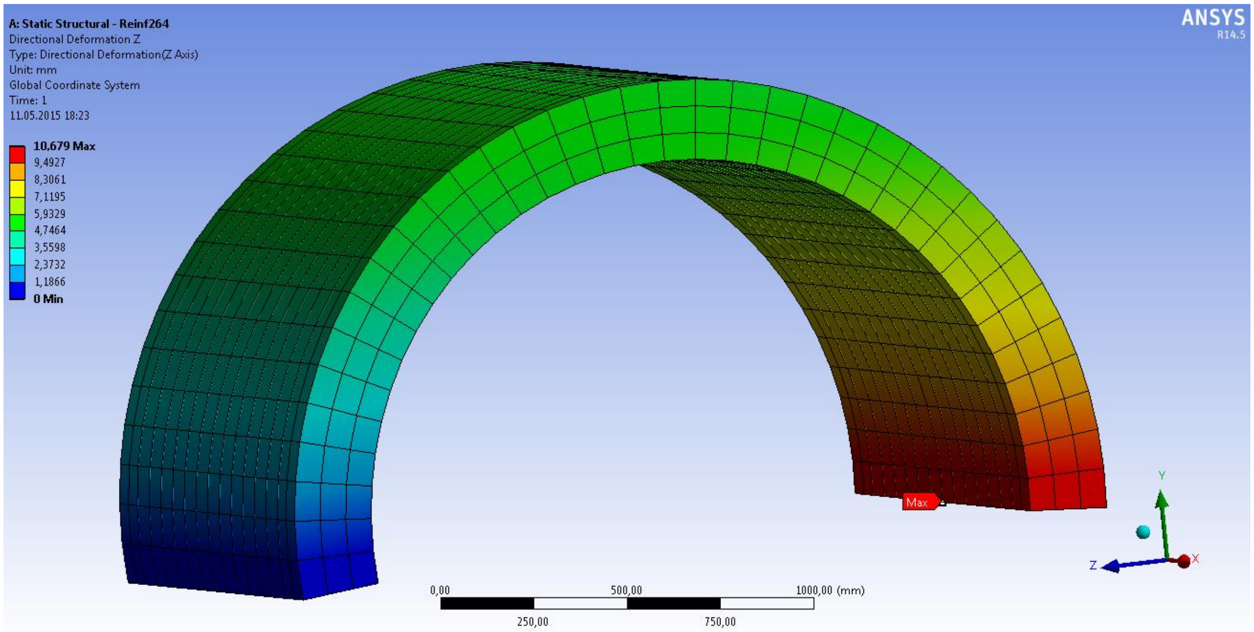

Figure A-53 Directional Deformation Z – Mid 2 load case. Source: ***Ansys® Workbench, Release 14.5***

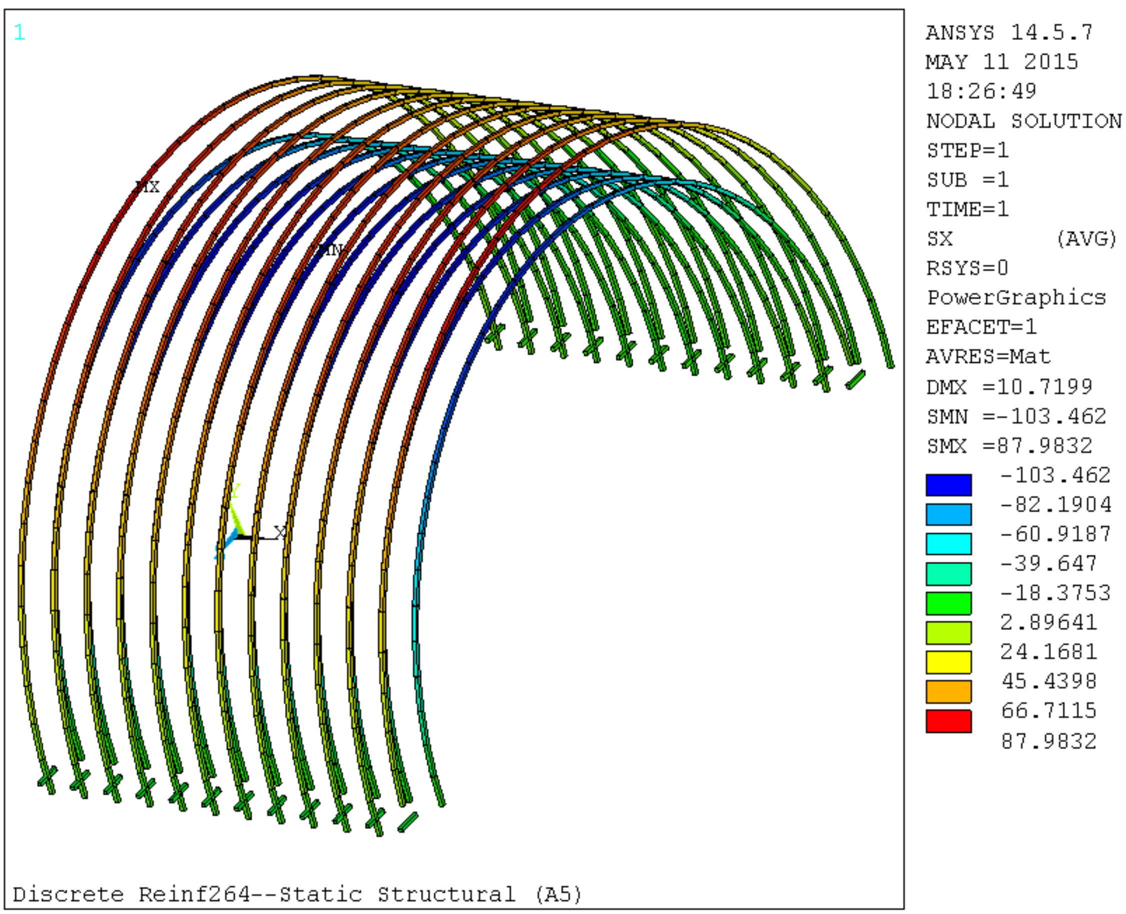

Figure A-54 Axial Stresses in Reinforcement – Mid 2 load case.
Source: ***Ansys® Workbench, Release 14.5***

Mid 3 load case:

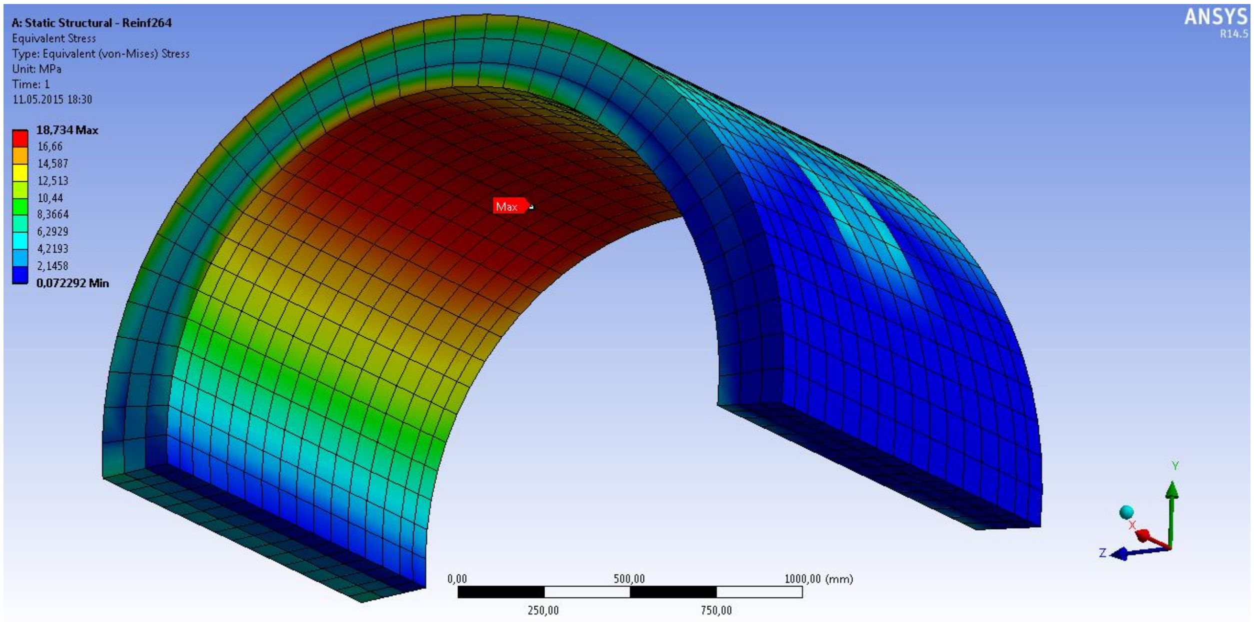

Figure A-55 Equivalent Stress – Mid 3 load case. Source: *Ansys® Workbench, Release 14.5*

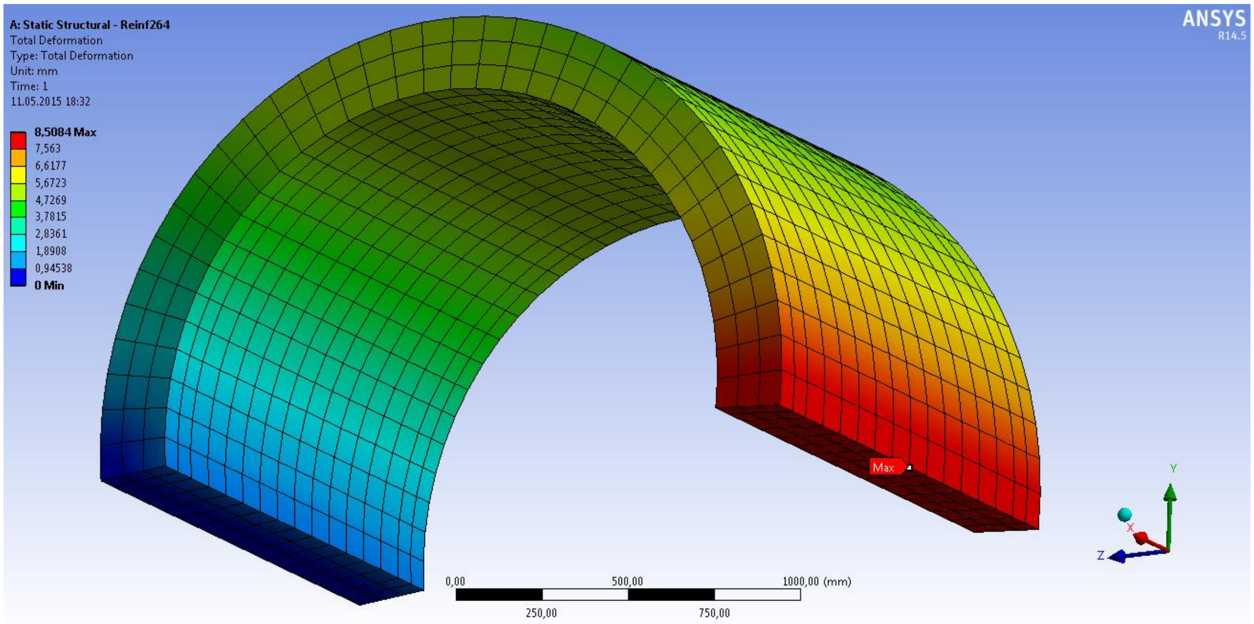

Figure A-56 Total Deformation – Mid 3 load case. Source: *Ansys® Workbench, Release 14.5*

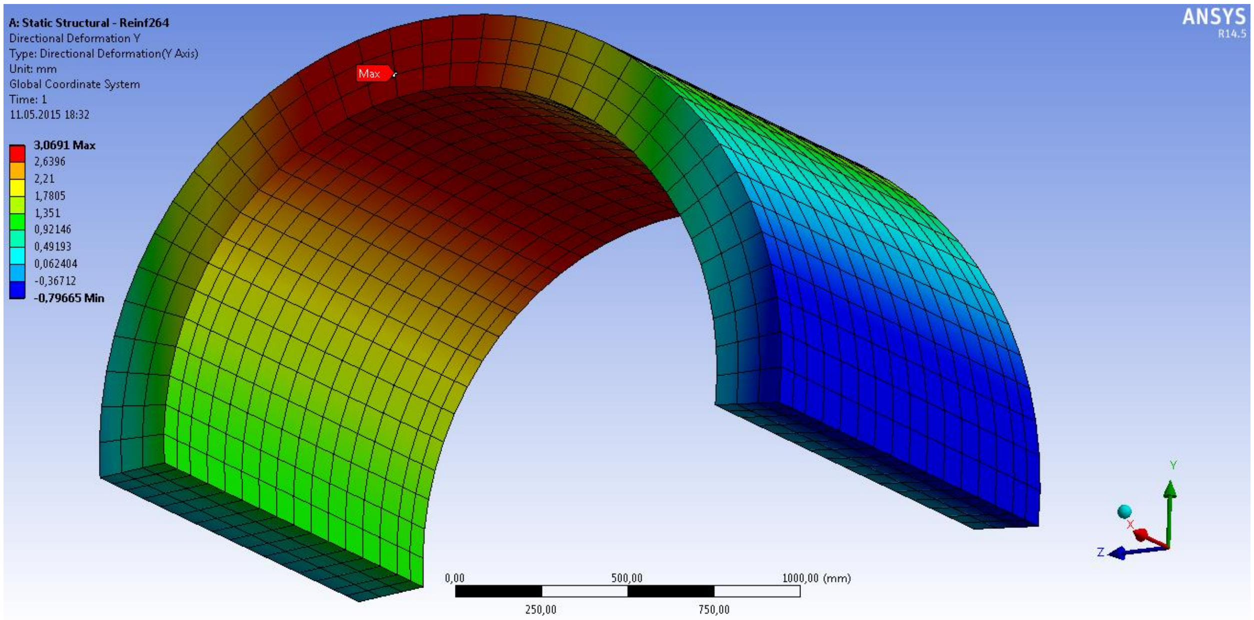

Figure A-57 Directional Deformation Y – Mid 3 load case. Source: ***Ansys® Workbench, Release 14.5***

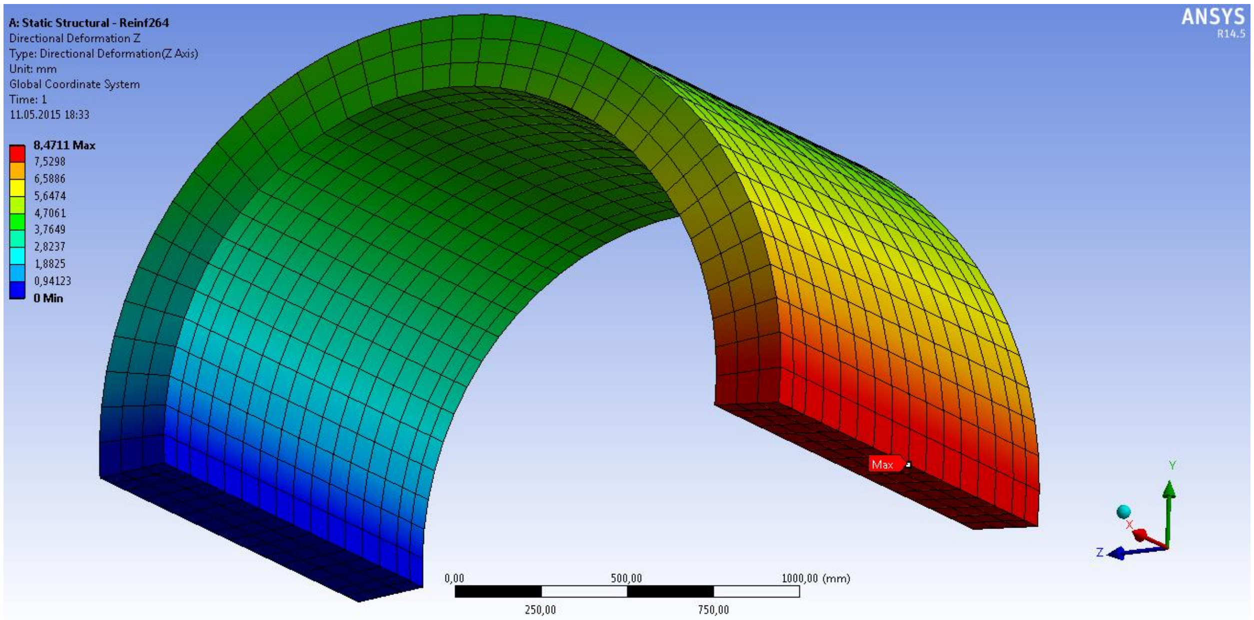

Figure A-58 Directional Deformation Z – Mid 3 load case. Source: ***Ansys® Workbench, Release 14.5***

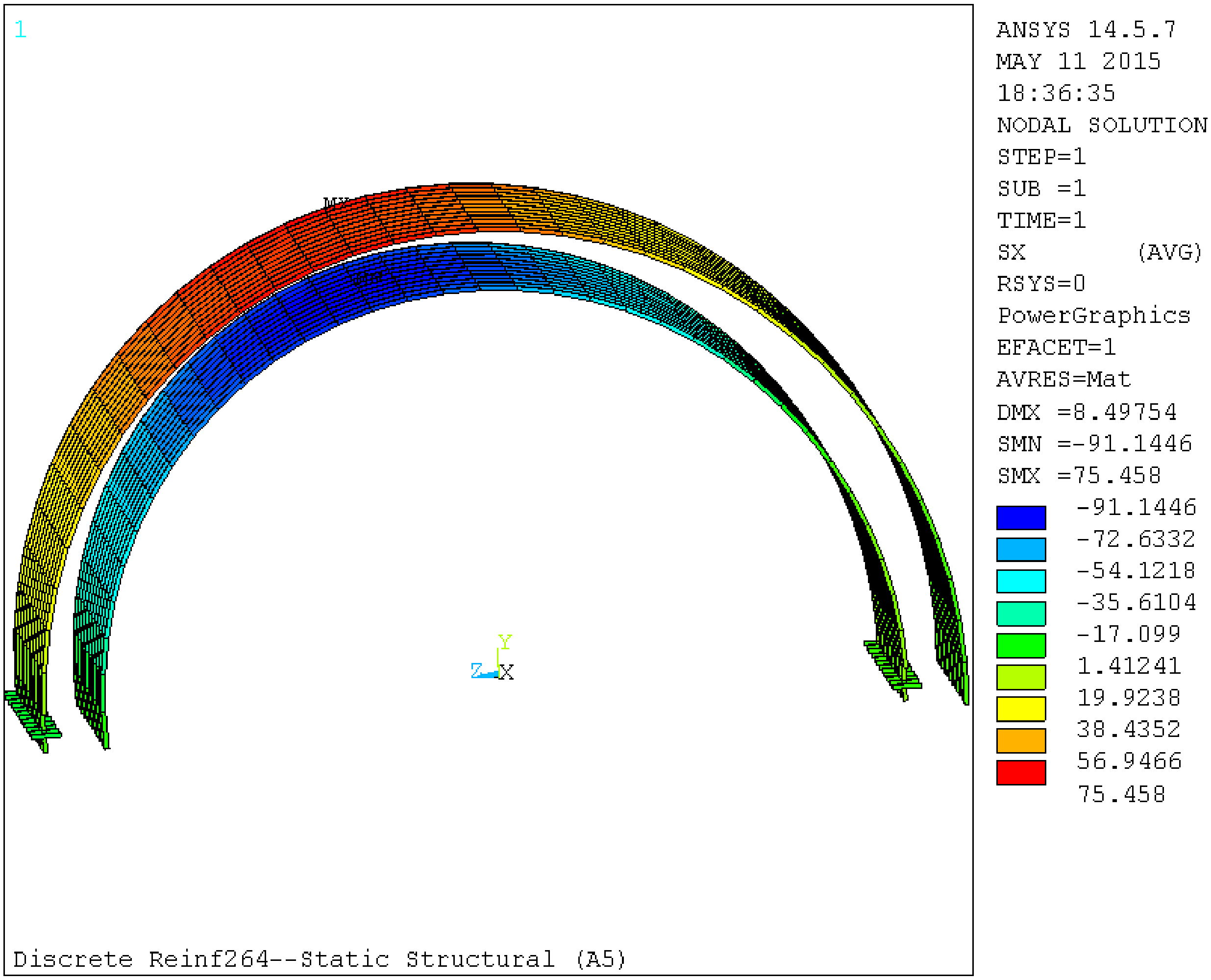

Figure A-59 Axial Stresses in Reinforcement – Mid 3 load case.
Source: ***Ansys® Workbench, Release 14.5***

Mid 4 load case:

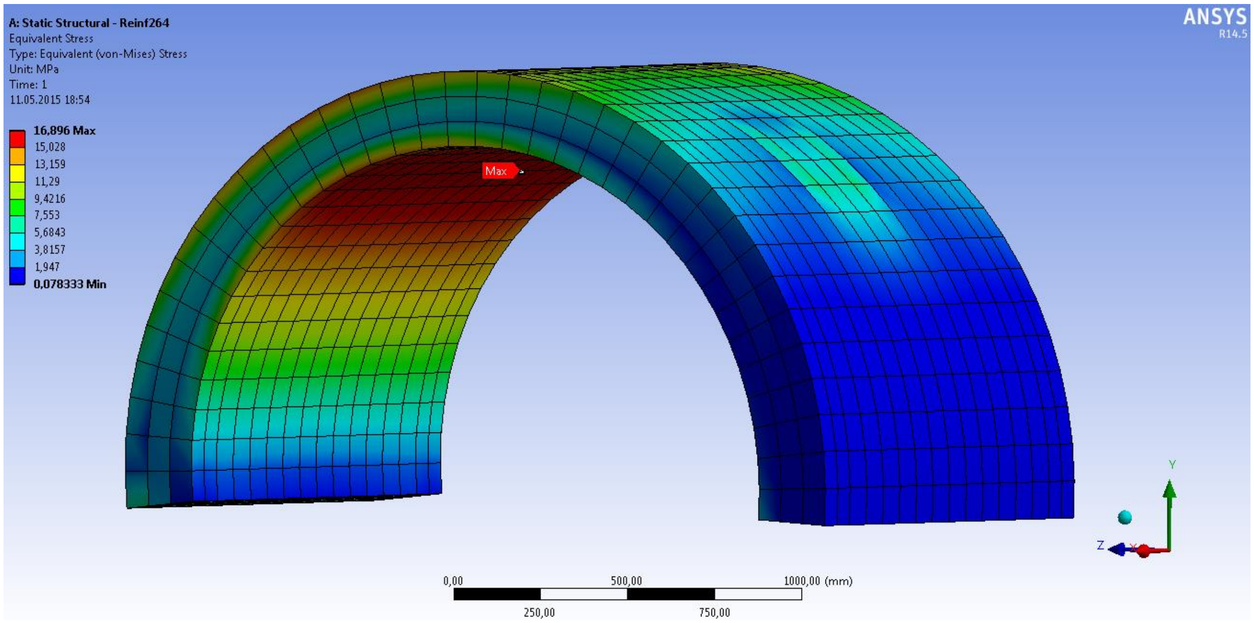

Figure A-60 Equivalent Stress – Mid 4 load case. Source: *Ansys® Workbench, Release 14.5*

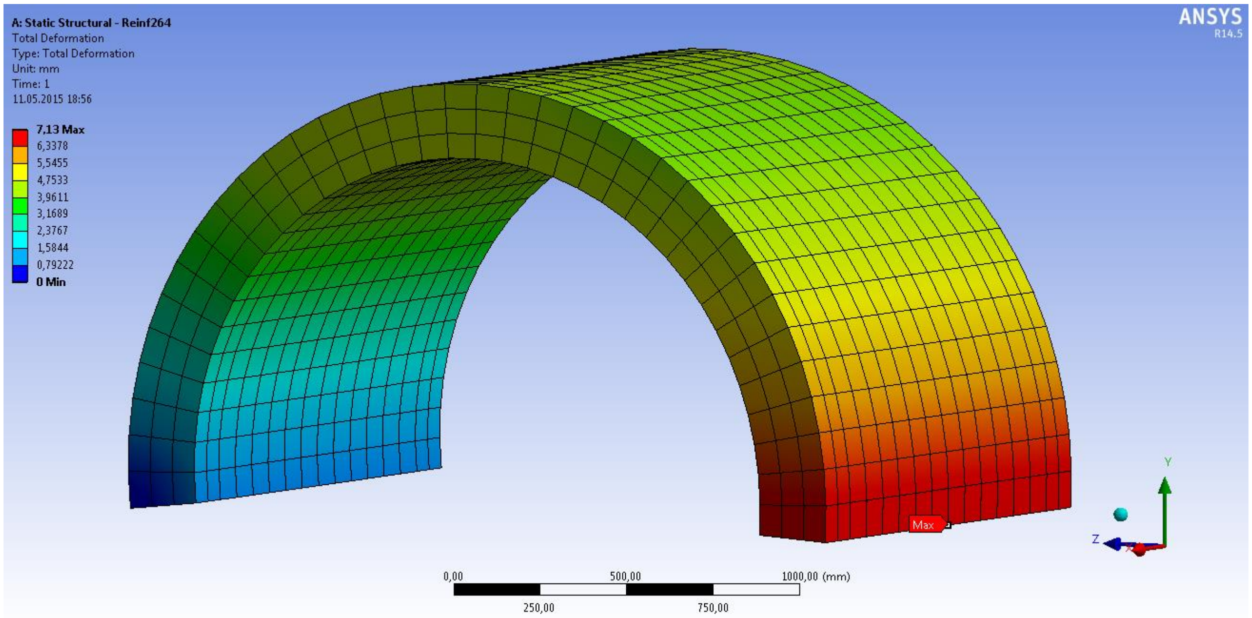

Figure A-61 Total Deformation – Mid 4 load case. Source: *Ansys® Workbench, Release 14.5*

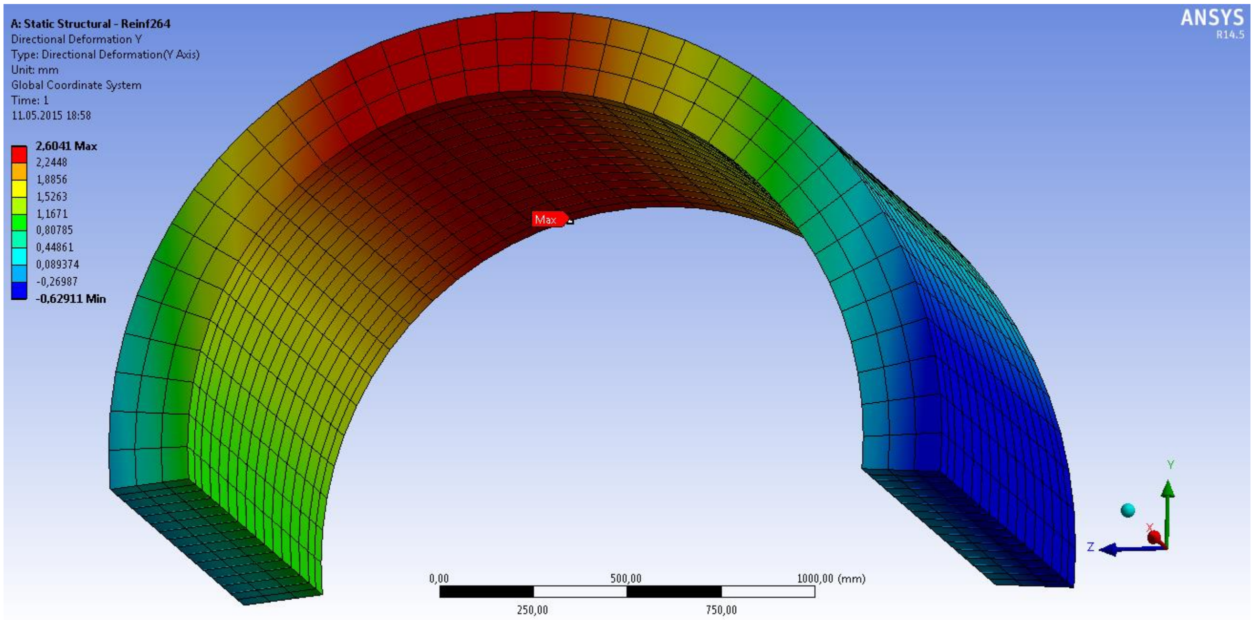

Figure A-62 Directional Deformation Y – Mid 4 load case. Source: ***Ansys® Workbench, Release 14.5***

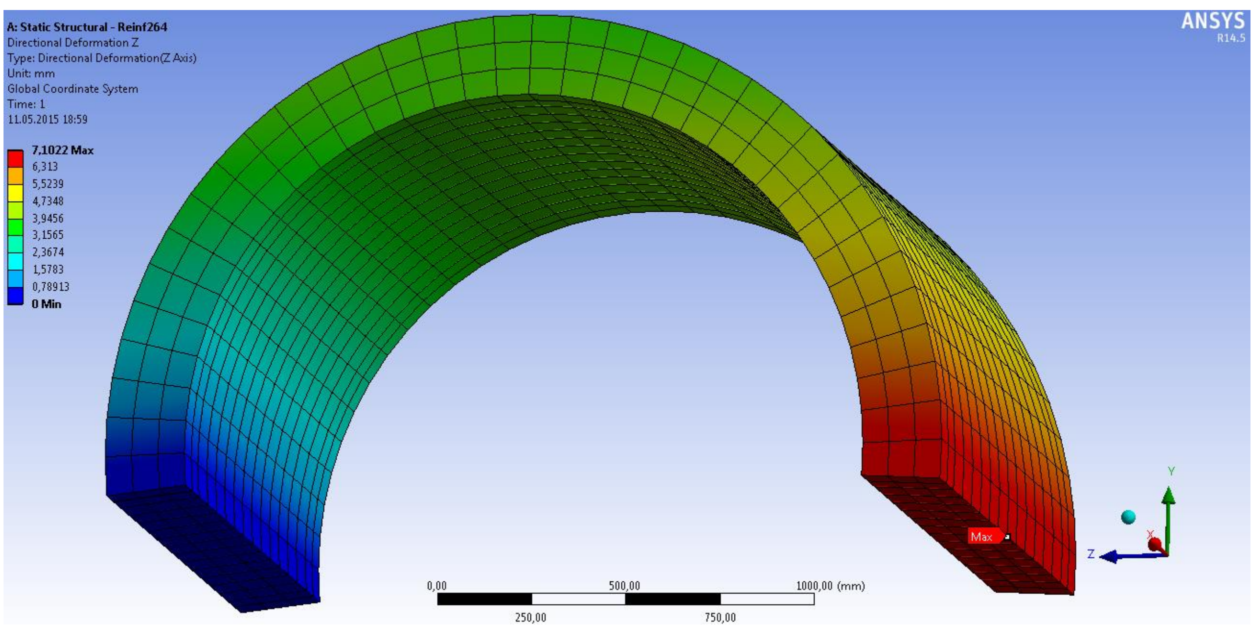

Figure A-63 Directional Deformation Z – Mid 4 load case. Source: ***Ansys® Workbench, Release 14.5***

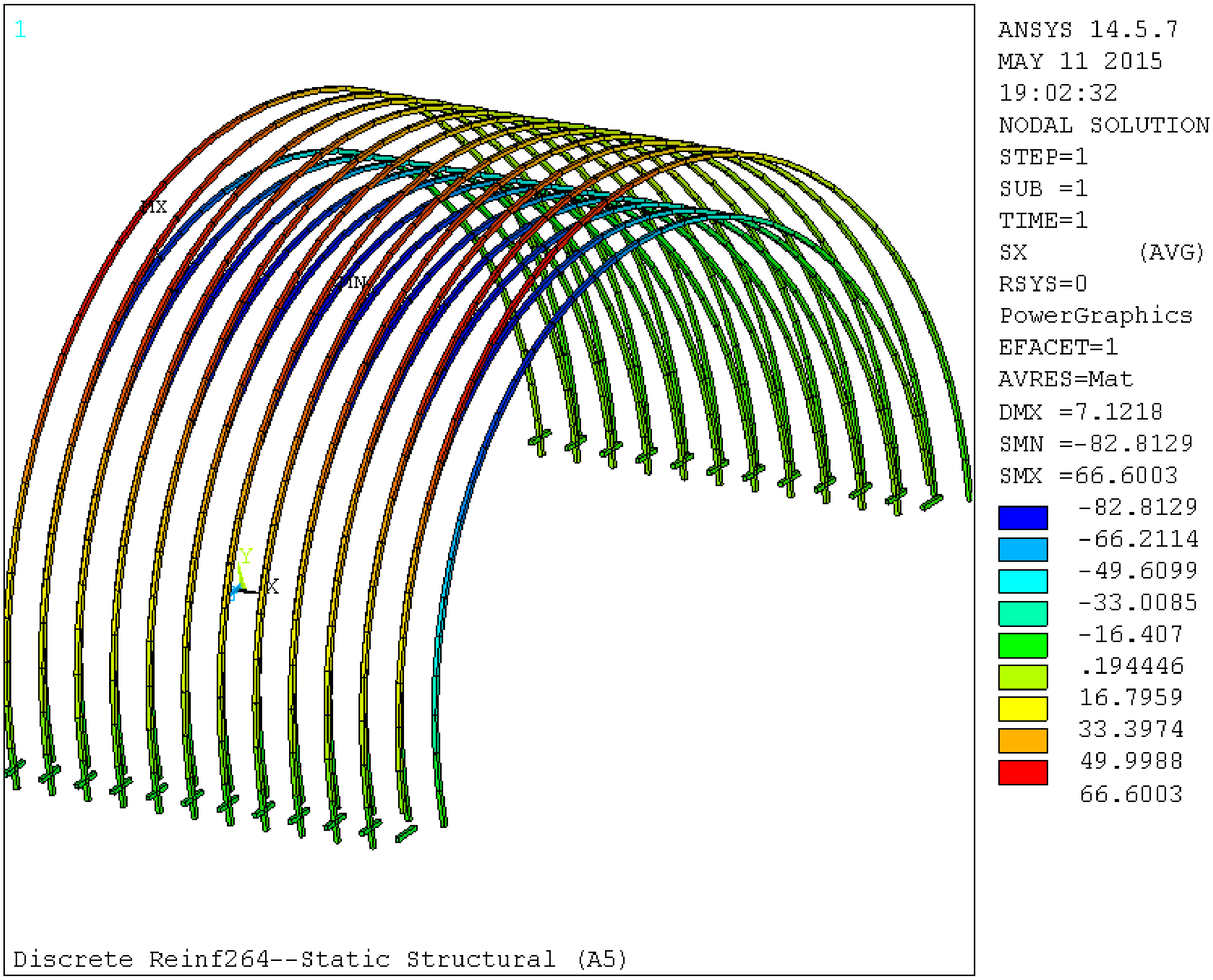

Figure A-64 Axial Stresses in Reinforcement – Mid 4 load case.
Source: ***Ansys® Workbench, Release 14.5***

B. Results from the Dropped object analysis in *Ansys® Workbench, Release 14.5*

50 kJ impact can be seen in chapter 5.1.2 Dropped object impact test – Explicit Dynamics.

5 kJ impact:

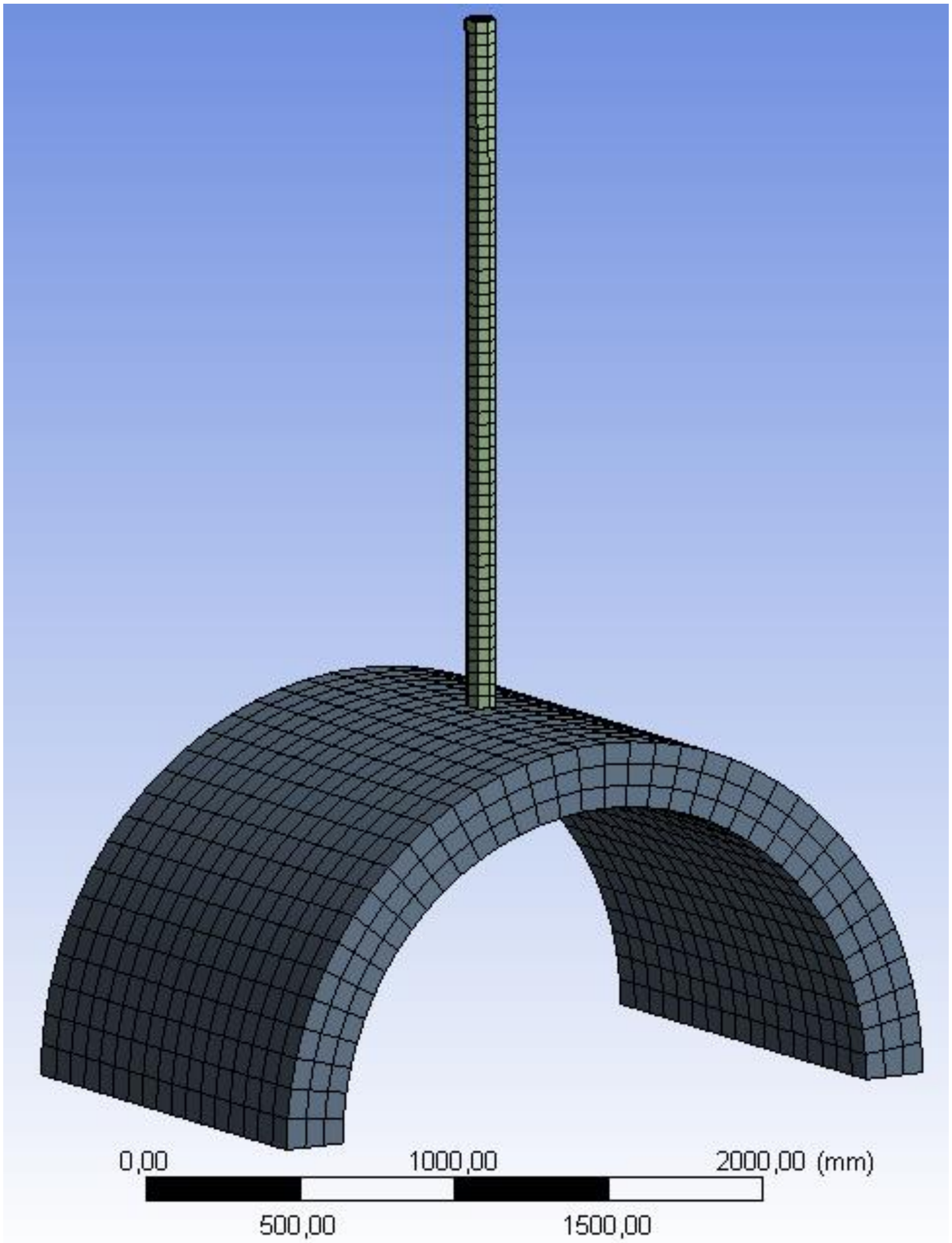

Figure B-1 Mesh of model for the 5 kJ impact. Source: *Ansys® Workbench, Release 14.5*

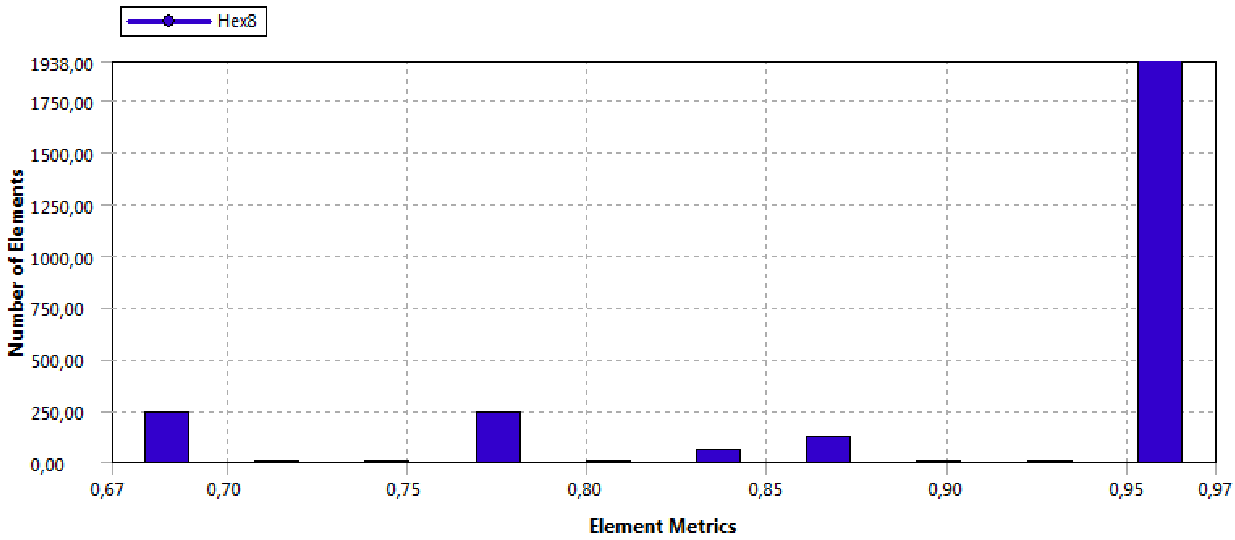

Figure B-2 Mesh metrics for the 5 kJ impact. Source: ***Ansys® Workbench, Release 14.5***

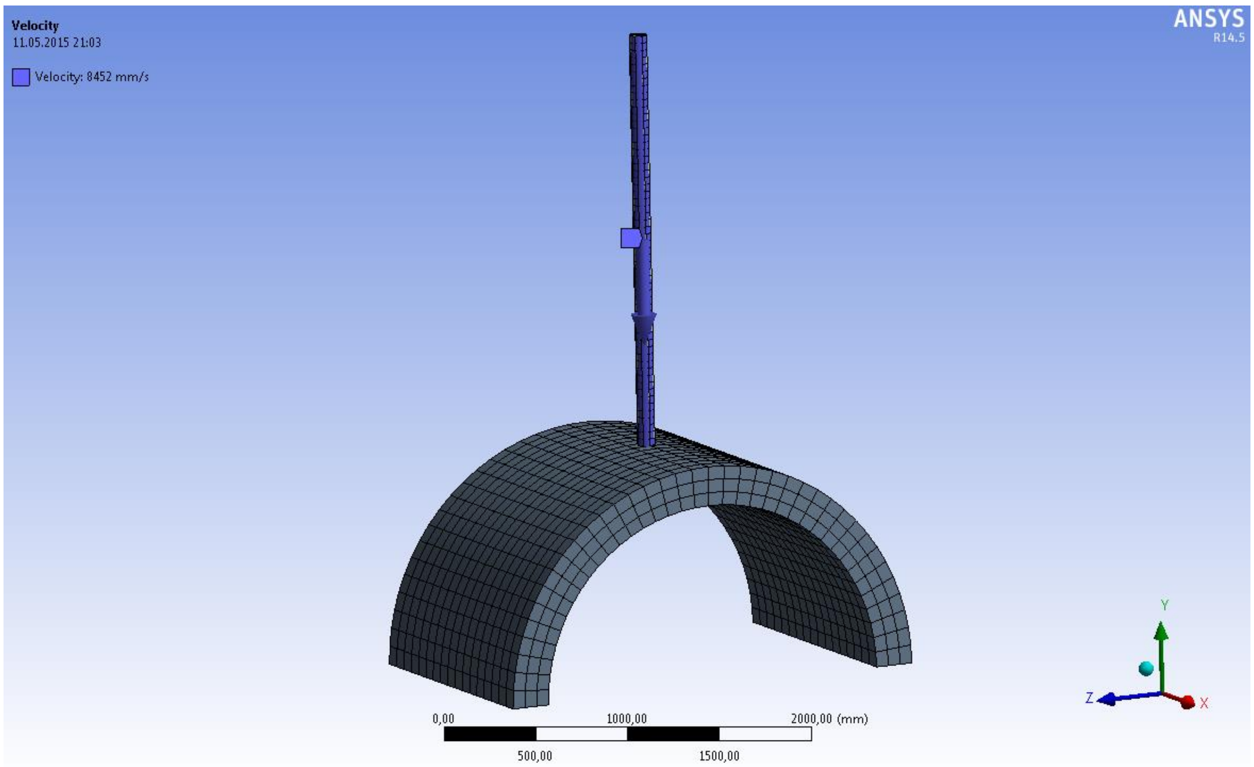

Figure B-3 Velocity of object for the 5 kJ impact. Source: ***Ansys® Workbench, Release 14.5***

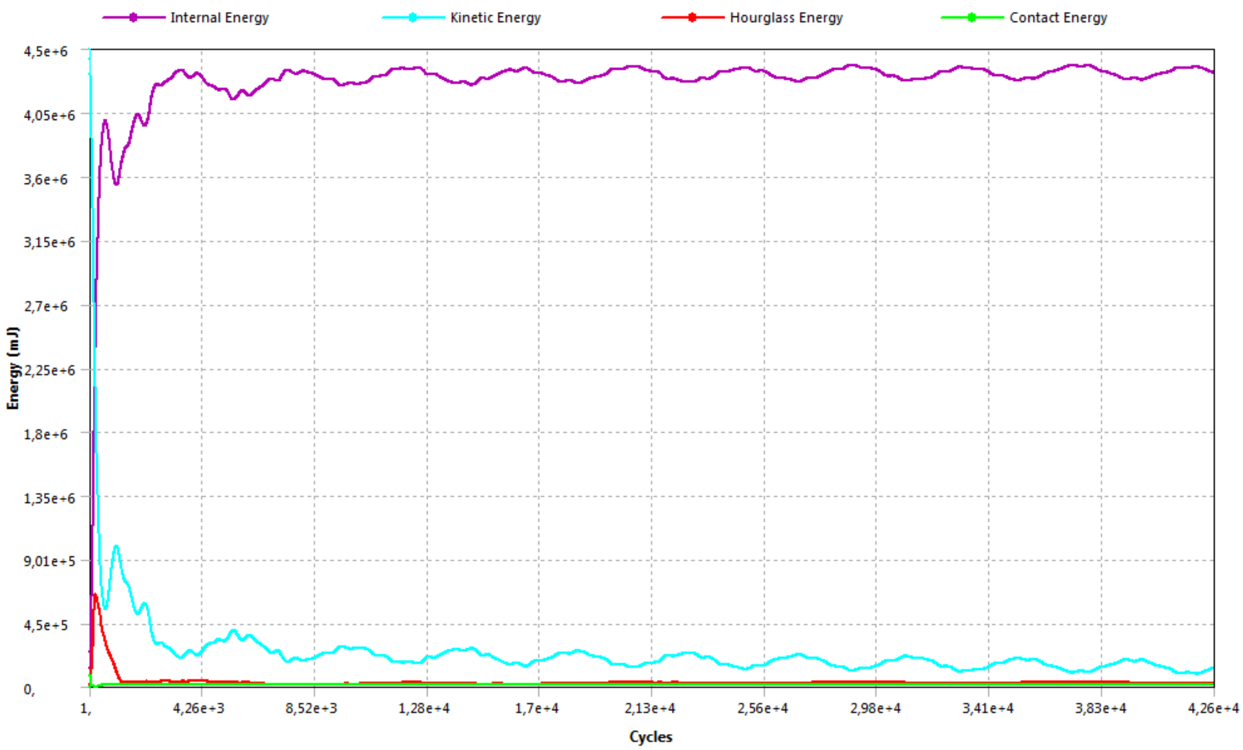

Figure B-4 Energy summary for the 5 kJ impact. Source: *Ansys® Workbench, Release 14.5*

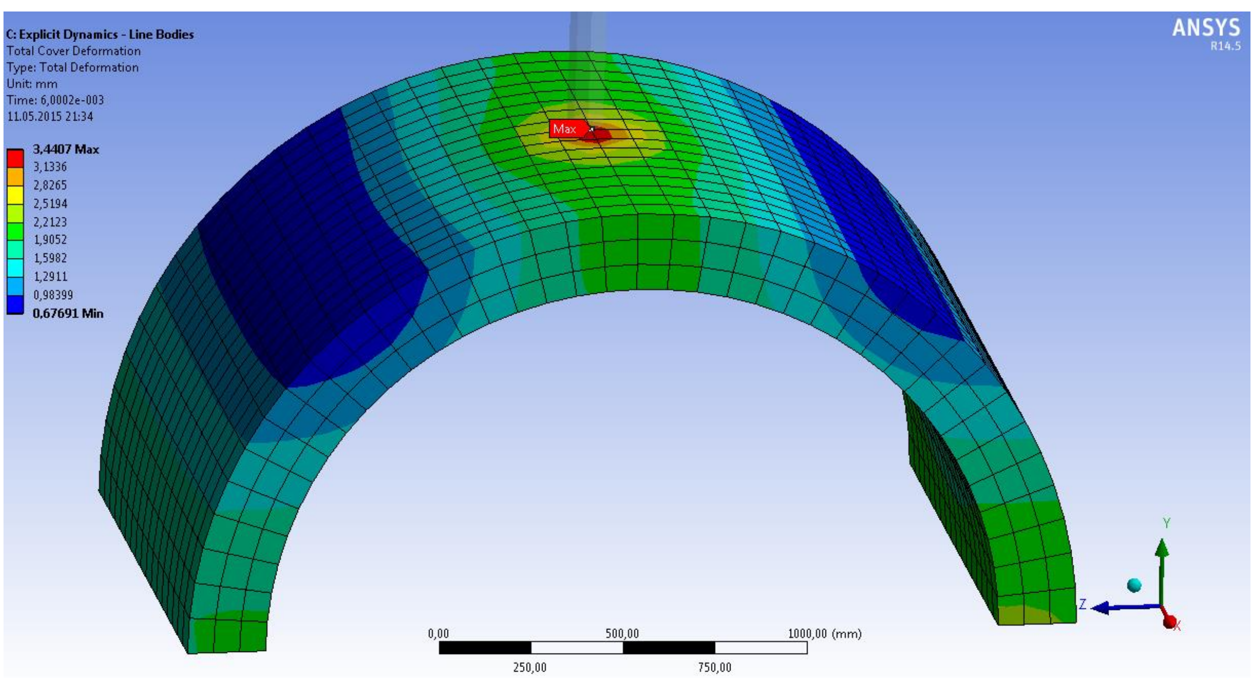

Figure B-5 Total Cover Deformation for the 5 kJ impact. Source: *Ansys® Workbench, Release 14.5*

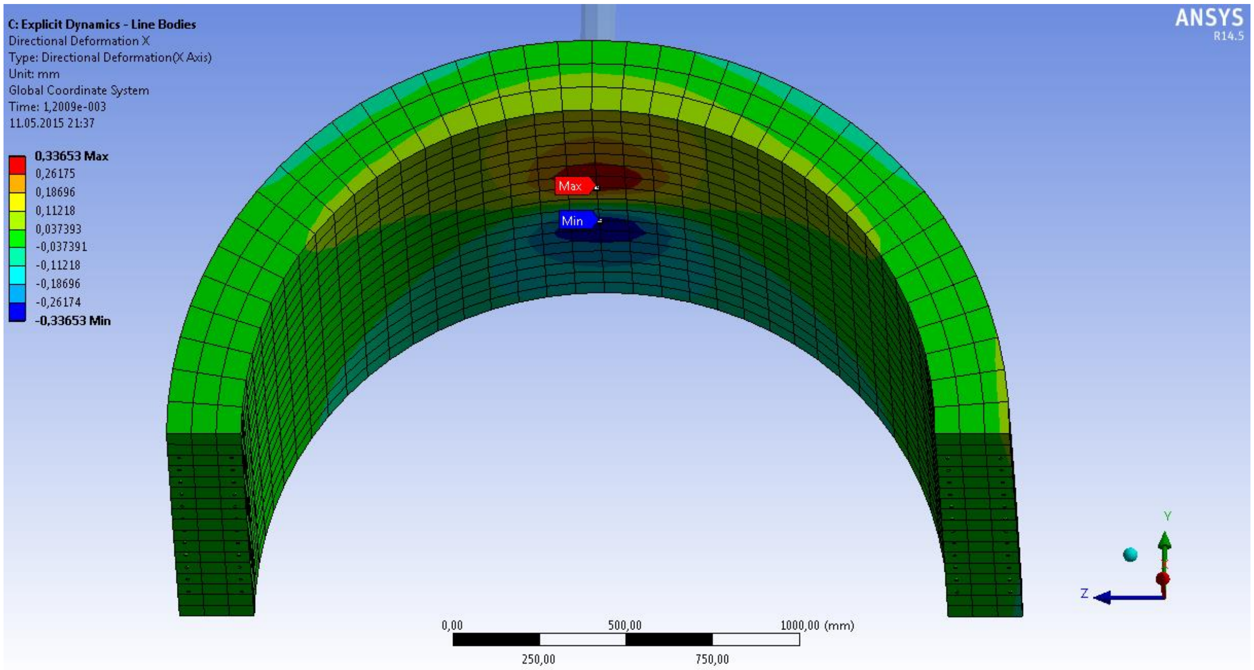

Figure B-6 Directional Deformation X for the 5 kJ impact. Source: ***Ansys® Workbench, Release 14.5***

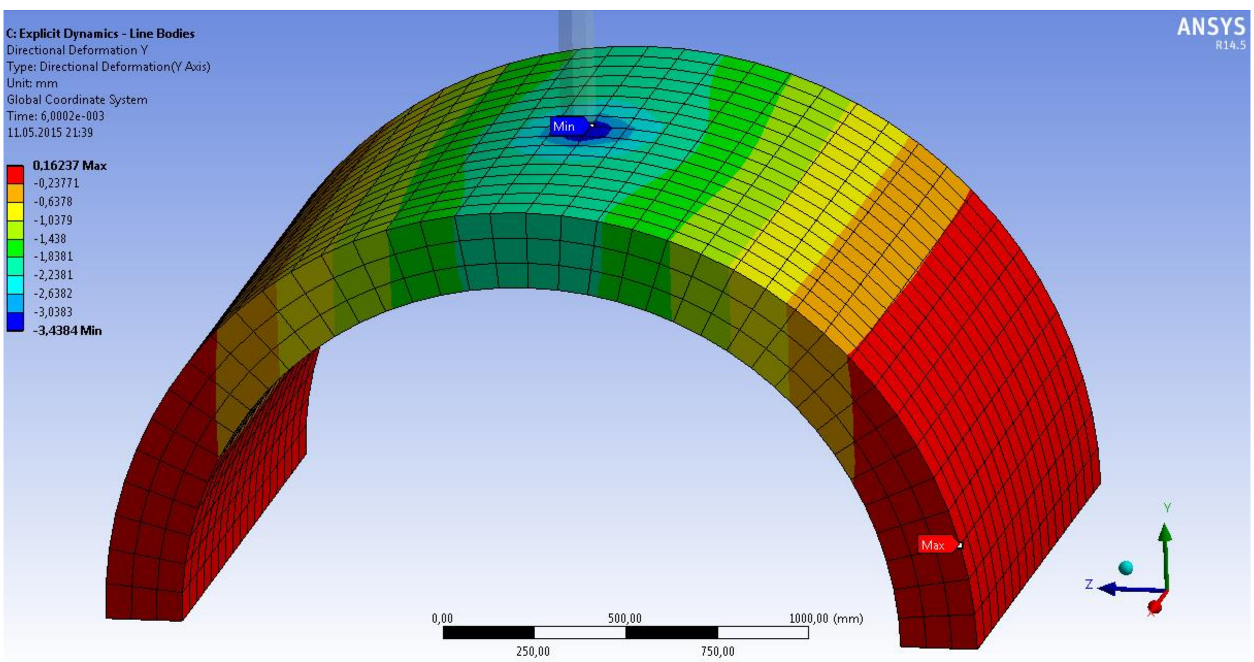

Figure B-7 Directional Deformation Y for the 5 kJ impact. Source: ***Ansys® Workbench, Release 14.5***

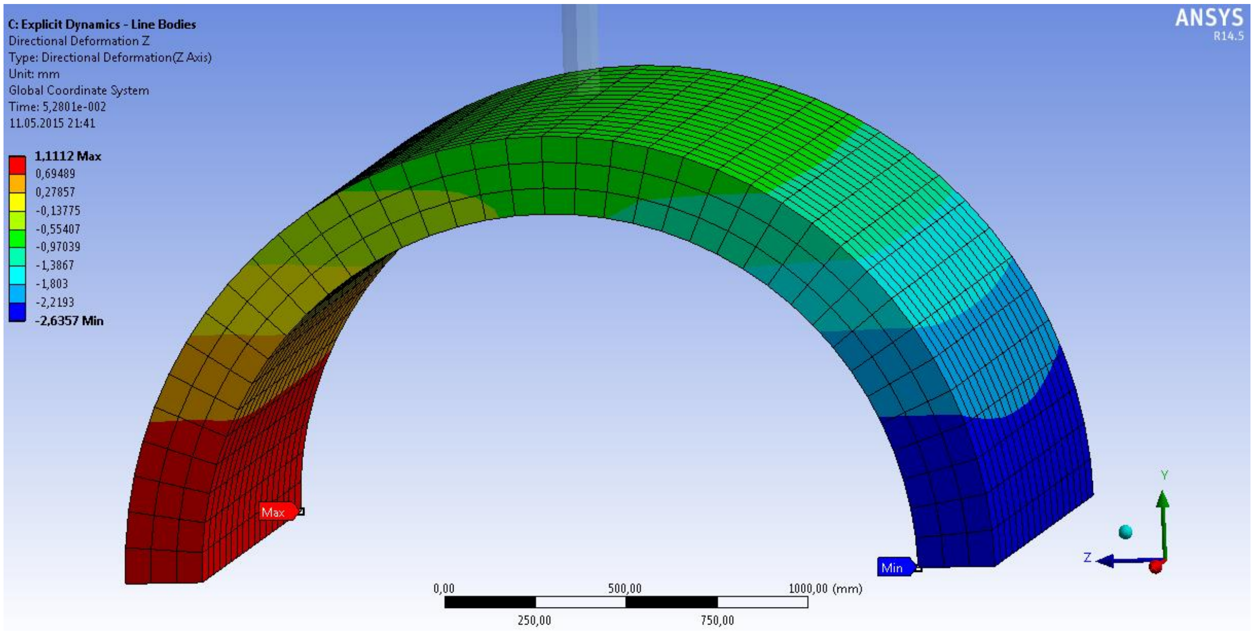

Figure B-8 Directional Deformation Z for the 5 kJ impact. Source: *Ansys® Workbench, Release 14.5*

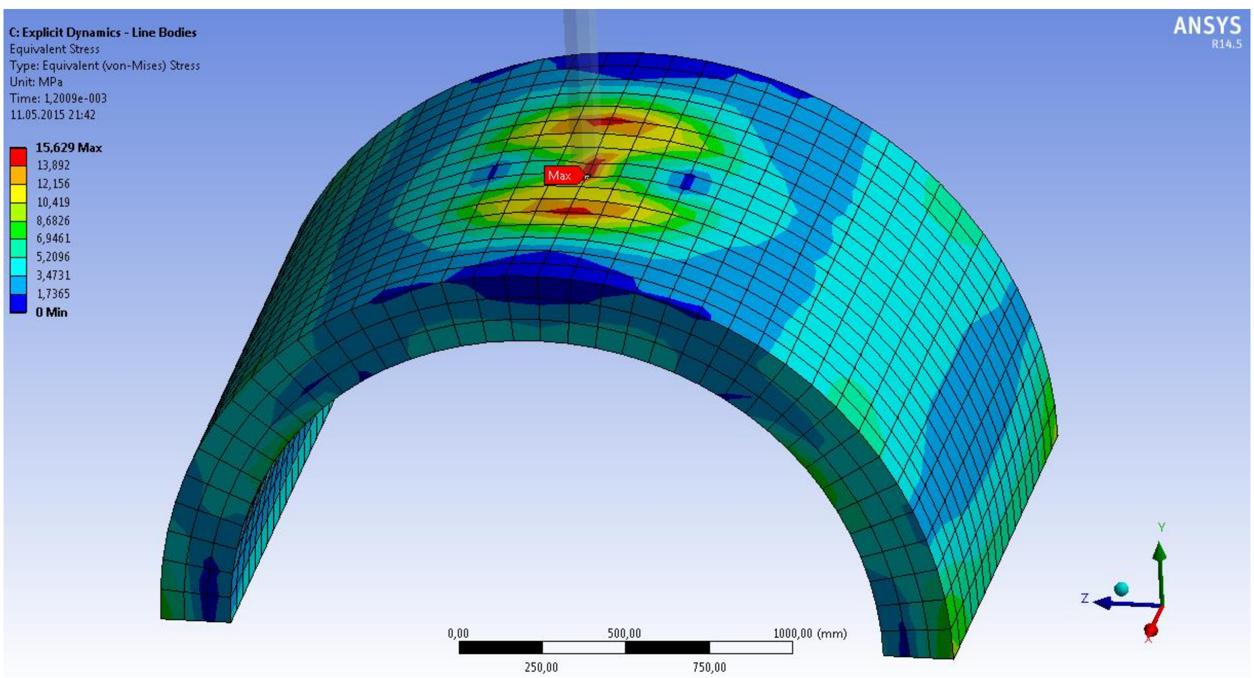

Figure B-9 Equivalent Stress for the 5 kJ impact. Source: *Ansys® Workbench, Release 14.5*

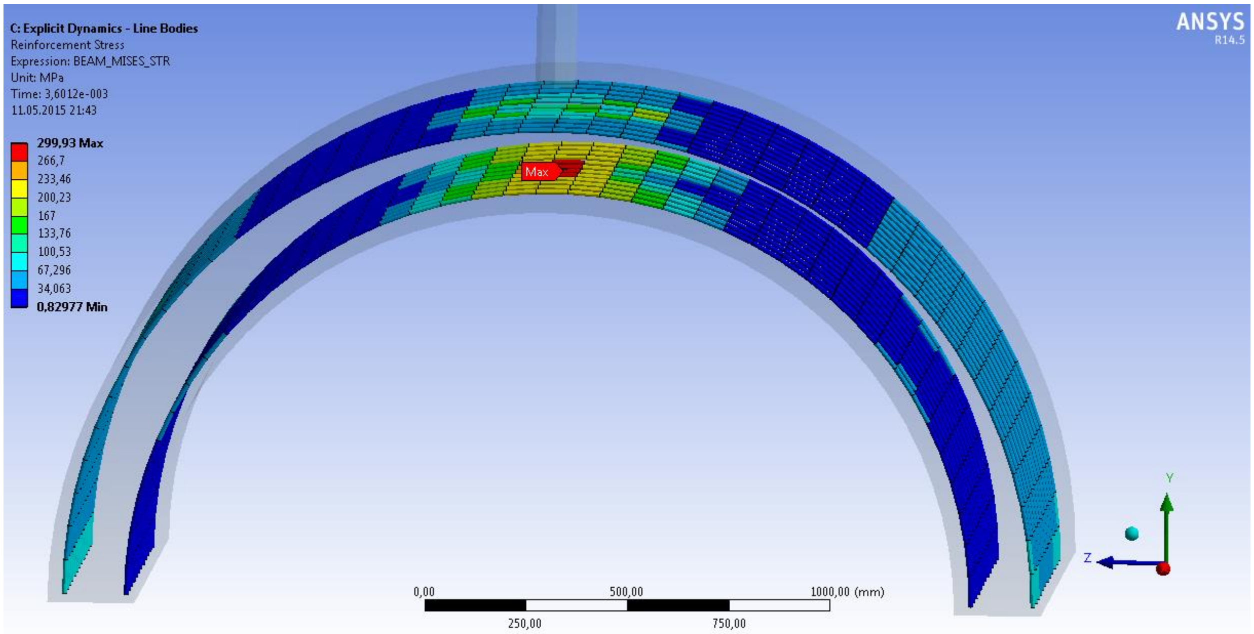

Figure B-10 Reinforcement Stress for the 5 kJ impact. Source: *Ansys® Workbench, Release 14.5*

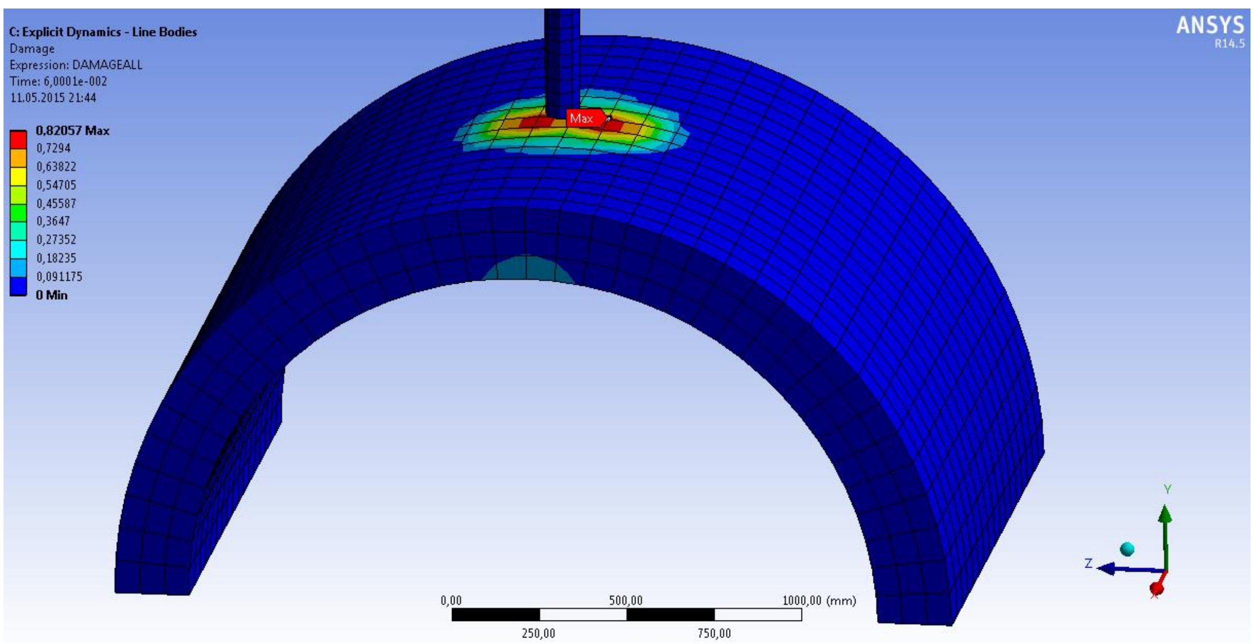

Figure B-11 Damage from the 5 kJ impact. Source: *Ansys® Workbench, Release 14.5*

20 kJ impact:

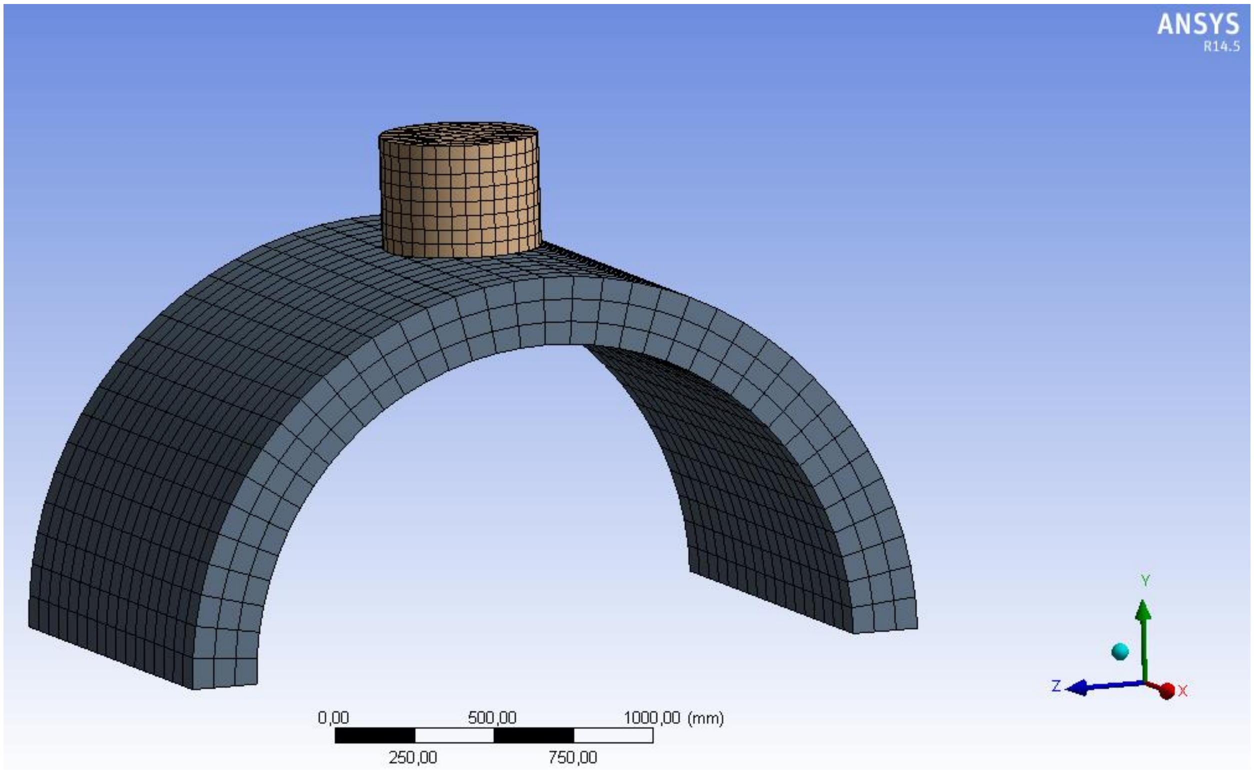

Figure B-12 Mesh of model for the 20 kJ impact. Source: ***Ansys® Workbench, Release 14.5***

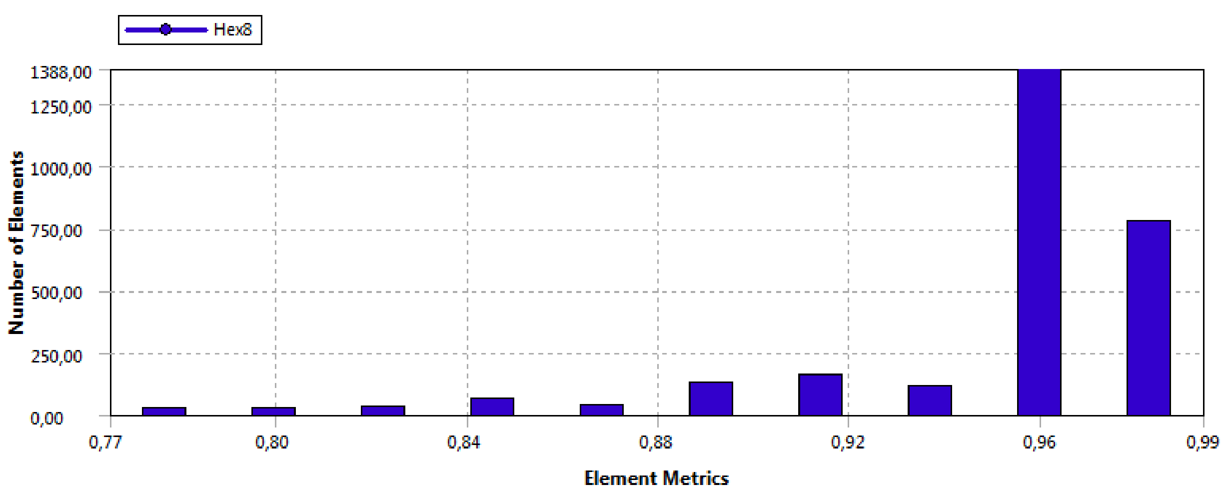

Figure B-13 Mesh metrics for the 20 kJ impact. Source: ***Ansys® Workbench, Release 14.5***

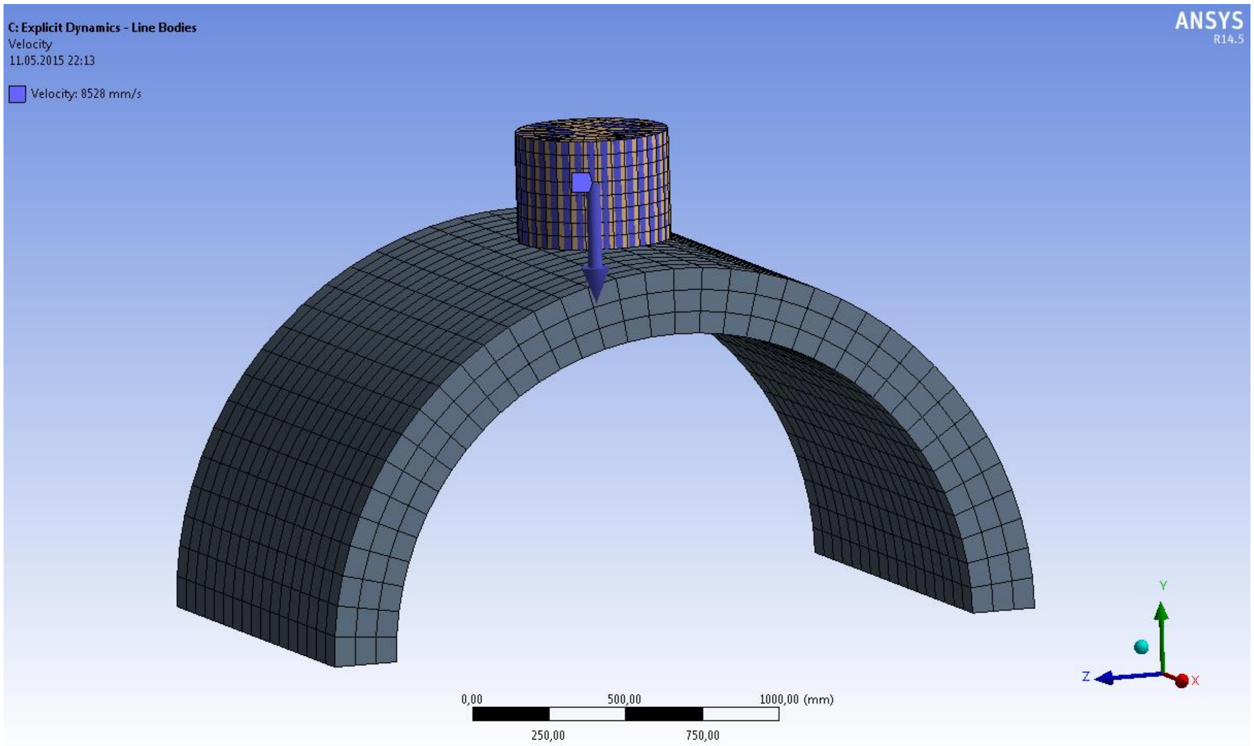

Figure B-14 Velocity of object for the 20 kJ impact. Source: ***Ansys® Workbench, Release 14.5***

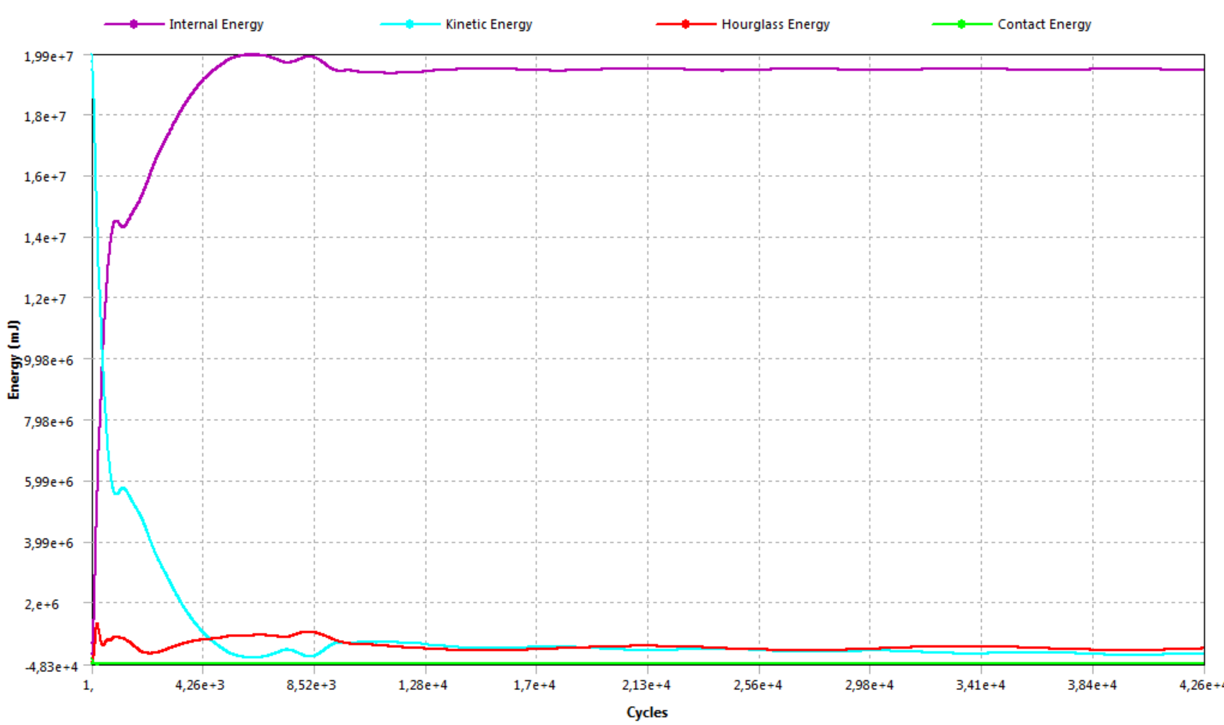

Figure B-15 Energy summary for the 20 kJ impact. Source: ***Ansys® Workbench, Release 14.5***

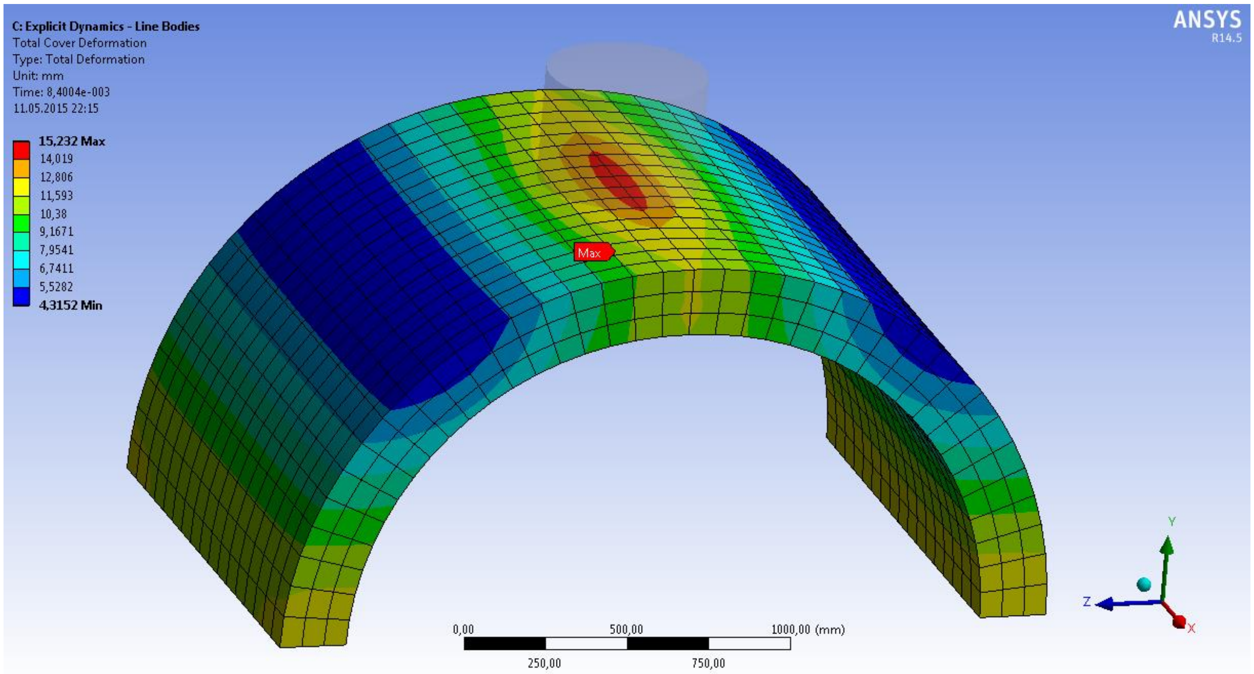

Figure B-16 Total Cover Deformation for the 20 kJ impact. Source: *Ansys® Workbench, Release 14.5*

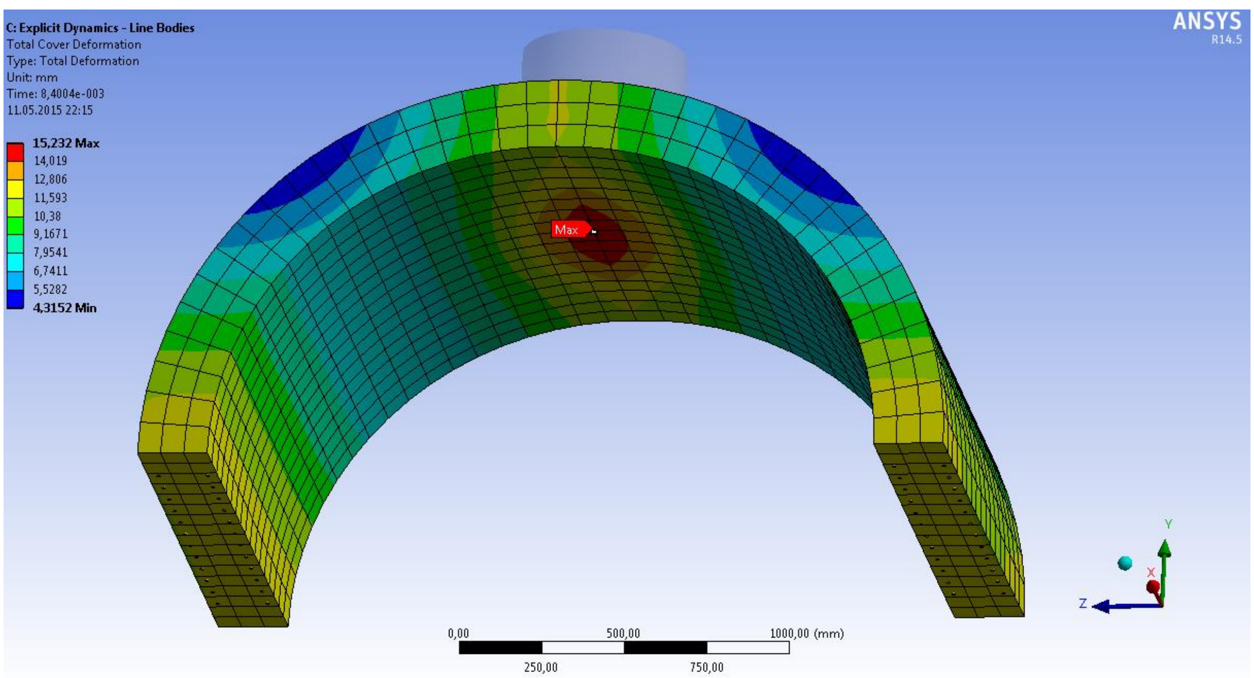

Figure B-17 Total Cover Deformation for the 20 kJ impact. Source: *Ansys® Workbench, Release 14.5*

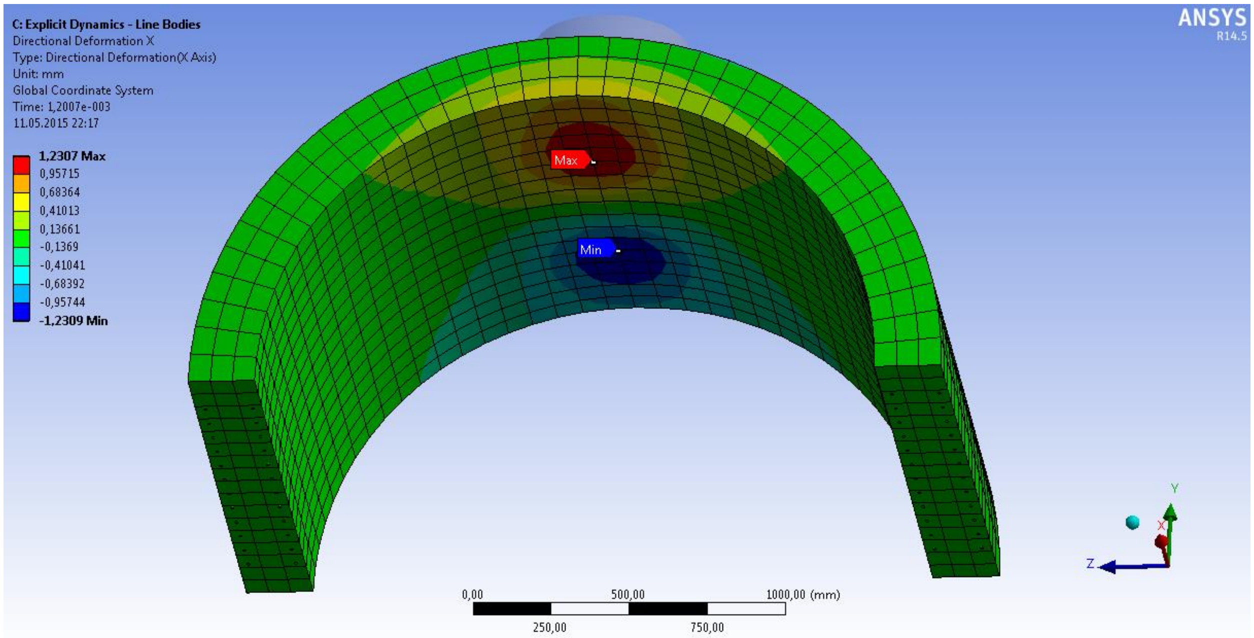

Figure B-18 Directional Deformation X for the 20 kJ impact. Source: ***Ansys® Workbench, Release 14.5***

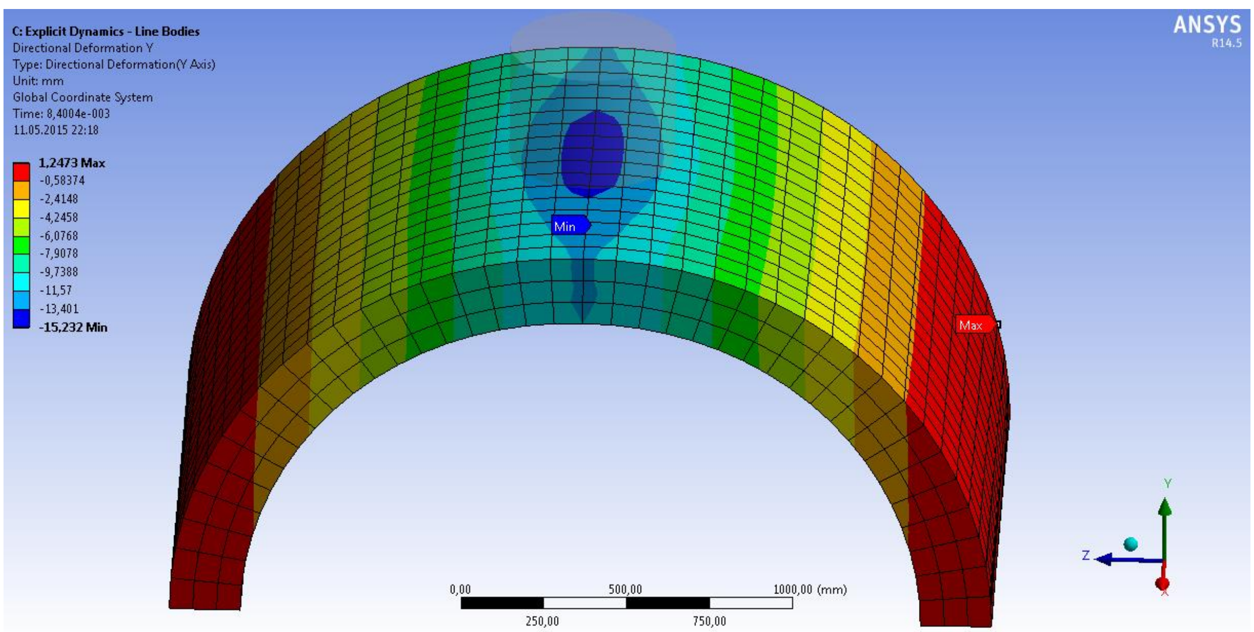

Figure B-19 Directional Deformation Y for the 20 kJ impact. Source: ***Ansys® Workbench, Release 14.5***

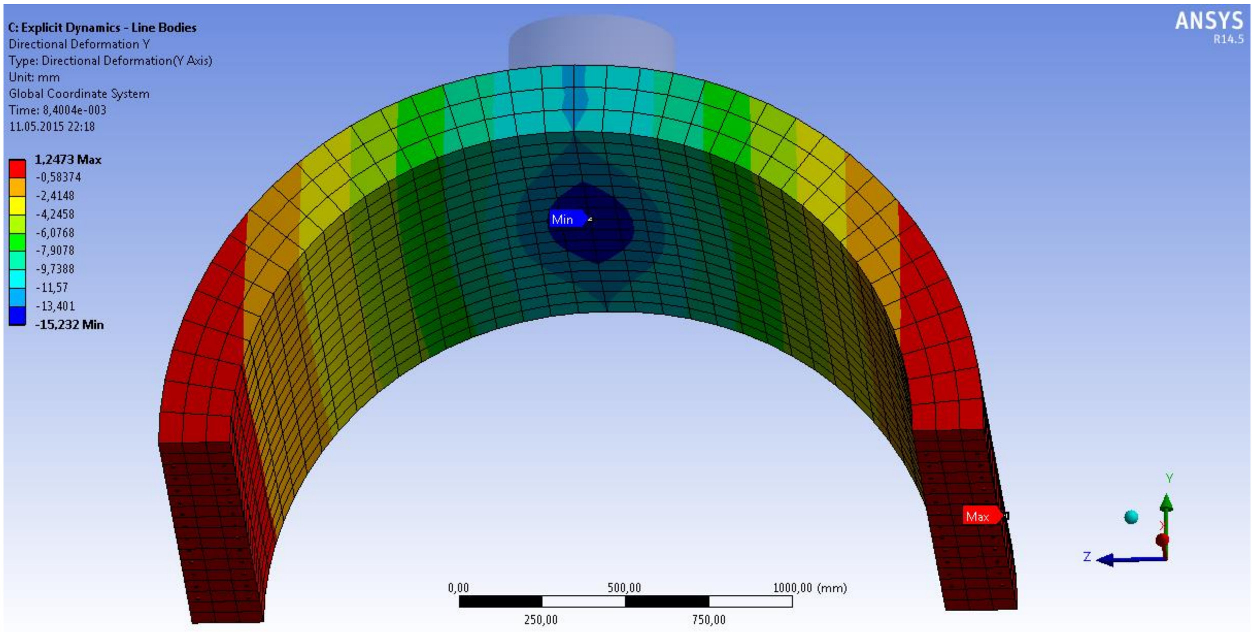

Figure B-20 Directional Deformation Y for the 20 kJ impact. Source: ***Ansys® Workbench, Release 14.5***

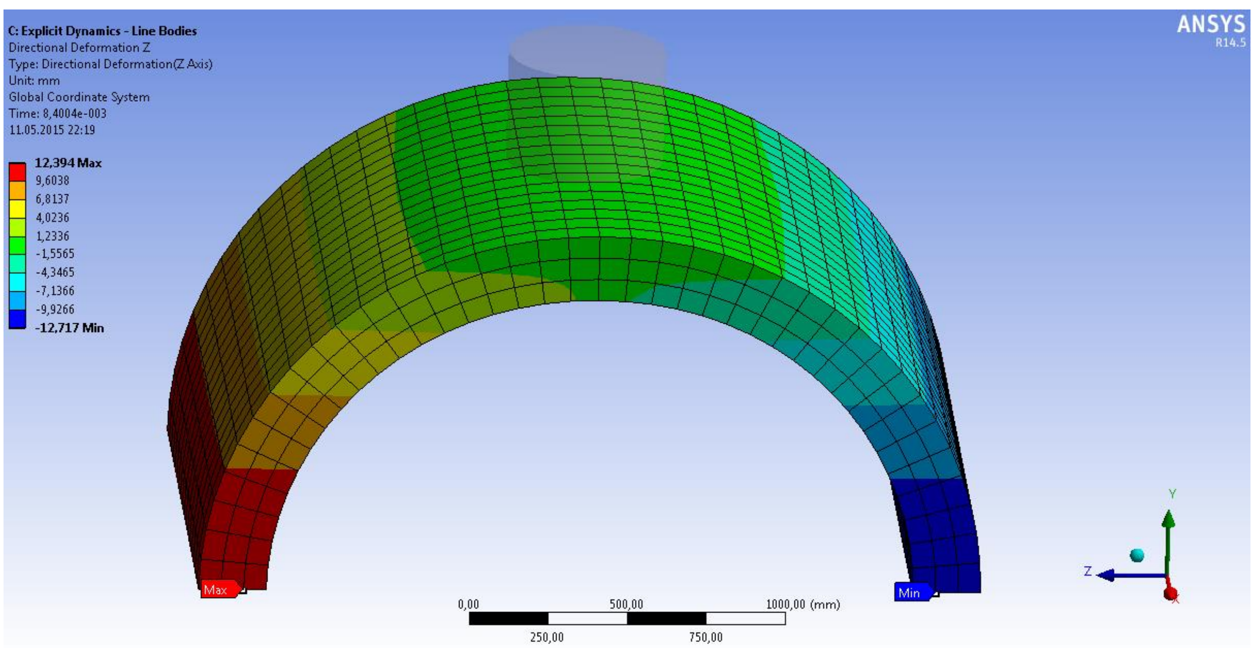

Figure B-21 Directional Deformation Z for the 20 kJ impact. Source: ***Ansys® Workbench, Release 14.5***

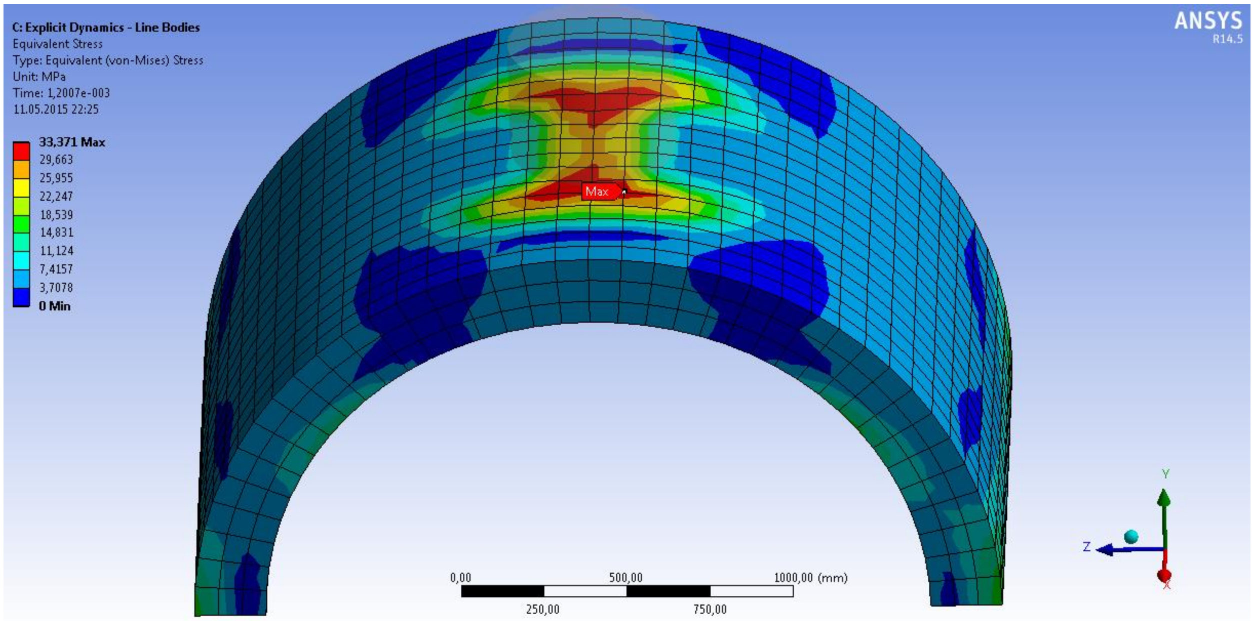

Figure B-22 Equivalent Stress for the 20 kJ impact. Source: *Ansys® Workbench, Release 14.5*

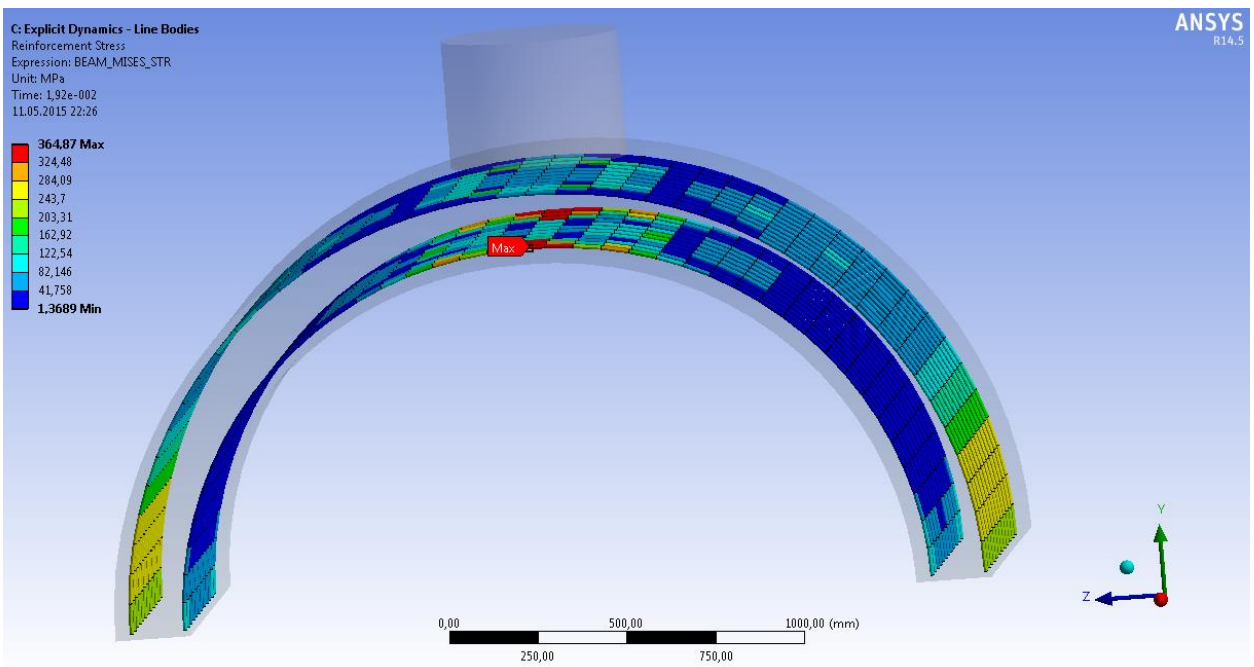

Figure B-23 Reinforcement Stress for the 20 kJ impact. Source: *Ansys® Workbench, Release 14.5*

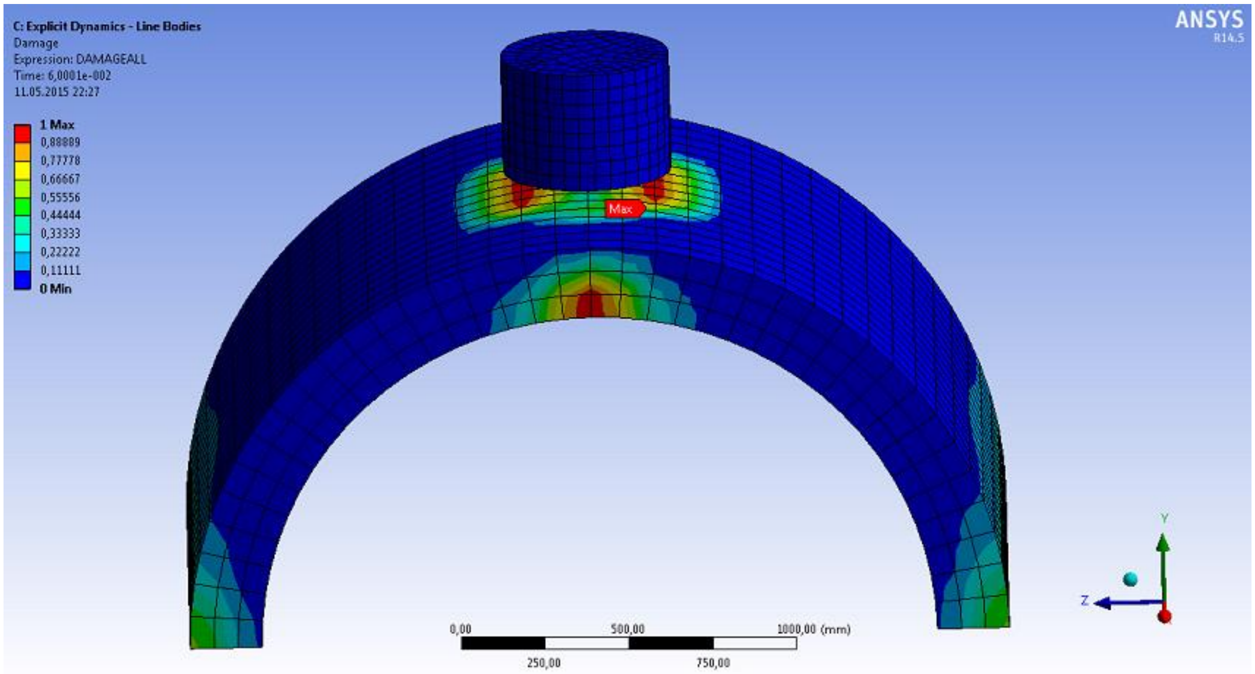

Figure B-24 Damage from the 20 kJ impact. Source: ***Ansys® Workbench, Release 14.5***

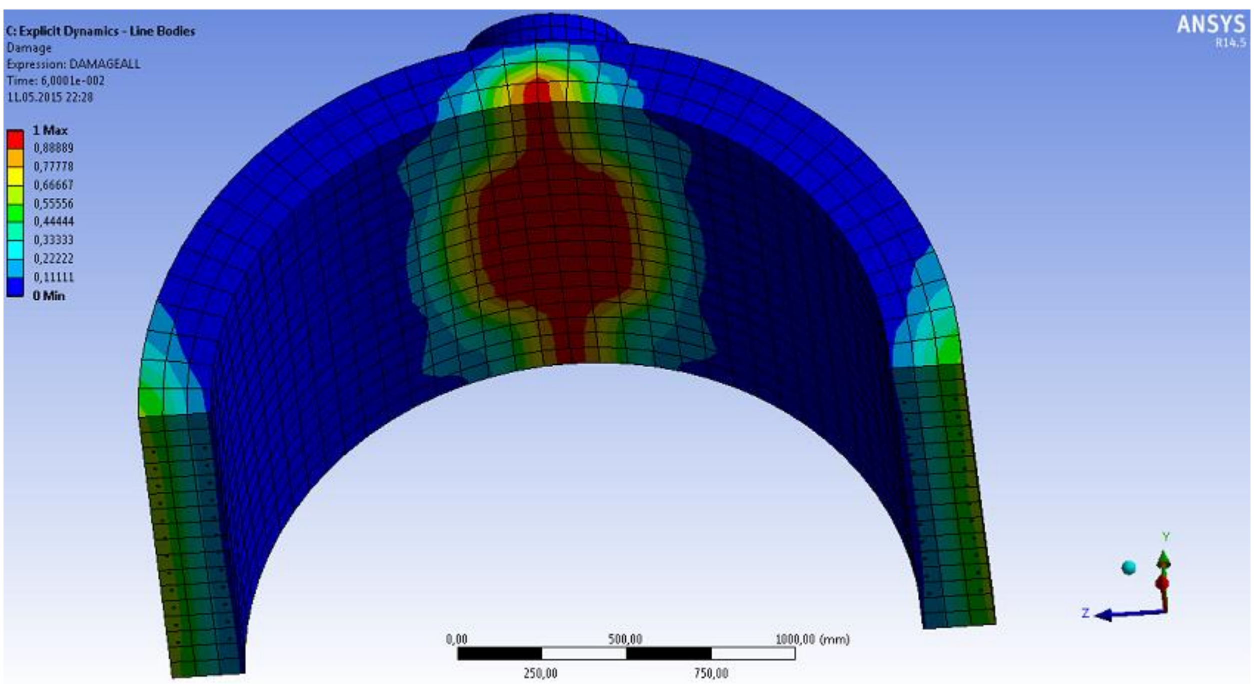

Figure B-25 Damage from the 20 kJ impact. Source: ***Ansys® Workbench, Release 14.5***

30 kJ impact:

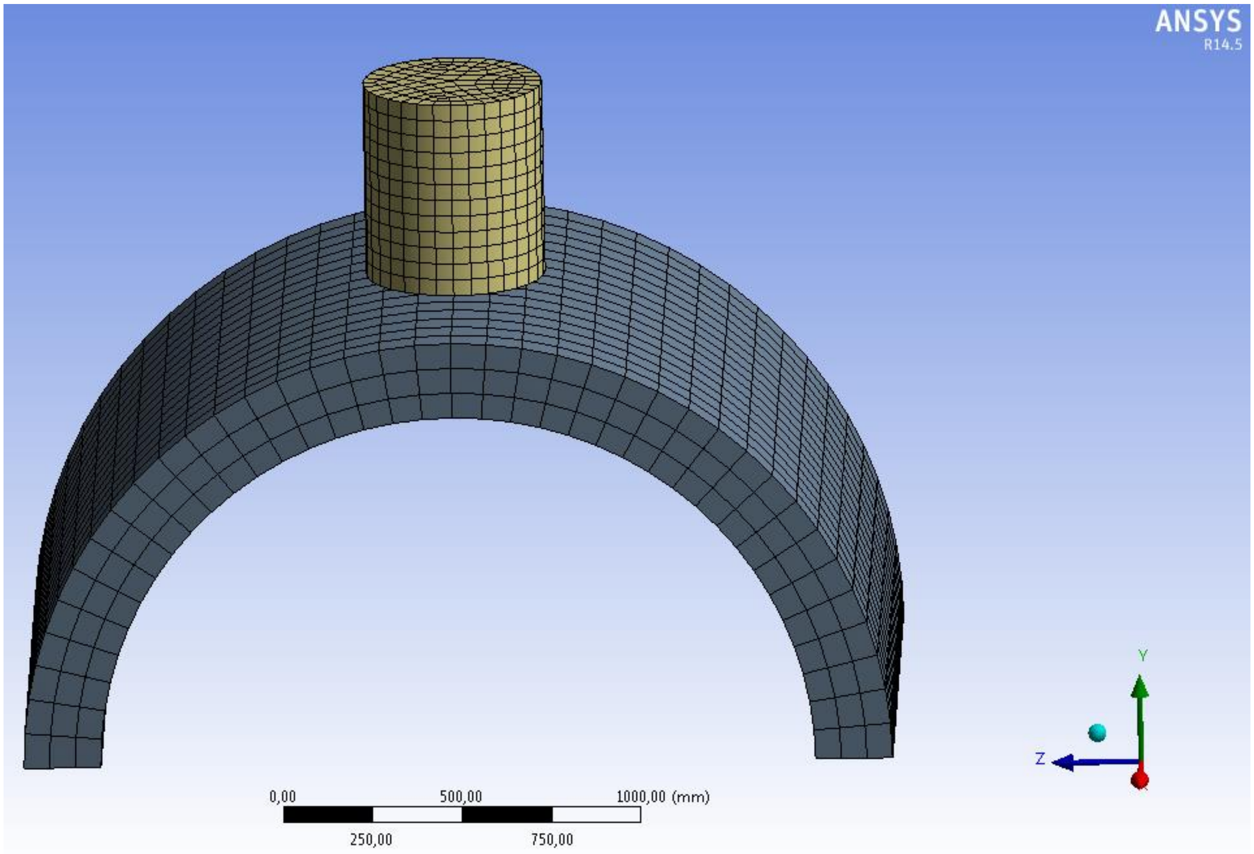

Figure B-26 Mesh of model for the 30 kJ impact. Source: ***Ansys® Workbench, Release 14.5***

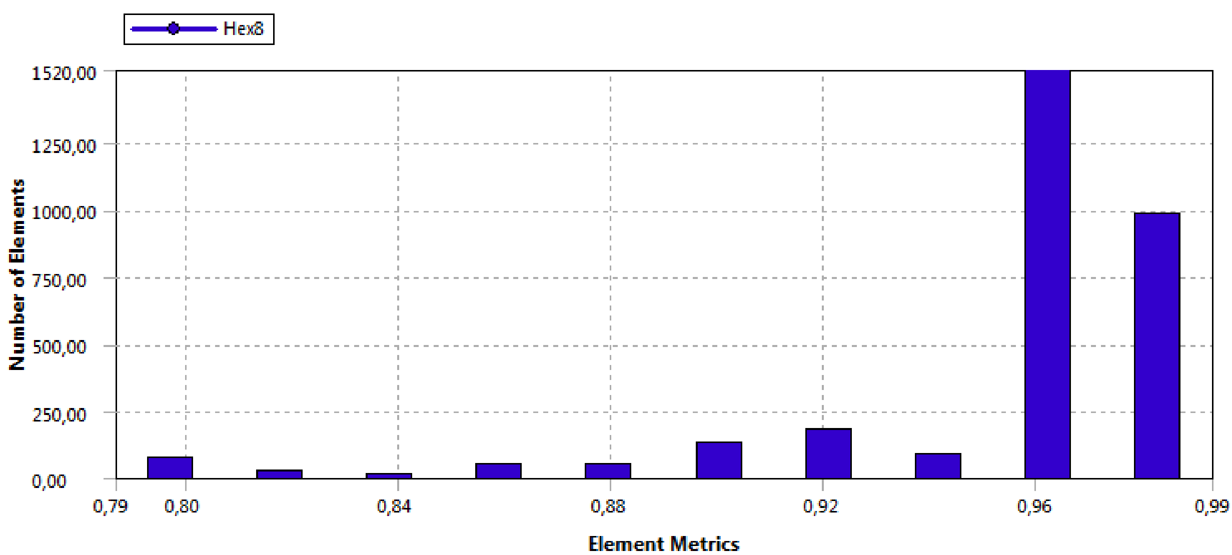

Figure B-27 Mesh metrics for the 30 kJ impact. Source: ***Ansys® Workbench, Release 14.5***

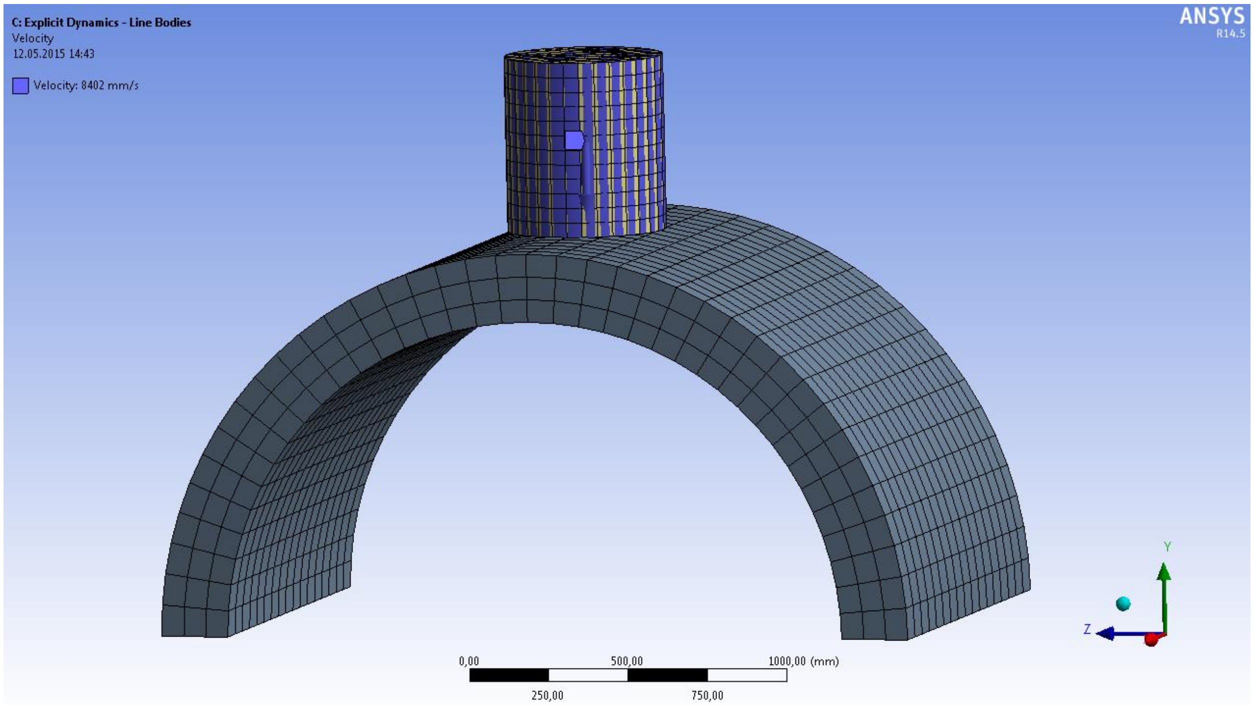

Figure B-28 Velocity of object for the 30 kJ impact. Source: *Ansys® Workbench, Release 14.5*

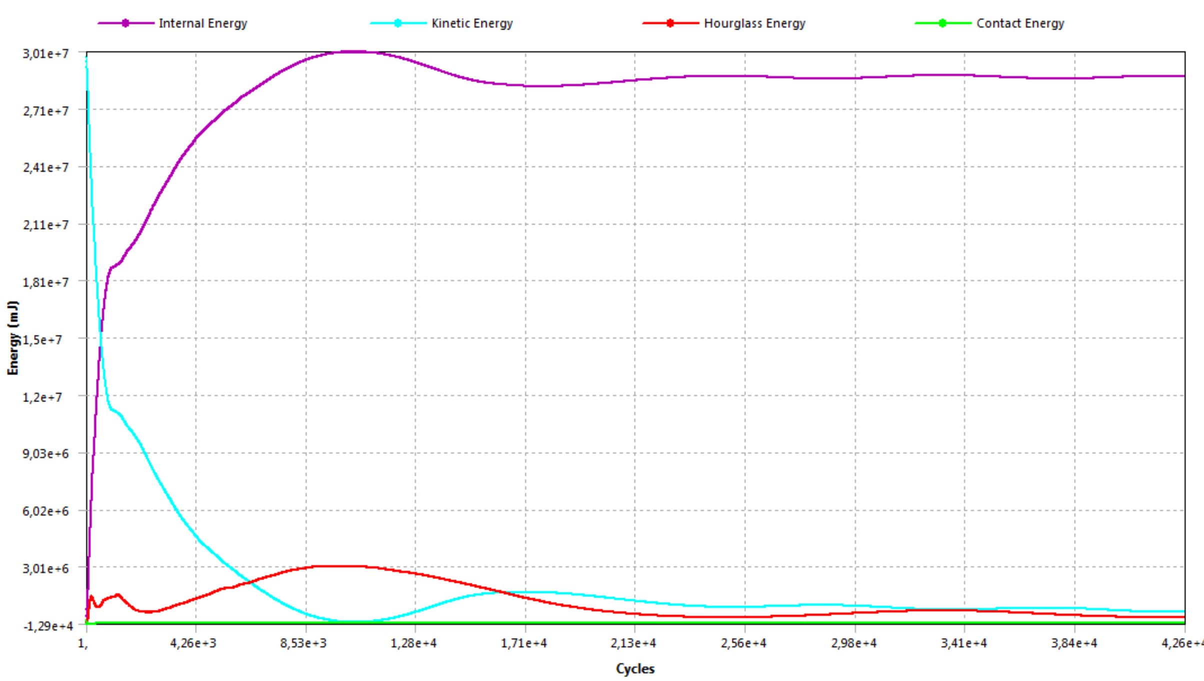

Figure B-29 Energy summary for the 30 kJ impact. Source: *Ansys® Workbench, Release 14.5*

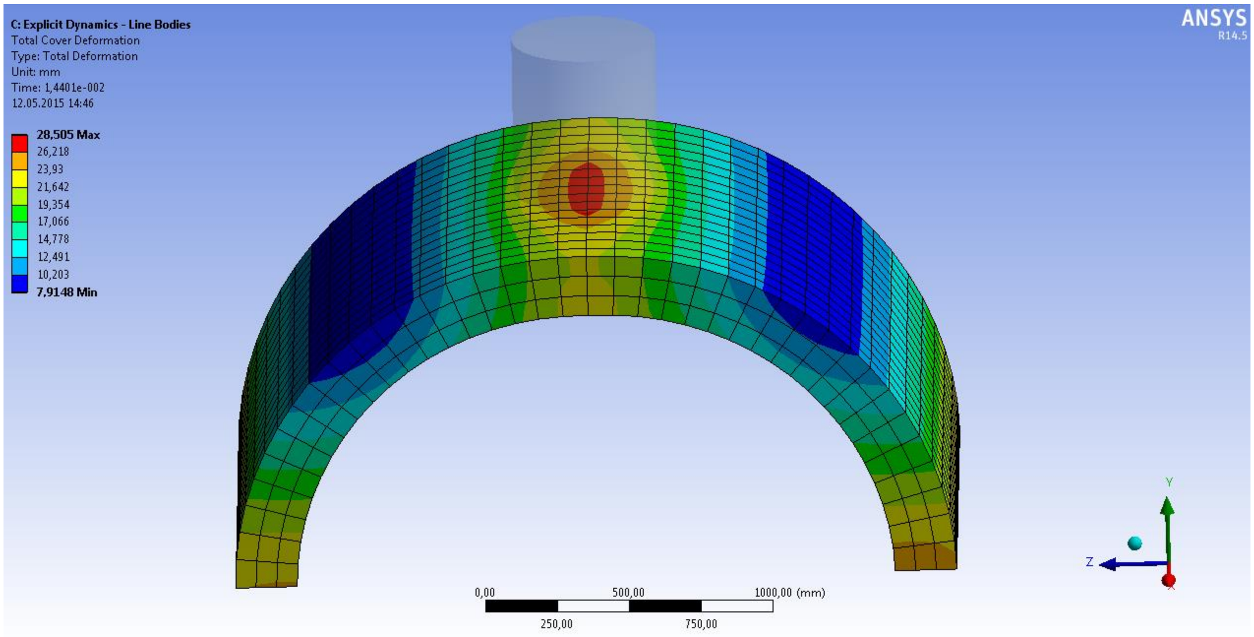

Figure B-30 Total Cover Deformation for the 30 kJ impact. Source: ***Ansys® Workbench, Release 14.5***

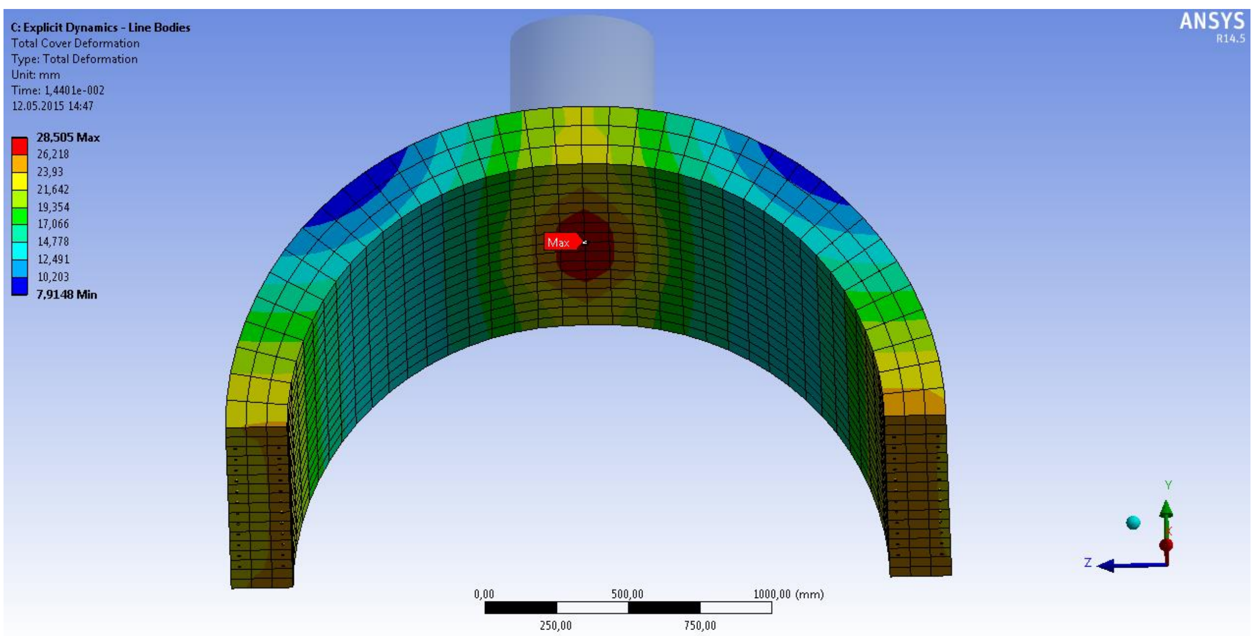

Figure B-31 Total Cover Deformation for the 30 kJ impact. Source: ***Ansys® Workbench, Release 14.5***

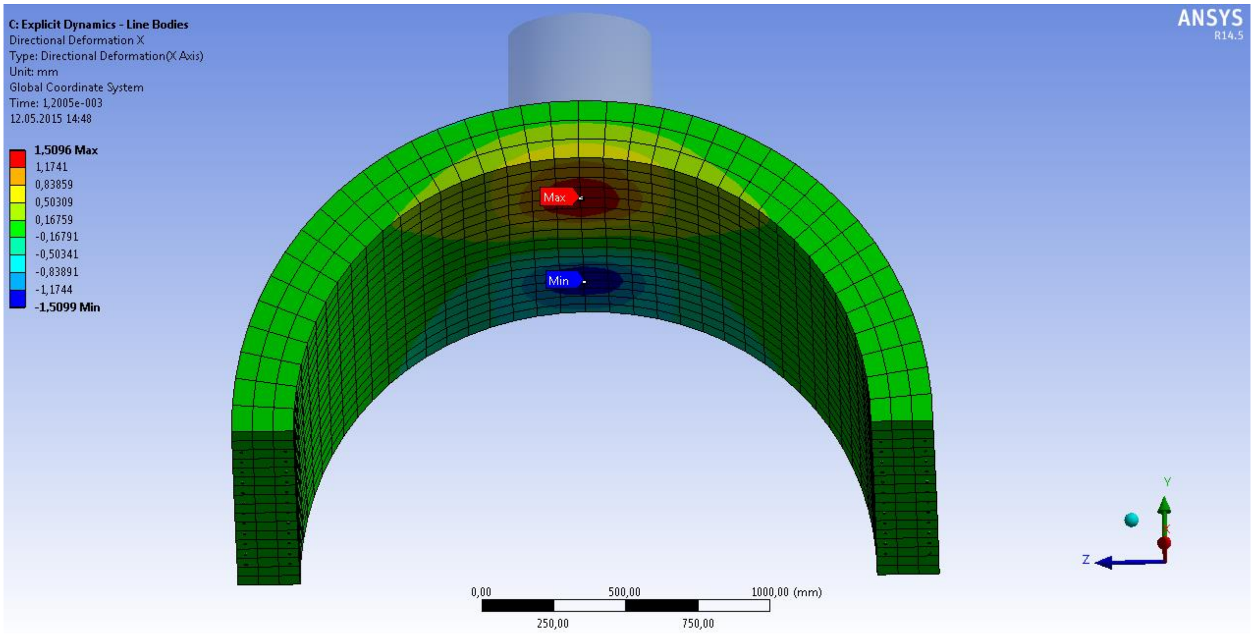

Figure B-32 Directional Deformation X for the 30 kJ impact. Source: *Ansys® Workbench, Release 14.5*

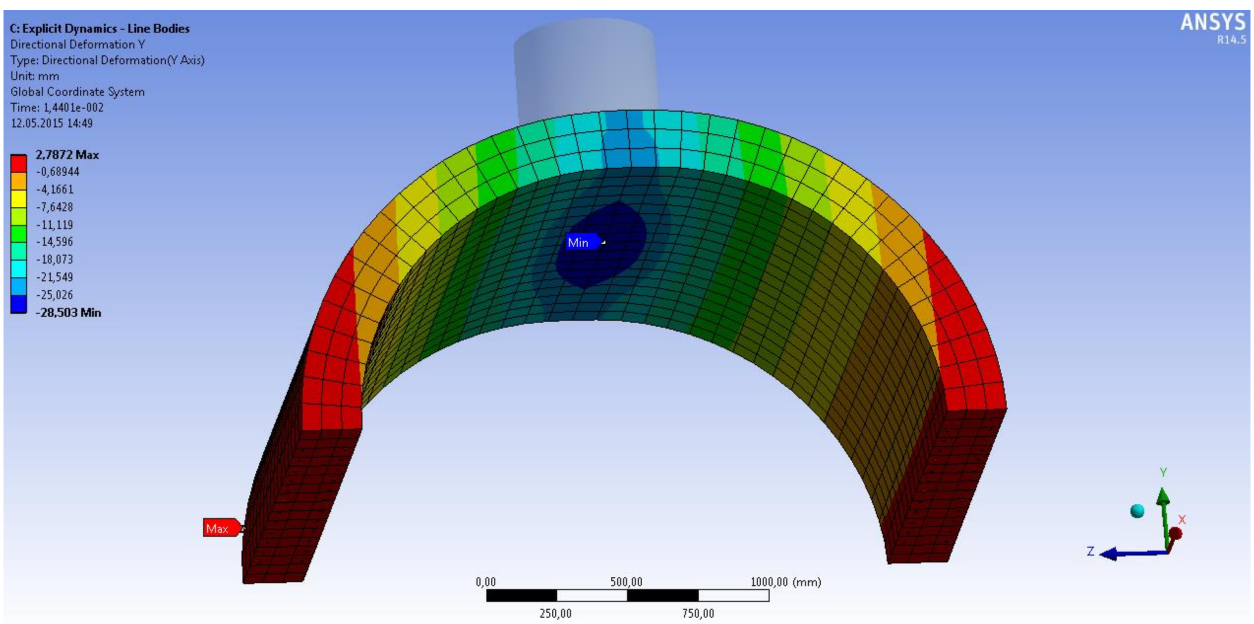

Figure B-33 Directional Deformation Y for the 30 kJ impact. Source: *Ansys® Workbench, Release 14.5*

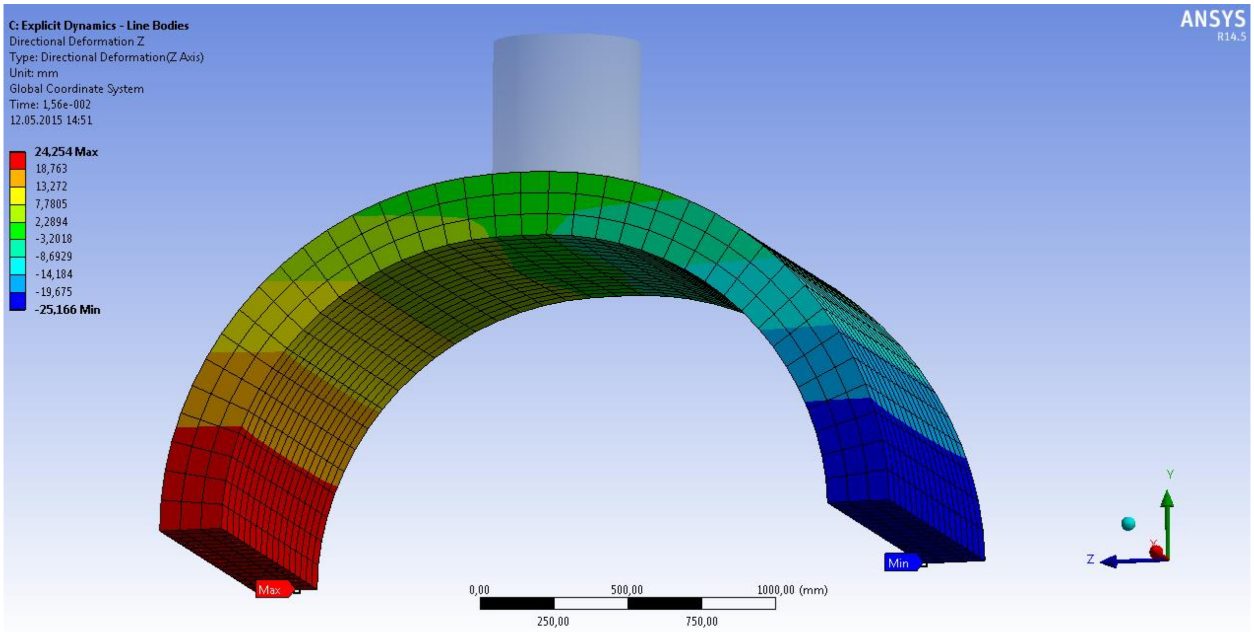

Figure B-34 Directional Deformation Z for the 30 kJ impact. Source: ***Ansys® Workbench, Release 14.5***

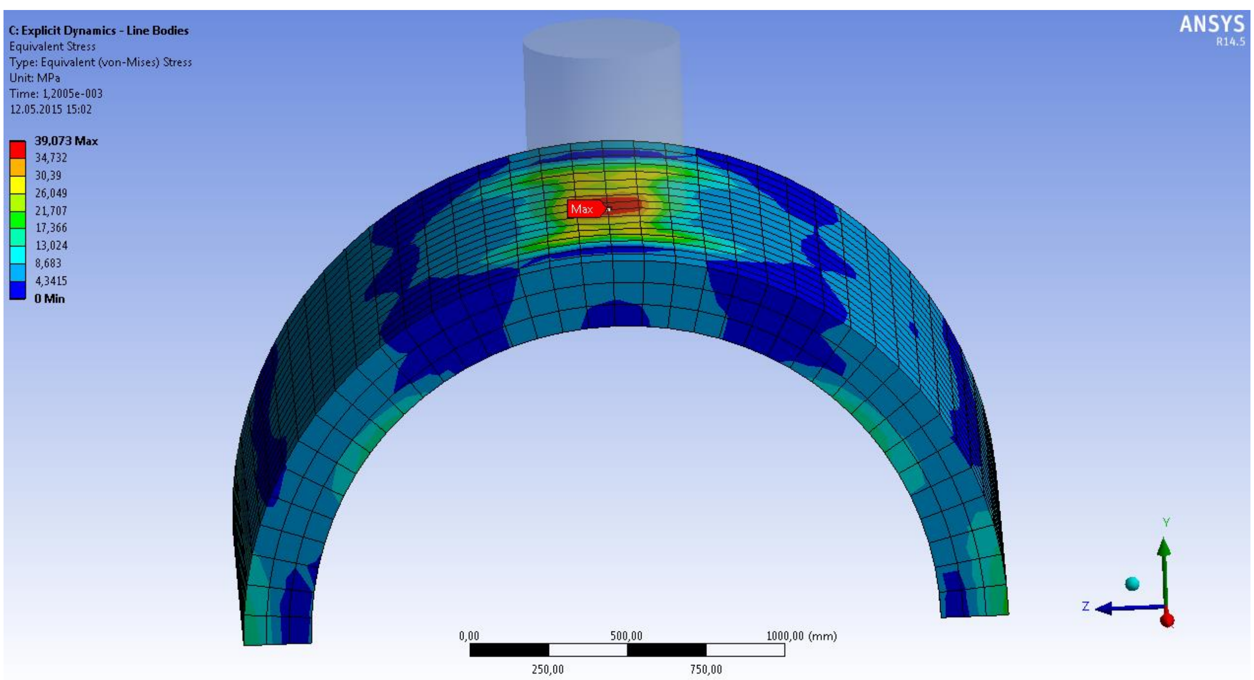

Figure B-35 Equivalent Stress for the 30 kJ impact. Source: ***Ansys® Workbench, Release 14.5***

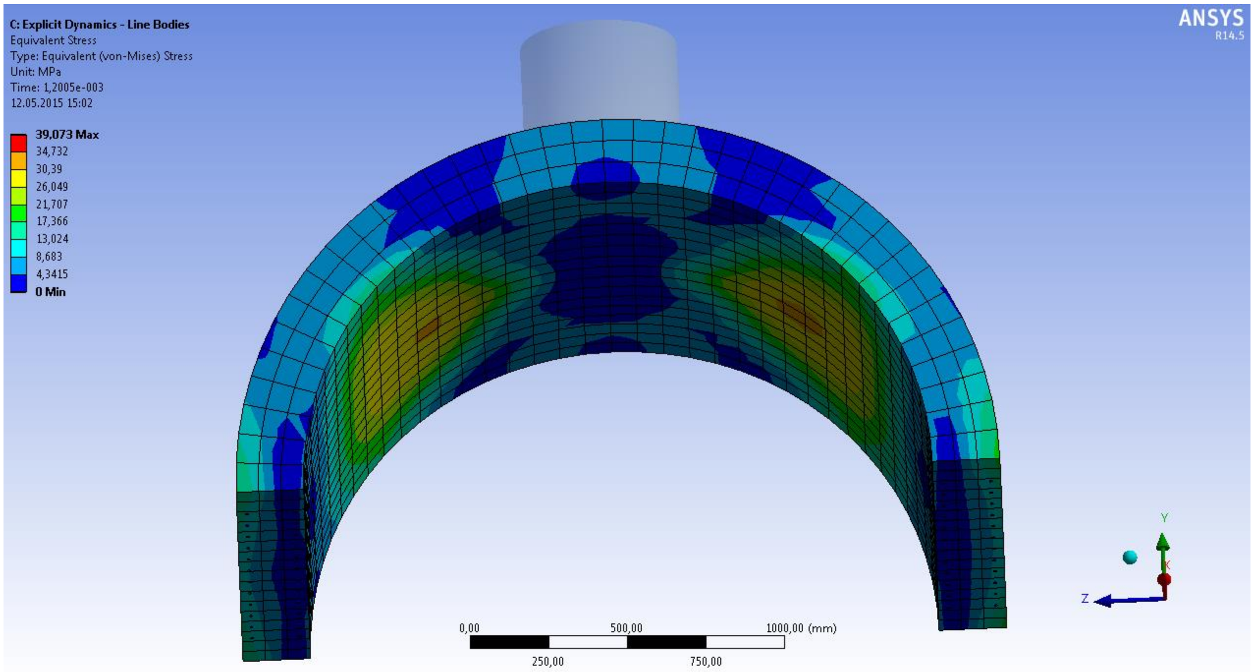

Figure B-36 Equivalent Stress for the 30 kJ impact. Source: ***Ansys® Workbench, Release 14.5***

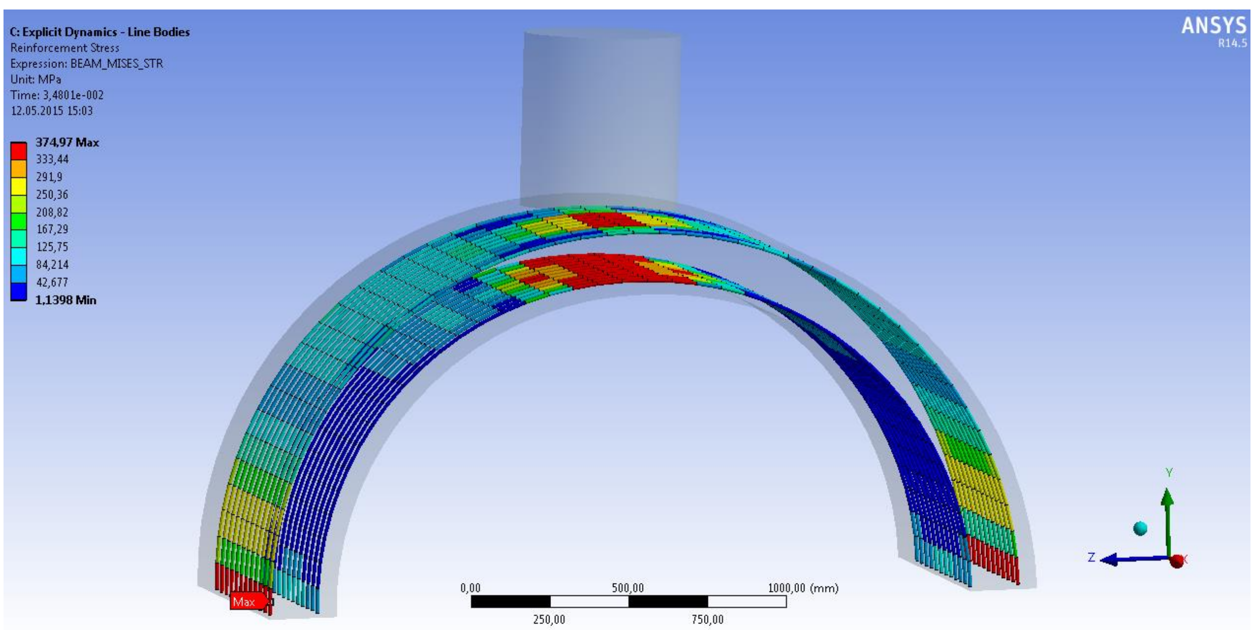

Figure B-37 Reinforcement Stress for the 30 kJ impact. Source: ***Ansys® Workbench, Release 14.5***

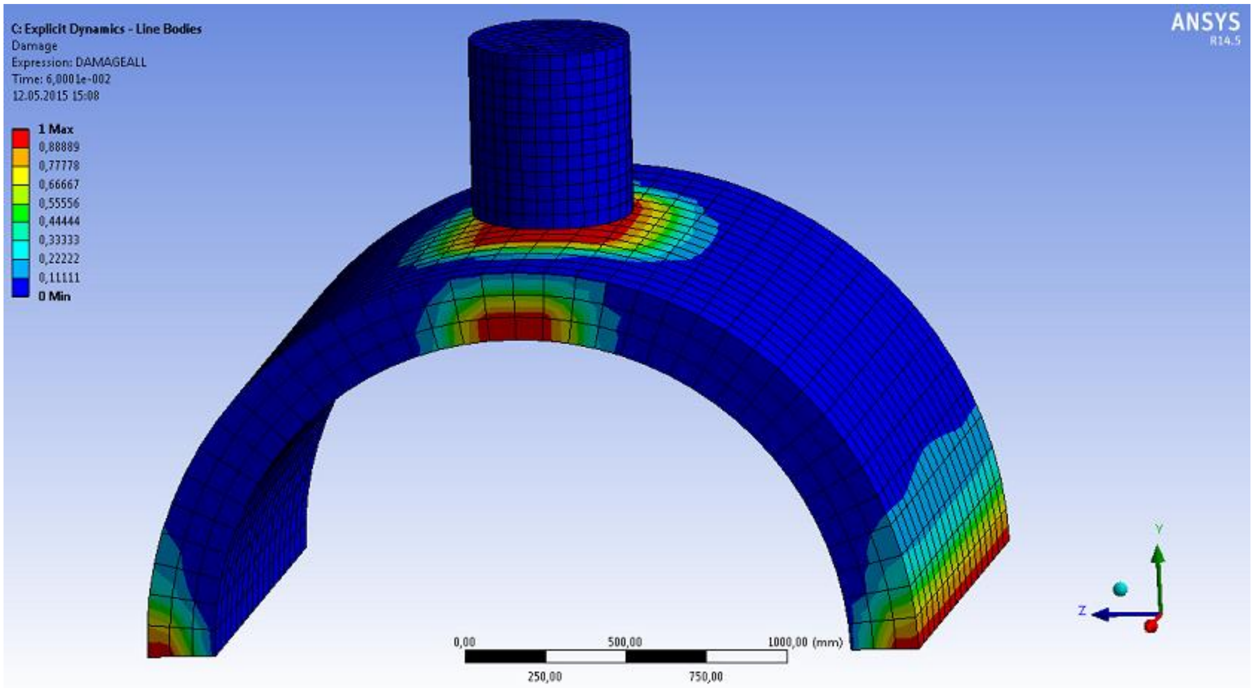

Figure B-38 Damage from the 30 kJ impact. Source: ***Ansys® Workbench, Release 14.5***

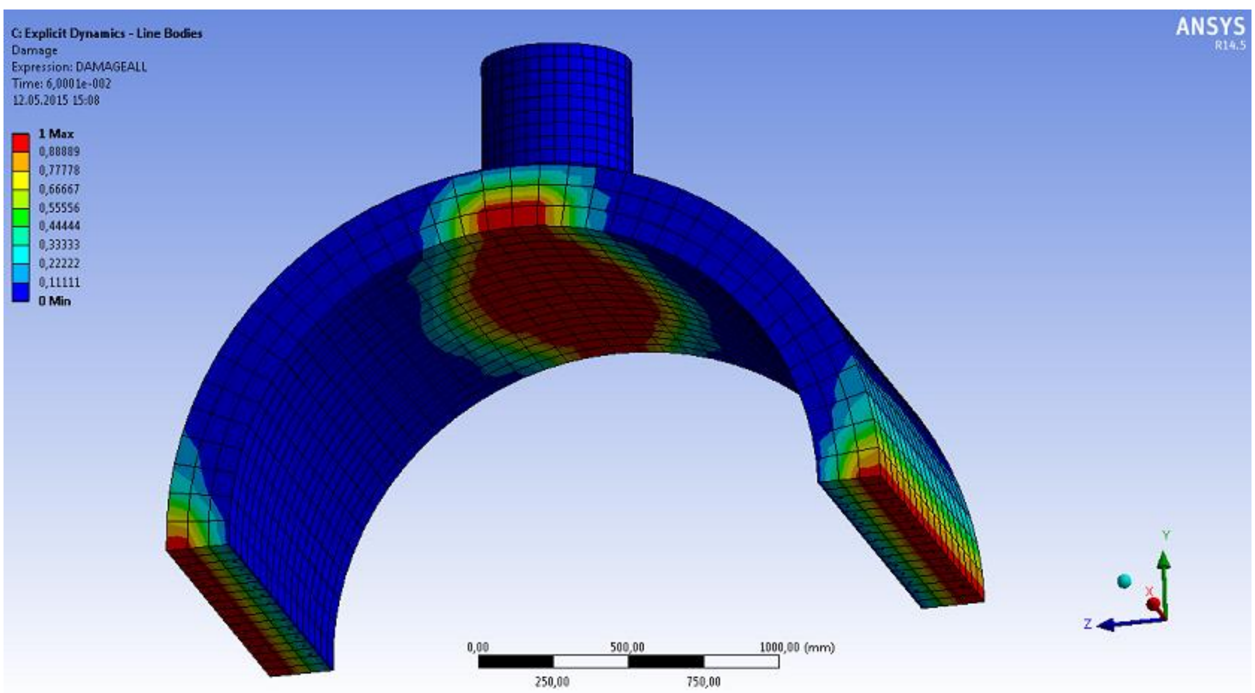

Figure B-39 Damage from the 30 kJ impact. Source: ***Ansys® Workbench, Release 14.5***

C. Stability Calculations

Stability calculations

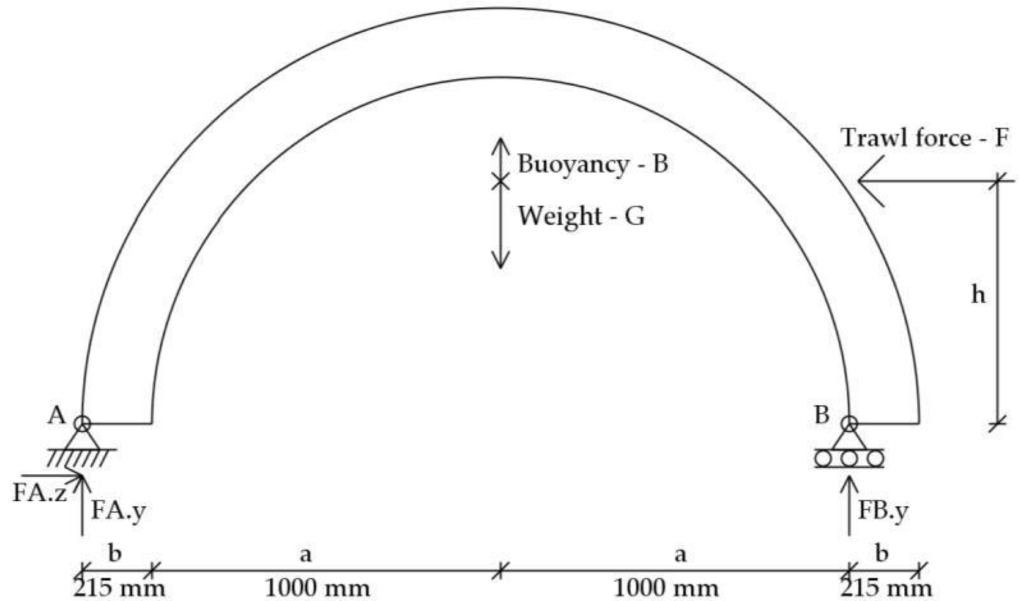

Assuming equal supporting conditions as used in *Ansys® Workbench, Release 14.5*.
Pinned support in A, and Roll support in B.

Archimedes' principle: Buoyancy = weight of displaced fluid

Density concrete $\rho_c := 2400 \frac{kg}{m^3}$

Density sea water $\rho_w := 1025 \frac{kg}{m^3}$

Resulting density of concrete $\rho := \rho_c - \rho_w = 1375 \frac{kg}{m^3}$

Trawl force $F := 300kN$

Height from ground to impact point $h := 0.50m$

Radius $a := 1000mm$

Thickness $b := 215mm$

Length in X-direction $L := 1500mm$

Volume of cover from Ansys $1.1221 \cdot 10^9 \text{mm}^3 = 1.122 \cdot \text{m}^3$

Area of cover $A := \dfrac{\pi \cdot \left[(a+b)^2 - a^2\right]}{2} = 0.748\, \text{m}^2$

Volume of cover control calculation $V := A \cdot L = 1.122 \cdot \text{m}^3$

Mass of cover $M_C := V \cdot \rho_c = 2692.989\, \text{kg}$

Effective mass of cover including buoyancy $M := V \cdot \rho = 1542.858\, \text{kg}$

Stability consideration: Sum of moment about tipping point A. Clockwise rotation positive.

$\Sigma M_A = 0$

$$G \cdot (a+b) - B \cdot (a+b) - F \cdot h - F_B \cdot (2 \cdot a + b) = 0$$

$$\rho \cdot V \cdot g \cdot (a+b) - F \cdot h - F_B \cdot (2a + b) = 0$$

Vertical reaction force FB

$$F_B := \frac{\rho \cdot V \cdot g \cdot (a+b) - F \cdot h}{(2a+b)} = -59.421 \cdot \text{kN}$$

$$F_B = -6.059 \cdot \text{tonne} \cdot g$$

The reaction force FB is negative, which means that it is in reality pointing downwards to counteract the tipping moment from the trawl force. This means that the weight of the cover is too low, and that it is unstable when applying the 300 kN trawl force to the cover when it is 1,5 m long.

As can be seen from the calculations above, an additional 6.0 tonne is required to keep the cover stable with its current supporting conditions.

The further up the Trawl force impacts, the more additional weight will be needed to keep the cover stable.

This downwards force will result in forced stresses in the supporting point B, due to the need to force the cover down to keep it stable. In a real situation, the cover will need to be heavy enough to be stable on its own even when impacted by the trawl load.

In order to make the covers overtrawlable, one suggestion is to shape the covers including "trawl deflectors" with an angle of maximum 58°. This effectively adds weight to the cover, changes the tipping point to A1 and positively increases the moment arms.

Lengths, volumes and masses of the deflectors are found from the model in Ansys® Workbench, Release 14.5, where the deflectors were modeled for this purpose. The pinned support is moved, while the roll support is kept at its original location.

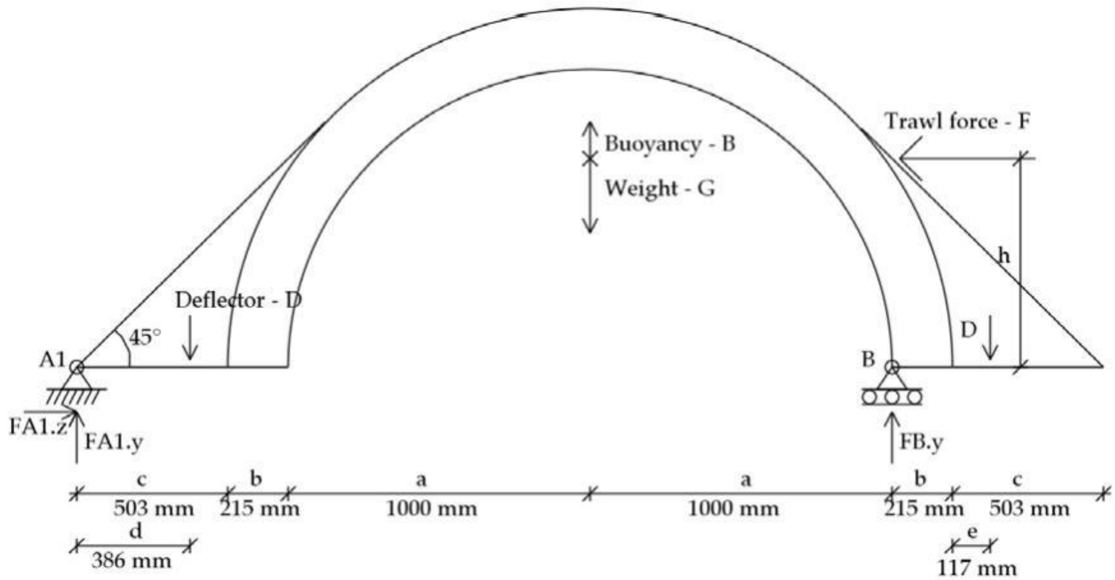

By assuming deflectors with an angle of 45°, the following data is found from the model in *Ansys® Workbench, Release 14.5*

Volume of one deflector $V_D := 2.376 \cdot 10^8 mm^3 = 0.238 \cdot m^3$

Area of one deflector $A_D := \dfrac{V_D}{L} = 0.158\,m^2$

Mass of one deflector $M_D := V_D \cdot \rho_c = 570.24\,kg$

Effective mass of one deflector including buoyancy $M_D := V_D \cdot \rho = 326.7\,kg$

Length of the deflector $c := 503mm$

According to the 3D model, the mass center of the deflector is at Z-coordinate 1332 mm

Attack point of weight of right deflector $e := 1332mm - (a + b) = 117 \cdot mm$

Attack point of weight of left deflector $d := c - e = 386 \cdot mm$

Total mass of cover $$M_T := \left(V + 2V_D\right)\cdot\rho_c = 3833.469\,\text{kg}$$

Effective total mass of cover including buoyancy $$M_T := \left(V + 2V_D\right)\cdot\rho = 2196.258\,\text{kg}$$

Stability consideration: Sum of moment about tipping point A1. Clockwise rotation positive.

$$\Sigma M_{A1} = 0$$

$$G_D\cdot d + G\cdot(a + b + c) - B\cdot(a + b + c) - F\cdot h - F_B\cdot(2\cdot a + b + c) + G_D\cdot(2a + 2b + c + e) = 0$$

$$\rho\cdot V_D\cdot g\cdot d + \rho\cdot V\cdot g\cdot(a + b + c) - F\cdot h - F_B\cdot(2\cdot a + b + c) + \rho\cdot V_D\cdot g\cdot(2a + 2\cdot b + c + e) = 0$$

Vertical reaction force FB

$$F_B := \frac{\rho\cdot V_D\cdot g\cdot d + \rho\cdot V\cdot g\cdot(a + b + c) - F\cdot h + \rho\cdot V_D\cdot g\cdot(2a + 2\cdot b + c + e)}{(2\cdot a + b + c)} = -41.574\cdot\text{kN}$$

$$F_B = -4.239\cdot\text{tonne}\cdot g$$

The reaction force FB is still negative, which means that it is in reality pointing downwards to counteract the tipping moment from the trawl force. This means that the weight of the cover is too low, and that it is unstable when applying the 300 kN trawl force to the cover when it is 1,5 m long, even after moving the tipping point to the outer point of the deflector and increasing the mass.

As can be seen from the calculations above, an additional 4.2 tonne is required to keep the cover stable with its current supporting conditions.

The further up the Trawl force impacts, the more additional weight will be needed to keep the cover stable.

In a real situation, the cover will need to be longer in the X-direction. The normal length for GRP covers are in the area of 5 m to 8 m, depending on several factors. This cover is only 1.5 m long, and it was decided to use this dimension in order to gain coherence between the covers supplied by Multiblokk AS for the drop test and the modeled cover in Ansys® Workbench, Release 14.5.

New length $L := 6500\text{mm}$

New volume of cover $V := A \cdot L = 4.862 \cdot \text{m}^3$

New volume of cover $V_D := A_D \cdot L = 1.03 \cdot \text{m}^3$

New total mass of cover $M_T := \left(V + 2V_D\right) \cdot \rho_c = 16611.699\,\text{kg}$

New effective total mass of cover including buoyancy $M_T := \left(V + 2V_D\right) \cdot \rho = 9517.119\,\text{kg}$

Stability consideration: Sum of moment about tipping point A1. Clockwise rotation positive.

$$\Sigma M_{A1} = 0$$

$$G_D \cdot d + G \cdot (a + b + c) - B \cdot (a + b + c) - F \cdot h - F_B \cdot (2 \cdot a + b + c) + G_D \cdot (2a + 2b + c + e) = 0$$

$$\rho \cdot V_D \cdot g \cdot d + \rho \cdot V \cdot g \cdot (a + b + c) - F \cdot h - F_B \cdot (2 \cdot a + b + c) + \rho \cdot V_D \cdot g \cdot (2a + 2 \cdot b + c + e) = 0$$

Vertical reaction force FB

$$F_B := \frac{\rho \cdot V_D \cdot g \cdot d + \rho \cdot V \cdot g \cdot (a + b + c) - F \cdot h + \rho \cdot V_D \cdot g \cdot (2a + 2 \cdot b + c + e)}{(2 \cdot a + b + c)} = 3.805 \cdot \text{kN}$$

$$F_B = 0.388 \cdot \text{tonne} \cdot g$$

The reaction force FB is now positive, which means that the when the cover weighs enough (16.6 tonne in the air in the case of h = 0.5 m), to be stable on its own without tipping over due to the trawl force. For GRP covers, this weight can be considerable less due to rockdumping. One of the premises of the thesis is however to study the possibility of using concrete covers without rock dumping.

The same stability considerations will need to be taken in regards to wave and current forces, but this is outside the scope of this thesis.

D. Impact Calculations

Dropped object - Impact calculations

$kJ := 1000 \cdot J$ $\qquad g = 9.807 \dfrac{m}{s^2}$

Equations:

Potential energy: $E_p = m \cdot g \cdot h$ Kinetic energy: $E_k = \dfrac{1}{2} m \cdot v^2$

The Kinematic Equations of free fall:

$$v_f = v_i + g \cdot t \qquad v_f^2 = v_i^2 + 2 \cdot a \cdot d$$

$$d = \frac{v_i + v_f}{2} \cdot t \qquad d = v_i \cdot t + \frac{1}{2} \cdot g \cdot t^2$$

d = displacement
t = time
a = acceleration
v.i = initial velocity
v.f = final velocity

Weight needed for NORSOK standard U-001 requirements:

Impact energy 5 kJ, Object diameter 100mm

Wanted impact energy: $E_1 := 5kJ$

Mass of dropped object: $M_1 := 140kg$

Needed drop height: $h_1 := \dfrac{E_1}{M_1 \cdot g} = 3.642\,m$

Resulting potential energy: $E_{p1} := M_1 \cdot g \cdot h_1 = 5 \cdot kJ$

Inital and wanted terminal velocity: $v_i := 0 \dfrac{m}{s}$ $\qquad v_t := 6 \dfrac{m}{s}$

Time to reach terminal vel. 6m/s: $t_t := \dfrac{v_t}{g} = 0.612\,s$ from height $h_t := \dfrac{1}{2} \cdot g \cdot t_t^2 = 1.835\,m$

Time to impact from drop height: $t_{i1} := \sqrt{\dfrac{h_1 \cdot 2}{g}} = 0.862\,s$

Impact velocity from drop height: $v_{i1} := t_{i1} \cdot g = 8.452 \dfrac{m}{s}$ Slightly over terminal velocity in water

---

Kinetic impact energy control - for Ansys Workbench simulations:

$E_{k1} := \dfrac{1}{2} \cdot M_1 \cdot v_{i1}^2 = 5 \cdot kJ$ will use: $M_1 = 140\,kg$ $\quad v_{i1} = 8.452 \dfrac{m}{s}$

Impact energy 20 kJ, Object diameter 500mm

Wanted impact energy: $E_2 := 20\text{kJ}$

Mass of dropped object: $M_2 := 550\text{kg}$

Needed drop height: $h_2 := \dfrac{E_2}{M_2 \cdot g} = 3.708\ \text{m}$

Resulting potential energy: $E_{p2} := M_2 \cdot g \cdot h_2 = 20 \cdot \text{kJ}$

Inital and wanted terminal velocity: $v_i := 0\dfrac{m}{s}$ $\quad v_t := 6\dfrac{m}{s}$

Time to reach terminal vel. 6m/s: $t_t := \dfrac{v_t}{g} = 0.612\ \text{s}$ from height $h_t := \dfrac{1}{2} \cdot g \cdot t_t^{\,2} = 1.835\ \text{m}$

Time to impact from drop height: $t_{i2} := \sqrt{\dfrac{h_2 \cdot 2}{g}} = 0.87\ \text{s}$

Impact velocity from drop height: $v_{i2} := t_{i2} \cdot g = 8.528\ \dfrac{m}{s}$ Slightly over terminal velocity in water

---

Kinetic impact energy control - for Ansys Workbench simulations:

$E_{k2} := \dfrac{1}{2} \cdot M_2 \cdot v_{i2}^{\,2} = 20 \cdot \text{kJ}$ will use: $M_2 = 550\ \text{kg}$

$v_{i2} = 8.528\ \dfrac{m}{s}$

Impact energy 30 kJ, Object diameter 500mm

New trawl requirement in NORSOK U-001

Wanted impact energy: $E_3 := 30\text{kJ}$

Mass of dropped object: $M_3 := 850\text{kg}$

Needed drop height: $h_3 := \dfrac{E_3}{M_3 \cdot g} = 3.599\,\text{m}$

Resulting potential energy: $E_{p3} := M_3 \cdot g \cdot h_3 = 30 \cdot \text{kJ}$

Inital and wanted terminal velocity: $v_i := 0\,\dfrac{\text{m}}{\text{s}}$ $\quad v_t := 6\,\dfrac{\text{m}}{\text{s}}$

Time to reach terminal vel. 6m/s: $t_t := \dfrac{v_t}{g} = 0.612\,\text{s}$ from height $h_t := \dfrac{1}{2} \cdot g \cdot t_t^{\,2} = 1.835\,\text{m}$

Time to impact from drop height: $t_{i3} := \sqrt{\dfrac{h_3 \cdot 2}{g}} = 0.857\,\text{s}$

Impact velocity from drop height: $v_{i3} := t_{i3} \cdot g = 8.402\,\dfrac{\text{m}}{\text{s}}$ Slightly over terminal velocity in water

** Note that 8.4 m/s is a conservative value for this case because this impact energy is due to impact from trawling activities, where typical velocities are in the area of 3 to 4 m/s.*

Kinetic impact energy control - for Ansys Workbench simulations:

$E_{k3} := \dfrac{1}{2} \cdot M_3 \cdot v_{i3}^{\,2} = 30 \cdot \text{kJ}$ will use: $M_3 = 850\,\text{kg}$ $\quad v_{i3} = 8.402\,\dfrac{\text{m}}{\text{s}}$

Impact energy 50 kJ, Object diameter 700mm

Wanted impact energy: $E_4 := 50\text{kJ}$

Mass of dropped object: $M_4 := 1400\text{kg}$

Needed drop height: $h_4 := \dfrac{E_4}{M_4 \cdot g} = 3.642\,\text{m}$

Resulting potential energy: $E_{p4} := M_4 \cdot g \cdot h_4 = 50 \cdot \text{kJ}$

Inital and wanted terminal velocity: $v_i := 0\,\dfrac{m}{s}$ $\qquad v_t := 6\,\dfrac{m}{s}$

Time to reach terminal vel. 6m/s: $t_t := \dfrac{v_t}{g} = 0.612\,\text{s}$ from height $h_t := \dfrac{1}{2} \cdot g \cdot t_t^{\,2} = 1.835\,\text{m}$

Time to impact from drop height: $t_{i4} := \sqrt{\dfrac{h_4 \cdot 2}{g}} = 0.862\,\text{s}$

Impact velocity from drop height: $v_{i4} := t_{i4} \cdot g = 8.452\,\dfrac{m}{s}$ Slightly over terminal velocity in water

---

Kinetic impact energy control - for Ansys Workbench simulations:

$E_{k4} := \dfrac{1}{2} \cdot M_4 \cdot v_{i4}^{\,2} = 50 \cdot \text{kJ}$ will use: $M_4 = 1400\,\text{kg}$ $\quad v_{i4} = 8.452\,\dfrac{m}{s}$

Impact velocities from actual drop heights:

Impact energy	Measured mass:	Calculated drop height:	Theoretical impact velocity:
Multiblokk:			
$E := 50kJ$	$M := 1350kg$	$h := \frac{E}{M \cdot g} = 3.777\,m$	$v := \sqrt{\frac{h \cdot 2}{g}} \cdot g = 8.607\,\frac{m}{s}$
UiS:			
$E := 5kJ$	$M := 171.6kg$	$h := \frac{E}{M \cdot g} = 2.971\,m$	$v := \sqrt{\frac{h \cdot 2}{g}} \cdot g = 7.634\,\frac{m}{s}$
$E := 20kJ$	$M := 576.6kg$	$h := \frac{E}{M \cdot g} = 3.537\,m$	$v := \sqrt{\frac{h \cdot 2}{g}} \cdot g = 8.329\,\frac{m}{s}$
$E := 30kJ$	$M := 883.3kg$	$h := \frac{E}{M \cdot g} = 3.463\,m$	$v := \sqrt{\frac{h \cdot 2}{g}} \cdot g = 8.242\,\frac{m}{s}$
$E := 50kJ$	$M := 1279.5kg$	$h := \frac{E}{M \cdot g} = 3.985\,m$	$v := \sqrt{\frac{h \cdot 2}{g}} \cdot g = 8.841\,\frac{m}{s}$

Impact object size calculations - pure concrete column:

Density concrete $\rho_c := 2400\,\dfrac{kg}{m^3}$

Mass	**Diameter**	**Area**	**Needed object height**
$m_1 := 140kg$	$d_1 := 100mm$	$A_1 := \pi \cdot \left(\dfrac{d_1}{2}\right)^2 = 7854.0 \cdot mm^2$	$h_{o1} := \dfrac{m_1}{\rho_c \cdot A_1} = 7.4 \cdot m$
$m_2 := 550kg$	$d_2 := 500mm$	$A_2 := \pi \cdot \left(\dfrac{d_2}{2}\right)^2 = 196349.5 \cdot mm^2$	$h_{o2} := \dfrac{m_2}{\rho_c \cdot A_2} = 1.2 \cdot m$
$m_3 := 850kg$	$d_3 := 500mm$	$A_3 := \pi \cdot \left(\dfrac{d_3}{2}\right)^2 = 196349.5 \cdot mm^2$	$h_{o3} := \dfrac{m_3}{\rho_c \cdot A_3} = 1.8 \cdot m$
$m_4 := 1400kg$	$d_4 := 700mm$	$A_4 := \pi \cdot \left(\dfrac{d_4}{2}\right)^2 = 384845.1 \cdot mm^2$	$h_{o4} := \dfrac{m_4}{\rho_c \cdot A_4} = 1.5 \cdot m$

This is essentially the solution chosen for the 1400kg object.
An object of 1.5m were made from concrete drain pipes filled with concrete.

For 140kg, 550kg and 850kg other methods listed below are chosen.

Impact object size calculations - pure steel column - for Ansys simulations:

Density steel Ansys $\rho_c := 7850\frac{kg}{m^3}$

Mass	**Diameter**	**Area**	**Needed object height**
$m_1 := 140kg$	$d_1 := 100mm$	$A_1 := \pi\cdot\left(\frac{d_1}{2}\right)^2 = 7854.0\cdot mm^2$	$h_{o1} := \frac{m_1}{\rho_c\cdot A_1} = 2.271\cdot m$
$m_2 := 550kg$	$d_2 := 500mm$	$A_2 := \pi\cdot\left(\frac{d_2}{2}\right)^2 = 196349.5\cdot mm^2$	$h_{o2} := \frac{m_2}{\rho_c\cdot A_2} = 0.357\cdot m$
$m_3 := 850kg$	$d_3 := 500mm$	$A_3 := \pi\cdot\left(\frac{d_3}{2}\right)^2 = 196349.5\cdot mm^2$	$h_{o3} := \frac{m_3}{\rho_c\cdot A_3} = 0.551\cdot m$
$m_4 := 1400kg$	$d_4 := 700mm$	$A_4 := \pi\cdot\left(\frac{d_4}{2}\right)^2 = 384845.1\cdot mm^2$	$h_{o4} := \frac{m_4}{\rho_c\cdot A_4} = 0.463\cdot m$

Impact object size calculations - concrete in steel pipe:

Density concrete $\rho_c := 2400 \frac{kg}{m^3}$ Density steel $\rho_s := 7850 \frac{kg}{m^3}$

Data:
500mm pipe from Dusavik Base

outer diameter $d_o := 500mm$

outer radius $r_o := \frac{d_o}{2} = 250 \cdot mm$

wall thickness $t := 19mm$

inner radius $r_i := r_o - t = 231 \cdot mm$

Needed height for object mass 550kg - 20kJ

$m_2 := 550kg$

mass steel $m_s := \left(\pi \cdot r_o^{\ 2} - \pi \cdot r_i^{\ 2}\right) \cdot \rho_s = 225.381 \frac{kg}{m}$

mass concrete $m_c := \left(\pi \cdot r_i^{\ 2}\right) \cdot \rho_c = 402.332 \frac{kg}{m}$

equation $\left(m_s + m_c\right) \cdot h_n = 550kg \cdot m$

needed height $h_n := \frac{550kg}{\left(m_s + m_c\right)} = 0.876\, m$

Needed height for object mass 850kg - 30 kJ

$m_3 := 850kg$

mass steel $m_s := \left(\pi \cdot r_o^{\ 2} - \pi \cdot r_i^{\ 2}\right) \cdot \rho_s = 225.381 \frac{kg}{m}$

mass concrete $m_c := \left(\pi \cdot r_i^{\ 2}\right) \cdot \rho_c = 402.332 \frac{kg}{m}$

equation $\left(m_s + m_c\right) \cdot h_n = 850kg \cdot m$

needed height $h_n := \frac{850kg}{\left(m_s + m_c\right)} = 1.354\, m$

100mm pipe from Dusavik Base - Concrete in steel pipe:

100mm pipe from Dusavik Base

outer diameter	$d_o := 100\text{mm}$
outer radius	$r_o := \dfrac{d_o}{2} = 50\cdot\text{mm}$
wall thickness	$t := 3\text{mm}$
inner radius	$r_i := r_o - t = 47\cdot\text{mm}$

Using only Ø100mm steel pipe:

$m_2 := 140\text{kg}$

mass steel $\quad m_s := \left(\pi\cdot r_o^{\ 2} - \pi\cdot r_i^{\ 2}\right)\cdot\rho_s = 7.176\,\dfrac{\text{kg}}{\text{m}}$

mass concrete $\quad m_c := \left(\pi\cdot r_i^{\ 2}\right)\cdot\rho_c = 16.655\,\dfrac{\text{kg}}{\text{m}}$

equation $\quad \left(m_s + m_c\right)\cdot h_n = 140\text{kg}\cdot\text{m}$

needed height $\quad h_n := \dfrac{140\text{kg}}{\left(m_s + m_c\right)} = 5.874\,\text{m}$

<u>Too high concrete column - not a suitable solution!</u>

Better alternative for 5kJ - 140kg
- Increase of cross section above impact diameter

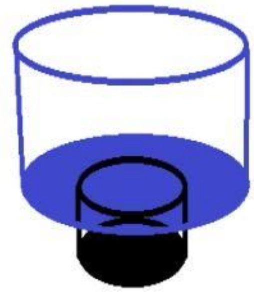

Concrete in 100mm steel pipe from Dusavik Base
+ 300mm concrete column on top in ventilation duct etc.

100mm pipe data

outer diameter $d_o := 100mm$

outer radius $r_o := \frac{d_o}{2} = 50 \cdot mm$

wall thickness $t := 10mm$

inner radius $r_i := r_o - t = 40 \cdot mm$

$m_2 := 140kg$

mass steel $m_s := \left(\pi \cdot r_o{}^2 - \pi \cdot r_i{}^2\right) \cdot \rho_s = 22.195 \frac{kg}{m}$

mass concrete $m_c := \left(\pi \cdot r_i{}^2\right) \cdot \rho_c = 12.064 \frac{kg}{m}$

mass of 20 cm of this pipe size $\left(m_s + m_c\right) \cdot 200mm = 6.852\,kg$

remaining mass $m_{1.300} := 140kg - 6.852\ kg = 133.15\,kg$

Needed height for 300mm concrete column

Mass	**Diameter**	**Area**	**Needed object height**
$m_{1.300} = 133.15\,kg$	$d_{1.300} := 300mm$	$A_1 := \pi \cdot \left(\frac{d_{1.300}}{2}\right)^2 = 70685.8 \cdot mm^2$	$\frac{m_{1.300}}{\rho_c \cdot A_1} = 0.785\,m$

E. Concrete and reinforcement design calculations according to *Eurocode 2*

Eurocode 2 - Concrete and Reinforcement Design Calculations

References are made to:
- *Eurocode 2: NS-EN 1992-1-1:2004+NA:2008,* Norsk Standard, Published by Standard Norge (2004)
- *Reinforced Concrete Design to Eurocode 2: Seventh Edition* by Bill Mosley, John Bungey and Ray Hulse, Published by Palgrave Macmillan (2012)
- *Betongkonstruksjoner - Formler og diagrammer - NS-EN 1992-1-1*, Høgskolen i Bergen (2011)

$kNm := kN \cdot m$

Cover data:

$b := 1500mm$ $\qquad h := 215mm$ $\qquad ø := 12mm$

Amount of reinforcement in cover:

$A_{s2} := 12 \cdot \pi \cdot (6mm)^2 = 1357.168 \cdot mm^2$ $\qquad A'_{s2} := A_{s2}$ $\qquad A_{tot} := A_{s2} + A'_{s2} = 2714.336 \cdot mm^2$

The concrete cover of the reinforcement bars is 31 mm, effective height d_2 is thus

$$d_2 := h - 31mm - \frac{ø}{2} = 178 \cdot mm$$

Material data - EC2 §3.1.3, §3.1.6 and §3.2:

$f_{ck} := 40MPa$ $\qquad f_{cd} := \frac{0.85 \cdot f_{ck}}{1.5} = 22.667 \cdot MPa$

$f_{ctk0.05} := 2.5MPa$ $\qquad f_{ctd} := \frac{0.85 \cdot f_{ctk0.05}}{1.5} = 1.417 \cdot MPa$

$f_{ctm} := 3.5MPa$

$f_{yk} := 500MPa$ $\qquad f_{yd} := \frac{f_{yk}}{1.15} = 434.783 \cdot MPa$

$\varepsilon_{cu} := 0.0035$ $\qquad \varepsilon_{sc} := 0.00217$

Design trawlboard overpull load on structure, from NORSOK U-001

$F = 300 \cdot kN$

Resulting design forces and moments on structure (ULS) from STAAD.Pro V8i

$M_{Ed} := 327.047kNm$ $\qquad V_{Ed} := 299.257kN$ $\qquad N_{Ed} := 337.026kN$

Concrete cover of reinforcement - EC2 §4.4.1.1

Exposure class: XS2 (permanent submersion in sea water) - EC2 Table NA.4.4N

$c_{min.dur} := 40mm$

$c_{min.b} := ø = 12 \cdot mm$ $\quad c_{min.\gamma} := 0mm$ $\quad c_{min.st} := 0mm$ $\quad c_{dur.add} := 0mm$

$c_{min} := \max(c_{min.b}, c_{min.dur} + c_{min.\gamma} - c_{min.st} - c_{dur.add}, 10mm) = 40 \cdot mm$

Cmin,b is the minimum cover requirements with regards to bonding. In this case, where the reinforcement used in testing was separated and had a diameter of 12 mm, 12 mm will be used.

Cmin,dur is the requirement according due to exposure class, 40 mm will be used.

Cmin,γ is an additive safety element, and is normally set to 0 mm. An increase to 10 mm will result in substantial increase of design working life with unchanged probability for corrosion damage, or a substantial decrease in probability for corrosion damage with unchanged design working life.

Δcdur,st is a reduction of concrete cover where stainless steel is used as reinforcement bars or other special measures have been taken. Recommended value is 0 mm, but can be reduced by up to 15 mm.

Δcdur,add is reduction of minimum cover if other protection measures are made. Recommended value is 0 mm.

The minimum concrete cover of the reinforcement c.nom is

$c_{nom} := c_{min} + 10mm = 50 \cdot mm$

Thus, the **effective height d** of the concrete beam is

$d' := c_{nom} + \frac{1}{2} \cdot ø = 56 \cdot mm$

$d := h - d' = 159 \cdot mm$

* Note that reinforcing links around the reinforcement has not been included in d for this cover

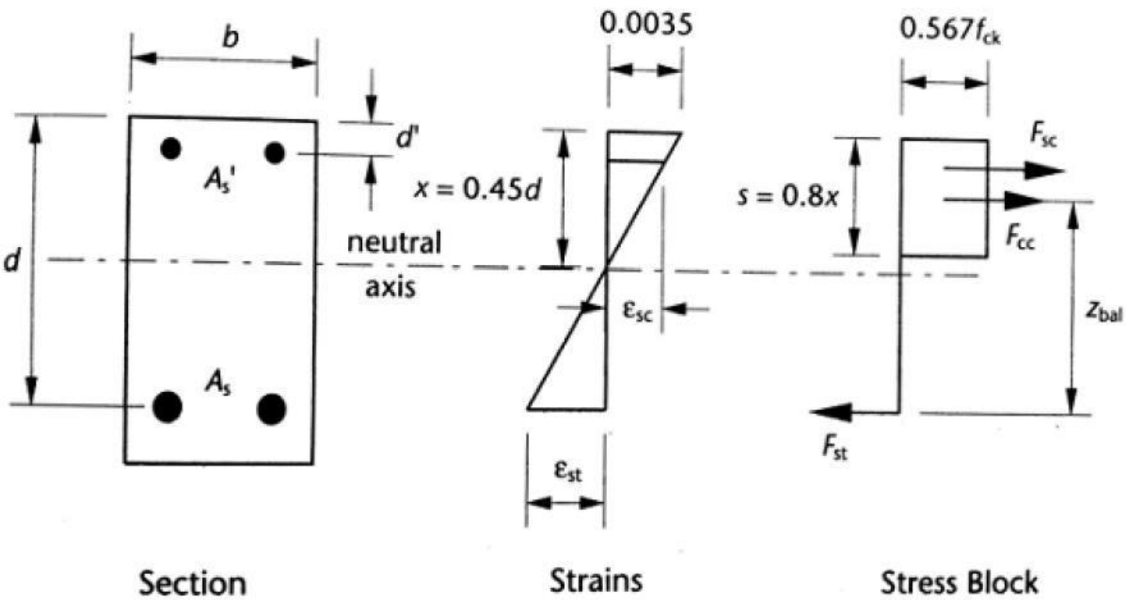

Source: *Reinforced Concrete Design to Eurocode 2: Seventh Edition*
by Bill Mosley, John Bungey and Ray Hulse, Published by Palgrave Macmillan (2012)

Minimum reinforcement requirements - EC2 §9.2.1.1 (1)

$$A_{s.min} := \max\left(0.26\cdot\frac{f_{ctm}}{f_{yk}}\cdot b\cdot d, 0.0013\cdot b\cdot d\right) = 434.07\cdot mm^2$$

Maximum reinforcement - EC2 §9.2.1.1 (3)

$$A_c := b\cdot h = 322500\cdot mm^2$$

$$A_{s.max} := 0.04\cdot A_c = 12900\cdot mm^2$$

Moment capacity - Mosley et al. (2012)

Simple test of Moment Capacity (only tensile reinforcement) according to p. 73 of Mosley et al.

$$M_{cd} := 0.167\cdot f_{ck}\cdot b\cdot d^2 = 253.316\cdot kNm$$

M_{cd} is lower than $M_{Ed} = 327.047\cdot kNm$ and compression reinforcement is needed.

A simple test of the moment capacity of the beam assessed in the thesis

$M_{cd.2} := 0.167 \cdot f_{ck} \cdot b \cdot d_2{}^2 = 317.474 \cdot kNm$ which is still lower than M_{Ed}

The cover has both tensile and compression reinforcement.
Thus the method described in Chapter 4.5 of Mosley et al. (2012) will be used.

The equations have been derived for the case of zero moment resdistribution,
Plastic behaviour of the reinforced concrete affects the moment distribution in the structure.
Zero moment redistribution is thus elastic calculation up to the yield strains.

The **depth to the neutral axis** x is

$x := 0.45 \cdot d = 71.55 \cdot mm$ $\qquad x_{bal} := x$

which is the max value allowed by EC2 in order to ensure tension failure with a ductile section.

Therefore

$$z_{bal} = d - \frac{s_{bal}}{s} = d - \frac{0.8 \cdot x_{bal}}{2} = d - \frac{0.8 \cdot 0.45 \cdot d}{2} = 0.82 \cdot d \qquad z_{bal} := 0.82 \cdot d = 130.38 \cdot mm$$

Equilibrium of section in figure above gives

$$F_{st} = F_{cc} + F_{sc}$$

with the reinforcement at yield

$$0.87 \cdot f_{yk} \cdot A_s = 0.567 \cdot f_{ck} \cdot b \cdot s + 0.87 \cdot f_{yk} \cdot A'_s$$

or with

$$s = 0.8 \cdot x = 0.8 \cdot 0.45 \cdot d = 0.36 \cdot d \qquad s := 0.36 \cdot d = 57.24 \cdot mm$$

we get

$$0.87 \cdot f_{yk} \cdot A_s = 0.204 \cdot f_{ck} \cdot b \cdot d + 0.87 \cdot f_{yk} \cdot A'_s$$

Taking moments about the centroid of the tension steel gives

$$M = F_{cc} \cdot z_{bal} + F_{sc}(d - d')$$

$$M = 0.204 \cdot f_{ck} \cdot b \cdot d \cdot 0.82 \cdot d + 0.87 \cdot f_{yk} \cdot A'_s(d - d')$$

$$M = 0.167 \cdot f_{ck} \cdot b \cdot d^2 + 0.87 \cdot f_{yk} \cdot A'_s(d - d')$$

Rearranging this, we get the necessary area of **compression reinforcement A´.s** where M is the design moment M.Ed

$$A'_s = \frac{M - 0.167 \cdot f_{ck} \cdot b \cdot d^2}{0.87 \cdot f_{yk} \cdot (d - d')} \qquad A'_s := \frac{M_{Ed} - 0.167 \cdot f_{ck} \cdot b \cdot d^2}{0.87 \cdot f_{yk} \cdot (d - d')} = 1645.606 \cdot mm^2$$

By multiplying both sides of the equation below by $z_{bal} = 0.82 \cdot d$ and rearranging gives the necessary area of **tensile reinforcement A.s**

$$0.87 \cdot f_{yk} \cdot A_s = 0.204 \cdot f_{ck} \cdot b \cdot d + 0.87 \cdot f_{yk} \cdot A'_s$$

$$0.87 \cdot f_{yk} \cdot A_s \cdot z_{bal} = 0.204 \cdot f_{ck} \cdot b \cdot d \cdot z_{bal} + 0.87 \cdot f_{yk} \cdot A'_s \cdot z_{bal}$$

$$A_s = \frac{0.204 \cdot f_{ck} \cdot b \cdot d \cdot 0.82 \cdot d}{0.87 \cdot f_{yk} \cdot z_{bal}} + \frac{0.87 \cdot f_{yk} \cdot A'_s \cdot 0.82 \cdot d}{0.87 \cdot f_{yk} \cdot 0.82 \cdot d}$$

$$A_s = \frac{0.167 \cdot f_{ck} \cdot b \cdot d^2}{0.87 \cdot f_{yk} \cdot z_{bal}} + A'_s \qquad A_s := \frac{0.167 \cdot f_{ck} \cdot b \cdot d^2}{0.87 \cdot f_{yk} \cdot z_{bal}} + A'_s = 6112.048 \cdot mm^2$$

In these calculations, it has been assumed that the compression steel has yielded.
This would mean that the steel stress $f_{sc} = 0.87 \cdot f_{yk}$

From the proportions of the strain distribution figure above we have

$$\frac{\varepsilon_{sc}}{x - d'} = \frac{\varepsilon_{cu}}{x} \qquad \text{where} \qquad \varepsilon_{cu} := 0.0035$$

so that

$$\frac{x - d'}{x} = \frac{\varepsilon_{sc}}{\varepsilon_{cu}} \qquad \text{or} \qquad \frac{d'}{x} = 1 - \frac{\varepsilon_{sc}}{\varepsilon_{cu}}$$

At yield with $f_{yk} = 500\text{MPa}$ the steel strain is $\varepsilon_{sc} = \varepsilon_y = 0.00217$ $\qquad \varepsilon_{sc} := 0.00217$

Therefore for yielding of the compression steel

$$\frac{d'}{x} < 1 - \frac{0.00217}{0.0035} < 0.38$$

or with $x = 0.45 \cdot d$ we get $\frac{d'}{d} < 0.171$

In this case, however, we get

$$\frac{d'}{x} = 0.783 \qquad > \qquad 0.38$$

or

$$\frac{d'}{d} = 0.352 \qquad > \qquad 0.171$$

Since $\frac{d'}{x} > 0.38$ and $\frac{d'}{d} > 0.171$ it is necessary to calculate the strain ε_{sc} from the equation above and then determine f_{sc} from $f_{sc} = E_s \cdot \varepsilon_{sc}$

$$\frac{\varepsilon_{sc}}{x - d'} = \frac{0.0035}{x} \qquad e_{sc} := \frac{0.0035}{x} \cdot (x - d') = 0.00076$$

$$E_s := 200000\text{MPa} \qquad f_{sc} := E_s \cdot \varepsilon_{sc} = 434 \cdot \text{MPa}$$

This value of stress for the compressive steel (f_{sc}) must be used in the denominator of the A´s equation in place of $0.87 \cdot f_{yk}$ in order to calculate the area A´s of **compression reinforcement**.

$$A'_s = \frac{M - 0.167 \cdot f_{ck} \cdot b \cdot d^2}{f_{sc} \cdot (d - d')} \qquad A'_s := \frac{M_{Ed} - 0.167 \cdot f_{ck} \cdot b \cdot d^2}{f_{sc} \cdot (d - d')} = 1649.398 \cdot mm^2$$

The area of **tension reinforcement** is then calculated from a modified equation such that

$$A_s = \frac{0.167 \cdot f_{ck} \cdot b \cdot d^2}{0.87 \cdot f_{yk} \cdot z_{bal}} + A'_s \cdot \frac{f_{sc}}{0.87 \cdot f_{yk}} \qquad A_s := \frac{0.167 \cdot f_{ck} \cdot b \cdot d^2}{0.87 \cdot f_{yk} \cdot z_{bal}} + A'_s \cdot \frac{f_{sc}}{0.87 \cdot f_{yk}} = 6112.048 \cdot mm^2$$

A'_s and A_s represents the needed amount of compression and tensile reinforcement for the beam with the given cross-section data and reinforcement cover requirements to withstand the ULS design moment M_{Ed}

$$A_s = 6112.048 \cdot mm^2 \qquad A'_s = 1649.398 \cdot mm^2 \qquad A_{s.min} = 434.07 \cdot mm^2 \qquad A_{s.max} = 12900 \cdot mm^2$$

The totalt is between minimum $A_{s.min}$ and maximum $A_{s.max}$ amount of reinforcement.

For the design moment $M_{Ed} = 327.047 \cdot kNm$ the amount of reinforcement bars of diameter $ø = 12 \cdot mm$ is needed:

Compression reinforcement $\dfrac{A'_s}{\pi \cdot \left(\frac{ø}{2}\right)^2} = 14.6$

Should be rounded up

Tension reinforcement $\dfrac{A_s}{\pi \cdot \left(\frac{ø}{2}\right)^2} = 54.0$

Moment capacity test according to
Betongkonstruksjoner - Formler og diagrammer - NS-EN 1992-1-1

Moment capacity due to the tensile reionforcement alone:

Height of compression zone

$$x_1 := \frac{f_{yd} \cdot A_s}{0.8 \cdot b \cdot f_{cd}} = 97.699 \cdot mm$$

$$x_{bal} := 0.617 \cdot d = 98.103 \cdot mm$$

$x_1 \leq x_{bal}$ --> yield in reinforcement, OK

The moment capacity of the compression zone of the concrete

$$M_{Rd} := 0.8 \cdot b \cdot x \cdot f_{cd} \cdot \left(d - \frac{0.8 \cdot x}{2} \right) = 253.74 \cdot kNm \qquad M_{Rd} < M_{Ed}$$

Will try to include the effects of the compression reinforcement

new height of compression zone:

$$x_1 := \frac{f_{yd} \cdot \left(A_s - A'_s \right)}{0.8 \cdot b \cdot f_{cd}} = 71.334 \cdot mm$$

$$h' := h - 2 \cdot c_{nom} - 2 \cdot \frac{ø}{2} = 103 \cdot mm$$

$$\Delta M := A'_s \cdot f_{yd} \cdot h' = 73.864 \cdot kNm$$

$$M_{Rd} := 0.8 \cdot b \cdot x_1 \cdot f_{cd} \cdot \left(d - \frac{0.8 \cdot x_1}{2} \right) = 253.142 \cdot kNm$$

$$M_{Rd} := M_{Rd} + \Delta M = 327.006 \cdot kNm \qquad M_{Ed} = 327.047 \cdot kNm$$

The calculated reinforcement amount gives a moment capacity $M_{Rd} \geq M_{Ed}$

Moment capacity test of cover investigated in thesis:

$h = 215 \cdot mm \qquad d'_2 := 31mm + \frac{ø}{2} = 37 \cdot mm \qquad d_2 = 178 \cdot mm$

$A_{s2} = 1357.168 \cdot mm^2 \qquad A'_{s2} = 1357.168 \cdot mm^2$

Moment capacity due to the tensile reionforcement alone:

Height of compression zone

$$x_2 := \frac{f_{yd} \cdot A_{s2}}{0.8 \cdot b \cdot f_{cd}} = 21.694 \cdot mm$$

$$x_{bal.2} := 0.617 \cdot d_2 = 109.826 \cdot mm$$

$x_2 \le x_{bal.2}$ --> yield in reinforcement, OK

The moment capacity of the compression zone of the concrete

$$M_{Rd.2} := 0.8 \cdot b \cdot x_2 \cdot f_{cd} \cdot \left(d_2 - \frac{0.8 \cdot x_2}{2} \right) = 99.913 \cdot kNm \qquad M_{Rd.2} < M_{Ed}$$

Include the effects of the compression reinforcement

new height of compression zone:

$$x_3 := \frac{f_{yd} \cdot \left(A_{s2} - A'_{s2} \right)}{0.8 \cdot b \cdot f_{cd}} = 0 \cdot mm$$

$$h'_2 := h - 2 \cdot 31mm - 2 \cdot \frac{ø}{2} = 141 \cdot mm$$

$$\Delta M_2 := A'_{s2} \cdot f_{yd} \cdot h'_2 = 83.2 \cdot kNm$$

$$M_{Rd.2} := 0.8 \cdot b \cdot x_3 \cdot f_{cd} \cdot \left(d_2 - \frac{0.8 \cdot x_3}{2} \right) = 0 \cdot kNm$$

Note: The fact that tension and compression reinforcement, A.s2 and A´.s2, are equal in this cover makes the formulas for M.Rd.2 yield only 0 moment capacity. This can not be entirely true.
One of the reasons for this could be the oddly shaped and reinforced "beam" assumed in the calculations.

$$M_{Rd.2} := M_{Rd.2} + \Delta M_2 = 83.2 \cdot kNm \qquad M_{Ed} = 327.047 \cdot kNm$$

The calculated reinforcement amount gives a moment capacity $M_{Rd.2} < M_{Ed}$

Shear force design according to EC2 §6.2.2

The acting shear force in the cover is $V_{Ed} = 299.257 \cdot kN$ at the ends of the beam when the trawl board impacts the cover in the bottom corner. Mind that this force is conservative, as it is implausible that the trawl board will impact the cover that far down. In addition, due to trawl board deflectors, the force will in reality most likely not act only in the Z-direction, but will have components in the Y-direction as well, possibly also X-direction.

According to EC2 §6.2.2, the shear capacity $V_{Rd.c}$ without shear reinforcement is

$k_2 := 0.15$ $\qquad \gamma_c := 1.5$ $\qquad C_{Rd.c} := \frac{k_2}{\gamma_c} = 0.1$ $\qquad d = 0.159\,m$

$$k := \min\left(1 + \sqrt{\frac{200}{\frac{d}{mm}}}, 2.0\right) = 2$$

$A_{sl} := A_s$ $\qquad \rho_I := \min\left(\frac{A_{sl}}{b \cdot d}, 0.02\right) = 0.02$

A.sl is the area of tensile reinforcement which extends > (l.bd + d) beyond the section considered. Not entirely applicable to this situation.

$k_1 := 0.15$ 0.15 at compression and 0.3 at tension

$\frac{N_{Ed}}{A_c} = 1.045 \cdot MPa$ < $0.2 \cdot f_{cd} = 4.533 \cdot MPa$ $\qquad \sigma_{cp} := \min\left(\frac{N_{Ed}}{A_c}, 0.2 \cdot f_{cd}\right) = 1.045 \cdot MPa$

Shear capacity without shear reinforcement $V_{Rd.c}$

$$V_{Rd.c} := \left[C_{Rd.c} \cdot k \cdot \left(100 \cdot \rho_I \cdot \frac{f_{ck}}{MPa}\right)^{\frac{1}{3}} + k_1 \cdot \frac{\sigma_{cp}}{MPa}\right] \cdot b \cdot d \cdot MPa = 242.919 \cdot kN$$

with a minimum value of

$\upsilon_{min} := 0.035 \cdot k^{\frac{3}{2}} \cdot \left(\frac{f_{ck}}{MPa}\right)^{\frac{1}{2}} = 0.626$ $\qquad V_{Rd.c.min} := \left(\upsilon_{min} + k_1 \cdot \frac{\sigma_{cp}}{MPa}\right) \cdot b \cdot d \cdot MPa = 186.711 \cdot kN$

$$V_{Rd.c} := \max\left(V_{Rd.c}, V_{Rd.c.min}\right) = 242.919 \cdot kN$$

The shear capacity without shear reinforcement $V_{Rd.c} = 242.919 \cdot kN$ is lower than the design shear force $V_{Ed} = 299.257 \cdot kN$. This means that the cover/beam needs shear reinforcement.

Shear force design with shear reinforcement according to EC2 §6.2.3

If the cover is designed with shear reinforcement, the shear force capacity is the smaller value of $V_{Rd.s}$ and V.Rd.max

$d = 0.159\,m$

$z := 0.9 \cdot d = 0.143\,m$

$A_{sw} := \pi \cdot \left(\frac{ø}{2}\right)^2 = 113.097 \cdot mm^2$ — A.sw is the cross-sectional area of the shear reinforcement
Assuming diameter ø=12mm

$f_{ywd} := f_{yd} = 434.783 \cdot MPa$ — f.ywd is the design yield strength of the shear reinforcement

$1 \le \cot(\theta) \le 2.5$ — First try with concrete strut angle $\theta := 21.8deg$

--> not enough, change to e.g. $\theta := 20deg$

$s := 60mm$ — s is the spacing of the stirrups (center distance between shear reinforcement)

Shear capacity from strut inclination method $V_{Rd.s}$ is

$$V_{Rd.s} := \frac{A_{sw}}{s} \cdot z \cdot f_{ywd} \cdot \cot(\theta) = 322.216 \cdot kN$$

The structure experiences axial pressure, thus α.cw is decided in NA.6.2.3 (3)

$\sigma_{cp} = 1.045 \cdot MPa \qquad 0 < \sigma_{cp} < 0.25 \cdot f_{cd}$

$0.25 \cdot f_{cd} = 5.667 \cdot MPa$

$0.5 \cdot f_{cd} = 11.333 \cdot MPa$

$1.0 \cdot f_{cd} = 22.667 \cdot MPa$

$$\alpha_{cw} := 1 + \frac{\sigma_{cp}}{f_{cd}} = 1.046$$

$$\upsilon_1 := 0.6 \cdot \left(1 - \frac{f_{ck}}{250 \cdot MPa}\right) = 0.504$$

Maximum allowed shear capacity V.Rd.max

$$V_{Rd.max} := \alpha_{cw} \cdot b \cdot z \cdot \upsilon_1 \cdot \frac{f_{cd}}{\cot(\theta) + \tan(\theta)} = 824.445 \cdot kN$$

Shear capacity V.Rd

$V_{Rd} := \min\left(V_{Rd.s}, V_{Rd.max}\right) = 322.216 \cdot kN \qquad V_{Ed} = 299.257 \cdot kN \qquad V_{Rd} > V_{Ed}$

Shear reinforcement requirements - EC2 §9.2.2

Minimum shear reinforcement ratio $\rho_{w.min}$

$$\rho_{w.min} := 0.1 \cdot \frac{\sqrt{\frac{f_{ck}}{MPa}}}{\frac{f_{yk}}{MPa}} = 0.00126$$

$\alpha := 90deg$ α is the angle between shear and longitudinal reinforcement

Shear reinforcement ratio ρ_w due to A_{sw} $s = 60 \cdot mm$

$$\rho_w := \frac{A_{sw}}{s \cdot b \cdot \sin(\alpha)} = 0.00126$$

$$\rho_w := \max\left(\rho_w, \rho_{w.min}\right) = 0.00126$$

Minimum distance between shear reinforcement s_{min}

$$s_{min} := \frac{A_{sw}}{b \cdot \rho_{w.min}} = 59.608 \cdot mm$$

Largest distance s_{max} allowed between shear reinforcement due to shear force V_{Ed}

$$s_{max} := \frac{A_{sw} \cdot z \cdot f_{yd} \cdot \cot(\theta)}{V_{Ed}} = 64.603 \cdot mm$$

The maximum longitudinal spacing between shear assemblies should not exceed $s_{I.max}$

$h' := h - 2 \cdot c_{nom} - 2 \cdot \frac{ø}{2} = 103 \cdot mm$ h´ is the distance between the centre lines of the tension and compression reinforcements

$$s_{I.max} := 0.6 \cdot h' \cdot (1 + \cot(\alpha)) = 61.8 \cdot mm$$

$s = 60 \cdot mm$ is within the limits of $s_{min} = 59.608 \cdot mm$ and $s_{I.max} = 61.8 \cdot mm$, as well as $s_{max} = 64.603 \cdot mm$

Moment capacity taking into account axial force and 2. order effects
- EC2 §5.8.3 and *Betongkonstruksjoner - Formler og diagrammer - NS-EN 1992-1-1*

Simplified criteria for second order effects

Length of beam $l := 2 \cdot 1215\text{mm} = 2430 \cdot \text{mm}$ or $l := \dfrac{\pi \cdot 2430\text{mm}}{2} = 3817.035 \cdot \text{mm}$

Effective length $l_0 := l$ According to Figure 5.7 of EC2, where a) is most similar to this case.

$h = 215 \cdot \text{mm}$ $h' = 103 \cdot \text{mm}$ $\dfrac{h'}{h} = 0.479$

Due to the odd shape of the cover, the ratio $\dfrac{h'}{h} = 0.479$ is not covered in the MN-diagrams provided in *Betongkonstruksjoner - Formler og diagrammer - NS-EN 1992-1-1*. Therefore, the closest available diagram for h'/h = 0.6 will be used, see last page of these calculations.

Relative axial force is

$n := \dfrac{N_{Ed}}{A_c \cdot f_{cd}} = 0.046$ decides n on the n-axis on the MN-diagram

Mechanical reinforcement ratio

$A_s = 6112.048 \cdot \text{mm}^2$ $A_c = 322500 \cdot \text{mm}^2$

$\omega := \dfrac{A_s \cdot f_{yd}}{A_c \cdot f_{cd}} = 0.364$ decides which curve to use in the MN-diagram

Will use the MN-diagram provided on the next page to read off the m (m.kap) value from the m-axis

$m_{kap} := 0.25$ approximately

A control of the moment capacity is thus

$M_{Rd.3} := m_{kap} \cdot f_{cd} \cdot A_c \cdot h = 392.913 \cdot \text{kNm}$ (in reality slightly lower, due to using 0.6 MN-diagram)

$M_{Rd} = 327.006 \cdot \text{kNm}$ Moment capacity from reinforcement calculations

Radius of gyration of the uncracked concrete section

$$i = \sqrt{\frac{I_c}{A_c}} \qquad i := \sqrt{\frac{b \cdot h^3}{12 \cdot A_c}} = 62.065 \cdot mm$$

Slenderness ratio

$$\lambda := \frac{l_0}{i} = 61.5$$

$$K_a = \left(\frac{i_s}{i}\right)^2 \quad \text{Simplified:} \quad K_a := 1$$

Normalized slenderness ratio

$$\lambda_n := \lambda \cdot \sqrt{\frac{n}{1 + 2 \cdot K_a \cdot \omega}} = 10.048$$

Effective creep ratio

$\varphi_{ef} := 0.011$ see calculations below accounting for φ.ef

$$A_\varphi := \min\left(\frac{1.25}{1 + 0.2 \cdot \varphi_{ef}}, 1.0\right) = 1 \qquad \frac{1.25}{1 + 0.2 \cdot \varphi_{ef}} = 1.247$$

$\lambda_{n.lim} := 13 \cdot A_\varphi = 13$ Because one end is roll supported

2. order effects can be overlooked if λ.n < λn.lim

$\lambda_n = 10.048 < \lambda_{n.lim} = 13$ and thus the 2. order effects can be overlooked.

An attempt on taking into account 2. order effects from N.Ed - EC2 - §5.8.2, §5.8.8.2 and Annex B

The moment including 2. order effects from N.Ed is

$$M_{Ed.2.order} = M_{Ed} + N_{Ed} \cdot e_i + N_{Ed} \cdot e_2$$

M_{Ed} is the 1. order moment

$N_{Ed} \cdot e_i$ is the 2. order moment due to geometrical deviation

$N_{Ed} \cdot e_2$ is the nominal 2. order moment due to deflection from the axial force

$M_{Ed} = 327.047 \cdot kNm \qquad N_{Ed} = 337.026 \cdot kN$

$e_i := \dfrac{l_0}{400} = 9.543 \cdot mm \qquad M_i := N_{Ed} \cdot e_i = 3.216 \cdot kNm$ EC2 §5.2 (7)

e_2 is the deflection and is dependant on the curvature of the normally straight beam. In this case the beam is arch shaped, so the applicability is uncertain. An attempt was made nonetheless, assuming and treating it like a straight beam.

$e_2 = \dfrac{1}{r} \cdot \dfrac{l_0^{\,2}}{10}$ where $\dfrac{1}{r}$ is the curvature K $\qquad K = K_r \cdot K_\varphi \cdot \dfrac{1}{r_0}$

K.r is a correction factor depending on axial load, and K.φ is a factor for taking account of creep.

$$\varepsilon_{yd} := \frac{f_{yd}}{E_s} = 0.00217$$

$K_0 = \dfrac{1}{r_0} = \dfrac{\varepsilon_{yd}}{0.45 \cdot d} \qquad K_0 := \dfrac{\varepsilon_{yd}}{0.45 \cdot d} = 0.03 \cdot \dfrac{1}{m}$

Correction factor for axial load K.r

$n_u := 1 + \omega = 1.364 \qquad n = 0.046 \qquad n_{bal} := 0.25$

n.bal is the value of n at maximum moment resistance (value of "nose tip" on MN-diagram at the bottom). The value 0.4 can be used. Note: for this case a 0.6 MN diagram was used instead of 0.4 MN diagram, and moment capacity is thus a little too high with n.bal = 0.4 or 0.3, and 0.25 was chosen instead.

$K_r := \min\left(\dfrac{n_u - n}{n_u - n_{bal}}, 1.0\right) = 1 \qquad \dfrac{n_u - n}{n_u - n_{bal}} = 1.183$

The correction factor for creep K.φ is a calculation with many assumptions and uncertanties

$K_{\varphi} = \max(1 + \beta \cdot \varphi_{ef}, 1)$

$\beta := 0.35 + \frac{f_{ck}}{200 \cdot MPa} - \frac{\lambda}{150} = 0.14$

φ.ef is the effective creep ratio according to EC2 - §5.8.4

$\varphi_{ef} = \varphi_{\infty.t0} \cdot \frac{M_{0Eqp}}{M_{0Ed}}$

where:
$\varphi_{t.t0}$ is the final creep coefficient according to §3.1.4
M_{0Eqp} is the first order bending moment in quasi-permanent load combination (SLS) - will assume moment from only self weight of cover
M_{0Ed} is the first order bending moment in design load combination (ULS)

The effect of creep can be ignored, i.e. φ.ef = 0, if the following three conditions are met:

$\lambda = 61.5$ < 75 OK

$M_{0Ed} := M_{Ed}$ $\frac{M_{0Ed}}{N_{Ed}} = 970.391 \cdot mm$ > $h = 215 \cdot mm$ not OK

$\varphi_{\infty.t0} = 1.45 \leq 2$ OK

Need to take creep into account.

Final creep coefficient $\varphi_{\infty.t0}$ is decided from Figure 3.1 of EC2

$E_c = 1.05 \cdot E_{cm}$ $E_c := 1.05 \cdot 35MPa$

t.0 is the time of loading in days. Hard to predict when trawl load is considered. Load from selfweight is the only other load, and can be assumed applied within a few days.
Assuming somewhere in between: $t_0 := 50$ $\varphi_{\infty.t0} := 1.45$

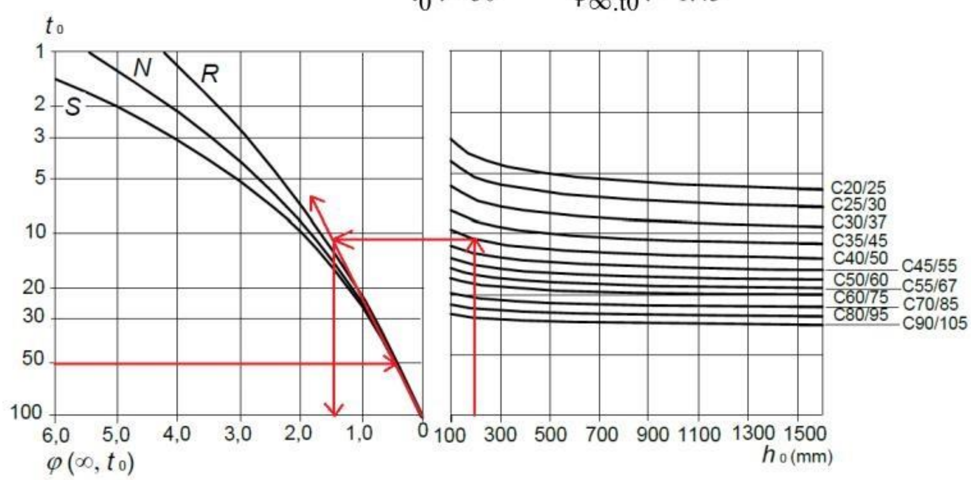

If we assume that $M_{0Ed} := M_{Ed} = 327.047 \cdot kNm$

and that $M_{0Eqp} := 5kNm$ is the maximum moment from selfweight alone (found from Staad.Pro V8i model)

The effective creep ratio is

$$\varphi_{ef} := \varphi_{\infty.t0} \cdot \frac{M_{0Eqp}}{M_{0Ed}} = 0.022$$

and the correction factor for creep K.φ is

$$K_{\varphi} := \max\left(1 + \beta \cdot \varphi_{ef}, 1.0\right) = 1.003$$

This gives the curvature K

$$K := K_r \cdot K_{\varphi} \cdot K_0 = 0.03 \frac{1}{m}$$

and thus the deflection e.2 is

$$e_2 := K \cdot \frac{{l_0}^2}{10} = 44.405 \cdot mm$$

Resulting 1. and 2. order moments

$M_{Ed} = 327.047 \cdot kNm$

$N_{Ed} \cdot e_i = 3.216 \cdot kNm$

$N_{Ed} \cdot e_2 = 14.966 \cdot kNm$

The total moment including second order effects can then be calculated as

$$M_{Ed.2.order} := M_{Ed} + N_{Ed} \cdot e_i + N_{Ed} \cdot e_2 = 345.229 \cdot kNm$$

The moment capacity is $M_{Rd} = 327.006 \cdot kNm$ which is now too low.

The amount of longitudinal reinforcement must be increased.

Compression reinforcement necessary:

$$A'_{s.2.order} := \frac{M_{Ed.2.order} - 0.167 \cdot f_{ck} \cdot b \cdot d^2}{f_{sc} \cdot (d - d')} = 2056.129 \cdot mm^2$$

Tension reinforcement necessary:

$$A_{s.2.order} := \frac{0.167 \cdot f_{ck} \cdot b \cdot d^2}{0.87 \cdot f_{yk} \cdot z_{bal}} + A'_{s.2.order} \cdot \frac{f_{sc}}{0.87 \cdot f_{yk}} = 6517.845 \cdot mm^2$$

Compression reinforcement $\frac{A'_{s.2.order}}{\pi \cdot \left(\frac{ø}{2}\right)^2} = 18.2$

Should be rounded up

Tension reinforcement $\frac{A_{s.2.order}}{\pi \cdot \left(\frac{ø}{2}\right)^2} = 57.6$

Test of moment capacity:

$$x_{2.order} := \frac{f_{yd} \cdot \left(A_{s.2.order} - A'_{s.2.order}\right)}{0.8 \cdot b \cdot f_{cd}} = 71.319 \cdot mm$$

$$M_{Rd.2.order} := 0.8 \cdot b \cdot x_{2.order} \cdot f_{cd} \cdot \left(d - \frac{0.8 \cdot x_{2.order}}{2}\right) = 253.1 \cdot kNm$$

$$\Delta M_{2.order} := A'_{s.2.order} \cdot f_{yd} \cdot h' = 92.079 \cdot kNm$$

$$M_{Rd} := M_{Rd.2.order} + \Delta M_{2.order} = 345.179 \cdot kNm \qquad M_{Ed.2.order} = 345.229 \cdot kNm$$

The rounded up reinforcement amount gives a moment capacity $M_{Rd} \geq M_{Ed}$

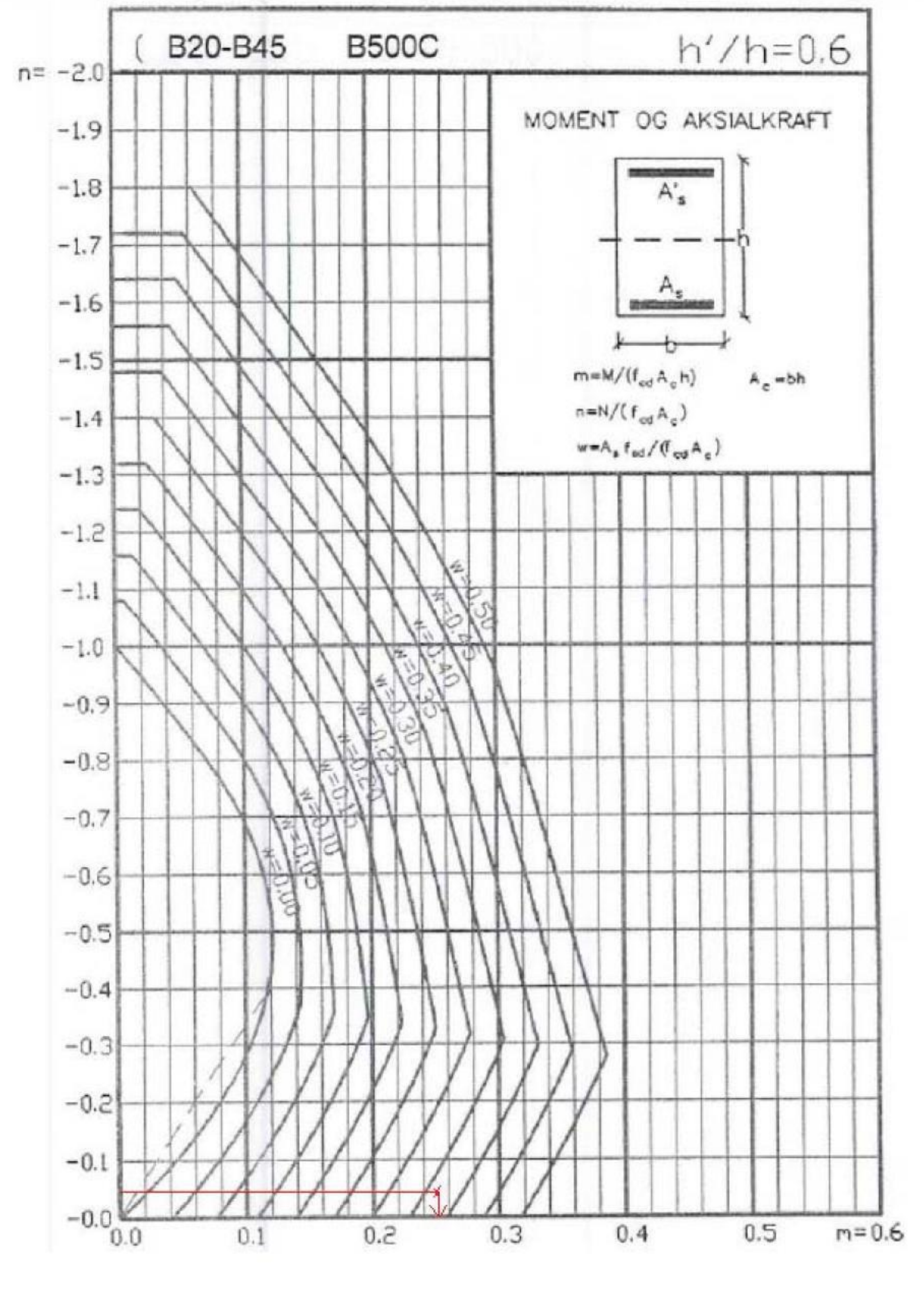
B20-B45 B500C
h'/h=0.6
MOMENT OG AKSIALKRAFT
A's
h
As
b
m=M/(fcd Ac h)
Ac=bh
n=N/(fcd Ac)
w=As fsd/(fcd Ac)
n= -2.0
-1.9
-1.8
-1.7
-1.6
-1.5
-1.4
-1.3
-1.2
-1.1
-1.0
-0.9
-0.8
-0.7
-0.6
-0.5
-0.4
-0.3
-0.2
-0.1
-0.0
0.0
0.1
0.2
0.3
0.4
0.5
m=0.6
w=0.50
w=0.45
w=0.40
w=0.35
w=0.30
w=0.25
w=0.20
w=0.15
w=0.10
w=0.05
w=0.00

F. Impact Test Sheets

Impact Test - Record Sheet

Date: 9/3-15

Location: Multiblokk AS

Conditions / Equipment: Dry weather, some wind, Pelican slip hook, Manitou lift, Deflection measuring devices

Test ID: 1.7, 50KJ, 1400kg

Diameter: 700 mm

Measured weight: 1350 kg → higher drop height

Wanted impact energy: 50 kJ

Calculated drop height: $\frac{50000J}{1350kg \cdot 9{,}81 \frac{m}{s^2}} = 3{,}77 m$

Measured deflections:

Telescope center: Before: 0,541m After: 0,454m MAX: 0,441m space: 13mm

Telescope outer: Before: 0,508m After: 0,435m MAX: 0,421m space: 14mm

Oasis: 7,3cm Ruler: 7,5cm

Comments: More heavy cracking/crushing than anticipated → Dry-cast. Reinforcement gives som "bounce back", tension that is "pulled back again." Concrete had good sound :) Would completely crush without reinf. → Too little reinf. Big cracks, concrete chunks came off, reinf. exposed underneath. Need new object for next test. Vertical deflection, expanded to the sides-horizontally. Double reinf. for next test.

Note: This is a standardized, stock pipe, not tested or made for impacts. Pressure tested.

Attendees:

Arnstein G. Waldeland

Ove Tobias Gudmestad (UiS)

Meric Pakkan (Subsea7)

Rune Egeland (Multiblokk)

Geir Lillebø (—"—)

Egil Lillebø (—"—)

Jan Herbert Sandsmark (—"—)

Martine Johnsen

$E = mgh$

$h = \frac{E}{mg} = \frac{5000\,J}{9{,}81\,\frac{m}{s^2} \cdot 171{,}6\,kg} = 2{,}97\,m$

Impact Test - Record Sheet

Date: 27/4 - 15

Location: UiS LABORATORIES

Conditions / Equipment: INSIDE, BASIN, SUBMERGED

Test ID: 2.7 / 2.2

Diameter: 100 mm

Measured weight: (160kg + 170kg + 185kg) / 3 = 171,6 kg

Wanted impact energy: 5 kJ

Calculated drop height: 2,97m

Measured deflections: ORIGINAL: 43cm AFTER: 43cm

NO DEFLECTION / PUSHED INTO SAND

Comments: TEST DONE 2 TIMES. FIRST TIME ON MID POINT OF COVER - LANDED A BIT ASKEW. SECOND TIME NEARER EDGE, MIDPOINT BETWEEN CENTER & EDGE - LANDED STRAIGHT.

NO MEASURABLE DEFLECTION OR PUSH DOWN INTO SAND.
LEFT ONLY TWO VISIBLE IMPACT "HOLES"/DIMPLES OF ~1cm DEPTH.
NO VISIBLE CRACKING → NEXT TEST PERFORMED ON SAME COVER. (20 kJ)

Attendees:

ARNSTEIN WALDELAND: Arnstein Waldeland

OVE TOBIAS GUDMESTAD: Ove T Gudmestad (UiS)

MERIC PAKKAN: (Subsea 7)

RUNE EGELAND: (MULTIBLOKK)

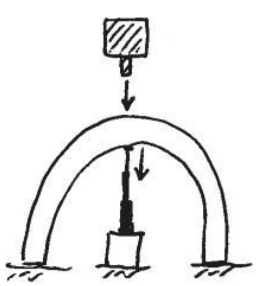

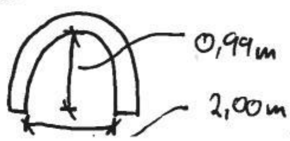

MEASURED AFTER REMOVAL FROM BASIN
MEASURED AFTER BOTH 5 kJ AND 20 kJ IMPACT TEST

$E = mgh$

$h = \frac{E}{mg} = \frac{20\,000\,J}{9{,}81\,\frac{m}{s^2} \cdot 576{,}6\,kg} = 3{,}53\,m$

Impact Test - Record Sheet

Date: 27/4 -15

Location: UiS LABORATORIES

Conditions / Equipment: BASIN, SUBMERGED

Test ID: 3.7

Diameter: 500 mm

Measured weight: (570kg + 580 kg + 580 kg)/3 = 576,6 kg

Wanted impact energy: 20 kJ

Calculated drop height: 3,53m

Measured deflections: ORIGINAL: 43cm , AFTER: 39 cm

4cm DEFLECTION / PUSHED DOWN INTO SAND

Comments: OBJECT LANDED SLIGHTLY ASKEW FORWARD, WHICH LEFT A 1,5cm DEEP IMPACT MARK AND SENT MOST OF THE IMPACT ENERGY FORWARD. THIS LED TO A ~3mm CRACK IN FRONT. IMPACT LEFT A VERTICAL CRACK FROM CENTER AND UP TO THE WEB OF SMALL CRACKS AROUND THE IMPACT AREA. OF BOTH SIDES SOME RATHER LARGE CRACKS UNDERNEATH COVER OF ~ 3mm ~~to ~1mm~~ TO ~0,01 mm ALONG THE ARCH. SOME SMALL LOOSE FLAKES OF CONCRETE IN THE AREAS WITH LARGE CRACKS.

Attendees:

ARNSTEIN WALDELAND: Arnstein Waldeland

OVE TOBIAS GUDMESTAD: Ove T. Gudmestad (UiS)

MERIC PAKKAN: [signature] (Subsea7)

RUNE EGELAND: [signature] (MULTIBLOKK)

JOHN GRØNLI: John Grønli (UiS)

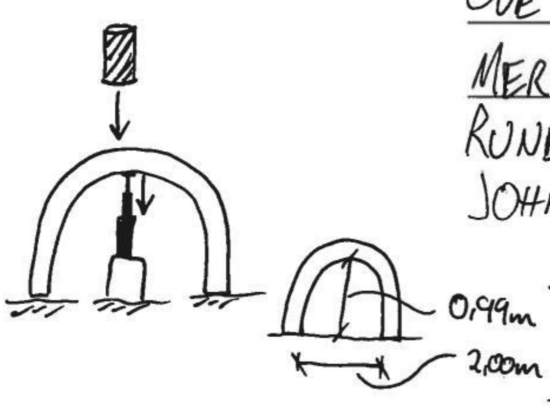

MEASURED AFTER REMOVAL FROM BASIN

MEASURED AFTER IMPACT FROM BOTH 5kJ AND 20 kJ

$E = mgh$

$h = \frac{E}{mg} = \frac{30\,000\ J}{9{,}81\ \frac{m}{s^2} \cdot 883{,}3\ kg} = 3{,}46\ m$

Impact Test - Record Sheet

Date: 27/4-15

Location: UiS LABORATORIES

Conditions / Equipment: BASIN, SUBMERGED

Test ID: 4.1

Diameter: 500 mm

Measured weight: (870 kg + 900 kg + 880 kg) / 3 = 883,3 kg

Wanted impact energy: 30 kJ

Calculated drop height: 3,46 m

FROM WATER SURFACE TO TOP OF COVER:

Measured deflections:

BEFORE: FRONT: 21,5 cm; BACK: 24 cm
AFTER: FRONT: 26,5 cm; BACK: 26 cm

Comments: OBJECT LANDED SLIGHTLY ASKEW FORWARD, WHICH LEFT A CLEAR IMPACT MARK. FOLLOWING THIS, A LOT OF ENERGY WAS ABSORBED FORWARD, AND THE FRONT WAS HEAVILY CRACKED (~6 mm). AROUND THE IMPACT AREA, A LARGE WEB OF CRACKS (~0,5 mm) CAN BE SEEN. A LARGE CRACK FROM MID SIDE (1 cm) STRETCHES UP TO THE IMPACT CRACK WEB. SEVERAL LARGE CHUNKS OF CONCRETE CAME LOOSE IN THE NETHER AREAS OF THIS CRACK. INSIDE, UNDERNEATH, AN EXTENSIVE WEB OF CRACKS (4mm-3mm-2mm-1mm-smaller) CAN BE OBSERVED, AS WELL AS SEVERAL LARGE CHUNKS OF CONCRETE ALMOST COME LOOSE IN FRONT UNDER IMPACT AREA. MAINLY ONE LARGE CRACK IN FRONT, ONE LARGE ON THE RIGHT SIDE ON THE INSIDE AND OUTSIDE OF COVER, AND A WEB OF SMALLER CRACKS - MOSTLY IN THE FRONT HALF OF THE COVER.

Attendees:
Arnstein Waldeland: ARNSTEIN WALDELAND
RUNE EGELAND: (MULTIBLOKK)
ARVID LILLEBØ: (SKIAEVELAND CEMENTSTØPERI)
ROLV RAVN WALDELAND: (SUBSEA 7)

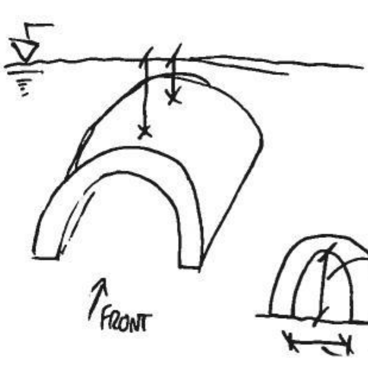

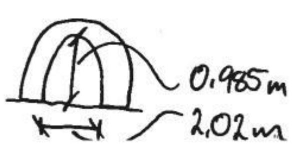

} MEASURED AFTER REMOVAL FROM BASIN

$E = mgh$

$h = \frac{E}{mg} = \frac{50\,000\,J}{9{,}81\frac{m}{s} \cdot 1279{,}5kg} = 3{,}98m$

Impact Test - Record Sheet

Date: 28/4-15

Location: UiS LABORATORIES

Conditions / Equipment: BASIN, SUBMERGED

Test ID: 5.1

Diameter: 700 mm

Measured weight: (1279 kg + 1280 kg)/2 = 1279,5 kg

Wanted impact energy: 50 kJ

Calculated drop height: 3,98m

Measured deflections: FROM WATER SURFACE TO TOP OF COVER

BEFORE: FRONT: 19 cm, BACK: 19 cm — AFTER: FRONT: 26 cm, BACK: 26,5 cm

Comments: OBJECT LANDED STRAIGHT AND LEFT AN EVEN MARK ON THE COVER. THIS LED TO LESS SEVERE DAMAGE AS FOR 30 kJ (ASKEW), BUT MORE EVEN OVERALL CRACKING, STRETCHING FROM ONE END OF COVER TO THE OTHER. SEVEN CRACKS CAN BE SEEN IN FRONT, ALONG THE ARCH, FOLLOWING THE LENGTH OF THE COVER ALL THE WAY TO THE BACK (CENTER: ~1,5mm, SIDES ~0,5mm-0,2mm) THE LARGEST CRACK IN FRONT IS APPROXIMATELY 2mm WIDE. INSIDE, UNDERNEATH, AN INTRICATE, AND RATHER SYMMETRIC WEB OF SMALL CRACKS (~1,5mm-1mm-0,5mm) CAN BE OBSERVED. THE CENTER OF THE WEB IS APPROX. WHERE CENTER OF IMPACT OCCURED. SOME FOLLOW THE ENTIRE LENGTH OF THE COVER, WHILE SOME TRAVEL DIAGONALLY OUTWARDS FROM CENTER. SOME ALSO FOLLOW THE ARCH OF THE COVER.

Attendees:

ARNSTEIN WALDELAND: Arnstein Waldeland

OVE TOBIAS GUDMESTAD: Ove T Gudmestad (UiS)

ARVID LILLEBØ: [signature] (SKJÆVELAND CEMENTSTØPERI)

JOHN GRØNLI: John Grønli (UiS)

ROLV RAVN WALDELAND: Rolv R Waldeland (SUBSEA

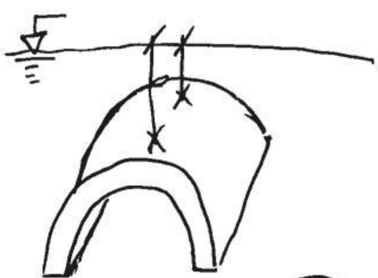

FRONT

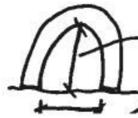

0,975m
2,02m } MEASURED AFTER REMOVAL FROM BASIN

G. Frame-by-Frame of dropped object tests

Frame-by-frame #1 of Test ID 1.1 – 50 kJ

Frame-by-frame #2 of Test ID 1.1 – 50 kJ

Frame-by-frame of Test ID 2.1 and 2.2 – 5 kJ

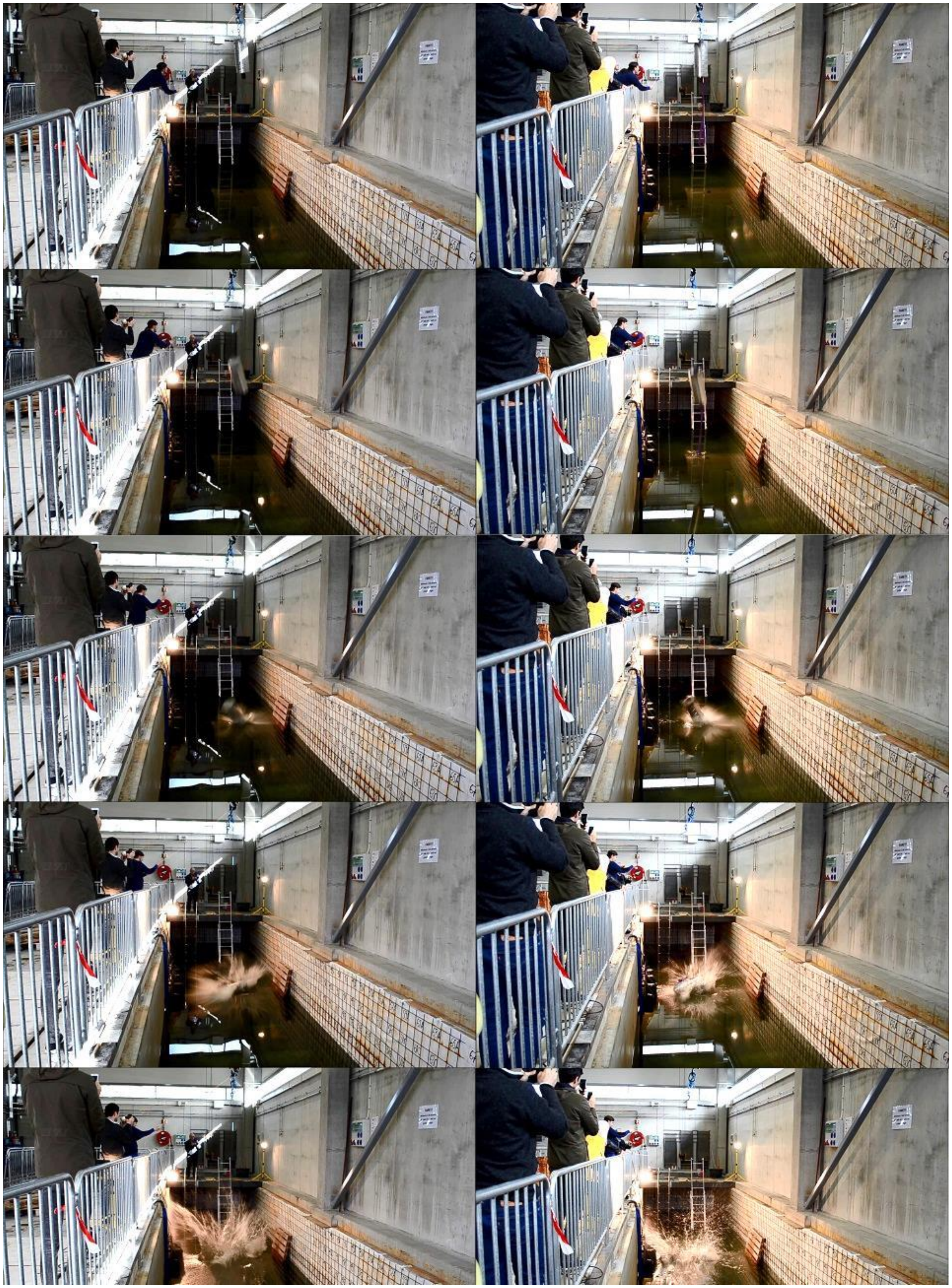

Frame-by-frame of Test ID 3.1 – 20 kJ

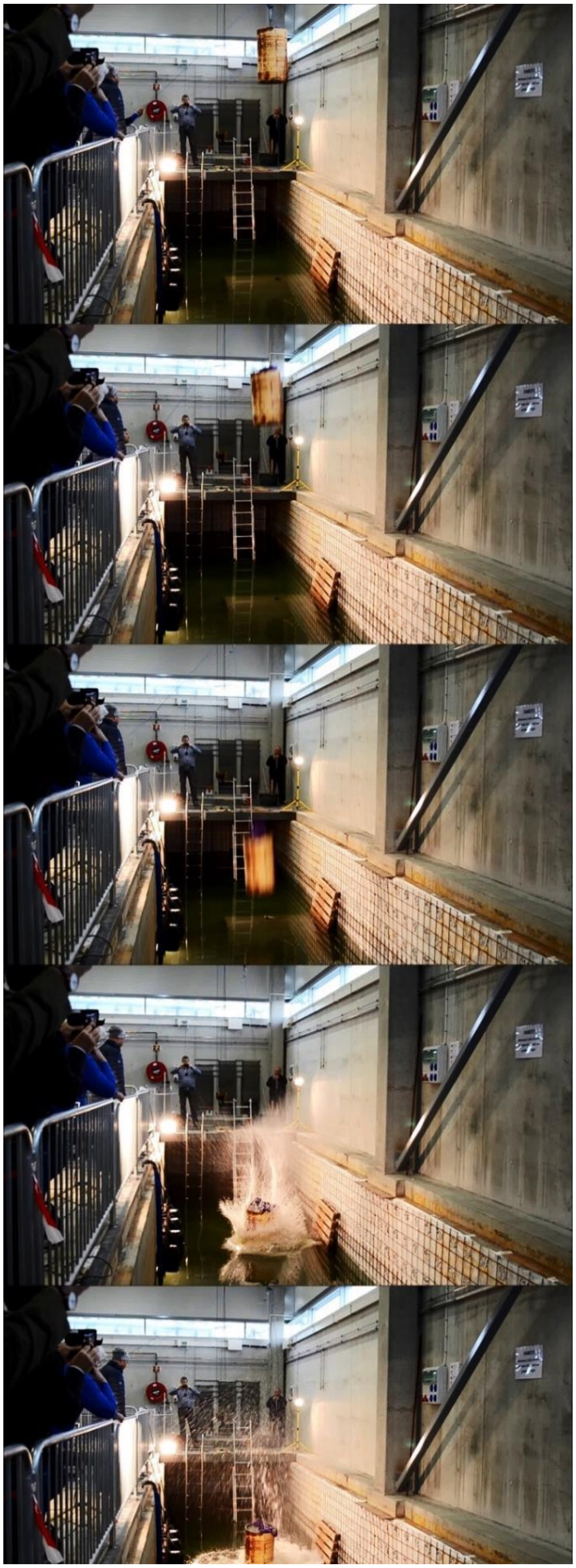

Frame-by-frame of Test ID 4.1 – 30 kJ

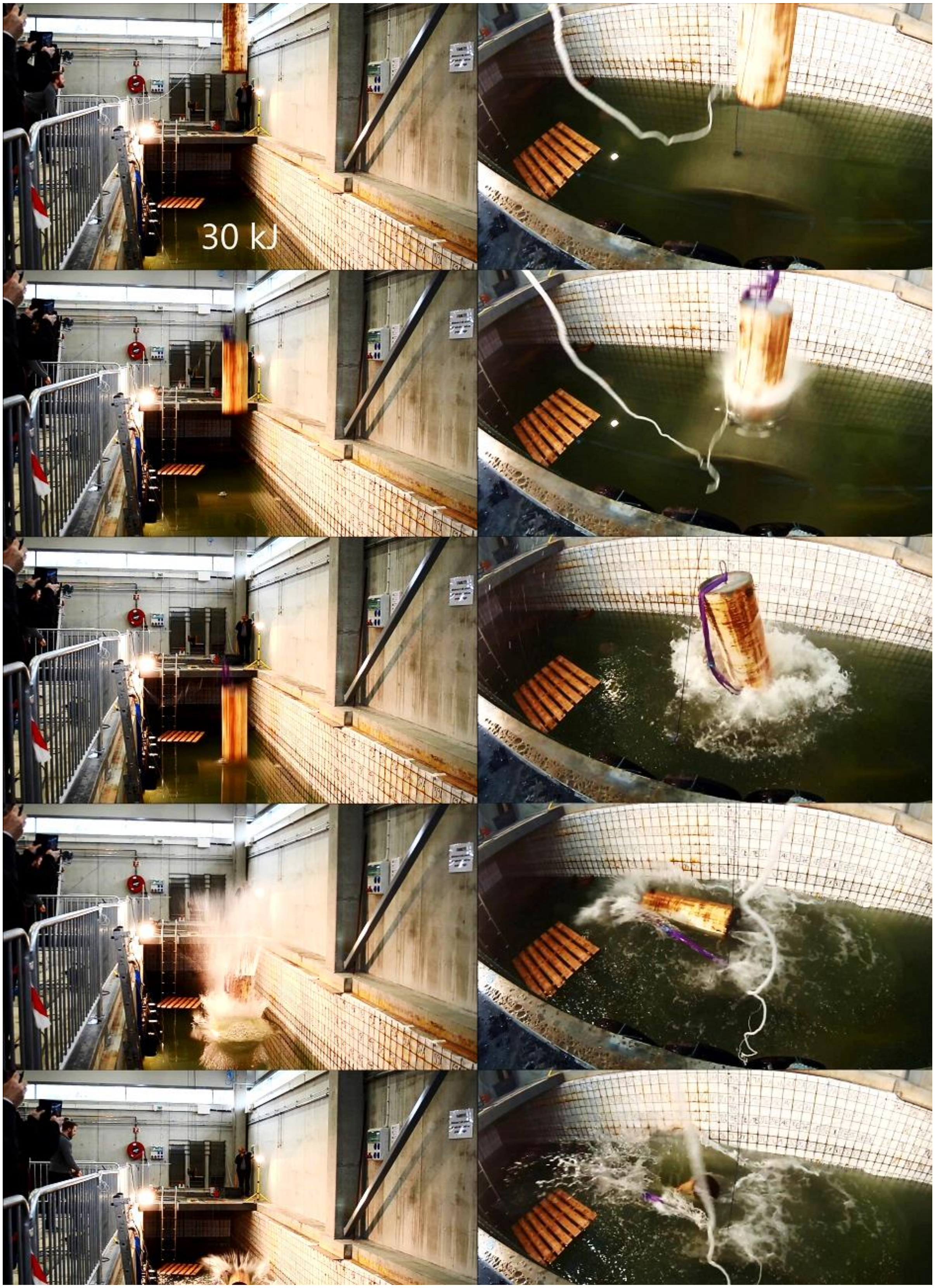

Frame-by-frame of Test ID 5.1 – 50 kJ